DISSERTATION

TRANSITION-METAL NANOCLUSTERS: KINETIC, MECHANISTIC AND ARENE HYDROGENATION CATALYSIS STUDIES

Submitted by

Jason A. Widegren

Department of Chemistry

In partial fulfillment of the requirements

for the Degree of Doctorate of Philosophy

Colorado State University

Fort Collins, Colorado

Fall 2002

COLORADO STATE UNIVERSITY

August 12, 2002

WE HEREBY RECOMMEND THAT THE DISSERTATION PREPARED UNDER OUR SUPERVISION BY JASON A. WIDEGREN ENTITLED TRANSITION-METAL NANOCLUSTERS: KINETIC, MECHANISTIC AND ARENE HYDROGENATION CATALYSIS STUDIES BE ACCEPTED AS FULFILLING IN PART REQUIREMENTS FOR THE DEGREE OF DOCTOR OF PHILOSOPHY.

Committee on Graduate Work

Anthony K. Rappé

Bruce A. Parkinson

Yian Shi

David S. Dandy

Richard G. Finke/Advisor

C. Michael Elliot/Department Head/Director

ABSTRACT OF DISSERTATION

TRANSITION-METAL NANOCLUSTERS: KINETIC, MECHANISTIC AND ARENE HYDROGENATION CATALYSIS STUDIES

Following a review of the appropriate literature, the research presented herein includes: (1) the development and testing of an indirect kinetic method for following transition-metal nanocluster formation under hydrogen: (2) the use of polyoxoanion-stabilized Rh(0) nanoclusters for monocyclic arene hydrogenation catalysis; and (3) a demonstration that precipitated ruthenium metal is the true catalyst in the benzene hydrogenation system based on the monometallic precatalyst, $Ru(II)(\eta^6\text{-}C_6Me_6)(OAc)_2$.

A few years ago a new kinetic method for following transition-metal nanocluster formation was developed in which the resultant nanocluster's catalytic activity was used as a reporter reaction. Herein this new kinetic method is tested and developed further: (i) by following nanocluster formation directly via H_2 uptake: (ii) by following nanocluster size vs time via TEM; (iii) by numerical integration simulations of the nanocluster formation reaction; and (iv) by showing that the new kinetic method can be used for a variety of metals and catalytic reactions. In the course of these studies it was discovered that heterolytic hydrogen activation is important for the formation of nanoclusters from higher valent metals.

Well-characterized polyoxoanion- and tetrabutylammonium-stabilized Rh(0) nanoclusters are synthesized by the reduction of $[Bu_4N]_5Na_3[(1,5\text{-}COD)Rh{\bullet}P_2W_{15}Nb_3O_{62}]$ with H_2 in propylene carbonate solvent. Propylene carbonate solutions of the Rh(0) nanoclusters catalyze the hydrogenation of anisole (methoxybenzene) under mild conditions (22–78 °C. 30–40 psig H_2). Proton donors such as water or $HBF_4{\bullet}Et_2O$ affect both nanocluster formation and nanocluster arene hydrogenation catalysis. These Rh(0) nanoclusters are 10-fold more active than a commercially available 5% Rh/Al_2O_3 catalyst of the same average metal-particle size. The Rh(0) nanoclusters are capable of ≥2600 catalytic turnovers. and also display an unusual selectivity for the partial hydrogenation of anisole to 1-methoxycyclohexene.

Finally. a literature arene hydrogenation system based on the precatalyst $Ru(II)(\eta^6\text{-}C_6Me_6)(OAc)_2$ is re-investigated. A previously developed. four-step. mechanistic approach is used to answer the question "is it homogeneous or heterogeneous catalysis?" The data presented herein provide compelling kinetic (and other) evidence that the true catalyst in this system is *not* a homogeneous metal complex or a soluble colloid: rather. the data are consistent with bulk ruthenium metal as the true catalyst.

Jason A. Widegren
Department of Chemistry
Colorado State University
Fort Collins. Colorado 80523
Fall 2002

DEDICATION

To Mom and Dad

TABLE OF CONTENTS

CHAPTER I

INTRODUCTION

This dissertation is written in the "journals-format" style (see Appendix A for a discussion of this type of dissertation), and is based on five separate publications, each written in a format set by Elsevier Science (Chapters II and III) or the American Chemical Society (Chapters IV-VI). A level of cohesiveness is achieved herein (i) by this introductory chapter, (ii) by the use of bridging paragraphs at the beginning of each subsequent chapter, and (iii) by a final summary chapter. The overall theme of this dissertation is the study of transition-metal nanoclusters. A brief overview of the contents of each chapter is presented below.

Chapter II is a review of the literature of transition-metal nanoclusters as arene hydrogenation catalysts. This review is most relevant to the material presented in Chapter V. This chapter is given first because it contains a brief introduction to nanocluster science and to the use of nanoclusters for catalysis, topics of importance throughout this dissertation. The reader is also referred to an in-depth review of nanocluster science and catalysis available elsewhere [1].

Chapter III is a review of the problem of distinguishing true homogeneous catalysis from soluble-metal-particle heterogeneous catalysis under reducing conditions. This review is most relevant to the material presented in Chapter VI.

Chapter IV describes the development and testing of a new kinetic method for following transition-metal nanocluster formation under hydrogen. This work is an extension of an important paper on the mechanism of transition-metal nanocluster formation [2]. Use of the new kinetic method led the discovery that heterolytic hydrogen activation is important for nanocluster nucleation when the nanocluster precursors contain metals in high oxidation states. The new kinetic method is also vital to the work described in Chapters V and VI.

Chapter V describes the use of polyoxoanion- and tetrabutylammonium-stabilized Rh(0) nanoclusters for anisole (i.e., methoxybenzene) hydrogenation. Among soluble nanocluster catalysts, these Rh(0) nanoclusters have a record catalytic lifetime for monocyclic arene hydrogenation. Additionally, such nanoclusters have an unexpected selectivity for the partial hydrogenation of arenes. The work described in this chapter probes the effects of proton donors, such as water and tetrafluoroboric acid, on arene hydrogenation catalysis. Finally, the catalytic properties of soluble polyoxoanion-stabilized Rh(0) nanoclusters are compared to a prototype heterogeneous metal-particle catalyst, Rh/Al_2O_3.

Chapter VI presents a re-investigation of a known [3,4] benzene hydrogenation catalyst system based on $Ru(II)(\eta^6\text{-}C_6Me_6)(OAc)_2$. The question asked in this chapter is, "is it homogeneous or heterogeneous catalysis?" Compelling kinetic (and other) evidence implicates ruthenium metal particles as the true catalyst in this system.

Chapter VII contains a brief summary of the material presented in this dissertation.

The most important hypotheses tested in this dissertation are the following: (i) soluble transition-metal nanoclusters are useful catalysts for monocyclic arene hydrogenation reactions; (ii) *polyoxoanion-stabilized* Rh(0) nanoclusters are interesting and exceptional catalysts for monocyclic arene hydrogenation; (iii) the kinetics of transition-metal nanocluster formation under hydrogen can be followed by using cyclohexene hydrogenation as a catalytic reporter reaction; (iv) the *in situ* formation of soluble nanocluster catalysts from monometallic precatalysts is common under reducing conditions; (v) kinetic experiments are the most important experiments for distinguishing true homogeneous catalysis from soluble-metal-particle heterogeneous catalysis; and (vi) the true catalyst in the benzene hydrogenation system based on $Ru(II)(\eta^6\text{-}C_6Me_6)(OAc)_2$ is a soluble nanocluster catalyst.

References:

[1] J.D. Aiken III, R.G. Finke, J. Mol. Catal. A: Chem. 145 (1999) 1.

[2] M.A. Watzky, R.G. Finke, J. Am. Chem. Soc. 119 (1997) 10382.

[3] M.A. Bennett, J.P. Ennett, Inorg. Chim. Acta 198-200 (1992) 583.

[4] J.P. Ennett, Ph.D. Dissertation, Department of Chemistry, Australian National University, 1984.

CHAPTER II

A REVIEW OF SOLUBLE TRANSITION-METAL NANOCLUSTERS AS ARENE HYDROGENATION CATALYSTS

This chapter contains (i) an introduction to arene hydrogenation, (ii) an introduction to nanocluster science, and (iii) a comprehensive, critical review of soluble transition-metal nanoclusters as arene hydrogenation catalysts. This chapter is intended to encompass the literature relevant to Chapter V, but the material herein, especially the introduction to nanocluster science, is pertinent to the entire dissertation.

This chapter, which is in press in the *Journal of Molecular Catalysis A: Chemical*, was written by J.A.W. and then lightly edited by R.G.F. in three sessions (11 hours total).

A review of soluble transition-metal nanoclusters as arene hydrogenation catalysts

Jason A. Widegren and Richard G. Finke

Abstract

A critical review of the use of soluble transition-metal nanoclusters for the hydrogenation of monocyclic aromatic compounds is presented. The review begins with a brief introduction to arene hydrogenation and to nanocluster science. The introductory material is followed by a detailed discussion of the approximately 20 papers in the literature that deal with the use of soluble transition-metal nanoclusters for the hydrogenation of monocyclic aromatic compounds. Metal particle catalysts on solid supports are not reviewed herein, and are considered only as far as they serve to compare and contrast with soluble transition-metal nanoclusters. The major findings of this review are: (i) soluble nanocluster catalysts are implicated as the true catalysts in many putatively "homogeneous" arene hydrogenations; (ii) with few exceptions, nanocluster

catalysts used for arene hydrogenation are poorly characterized; (iii) soluble nanocluster catalysts for arene hydrogenation have modest activity and lifetime; (iv) Rh and Ru are used almost exclusively as the active metals; (v) two catalyst systems, one developed by Roucoux and coworkers and the other by our own research group, stand out from the rest in terms of activity and lifetime; and (vi) selective arene hydrogenation, especially for the synthesis of the all-*cis* diastereomer of substituted cyclohexanes, has received considerable attention and is a promising area for future study and, perhaps, fine chemical applications (selectivities >90% for the all-*cis* diastereomer have been achieved by several groups).

1. Introduction

1.1. Arene hydrogenation

Sabatier and Senderens hydrogenated benzene for the first time a century ago using finely divided nickel as the catalyst [1,2]. For his studies of the hydrogenation of organic compounds in the presence of metallic catalysts, Sabatier shared the Nobel Prize in Chemistry with Victor Grignard in 1912. To this day, the hydrogenation of monocyclic arenes is an active area of research [3,4,5,6,7,8,9,10,11]. The production of substituted cyclohexanes from the corresponding substituted arenes is a goal of much of this research [12,13,14,15]. The hydrogenation of benzene to cyclohexane is probably the most important industrially practiced arene hydrogenation reaction, the cyclohexane being used primarily in the production of adipic acid, a precursor to nylon [16,17].

Partial arene hydrogenation to cyclohex*enes* is also an active area of research [3,18,19,20]. An example of this chemistry is the partial hydrogenation of benzene to cyclohexene, Eq. 1, which is practiced industrially by Asahi Chemical Industry in Japan using a heterogeneous Ru catalyst [21].

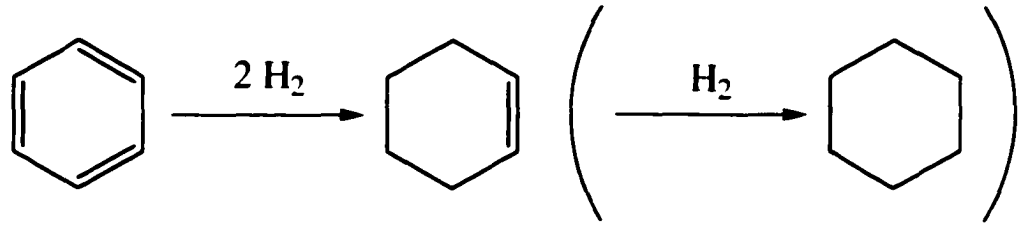

(1)

Arene hydrogenation has also garnered interest because of the demand for cleaner-burning, low-aromatic-content diesel fuels [6], which has been stimulated in part by the discovery that diesel exhaust particles contain powerful carcinogens [22], particles which also contribute to the prevalence of asthma and nasal allergies [23,24]. Hydrogenating aromatic polymers is also of current interest because the resultant polymers can have dramatically improved thermal and oxidative stability as well as improved optical properties [25]. For example, hydrogenation of polystyrene to poly(cyclohexylethylene) [25], Eq. 2, converts benzylic C–H bonds into more stable aliphatic C–H bonds. Dow Plastics is developing a commercial polystyrene hydrogenation process, and intends to use the poly(cyclohexylethylene) in optical media applications such as digital versatile discs (DVDs) [26]. As a second example, hydrogenation of aromatic rings in lignin, a biopolymer, has been suggested as a way to inhibit the oxidative yellowing (from quinone formation) of paper made from mechanical

pulps [27,28,29,30]. In short, monocyclic arene hydrogenation is still a very important research area in catalysis.

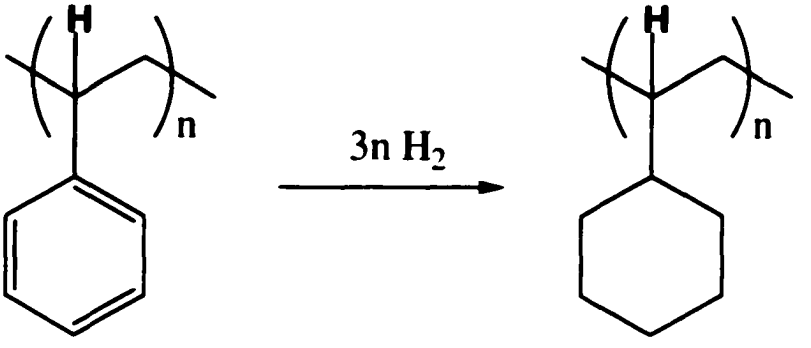

(2)

The hydrogenation of arenes is more difficult to catalyze than the hydrogenation of simple olefins [31]. This is as expected because at least some fraction of the resonance stabilization energy that is lost during arene hydrogenation appears in the transition state of the rate-determining step. Herein a distinction is made between monocyclic arenes (e.g., benzene and toluene) and polycyclic arenes (e.g., naphthalene and anthracene [32,33,34])[1] because, at least under mild conditions, monocyclic arenes are more difficult to hydrogenate [6,35].[2]

Monocyclic arene hydrogenation is typically performed with heterogeneous catalysts of Group VIII metals, such as Rh/Al_2O_3 and Raney nickel [36]. The catalytic

---

[1] The hydrogenation of *polycyclic* arenes such as naphthalene and anthracene with homogeneous, mononuclear catalysts is well established. For example, Halpern and coworkers present compelling kinetic plus other evidence that certain *mononuclear* Ru and Rh hydrido complexes are homogeneous catalysts for polycyclic arene hydrogenation [32,33,34].

[2] The hydrogenation of a monocyclic arene results in a greater loss of resonance stabilization energy than the hydrogenation of one of the rings in a polycyclic arene. Consider the following comparison as an illustration of this point. The resonance stabilization energies of benzene and naphthalene can be estimated as 36 and 61 kcal/mol, respectively [35]. Upon hydrogenation, benzene loses all 36 kcal/mol of resonance stabilization energy. In comparison, when naphthalene is hydrogenated to tetralin (i.e., 1,2,3,4-

activity of such metals for the hydrogenation of benzene and alkylbenzenes decreases in the order Rh > Ru > Pt > Ni > Pd > Co [36,37]. Metal sulfides, including MoS_2 and WS_2, are another important class of heterogeneous arene hydrogenation catalysts, especially for petroleum refining [38,39,40,41]. In general, and as Gates has noted, "the most active metal sulfides are typically several orders of magnitude less active than the most active metal catalysts", but metal sulfide catalysts are useful because sulfur compounds do not (further) poison them [41].

There have also been several claims of homogeneous, single-metal-complex catalysts capable of *monocyclic arene* hydrogenation [4,42].[1] Unfortunately, these catalysts typically have poor catalytic activity [42], there is usually little evidence to support the hypothesis that the true catalyst in these systems is homogeneous,[3] and several such claimed mononuclear "homogeneous" catalysts have more recently been shown to be heterogeneous, soluble nanocluster catalysts [43,44,45], a point we will return to in a moment. The use of soluble nanoclusters as catalysts for monocyclic arene hydrogenation has received increased attention in recent years, and is the focus of this review.

---

tetrahydronaphthalene) it retains ~36 kcal/mol of resonance stabilization energy in the remaining aromatic ring, so only ~25 kcal/mol is lost.

[3] The monocyclic arene hydrogenation catalysts developed by Rothwell and coworkers, such as $[Ta\{OC_6H_3(C_6H_{11})_2\text{-}2,6\}_2(H)_3(PMe_2Ph)_2]$, are an exception to this statement [4]. These Nb^V or Ta^V hydrido aryloxide complexes are almost surely true homogeneous catalysts based on the following evidence: (i) the reduction of Nb^V or Ta^V by hydrogen is implausible under the reaction conditions, so the formation of Nb(0) or Ta(0) metal particles is extremely unlikely; and (ii) the observed selectivity of the catalyst for the intramolecular hydrogenation of the aryloxide ligands is consistent with a homogeneous mononuclear catalyst, but difficult to explain if the true catalyst is heterogeneous (*ortho*-phenyl substituents on the

1.2. Background information on transition-metal nanoclusters

For the purposes of this review, transition-metal nanoclusters [46,47,48,49,50,51,52,53,54,55,56,57,58,59,60,61] are defined as metal particles with a diameter in the 1–10 nm range [49]. Such particles have generated intense interest in recent years because of the fundamental interest in these "strange morsels of matter" [62], and because of their many potential uses [48,50,58]. Modern transition-metal nanoclusters differ from classical colloids in several important respects [46,49]. Modern transition-metal nanoclusters are generally: (i) smaller (1–10 nm in diameter) than classical colloids (typically >10 nm in diameter); (ii) isolable and redissolvable ("bottleable"), unlike classical colloids; (iii) soluble in organic solvents (classical colloid chemistry is typically aqueous); and (iv) well defined compositionally, unlike classical colloids. Additionally, modern transition-metal nanoclusters typically have: (v) narrower size dispersions than classical colloids; (vi) clean surfaces (less to none of the X^-, O^{2-}, OH^-, H_2O or polymers that are prevalent in classical colloid chemistry); (vii) reproducible syntheses; and (viii) reproducible ($\leq\pm$15–20%) catalytic activities (unlike the irreproducible, often $\geq\pm$500%, catalytic activities of classically prepared colloids [46,63]). Catalysis is an especially important area of nanocluster science in that processes already exist that could potentially use nanoclusters as "soluble analogs of heterogeneous catalysts" [49] to improve catalytic rates, selectivities or possibly even lifetimes.

---

aryloxide ligand are hydrogenated, while hydrogenation of phenyl rings *meta* or *para* to the aryloxide

1.2.1 Synthesis

The synthesis of soluble transition-metal nanoclusters has been accomplished using five general methods [48,58]: (i) the chemical reduction of transition-metal salts, (ii) the electrochemical reduction of transition-metal salts, (iii) thermal or photochemical decomposition of transition-metal precursors, (iv) ligand reduction and displacement from organometallic compounds, and (v) metal vapor synthesis. Some synthetic techniques use a combination of these five methods; for example, sonochemical [64] preparations of nanoclusters involve either (i) or (iii) or a combination of (i) and (iii) [64,65,66,67,68,69]. Of the five methods, the chemical reduction of transition-metal salts is by far the most common. For example, all but one [159] of the nanocluster arene hydrogenation catalysts in Table 2.1 were prepared by the chemical reduction of a transition metal salt. Solubility is often an advantage in nanocluster syntheses, and has even allowed the use of powerful HPLC separation methodologies [70,71,72,73,74].[4]

1.2.2 Stabilization

Transition-metal nanoclusters are only kinetically stable because the formation of bulk metal is the thermodynamic minimum [49,75].[5] Therefore, nanoclusters that are freely dissolved in solution must be stabilized in a way that prevents the nanoclusters from diffusing together and coalescing—any such agglomeration would eventually lead

---

oxygen is not observed nor is hydrogenation of the phenoxide nucleus itself ever observed) [4].

[4] The use of chromatographic techniques, such as HPLC, for the purification of transition-metal nanoclusters is still rare, however, with the work to date focusing on gold nanoclusters. Hence, it is not yet clear how widely applicable chromatographic techniques will be in nanocluster science.

[5] From the enthalpies of vaporization (i.e., ignoring solvation effects), one finds that the bulk metal is 133, 155 and 160 kcal/mol more stable than single Rh(0), Ru(0) and Ir(0) atoms, respectively [75]. Obviously, nanoclusters are more stable than isolated metal atoms because they have many metal–metal bonds, but

to the formation of the thermodynamically favored bulk metal [49]. Nanocluster stabilization is usually discussed in terms of two general categories of stabilization, electrostatic and steric [76,77]. Electrostatic stabilization is achieved by the coordination of anionic species, such as halides, carboxylates or polyoxoanions, to the coordinatively unsaturated surface metal atoms of the metal particles [76]. This results in the formation of an electrical double-layer (really a diffuse electrical multi-layer) [78], which causes coloumbic repulsion between the nanoclusters. Steric stabilization is achieved by the presence of bulky, typically organic materials that, due to their bulk, impede the nanoclusters from diffusing together [76]. Polymers, dendrimers and large alkylammonium cations are examples of organic steric stabilizers. Some types of stabilizers provide both steric and electrostatic stabilization—the 15×12 Å, highly charged $P_2W_{15}Nb_3O_{62}^{9-}$ polyoxoanion is presently the premier example of such a "Gold Standard" [79] nanocluster stabilizing anion [48,49,79]. The choice of stabilizer also allows one to tune the solubility of the nanoclusters [80,81]. For example, the transfer of nanoclusters from organic solvents to water (and *vice versa*) has been demonstrated using phosphine [80] or pyridine [82] stabilizers.[6]

1.2.3 Advantages of nanoclusters as soluble metal-particle catalysts

The use of soluble nanocluster catalysts for arene hydrogenation provides some advantages over traditional metal-particle heterogeneous catalysts on solid supports.

---

they are still less stable than the thermodynamic sink of bulk metal, in which every metal atom has the maximum possible number of metal–metal bonds.

[6] As a third example, with the use of appropriate thiolates the solubility of thiolate-stabilized nanoclusters can be changed easily, ranging from water to nonpolar solvents [81]. Of course such nanoclusters are of little interest for catalysis because they are thiolate-poisoned (*vide infra*).

Figure 2.1. To begin with, nanoclusters are often more active under mild conditions than corresponding supported metal particle catalysts [13,162]. This must be due to the number and type (degree of coordinative unsaturation) of the active sites present, which is a function of the conditions under which the catalysts are prepared. Traditional heterogeneous catalysts are typically prepared at high temperatures, which causes annealing to the most stable (but probably not the most active) surface structure [83]. On the other hand, soluble nanoclusters are typically synthesized under mild conditions, resulting in a tendency towards kinetically controlled surface structures [84]. Based on studies of CO adsorption on nanocluster surfaces, de Caro and Bradley conclude that "surface irregularity is probably to be found for colloidal metal particles in most, if not all, cases where the preparation conditions do not lead to annealing of the as-prepared surface" [83].

A second advantage of soluble nanocluster catalysts is that they have been found to be more selective than corresponding traditional heterogeneous catalysts for some reactions [48,85]. Relevant here is Schmid's study of the ligand-modified selectivity of nanocluster catalysts for the hydrogenation of 2-hexyne [85], an important precedent that *presages a new area of ligand-modified, highly selective, nanocluster catalysts.*

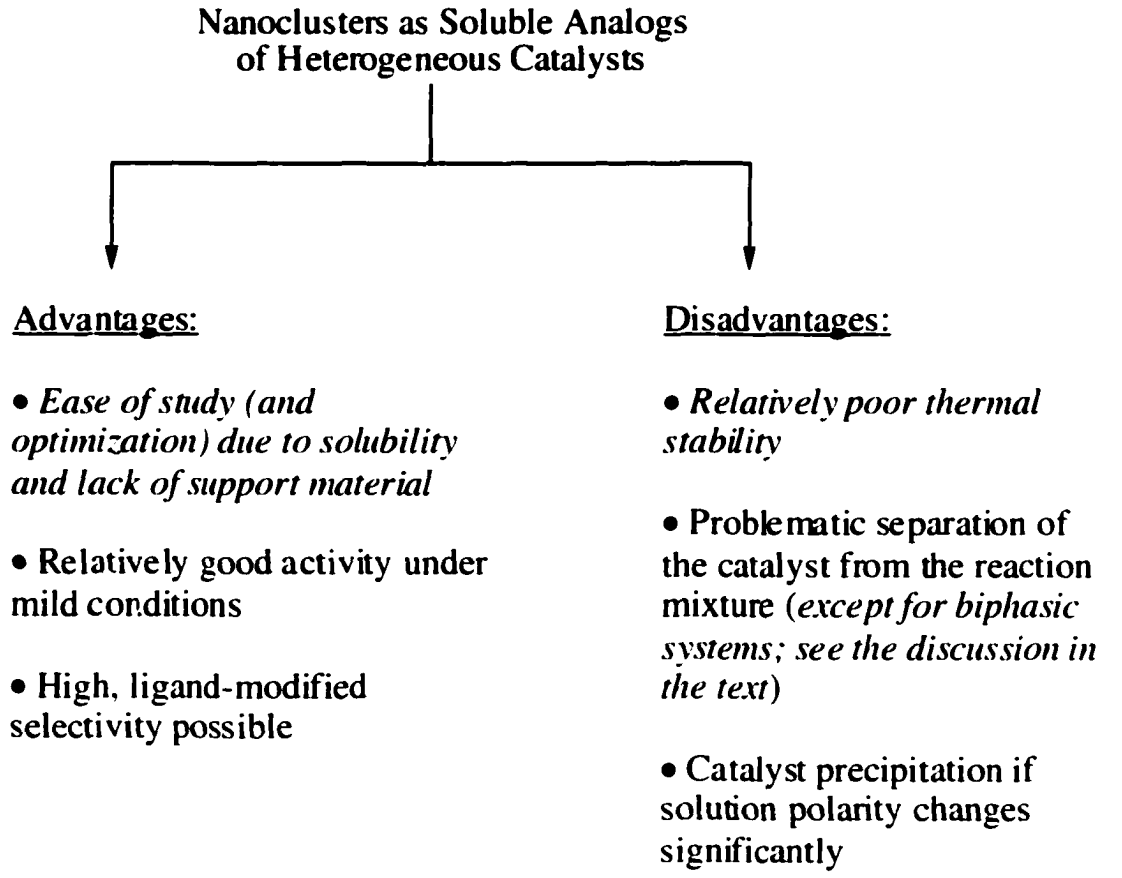

Figure 2.1. Some advantages and disadvantages of using nanoclusters as soluble analogs of heterogeneous catalysts.

Perhaps the most important, albeit still under-exploited, advantage of soluble nanocluster catalysts is that they are easier to study and, therefore, to optimize than traditional heterogeneous catalysts. Their solubility allows the use of analytical techniques in solution such as high resolution NMR [86,87,88,89,90], solution-phase IR [83,91,92,93,94,95,96], and *homogeneous* solution-phase kinetic and mechanistic studies [97]. The absence of support material generally simplifies characterization of soluble nanoclusters by eliminating the heterogeneity and other effects of the solid support [98].

1.2.4 Disadvantages of nanoclusters as soluble metal-particle catalysts

Soluble nanocluster catalysts also have disadvantages compared to traditional heterogeneous catalysts, Figure 2.1. The greatest disadvantage of at least the presently known soluble nanocluster catalysts is their poorer stability towards agglomeration in comparison to metal particle catalysts on solid supports. Reports of nanoclusters that are thermally stable *in solution* at ≥100°C are rare [99,100,101,102,103,104,105,106]. Of these, the solvent- (and chloride- [48]) stabilized Pd nanoclusters prepared by Reetz and Lohmer have the highest demonstrated thermal stability: a propylene carbonate solution of the Pd nanoclusters shows no visually observable formation of bulk metal even after several days at 140–155°C [104]; unfortunately, the apparent absence of agglomeration was not verified by transmission electron microscopy (TEM) in that study. Reetz's nanoclusters were also shown to catalyze Heck coupling reactions at temperatures as high as 160°C [104], a record reaction temperature for a soluble nanocluster catalyst. Two other thermally stable nanocluster systems of note are the polymer-stabilized Pd nanoclusters developed by Bradley and coworkers [102] and Antonietti and coworkers [103], both of which were used to catalyze Heck coupling reactions. These two nanocluster systems show excellent stability and catalytic lifetime at 140°C: Bradley's poly(vinylpyrrolidone)-stabilized nanoclusters are capable of 100 000 total turnovers (TTO) [102], and Antonietti's polystyrene-*b*-poly-4-vinylpyridine-stabilized (i.e., block copolymer-stabilized) nanoclusters are capable of at least 50 000 TTO [103]. In contrast to these soluble nanocluster catalysts, metal particle catalysts on solid supports are routinely used at several hundred degrees Celsius: for example, naphtha reforming with Pt/Al_2O_3 is performed industrially at 500°C [98]. An added difficulty in the stabilization

of soluble nanoclusters for catalysis is that the substrate must have some access to the nanocluster surface. Some types of stabilizers, such as thiols[7] [81,107,108,109,110,111,112] and silica[8] [113,114,115,116,117,118,119,120], effectively poison the nanoclusters.

Another disadvantage of soluble nanocluster catalysts is the problem of separating the catalyst from the reaction products; in this respect soluble nanocluster catalysts are similar to traditional homogeneous catalysts. Nevertheless, this separations problem is probably surmountable with the use of aqueous/organic biphasic systems (*vide infra*) or other modern immobilization systems for soluble catalysts. Two such modern immobilization systems are Horvath's fluorous phase methods [121,122,123,124] and Davis' immobilization of homogeneous hydrophilic catalysts in thin films of hydrophilic liquids on a porous hydrophilic support (the reactants and products form a hydrophobic phase) [125,126]. Nanoclusters in biphasic organic substrate/ionic liquids are another

---

[7] Thiol-stabilized nanoclusters, often referred to as "monolayer-protected" clusters [81], can be repeatedly isolated and redissolved without agglomeration or decomposition, they can be chromatographed, and they are generally air- and solvent-stable [81]. Of course, the nanocluster surface is poisoned by the thiols, and so is of little interest for catalytic studies. However, there are reports describing the use of thiol ligands to tether homogeneous catalysts to nanoclusters, thereby making catalysis with such nanoclusters possible [110,111]. There is also a report of thiols anchoring nanoclusters to a silica support (i.e., Si-SH groups on the silica particles tether the nanoclusters to the silica surface), resulting in an alkene hydrogenation catalyst, presumably because it is not possible to achieve a full monolayer of thiol on the nanocluster under these conditions [112].

[8] The interesting silica-coated nanoclusters developed by Mulvaney and co-workers [113,114,115,116,117] have good thermal stability. It is reported, for example, that gold nanoclusters coated with a 5-nm layer of silica show excellent stability against agglomeration at 70°C (higher temperatures were not tested) [115]. More work is needed to determine if these nanoclusters will be of any use for catalysis, however. The silica layer appears to smoothly coat the entire surface of the nanocluster (see the electron micrographs in reference [116]), which would effectively poison it by limiting access of the substrate to the metal. However, the silica-coated metal core can be etched by cyanide or I_2 [118,119,120], demonstrating that at least small molecules can penetrate the silica layer.

possible solution to the problem of separating the product from soluble nanocluster catalysts [127,128,129].[9]

A final disadvantage of soluble nanocluster catalysts is that they must remain in solution to be effective. This can be problematic, for example, if the polarity of the solution changes during the course of the reaction, causing the nanoclusters to precipitate from solution (a phenomenon observed when using a batch reactor for the hydrogenation of cyclohexene with a record-lifetime Rh(0) nanocluster catalyst which showed 190 000 total turnovers of cyclohexene hydrogenation [130]).

1.3. The historically perplexing problem of distinguishing soluble nanocluster catalysts from homogeneous, single-metal-complex catalysts

A problem that has caused considerable consternation in the study of arene hydrogenation catalysis is the difficult task of distinguishing homogeneous, single-metal-complex catalysts from soluble nanocluster or colloid (*vide supra*) catalysts. The literature in this area dates back to about 1980 and includes contributions from Maitlis [131], Whitesides [132,133], Crabtree [134,135,136], Collman [42,137], Lewis [138,139] and our group [140,141]. A more general approach for distinguishing the two was developed only recently [140,141], and involves the four-pronged approach outlined in Figure 2.2. This method emphasizes: (1) the early use of TEM as a simple, powerful (but before the 1994 study [140], underutilized) way to detect soluble nanoclusters; (2) kinetic studies (because catalysis is a wholly kinetic phenomenon [142,143]); (3) catalyst

---

[9] It is unclear if the true catalyst in reference [127], employing $[H_4Ru_4(\eta^6\text{-}C_6H_6)_4][BF_4]_2$ as the precatalyst, is a nanocluster or not.

poisoning experiments using mercury or added ligand (PPh_3, CS_2, H_2S, etc.),[10] especially if performed quantitatively (the mercury test is easy to perform and is perhaps the best single test for metal particle catalysis, but it is not definitive by itself because mercury can react with single metal complexes [133]); and (4) the important concept that *the identity of the true catalyst will be consistent with all the data.*

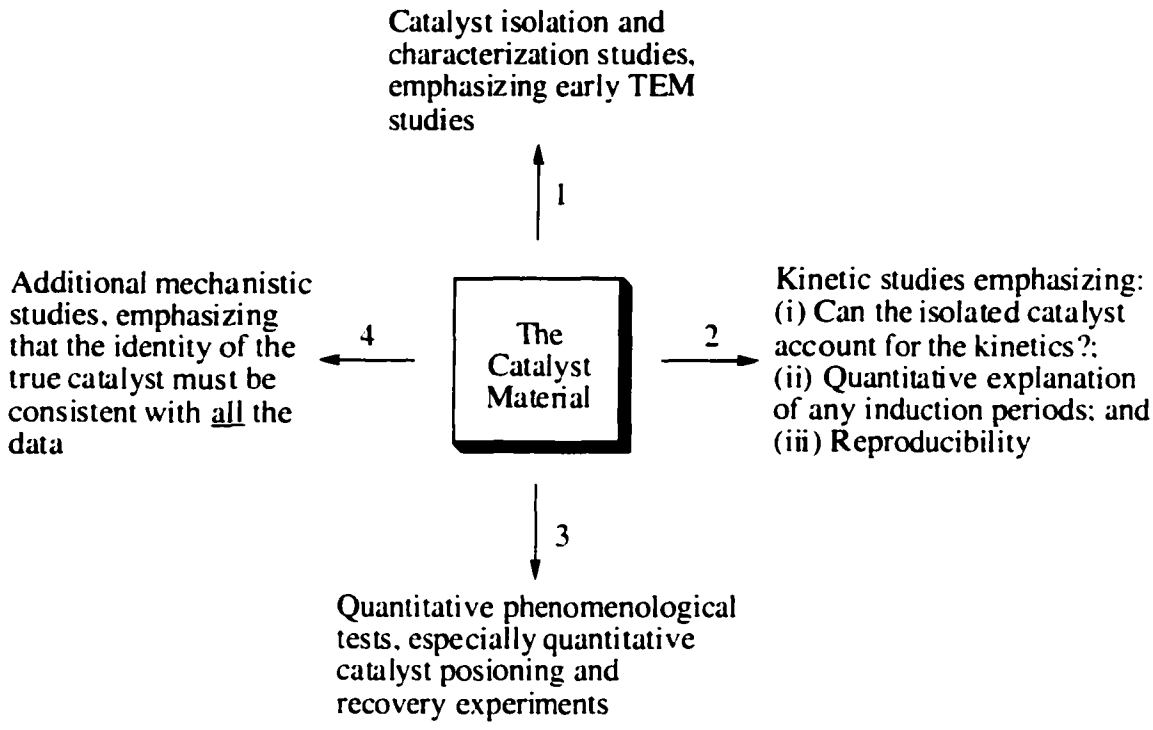

Figure 2.2. A more general approach to distinguishing between a "heterogeneous" nanocluster (colloid) catalyst and a discrete, "homogeneous" catalyst.

---

[10] Though underutilized, poisoning experiments using added ligands, such as PPh_3, CS_2 and H_2S, can be powerful if performed quanititatively [140]. If a catalyst can be completely poisoned with <<1.0 equivalent of the added ligand (per metal atom), then this is excellent evidence for a heterogeneous, metal particle catalyst. The logic here is that in a metal particle catalyst only a fraction of the metal atoms are on the surface; hence, even if every surface atom is active, <<1.0 equivalent of ligand will be sufficient to poison the catalyst. On the other hand, if ≥1.0 equivalent of ligand is required to completely poison the catalyst that is compelling evidence that the catalyst is a homogeneous, probably even monometallic, catalyst (and if control experiments show that the added ligand is unable to dissociate authentic nanoclusters of the same

There are now several examples in the literature of arene hydrogenation catalysts that were initially believed to be homogeneous, but later evidence suggests that a soluble nanocluster is the true catalyst. Perhaps the best example is the important arene hydrogenation catalyst based on $RhCl_3$ and $[(C_8H_{17})_3NCH_3]Cl$ [144,145]. Initially, it was believed that the $[(C_8H_{17})_3NCH_3]^+[RhCl_4]^-$ ion-pair was the true arene hydrogenation catalyst [144]. Later work using the more general approach to the "is it homogeneous or heterogeneous catalysis problem" [140] mentioned above, including TEM plus powerful solution-phase kinetic studies, convincingly shows that the true catalyst is actually a distribution of Rh(0) nanoclusters stabilized by Cl^- and $[(C_8H_{17})_3NCH_3]^+$ [43].

A second example involves the use of $[Rh(\eta^5\text{-}C_5Me_5)Cl_2]_2$ for arene hydrogenation [146,147]. The catalyst in this system was originally claimed to be homogeneous on the basis of light scattering experiments. However, later work suggests that the true catalyst may be heterogeneous, though the evidence is not definitive [44]. Briefly, the evidence for heterogeneity includes (i) the observation of dark colored reaction solutions, (ii) the routine observation of 1–2 h induction periods, an observation characteristic of nanoparticle formation [140,141], (iii) the deposition of Rh metal on the reactor walls, an observation which virtually demands the formation of Rh_n nanoparticles since the precatalyst is monometallic [140,141], and (iv) the observation that the catalyst is much more active for the hydrogenation of benzene and cumene than it is for the hydrogenation of polystyrene [44].

A third example involves $Ru_2Cl_2(\mu\text{-}H)_2(\mu\text{-}Cl)(\eta^6\text{-}C_6Me_6)_2$ as a precatalyst for arene hydrogenation [148,149]. This catalyst was originally thought to be homogeneous:

---

metal). See elsewhere [140,141] for a prototypical example of how this "fractional poisoning" experiment

however, a later study shows that the catalyst is inactive in the presence of elemental mercury [45], implying that the catalyst is colloidal in nature [140,150].[11] A fourth example involves the use of $Ru(\eta^6\text{-}C_6Me_6)(O_2CMe)_2$ for benzene hydrogenation [151,152,153,154]. Early catalytic studies [151,152] were unable to determine the nature of the true catalyst [151], but recent work, including TEM and kinetic studies, shows that the true catalyst is colloidal Ru [154]. These examples show that soluble nanoclusters are fairly pervasive in known ("homogeneous") arene hydrogenation. On this basis alone nanocluster arene hydrogenation catalysts merit further study.

The problem of distinguishing homogeneous vs heterogeneous catalysis is not limited to arene hydrogenation catalysis. The pervasiveness of this problem in catalytic science is illustrated by the identification of *homogeneous species* as the true catalysts for initially *heterogeneous* oxidation catalysts based on molecular sieves [155,156], and for carbonylation and Heck coupling catalysts where Pd/C and Pd/Al_2O_3 are the *precatalysts* [157].

---

can be used to identify a nanocluster catalyst.

[11] Additionally, and in hindsight, poisoning experiments reported in the original study [149] are more consistent with the hypothesis that the catalyst is colloidal than with the hypothesis that it is homogeneous. For example, the presence of only 0.05 equivs of thiophene (per Ru atom) dramatically slows the turnover frequency (from 4.1 min^{-1} in an unpoisoned experiment to 0.3 min^{-1} with 0.05 equivs of thiophene) [149].

2. The use of soluble transition-metal nanoclusters as arene hydrogenation catalysts

2.1. Introduction and description of the nanocluster catalysts

Most arene hydrogenation to date has been done with traditional heterogeneous catalysts [3,6]. However, the use of soluble transition-metal nanoclusters for arene hydrogenation has increased dramatically in recent years [12,13,14,27,28,43,45,158,159,160,161,162,163,164,165,166,167,168]. To the best of our knowledge, Table 2.1 is a complete list of the papers (including brief descriptions) in chronological order dealing with monocyclic arene hydrogenation with soluble nanocluster catalysts.

Much of the work using soluble nanocluster arene hydrogenation catalysts follows a seminal paper by Januszkiewicz and Alper [158]. The colloidal nature of the catalyst was not known at the time of this 1983 paper, but these authors insightfully suggest in a 1984 paper that the true catalyst is "a highly active form of colloidal rhodium" [169]. (Additional study by others on very similar systems, and where colloidal Rh is also identified [28,45,163,164], leaves little doubt that Rh(0) nanoclusters are the true arene hydrogenation catalyst.) Januszkiewicz and Alper performed hydrogenations under biphasic, aqueous/organic reaction conditions using $[RhCl(1,5\text{-hexadiene})]_2$ as the precatalyst, and tetraalkylammonium hydrogen sulfate or tetraalkylammonium bromide as the phase transfer agent and nanocluster stabilizer. Note here that (i) halide and tetraalkylammonium salts are well-known, widely used nanocluster stabilizers [48,49], and (ii) there is a close correspondence of this system to established Rh(0) nanocluster

---

Such a result is difficult to explain for a homogeneous catalyst, but makes perfect sense for a nanocluster

systems [28,45,163,164]. Using mild reaction conditions (room temperature, 1 atm H_2) Januszkiewicz and Alper demonstrated [158] up to 100 TTO for a variety of arenes. Unfortunately, no reaction times were given, so the catalytic activity or turnover frequency (TOF, i.e., turnovers divided by time) is unknown.

A perusal of the literature studies of soluble nanocluster arene hydrogenation catalysis in Table 2.1 demonstrates the following points: (i) most studies use Rh(0), which is not surprising because the literature of heterogeneous arene hydrogenation generally shows Rh to be the most active metal [36,37,170]; (ii) Ru(0) nanoclusters are the second most common catalyst in this literature, paralleling the extensive use of Ru in the heterogeneous catalysis of arene hydrogenation; (iii) the three most commonly used nanocluster precursor compounds are $[RhCl(diene)]_2$, $RhCl_3 \cdot 3H_2O$ and $RuCl_3 \cdot 3H_2O$; and (iv) most soluble nanocluster arene hydrogenation catalysts use tetraalkylammonium salts to stabilize the nanoclusters against agglomeration. In addition, (v) the reaction conditions are typically mild (approximately room temperature and 1 atm H_2) and often biphasic (aqueous/organic); and (vi) there is scant (often nonexistent) characterization of the nanocluster catalyst in most studies.

---

catalyst where only a fraction of the total metal atoms are on the surface and active.[10]

Table 2.1. Summary of monocyclic arene hydrogenation with soluble nanocluster catalysts

	Authors (date)	System	Results	Ref
1	Januszkiewicz, K. R. Alper, H. (1983)	This is an important paper because much of the other work in the area is based directly upon it. The precatalyst is $[RhCl(1,5\text{-hexadiene})]_2$ and a tetraalkylammonium halide. Several substrates were tried, including benzene, o-xylene, p-methylanisole and phenol. The conditions are room temperature and 1 atm H_2; biphasic benzene/water or hexane/water is the reaction medium. The authors don't probe whether or not the catalyst is homogeneous or heterogeneous, but in a 1984 paper by the same authors they suggest that the actual catalyst is "a highly active form of colloidal rhodium", and reference "unpublished results". Use of variations of this catalyst system (see below) by later groups, who recognize its colloidal nature, makes it fairly certain that the catalyst described in this paper is indeed colloidal.	Up to 100 TTO are demonstrated for some substrates; pH is shown to be an important variable. No activity is given (i.e., the authors don't say how long their hydrogenation experiments last) so the catalytic results cannot be compared to later work. Only the *cis* product is observed in the hydrogenation of 2-methylanisole (at 92% yield).	158
2	Foise, J. Kershaw, R. Dwight, K. Wold, A. (1985)	In this study the electrochemical reduction of benzene is combined with direct catalytic hydrogenation of benzene. Platinum and ruthenium colloids are used as the hydrogenation catalysts in solution and are prepared from the decomposition of Pt and Ru sulfite acid solutions. The conditions are room temperature and 1.7 atm H_2. The solvent is ethanol mixed with HMPA.	Only the ruthenium colloids are active. However, the colloids are poorly characterized by today's standards and it is not possible to calculate an activity or lifetime for the hydrogenation.	159
3	Duan, Z. Hampden-Smith, M. J. Sylwester, A. P. (1992)	$[(1,5\text{-COD})RhH]_4$ is synthesized from $[(1,5\text{-COD})RhCl]_2$ and used as the nanocluster precursor. NMR monitoring of the concentration of $[(1,5\text{-COD})RhH]_4$ and cyclooctane shows that activity is still seen after all of the $[(1,5\text{-COD})RhH]_4$ is gone, evidence that the nanoclusters are the (primary) active species. Cyclohexane-d_{12} is sometimes used as a solvent. Toluene is the primary substrate. The conditions are room temperature and one(?) atm H_2.	A lifetime of at least 127 TTO is demonstrated, though this seems to be based on substrate/$[(1,5\text{-COD})RhH]_4$, not on substrate/Rh atom. The authors calculate an activity of 1.83×10^{-3} molecules of toluene/(Rh atom • sec). TEM shows the presence of agglomerated 2-nm-sized nanoclusters.	160

4	Drognat Landré, P. Lemaire, M. Richard, D. Gallezot, P. (1993)	The precatalyst is $RhCl_3 \bullet 3H_2O$ in the presence of Aliquat 336 (tricaprylylmethyammonium chloride) and/or trioctylamine. Dibenzo-18-crown-6 ether is the only substrate. The conditions are room temperature and 1–50 atm H_2; biphasic CH_2Cl_2/water is the solvent.	The authors demonstrate the hydrogenation of about 20 mol of crown ether per mole of Rh in <1 h. TEM shows the presence of nanoclusters in the 2–3 nm size range. At higher pressure, the stereoselectivity increases to a 95/5 ratio of the *syn/anti* isomers of the dicyclohexyl-18-crown-6 ether.	161
5	Nasar, K. Fache, F. Lemaire, M. Beziat, J. C. Besson, M. Gallezot, P. (1994)	The precatalyst is $RhCl_3 \bullet 3H_2O$ in the presence of Aliquat 336 (tricaprylylmethyammonium chloride), trioctylamine or dioctylcyclohexylethylamine. The substrates are 2-methylanisole (for which the cis/trans hydrogenation selectivity is investigated) and o-cresol derivatives (for which the enantioselective hydrogenation is investigated). The conditions are room temperature and 1–50 atm H_2; biphasic CH_2Cl_2/water is the solvent.	The authors demonstrate 40 TTO in 24 h for the hydrogenation of 2-methylanisole. About 10% hydrogenolysis of the methoxy group of 2-methylanisole is observed. No activity is observed in the absence of water, but this may be due to the low solubility of $RhCl_3 \bullet 3H_2O$ in the organic phase. About 5% ee is observed in the enantioselective reductions using a chiral amine as the nanocluster stabilizer. TEM shows the presence of nanoclusters in the 2–3 nm size range.	14
6	Drognat Landré, P. Richard, D. Draye, M. Gallezot, P. Lemaire, M. (1994)	The authors survey colloidal catalysts based on various metal chlorides ($RhCl_3$, $RuCl_3$, $NiCl_2$, $PdCl_2$, $IrCl_3$, K_2PtCl_6) with tertiary amines or Aliquat-336 (tricaprylylmethylammonium chloride) as the stabilizer. They also survey several supported heterogeneous catalysts (e.g., Ru/Al_2O_3, Rh/C, $Rh/SrTiO_3$). Dibenzo-18-crown-6 ether is the only substrate. The reaction conditions are varied from 25–60°C and 1–50 atm H_2; the solvent is biphasic CH_2Cl_2/water.	The Rh colloids are by far the most active, exhibiting the hydrogenation of 20 mol of crown ether per mol of Rh in 42 min at 5 MPa H_2. The authors observe hydrogenolysis of the crown ether. At 5 MPa H_2 pressure the *cis-syn-cis/cis-anti-cis* isomer ratio is 95/5. TEM shows the presence of colloids. Also, a "Maitlis test" (a reaction rate comparison before and after filtration) points to nanoclusters as the true catalyst.	162
7	Fache, F. Lehuede, S. Lemaire, M. (1995)	The authors use $RuCl_3 \bullet 3H_2O$ (and $RhCl_3 \bullet 3H_2O$) in the presence of trioctylamine as the precursor to their colloidal catalyst. Several mono- and di-substituted benzene derivatives are hydrogenated (containing a variety of different functional groups), including 2-methylanisole and 2-methylbenzoate. The conditions are room temperature and 50 atm H_2; the solvent is methanol/water.	The authors appear to demonstrate about 40 TTO in 1 h for the most easily hydrogenated substrates. No hydrogenolysis is observed. The activity of Ru/Al_2O_3 is 5- or 10-fold lower (on a per-metal-atom basis) than the colloidal catalyst. *Cis/trans* selectivities up to 60 are observed in the hydrogenation of di-substituted arenes. No attempt is made to characterize the putative nanocluster catalyst. The rate is slower without water.	13

8	James, B. R. Wang, Y. Hu, T. Q. (1996)	Much of this work is based on the catalyst system developed by Januszkiewicz and Alper (entry 1 in this table). $[RhCl(\eta^4\text{-}1,5\text{-hexadiene})]_2$, $[RhCl(\eta^4\text{-}1,5\text{-cyclooctadiene})]_2$, $RhCl_3 \bullet 3H_2O$, $Rh_6(CO)_{16}$ and $[Rh(OC_6H_5)(\eta^4\text{-}1,5\text{-cyclooctadiene})]_2$ are used as nanocluster precursors; tetrabutylammonium hydrogen sulfate is the nanocluster stabilizer. The substrates are 4-propylphenol, 2-methoxy-4-propylphenol and 2,6-dimethoxy-4-propylphenol. The reaction is performed in a biphasic (aqueous/organic) medium at 20°C and 1 atm H_2.	The initial red or yellow solutions darken within 0.5 h to give the catalytically active solutions; over longer periods, bulk Rh metal precipitates with a resulting loss of activity. The formation of Rh metal, and a comparison to literature colloids (noting the necessity of the tetrabutylammonium hydrogen sulfate), are given as evidence that nanoclusters are the real catalyst. The TTO and TOF cannot be determined from the information given, but appear to be in the same range as later papers published by these researchers.	163
9	Hu, T. Q. James, B. R. Rettig, S. J. Lee, C.-L. (1997)	This catalyst system is based on that of Januszkiewicz and Alper (entry 1 in this table). $[RhCl(\eta^4\text{-}1,5\text{-hexadiene})]_2$ is the nanocluster precursor. A tetrabutylammonium salt is the nanocluster-stabilizing agent. The substrates are lignin model compounds: 4-propylphenol, 2-methoxy-4-propylphenol, and 2,6-dimethoxy-4-propylphenol. The reaction conditions include room temperature and 1–13.6 atm H_2; the solvent is biphasic hexane/water.	The authors demonstrate about 50 TTO in about 50 h at 1 atm H_2. The reaction time decreases to about 6 h at 13.6 atm H_2. No nanocluster characterization is done. The authors simply say, probably correctly, that "the active Rh catalyst is probably present in a colloidal form: as the hydrogenation proceeds, metal particles accumulate and these are not active for subsequent hydrogenation reactions". The all-*cis* diastereomer is obtained selectively when the phenolic hydroxyl group is protected as a methyl ether or when a model compound possessing two methoxy substituents adjacent to the phenolic hydroxyl group is used.	164
10	Hu, T. Q. James, B. R. Lee, C.-L. (1997)	A water-soluble, polymer-stabilized, colloidal Rh catalyst is prepared by reducing $RhCl_3 \bullet 3H_2O$ with ethanol in the presence of polyvinylpyrrolidone and triethylamine. The substrates are benzyl acetone, 4-propylphenol, 2-methoxy-4-propylphenol, and 1,2-dimethoxy-4-propylbenzene. The reaction conditions include 25°C and 1 atm H_2; monophasic, aqueous ethanol is the solvent.	The authors demonstrate about 50 TTO for the hydrogenation of benzyl acetone in <43 h. About 20% hydrogenolysis is observed for compounds with methoxy groups. The authors attempt to use small, *neutral* organic molecules to stabilize their colloids, but with little success. The polymer-stabilized nanoclusters are prepared using a literature method, and no further characterization of the catalyst is done.	27

11	Hu, T. Q. James, B. R. Lee, C.-L. (1997)	This work is based on that of Januszkiewicz and Alper (entry 1 in this table). $[RhCl(\eta^4\text{-}1,5\text{-hexadiene})]_2$ is the primary catalyst precursor. A tetrabutylammonium salt is used as the nanocluster-stabilizing agent. The authors describe the hydrogenation of benzyl acetone, 4-propylphenol, eugenol, 1,2-dimethoxy-4-propylbenzene, and 2,6-dimethoxy-4-propylphenol under mild conditions (25 °C, 1 atm H_2) in a biphasic (water/hexane) medium at pH 7.5.	The authors demonstrate about 50 TTO in <24 h for the hydrogenation of benzyl acetone. Moderate to high diastereoselectivities are observed for the hydrogenated products; only the all-*cis* diastereomer is obtained for substrates where the phenolic hydroxyl group is protected as a methyl ether or where the substrate possesses two methoxy substituents adjacent to the phenolic hydroxyl group. $[RhCl(\eta^4\text{-}1,5\text{-cyclooctadiene})]_2$, $RhCl_3 \bullet 3H_2O$ and $RuCl_3 \bullet 3H_2O$ are found to be less active precatalysts.	28
12	Weddle, K. S. Aiken, J. D., III Finke, R. G. (1998)	This paper re-examines a putative "homogeneous" arene hydrogenation catalyst developed by others (*J. Org. Chem.* **1987**, *52*, 2804). Several experiments (TEM, reaction kinetics, Hg poisoning, H/D exchange) provide definitive evidence for Rh(0) nanoclusters being the true catalyst when using $RhCl_3 \bullet 3H_2O$ and trioctylamine and Aliquat 336 as the catalyst precursor. Benzene is the only substrate used in this paper (benzene and anisole were the primary substrates in the **1987** *J. Org. Chem.* paper). Reaction conditions include 30°C and 0.9 atm H_2; the reactions are done in biphasic dichloroethane/water or in monophasic THF.	A total of 40 TTO are demonstrated in an experiment where the catalyst is re-used once (i.e., after doing 20 TTO in about 2 h, more benzene is added and another 20 TTO are demonstrated in an additional 4 h). Additional notes from the **1987** *J. Org. Chem.* paper: Those authors say that, "In general, hydrogenation of benzenes did not give partially hydrogenated products . . . . Cyclohexene derivatives were, however, isolated when sterically hindered compounds were reduced." Water has a big effect on the catalytic activity and a minimum of 2 equivs of water (in addition to the waters of hydration on the $RhCl_3 \bullet 3H_2O$) are necessary for activity; H/D exchange between water and substrate occurs under catalytic conditions.	43
13	James, B. R. Wang, Y. Alexander, C. S. Hu, T. Q. (1998)	The nanoclusters are synthesized from $RhCl_3 \bullet 3H_2O$, $[RhCl(diene)]_2$ or $RuCl_3/(n\text{-}C_8H_{17})_3N$. A Ziegler-Natta catalyst and a Bennett-type Ru catalyst are also tried. The nanocluster stabilizers are tetraalkylammonium salts, R_4NX (R = alkyl, X = Cl, Br or HSO_4). The substrates are 4-propylphenols and "milled wood lignin". Reaction conditions include 1–50 atm H_2 and 20–100 °C; biphasic (aqueous/organic) solvent systems are used.	This paper discusses the effects of water in detail. D-labeling studies show that some of the H in the product comes from water. Hydrogenolysis of the methoxy group is observed. The authors demonstrate up to 300 TTO in 24 h for the hydrogenation of 2-methoxy-4-propylphenol with $RuCl_3/(n\text{-}C_8H_{17})_3N$ as the catalyst. Some *cis*/*trans* selectivity is observed.	45

14	Schulz, J. Roucoux, A. Patin, H. (1999)	What separates this system from several of the others is the use of *hydroxy*alkylammonium bromide salts (which are highly water soluble) as the nanocluster stabilizer. The nanoclusters are synthesized by reducing $RhCl_3 \bullet 3H_2O$ with $NaBH_4$ in dilute aqueous solutions of the hydroxyalkylammonium salts. The organic phase apparently consists of just the substrate and products. Various mono- and di-substituted arenes are hydrogenated including benzene, toluene, anisole and xylene. The conditions include 20°C and 1 atm H_2; the reaction solutions are biphasic (aqueous/organic).	The nanoclusters have an average diameter of 3.6 nm by TEM. The authors demonstrate 1000 TTO for anisole hydrogenation in 47 h. Some *cis/trans* selectivity is observed for the hydrogenation of multiply-substituted arenes. No hydrogenolysis products are seen.	165
15	Albach, R.-W. Jautelat, M. (1999)	In this patent nanoclusters are synthesized from a number of different precursors [$RuCl_3$, $RhCl_3$, $PdCl_2$, $NiBr_2$, $Pd(OAc)_2$]. The sulfobetaine 3-(dodecyldimethylammonium)propanesulfonate was used as a nanocluster stabilizer. Substrates include isopropylbenzene and benzene. The reaction conditions include 50–180°C and 10–400 atm H_2; the reaction solutions are biphasic (aqueous/organic).	The authors appear to demonstrate 200 TTO for the hydrogenation of benzene and isopropyl benzene.	12
16	Schulz, J. Roucoux, A. Patin, H. (2000)	This is the follow-up full paper to these authors' 1999 *Chem. Commun.* paper (see entry 14 in this table). The nanoclusters are synthesized by reducing $RhCl_3 \bullet 3H_2O$ with $NaBH_4$ in dilute aqueous solutions of the hydroxyalkylammonium salts. Various mono- and di-substituted arenes are hydrogenated including benzene, toluene, anisole and xylene. The conditions include 20°C and 1 atm H_2; the reaction solutions are biphasic (aqueous/organic).	The nanoclusters are 2–2.5 nm in diameter by TEM. The metal particle nature of the catalyst is confirmed with a Hg(0) poisoning experiment. No hydrogenolysis products are formed. The activity of the nanocluster catalyst for anisole hydrogenation is compared with the activity of Hirai's polymer-stabilized Rh nanoclusters and with 5% Rh/C, all under identical conditions. The authors observe a TOF of 20 h^{-1} for Rh/C, of 47 h^{-1} for the PVP stabilized nanoclusters, and of 60 h^{-1} for the nanoclusters. The Rh nanoclusters give 2000 TTO for anisole hydrogenation in 37 h. The maximum TOF for the same experiment is 188 mol H_2/(mol Rh • hour). *Cis/trans* selectivities up to 99:1 are observed for the hydrogenation of di-substituted benzenes.	166

17	Bonilla, R. J. Jessop, P. G. James, B. R. (2000)	$[RhCl(1,5\text{-}COD)]_2$ is the nanocluster precursor and tetrabutylammonium hydrogen sulfate is the surfactant and nanocluster stabilizer. Several arenes are used as substrates, including lignin model compounds, anisole, phenol and p-xylene. The reaction conditions include 36°C and 10 atm H_2. The reactions are performed in a biphasic aqueous/supercritical ethane reaction medium.	The authors demonstrate as many as 110 TTO in 62 h for the hydrogenation of benzyl alcohol. Some *cis/trans* selectivity is observed for the hydrogenation of multiply-substituted arenes. The nanoclusters are not characterized.	167
18	Widegren, J. A. Finke, R. G.	The nanocluster catalyst is formed in situ by reducing $[Bu_4N]_5Na_3[(1,5\text{-}COD)Rh{\bullet}P_2W_{15}Nb_3O_{62}]$ with H_2 in a monophasic propylene carbonate solution, which gives polyoxoanion- and tetrabutylammonium-stabilized Rh(0) nanoclusters. Anisole is the only substrate. The reaction conditions include 22°C and 3.7 atm H_2; propylene carbonate is the solvent.	With 10 equivalents (vs Rh) of $HBF_4{\bullet}Et_2O$ added, the authors demonstrate 2600 TTO for anisole hydrogenation in 144 hours. The Rh(0) nanoclusters are shown by TEM to have an average diameter of between ~4–6 nm, depending on the nanocluster formation conditions. A combination of hydrogenation kinetics and the kinetics and stoichiometry of nanocluster formation provide excellent evidence that the nanoclusters are the true catalyst. These nanoclusters also display an unprecedented selectivity for the partial hydrogenation of anisole to 1-methoxycyclohexene, with initial selectivities of ~30% and overall yields up to 8%.	168

Additionally, there is often little to no compelling evidence that nanoclusters are indeed the active catalyst—recall the earlier discussion and Figure 2.2 concerning the problem of distinguishing homogeneous, single-metal-complex catalysts from soluble nanocluster catalysts. We recommend the following minimum criteria for any work that claims the use of nanoclusters for catalysis. First, there must be evidence that nanoclusters are present during catalysis; transmission electron microscopy (TEM) is the single most powerful technique for this purpose. Second, there must be kinetic evidence that the nanoclusters are the actual catalyst. If properly performed [43,140,150], poisoning studies can be used for this purpose (the underutilized fractional poisoning experiment described earlier[10] is particularly powerful). It is instructive to re-examine Table 2.1 with these criteria in mind. Only five [43,160,162,166,168] of the eighteen papers in Table 2.1 satisfy both criteria.

A final issue is the general lack of information regarding reproducibility for these nanocluster catalysts. Are reproducible results obtained from different laboratories on the same system? To date, only one of the nanocluster catalysts described herein has been studied by two different laboratories under the exact same conditions [43,144]. In that case the catalytic results were reproducible [43,144]. Nevertheless, more information about the repeatability of these nanocluster catalysts is needed.

2.2. Catalytic lifetime and activity of the nanocluster catalysts for the hydrogenation of monocyclic arenes

Practical catalytic applications as well as mechanistic studies of meaningful catalysts both require a reasonable catalyst lifetime. Table 2.1 documents that, to date,

most of the literature systems using soluble nanoclusters as arene hydrogenation catalysts have modest lifetimes at best, generally in the range of ≤100 TTO. Two nanocluster systems in Table 2.1 are exceptional in that they are capable of ≥2000 TTO. The first of these longer-lived nanocluster catalysts was developed by Roucoux and co-workers [165,166], Eq. 3, and the second was developed in our own labs [168], Eq. 4. These two catalyst systems are discussed in detail next.

The nanocluster catalyst developed by Roucoux and coworkers [165,166] is formed by the reduction of $RhCl_3 \cdot 3H_2O$ with $NaBH_4$ in an aqueous solution of N-alkyl-N-(2-hydroxyethyl)ammonium bromide. TEM shows the presence of nanoclusters with a diameter of 2–2.5 nm [166]. Adding a large excess of Hg(0) to a catalytically active solution after 50% conversion completely deactivates the catalyst [166], a single piece of good evidence that the Rh nanoclusters are the true catalyst [43]. Compelling kinetic or fractional poisoning evidence for nanocluster catalysis is not available, however, and would be of interest for this important catalyst. The arene hydrogenations were performed as biphasic (aqueous/organic) reactions simply by adding the substrate to an aqueous solution of the nanoclusters. The nanoclusters remain in the aqueous phase because of the water-solubility of the nanocluster stabilizing agent, N-alkyl-N-(2-hydroxyethyl)ammonium bromide; the organic substrate and products form the second phase in the reaction. Because of the biphasic reaction solution, the nanocluster catalyst can be separated from the reaction products by simple decantation. This experimental design is a possibly general way to overcome the problematic catalyst/product separation discussed earlier (Figure 2.1). Roucoux and coworkers demonstrate 2000 TTO for anisole (methoxybenzene) hydrogenation in 37 hours at 20°C and 1 atm H_2 [166], with a

reported selectivity to methoxycyclohexane of 100% (determined by GC analysis). Eq. 3. It is not stated if the catalyst is still active after 2000 TTO, although it appears that it probably is. For the lifetime experiment the average TOF is 54 mol anisole converted/(mol of Rh • h), the highest known TOF for monocyclic arene hydrogenation with a soluble nanocluster catalyst.

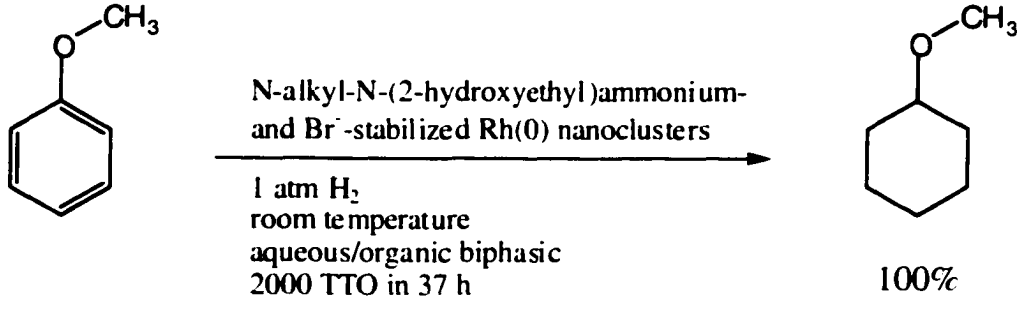

(3)

The other best soluble nanocluster arene hydrogenation catalyst in terms of catalytic lifetime was developed in our own labs [168]. Eq. 4. The nanocluster catalyst is formed in situ by reducing $[Bu_4N]_5Na_3[(1,5\text{-COD})Rh{\bullet}P_2W_{15}Nb_3O_{62}]$ with H_2 in a monophasic propylene carbonate solution. The resulting polyoxoanion- and tetrabutylammonium-stabilized Rh(0) nanoclusters are shown by TEM to have an average diameter between ~4–6 nm, depending on the nanocluster formation conditions [168]. A combination of TEM, hydrogenation kinetics, and the kinetics and stoichiometry of nanocluster formation provide compelling evidence that nanoclusters are the true catalyst.[12] Polyoxoanion- and tetrabutylammonium-stabilized Rh(0) nanoclusters

---

[12] Briefly, the evidence for nanocluster catalysis includes: (i) a quantitative curve fit of the precatalyst concentration vs time to the nucleation ($A \rightarrow B$, rate constant k_1) and autocatalytic surface-growth ($A + B \rightarrow 2B$, rate constant k_2) mechanism that is the *kinetic signature for nanocluster formation from a monometallic precatalyst ("A") when using H_2 as the reductant* [43]; (ii) direct confirmation of the

[130,171] were previously known to have a record catalytic lifetime in solution for olefin hydrogenation [130]. Consequently, it is not surprising that they also have a relatively long lifetime for arene hydrogenation in solution. With 10 equivalents (vs Rh) of $HBF_4 \bullet Et_2O$ added, 2600 TTO are demonstrated for anisole hydrogenation in 144 hours at 22°C and 3.7 atm of H_2 [168], which corresponds to an average TOF of 18 mol anisole converted/(mol of Rh · h). Although this anisole hydrogenation reaction went to completion (2600 TTO), preliminary experiments with larger amounts of substrate have failed to give more than this modest 2600 TTO [172].

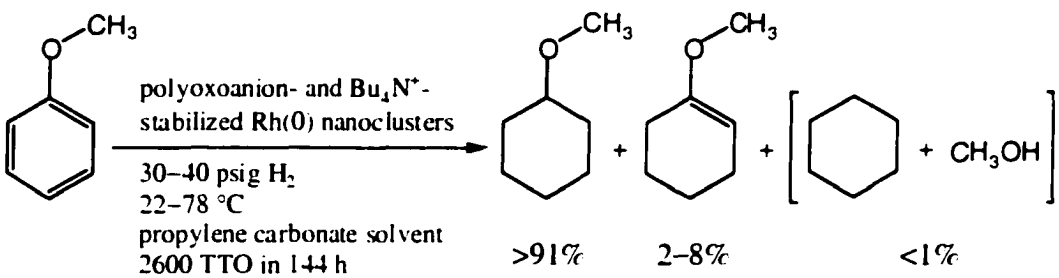

(4)

The development of soluble nanocluster catalysts with better lifetime and activity for arene hydrogenation remains an important goal. In this respect, state-of-the-art soluble nanocluster catalysts lag behind some types of supported catalysts. For example, Angelici and coworkers recently reported the use Rh complexes tethered to the SiO_2 of Pd/SiO_2 for the hydrogenation of anisole [173]. They demonstrate 14 500 TTO in 6 h *at 70°C and 4 atm of* H_2, which corresponds to an average TOF of 2400 mol anisole

---

expected stoichiometry of reduction of the precatalyst $[Bu_4N]_5Na_3[(1,5\text{-COD})Rh \bullet P_2W_{15}Nb_3O_{62}]$ with H_2 using GC analysis for cyclooctane formation and H_2 gas-uptake experiments; (iii) TEM confirmation that nanoclusters are indeed product "B" formed from the reduction of the precatalyst; (iv) the observation of induction periods that are identical within experimental error for the nanocluster formation reaction and the

converted/(mol of Rh • h). Although more forcing reaction conditions are used, the absolute performance of Angelici's catalyst is clearly better than the best soluble nanocluster catalysts known for the hydrogenation of anisole. A second example is Ahn and Marks' heterogeneous arene hydrogenation catalyst consisting of an organozirconium complex chemisorbed on sulfated zirconia [174]. They demonstrate an initial TOF of 970 mol benzene converted/(mol of Zr • h) at 25°C and 1 atm of H_2 (no TTO was reported for this catalyst). Even under these mild, directly comparable conditions, the activity of Ahn and Marks' catalyst is more than an order of magnitude better than the most active nanocluster catalyst.

2.3. Selectivity studies

Much of the effort in monocyclic arene hydrogenation with soluble nanocluster catalysts has been towards selective hydrogenation. Several types of selectivity have been studied: (i) the hydrogenation of arenes with two or more substituents on the benzene ring allows for selectivity to *cis* or *trans* diastereomers in the hydrogenated products; (ii) multi-substituted arenes can also contain prochiral carbons on the benzene ring, so enantioselective hydrogenation is possible; (iii) side reactions such as the hydrogenolysis of substituents can compete with the arene hydrogenation, so that there is a selectivity issue there; and (iv) selectivity for the partial hydrogenation of arenes (to form cyclic olefins) is also possible. Each of these types of selectivity will be considered in the following sections.

---

arene hydrogenation reaction; and (v) catalytic arene hydrogenation activity long after the precatalyst.

2.3.1. Cis/trans *diastereomers*

The most widely studied type of selectivity in the hydrogenation of monocyclic arenes with soluble nanocluster catalysts is the selectivity for the formation of *cis* diastereomers in the hydrogenation of di- or multi-substituted benzenes (Table 2.1). Arenes hydrogenated with metal particles are known to favor formation of the thermodynamically less favorable all-*cis* diastereomer [162]. This selectivity is rationalized by a continuous coordination of the substrate to the catalyst during hydrogenation, leading to the addition of hydrogen to only one "face" of the arene [164]. The studies of nanocluster catalysis have typically used di-substituted benzenes such as 2-methylanisole or xylenes. Without exception, the all-*cis* diastereomer is the major product; *trans* diasteriomers, commonly observed as minor products, are formed when a partially hydrogenated intermediate dissociates from the catalyst surface and then re-associates with the opposite "face" before further hydrogenation [36].

Several nanocluster catalysts display high selectivity for the *cis* diastereomer, as the following examples demonstrate. Januszkiewicz and Alper obtained *cis*-4-methylcyclohexyl methyl ether as the only product (in 92% yield) from the hydrogenation of 4-methylanisole [158], Eq. 5. Lemaire and co-workers found that the *cis* diastereomer was formed with selectivities of >97% for the hydrogenation of 2-methylanisole [14], Eq. 6. James and co-workers found that the all-*cis* diastereomer was formed exclusively in the hydrogenation of 2,6-dimethoxy-4-proplyphenol [164], Eq. 7. Roucoux and co-workers observed a *cis*/*trans* ratio of 99:1 in the hydrogenation of *m*-

---

$[Bu_4N]_6Na_3[(1,5\text{-}COD)Rh{\bullet}P_2W_{15}Nb_3O_{62}]$, has been completely consumed by reduction.

cresol [166], Eq. 9. Note that the lack of a mirror plane in the reactants of Eq. 6 and Eq. 8 leads to the formation of both enantiomers of the *cis* diastereomer.

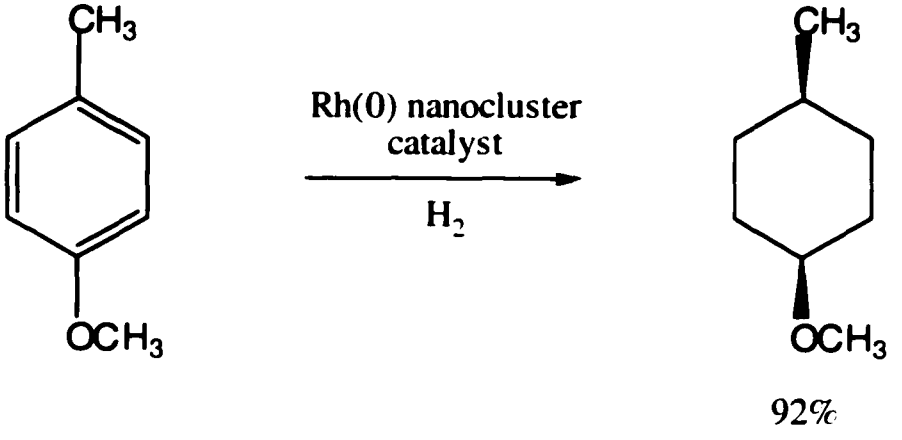

(5)

92%

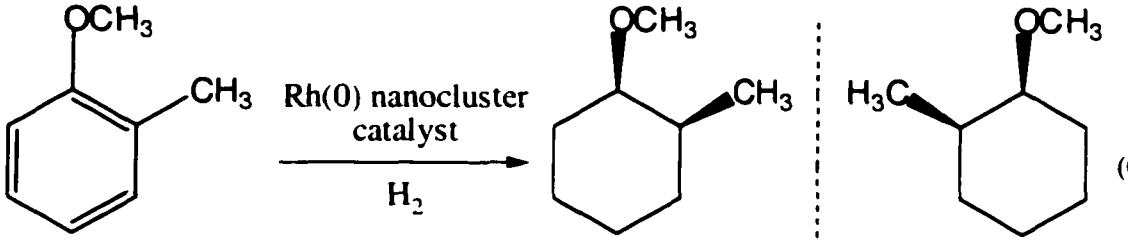

(6)

>97%

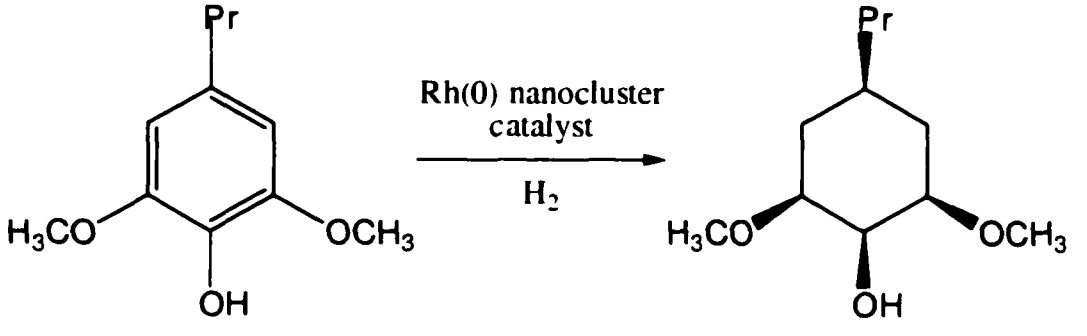

(7)

~100%

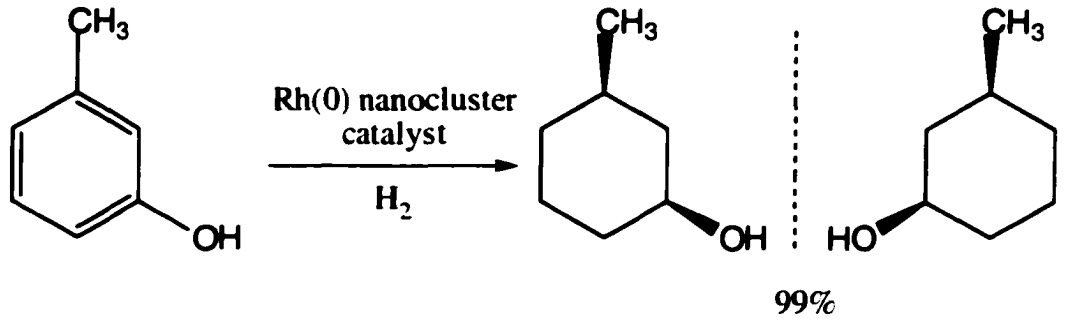

(8)

Traditional heterogeneous metal particle catalysts are also known to favor the formation of the *cis* diastereomer [162,175]. Using heterogeneous catalysts it was found that the ratio of *cis* to *trans* diastereomers was affected by: (i) the identity of the metal; (ii) the nature and position of the substituents; and (iii) the reaction temperature (lower temperatures favored the *cis* diastereomer) [162,175]. It is not clear if all the same trends will hold for soluble nanocluster catalysts. It is also not clear how the selectivities of the traditional heterogeneous metal particle catalysts compare to the selectivities of soluble nanocluster catalysts. Although three of the studies using nanocluster catalysts also use heterogeneous catalysts, either the reaction conditions are different for the two kinds of catalysts [162], or no selectivities are reported for the heterogeneous catalysts [13,166]; hence, more comparisons of selectivity between the same metal nanocluster and supported metal heterogeneous catalysts, under otherwise identical conditions, would be useful. Overall, the high diastereoselectivities commonly observed for nanocluster arene hydrogenation catalysts makes them promising as a way to produce the kinetically controlled *cis* isomers of a variety of cyclohexanes in smaller scale, fine chemical applications.

2.3.2. Enantioselectivity

The enantioselective hydrogenation of arenes with soluble nanoclusters has apparently only been attempted once [14].[13] In that study *o*-cresol derivatives were enantioselectively reduced using Rh(0) nanoclusters. Enantioselectivity was induced either by covalently binding a chiral auxiliary, menthoxyacetic acid, to the substrate or by using a chiral amine, R-(−)-dioctylcyclohexyl-1-ethylamine, as the nanocluster stabilizer. When the chiral auxiliary was added, a very modest enantiomeric excess of 10% was observed. Smaller enantiomeric excesses were observed in experiments using the chiral amine stabilizer. Obviously, these enantiomeric excesses are too small for useful preparative chemistry. However, future work in this area will very likely yield better nanocluster asymmetric arene hydrogenation catalysts, an interesting topic for further research and perhaps one of the best opportunities for fine chemical synthesis from nanocluster catalyzed arene hydrogenation.

2.3.3. Hydrogenolysis vs hydrogenation

Hydrogenolysis is commonly observed as a side reaction in the hydrogenation of some types of substituted arenes (aryl ethers, for example). Generally, hydrogenolysis is slow compared to the hydrogenation reaction. There is, however, one noteworthy exception to this rule in the literature of arene hydrogenation with soluble nanoclusters. For the hydrogenation of dibenzo-18-crown-6 ether with Rh(0) nanoclusters, Lemaire and co-workers found that under certain conditions the main product is a hydrogenolysis

---

[13] In a related case, bovine serum albumin was used as an additive in an attempt to induce chirality in the hydrogenation of acetophenone [158]. Unfortunately, the hydrogenation afforded only racemic products.

product [162]. Eq. 9. The uses or value of such compounds were not stated or studied, however [162].

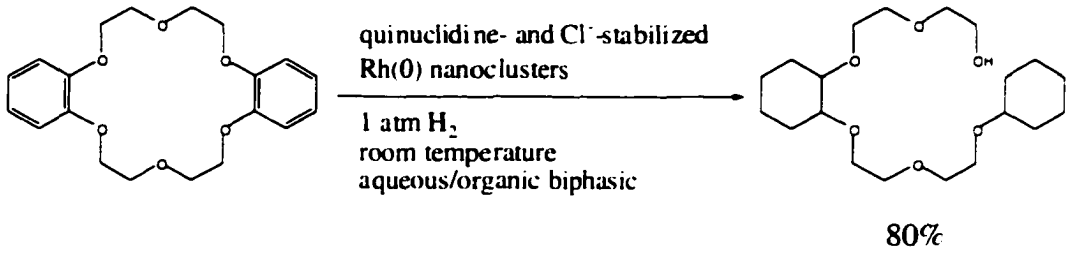

(9)

2.3.4. Partial hydrogenation

As mentioned in the introduction, the partial hydrogenation of monocyclic arenes is an important goal in arene hydrogenation [3,18,19]. Unfortunately, the valuable partial hydrogenation products are rarely observed when using soluble nanocluster catalysts. There are only two reports in the literature of soluble nanocluster catalysts that yield observable amounts of partial hydrogenation products [144,168]. In the first report [144] Blum and coworkers simply note that cyclohexene derivatives are observed only when very sterically hindered substrates like durene (1,2,4,5-tetramethylbenzene) are hydrogenated—sterically bulky substrates dissociate more readily from the catalyst surface and, therefore, favor partial hydrogenation. Recall that the true arene hydrogenation catalyst in this system was later found to be a nanocluster catalyst [43]. In the other available report, the partial hydrogenation of anisole was observed when polyoxoanion- and tetrabutylammonium-stabilized Rh(0) nanoclusters were used as the catalyst [168], an unprecedented selectivity among known soluble nanocluster catalysts

[176].[14] The partial hydrogenation product, 1-methoxycyclohexene, was formed with an initial selectivity of ~30% and overall yields up to 8% [168]. Although the selectivity and yield are modest, this system is of interest as a model for the study of the many important variables that increase selectivity to the monoene in the partial hydrogenation of monocyclic arenes with heterogeneous catalysts (e.g., higher temperatures, added H_2O or glycol solvents, added salts, H_2 mass-transfer (i.e., H_2-starved) conditions, or pH [3,18,19]). Temperature is an especially important variable, with a ~70% selectivity for benzene to cyclohexene being observed at 200°C vs a ~5% selectivity at 50°C when using a heterogeneous Ru catalyst [19]. Hence, the development of high-temperature stable nanocluster arene hydrogenation catalysts for monoene production is another important goal, as is further study of polyoxoanion and other ligand-modified nanoclusters as high selectivity catalysts.[14]

3. Summary and future outlook

The major findings of this review of arene hydrogenation with soluble nanocluster catalysts are: (i) soluble nanocluster catalysts have been identified as the true catalysts in

---

[14] Of course, it is possible that other researchers using soluble nanocluster catalysts for arene hydrogenation simply missed the alkene intermediate because of low yields or the eventual complete hydrogenation to alkane. However, some researchers specifically mention that no partial hydrogenation intermediates are observed [163,166]. For example, Roucoux and co-workers state, "Unfortunately, we did not observe any cyclohexene or cyclohexadiene derivatives as intermediates which ideally would have been desirable" [166]. Additionally, many of the reports in this area include careful product studies and most of the reports mention GLC as a means of product quantitation. Therefore, it seems likely that, among known soluble nanocluster catalysts, the polyoxoanion- and tetrabutylammonium-stabilized Rh(0) nanoclusters display a unique selectivity for the partial hydrogenation of arenes. The reason for this unique selectivity is not completely clear, but the available evidence suggests that the polyoxoanion stabilizer is involved [168]. In this regard, a recent report describes the use of a $Pd(0)_n$/C catalyst, prepared from the precursor $K_5PPd(H_2O)W_{11}O_{39}\cdot 12H_2O$, for the selective hydrogenation of arenes in the presence of distal ketone moieties; the $PW_{11}O_{39}^{7-}$ polyoxoanion is implicated as the key to the selectivity in that case as well [176].

several putatively "homogeneous" arene hydrogenation systems, suggesting that they are considerably more common than realized at present; (ii) with only a few exceptions [43,160,162,166,168], nanocluster catalysts used for arene hydrogenation are poorly characterized; (iii) Rh and Ru are used almost exclusively as the active metals; (iv) it would be of interest, however, to study in more detail nanoclusters composed of Pd [173,177], Pt [25,178], Ni [179,180] as well as bimetallics [181,182] for arene hydrogenation; and (v) soluble nanocluster catalysts for arene hydrogenation have modest activity and lifetime, with current records being an activity of 54 mol product/(mol metal · h) [166] and a lifetime of 2600 TTO [168]. Other major findings are: (vi) two catalyst systems, one developed by Roucoux and coworkers and one developed in our group, stand out from the rest in terms of activity and lifetime (the values cited just above); and (vii) much attention has been given to selective arene hydrogenation, especially for the synthesis of the all-*cis* diastereomer of substituted cyclohexanes, where selectivities of >90% are often observed [13,14,28,45,158,163,164,165,166], so that the application of nanocluster catalysts to produce all-*cis* substituted cyclohexanes is a promising area of future research and, perhaps, fine chemical synthesis.

Reasonable lifetime, activity and good selectivity have all been demonstrated for the hydrogenation of monocyclic arenes, so that additional studies of soluble nanocluster catalysts, leading to further improvements in arene hydrogenation, are warranted:

- Further examination of the many claimed "homogeneous" arene hydrogenation catalysts is of interest, since it is likely that many of these catalysts are soluble nanoclusters.

• *Development of nanoclusters that will withstand more forcing conditions (e.g., higher temperatures and pressures) is a key goal, one important not only to arene hydrogenation, but also to nanocluster catalysis in general.*

• Synthesis of the all-*cis* diastereomer of substituted cyclohexanes is probably the most promising practical application for nanocluster catalysts that has been demonstrated to date, an area that warrants further study as noted above.

• Nanocluster catalysis of enantioselective hydrogenations of substituted arenes is an interesting, but largely unexplored, area.

• The study of partial arene hydrogenation with nanocluster catalysts is an intriguing line of future inquiry.

• The hydrogenation of aromatic polymers with nanocluster catalysts is little studied, yet deserves a careful investigation with one or two prototype systems and in comparison to supported catalysts of the same metal(s).

• More information is needed regarding the repeatability of nanocluster catalyzed arene hydrogenations when the exact same system is used in different laboratories; the examination of supported heterogeneous catalysts of the same metal should also be part of these studies.

• Studies of the kinetics and mechanism of nanocluster arene hydrogenation reactions by powerful solution-phase spectroscopic techniques and homogeneous kinetic studies are needed and should provide insights to help optimize these reactions.

• The use of polyoxoanion and other ligands to change and improve the selectivity of nanocluster catalysts [85,168,176] is quite promising and, therefore, deserves further study.

• Methods to immobilize soluble arene hydrogenation catalysts hold promise [121,122,123,124,125,126], for example taking advantage of two-phase, aqueous/organic or organic/ionic liquid [127,128] systems in synthetically driven studies.

• The direct comparison of the arene hydrogenation selectivity of soluble nanocluster catalysts to their same-metal heterogeneous (supported) analogs under identical reaction conditions is rarely done [168], but is, of course, essential if one is to understand the strengths and weaknesses of nanocluster catalysts in comparison to their heterogeneous counterparts.

• The use of nanocluster catalysts in systems with confined spaces (such as inside mesoporous solids) is a conceivable application that takes advantage of the solubility and small size of the nanoclusters. In this regard, it would be especially interesting to make small, narrow size-distribution, clean-surface $Pt(0)_n$ nanoclusters for placement within Dow's ultra-wide-pore silica, and test them as polystyrene hydrogenation catalysts [25].

In short, nanocluster arene hydrogenation research is an area still wide open for additional, creative developments and practical applications.

Acknowledgments

Financial support was provided by the Department of Energy, Chemical Sciences Division, Office of Basic Energy, grant DOE FG06-089ER13998.

References

[1] P. Sabatier, Ind. Eng. Chem. 18 (1926) 1004.

[2] P. Sabatier, J.-B. Senderens, C. R. Hebd. Seances Acad. Sci. 132 (1901) 210.

[3] S.-C. Hu, Y.-W. Chen, J. Chin. Inst. Chem. Eng. 29 (1998) 387.

[4] I.P. Rothwell, Chem. Commun. (1997) 1331.

[5] W.D. Harman, Chem. Rev. 97 (1997) 1953.

[6] A. Stanislaus, B.H. Cooper, Catal. Rev. - Sci. Eng. 36 (1994) 75.

[7] M. Bennett, Chemtech 10 (1980) 444.

[8] E.L. Muetterties, J.R. Bleeke, Acc. Chem. Res. 12 (1979) 324.

[9] P.M. Maitlis, Acc. Chem. Res. 11 (1978) 301.

[10] R.B. Moyes, P.B. Wells, Advan. Catal. 23 (1973) 121.

[11] J.L. Garnett, Catal. Rev. 5 (1971) 229.

[12] R.-W. Albach, M. Jautelat, Two-phase hydrogenation method and colloidal catalysts for the preparation of cyclohexanes from benzenes, Bayer A.-G., German patent, DE 19807995, 1999.

[13] F. Fache, S. Lehuede, M. Lemaire, Tetrahedron Lett. 36 (1995) 885.

[14] K. Nasar, F. Fache, M. Lemaire, J.C. Beziat, M. Besson, P. Gallezot, J. Mol. Catal. 87 (1994) 107.

[15] P.N. Rylander, Catalytic Hydrogenation in Organic Synthesis, Academic Press, New York, 1979.

[16] K. Weissermel, H.-J. Arpe, Industrial Organic Chemistry, VCH, New York, 1993.

[17] G.W. Parshall, S.D. Ittel, Homogeneous Catalysis, 2nd Edition, The Applications and Chemistry of Catalysis by Soluble Transition Metal Complexes, Wiley, New York, 1992.

[18] J. Struijk, R. Moene, T. Van der Kamp, J.J.F. Scholten, Appl. Catal., A 89 (1992) 77.

[19] J. Struijk, M. D'Angremond, W.J.M. Lucas-De Regt, J.J.F. Scholten, Appl. Catal., A 83 (1992) 263.

[20] H. Arnold, F. Döbert, J. Gaube, in: G. Ertl, H. Knözinger, J. Weitkamp (Eds.), Handbook of Heterogeneous Catalysis, Vol. 5, VCH, Weinheim, 1997, pp. 2181–2182.

[21] A more efficient route for making cyclohexanol, Chem. Eng. 97 (1990) 25.

[22] T. Enya, H. Suzuki, T. Watanabe, T. Hirayama, Y. Hisamatsu, Environ. Sci. Technol. 31 (1997) 2772.

[23] A.M. Casillas, T. Hiura, N. Li, A.E. Nel, Ann. Allergy, Asthma, Immunol. 83 (1999) 624.

[24] A.E. Nel, D. Diaz-Sanchez, D. Ng, T. Hiura, A. Saxon, J. Allergy Clin. Immunol. 102 (1998) 539.

[25] D.A. Hucul, S.F. Hahn, Adv. Mater. 12 (2000) 1855.

[26] A. Tullo, "New DVDs Provide Opportunities for Polymers", Chemical and Engineering News 77 (1999) 14.

[27] T.Q. Hu, B.R. James, C.-L. Lee, J. Pulp Pap. Sci. 23 (1997) J200.

[28] T.Q. Hu, B.R. James, C.-L. Lee, J. Pulp Pap. Sci. 23 (1997) J153.

[29] T.Q. Hu, B.R. James, Y. Wang, J. Pulp Pap. Sci. 25 (1999) 312.

[30] T.Q. Hu, B.R. James, J. Pulp Pap. Sci. 26 (2000) 173.

[31] J. March, Advanced Organic Chemistry: Reactions, Mechanisms, and Structure, 4th edition, Wiley-Interscience, New York, 1992, pp. 780.

[32] D.E. Linn, Jr., J. Halpern, J. Am. Chem. Soc. 109 (1987) 2969.

[33] C.R. Landis, J. Halpern, Organometallics 2 (1983) 840.

[34] R. Wilczynski, W.A. Fordyce, J. Halpern, J. Am. Chem. Soc. 105 (1983) 2066.

[35] R.J. Fessenden, J.S. Fessenden, Organic Chemistry, 5th edition, Chap. 11, Brooks/Cole Publishing Company, Pacific Grove, 1993.

[36] R.L. Augustine, Heterogeneous Catalysis for the Synthetic Chemist, Chap. 17, Marcel Dekker, New York, 1996.

[37] H. Greenfield, Ann. N. Y. Acad. Sci. 214 (1973) 233.

[38] A.N. Startsev, G.I. Aleshina, D.G. Aksenov, V.N. Rodin, Kinet. Catal. 39 (1998) 363.

[39] A.N. Startsev, I.I. Zakharov, V.N. Rodin, G.I. Aleshina, D.G. Aksenov, Kinet. Catal. 39 (1998) 507.

[40] A.N. Startsev, V.N. Rodin, G.I. Aleshina, D.G. Aksenov, Kinet. Catal. 39 (1998) 221.

[41] B.C. Gates, Catalytic Chemistry, Chap. 6, John Wiley & Sons, New York, 1992.

[42] J.P. Collman, L.S. Hegedus, J.R. Norton, R.G. Finke, Principles and Applications of Organotransition Metal Chemistry, Chap. 10, University Science Books, Mill Valley, 1987.

[43] K.S. Weddle, J.D. Aiken, III, R.G. Finke, J. Am. Chem. Soc. 120 (1998) 5653.

[44] J.P. Collman, K.M. Kosydar, M. Bressan, W. Lamanna, T. Garrett, J. Am. Chem. Soc. 106 (1984) 2569.

[45] B.R. James, Y. Wang, C.S. Alexander, T.Q. Hu, Chem. Ind. 75 (1998) 233.

[46] R.G. Finke, in: D.L. Feldheim, C.A. Foss, Jr. (Eds.), Metal Nanoparticles: Synthesis, Characterization, and Applications, Chap. 2, Marcel Dekker, Inc., New York, 2001.

[47] R.J. Puddephatt, Met. Clusters Chem. 2 (1999) 605.

[48] J.D. Aiken, III, R.G. Finke, J. Mol. Catal. A: Chem. 145 (1999) 1.

[49] J.D. Aiken, III, Y. Lin, R.G. Finke, J. Mol. Catal. A: Chem. 114 (1996) 29.

[50] G. Schmid, M. Baumle, M. Geerkens, I. Heim, C. Osemann, T. Sawitowski, Chem. Soc. Rev. 28 (1999) 179.

[51] M.N. Vargaftik, N.Y. Kozitsyna, N.V. Cherkashina, R.I. Rudyi, D.I. Kochubei, B.N. Novgorodov, I.I. Moiseev, Kinet. Catal. 39 (1998) 740.

[52] N. Herron, D.L. Thorn, Adv. Mater. 10 (1998) 1173.

[53] J.S. Bradley, Schr. Forschungszent. Juelich, Mater. Mater. 1 (1998) D6.1.

[54] H. Bönnemann, W. Brijoux, A.S. Tilling, K. Siepen, Top. Catal. 4 (1998) 217.

[55] H. Bönnemann, W. Brijoux, Adv. Catal. Nanostruct. Mater. (1996) 165.

[56] H. Bönnemann, G. Braun, G.B. Brijoux, R. Brinkman, A.S. Tilling, K. Seevogel, K. Siepen, J. Organomet. Chem. 520 (1996) 143.

[57] G. Schmid, V. Maihack, F. Lantermann, S. Peschel, J. Chem. Soc., Dalton Trans. (1996) 589.

[58] J.S. Bradley, in: G. Schmid (Ed.), Clusters and Colloids: From Theory to Applications, VCH Publishers, New York, 1994, p. 459-544.

[59] L.N. Lewis, Chem. Rev. 93 (1993) 2693.

[60] G. Schmid, Chem. Rev. 92 (1992) 1709.

[61] G. Schmid, Endeavour 14 (1990) 172.

[62] R. Pool, Clusters: strange morsels of matter, Science 248 (1990) 1186.

[63] I. Willner, D. Mandler, J. Am. Chem. Soc. 111 (1989) 1330.

[64] K.S. Suslick, G.J. Price, Annu. Rev. Mater. Sci. 29 (1999) 295.

[65] T. Fujimoto, Y. Mizukoshi, Y. Nagata, Y. Maeda, R. Oshima, Scr. Mater. 44 (2001) 2183.

[66] E. Tagaki, Y. Mizukoshi, R. Oshima, Y. Nagata, H. Bandow, Y. Maeda, Stud. Surf. Sci. Catal. 132 (2001) 335.

[67] Y. Mizukoshi, E. Takagi, H. Okuno, R. Oshima, Y. Maeda, Y. Nagata, Ultrason. Sonochem. 8 (2001) 1.

[68] R.A. Caruso, M. Ashokkumar, F. Grieser, Colloids and Surfaces, A 169 (2000) 219.

[69] T. Fujimoto, S. Terauchi, H. Umehara, I. Kojima, W. Henderson, Chem. Mater. 13 (2001) 1057.

[70] J.P. Wilcoxon, J.E. Martin, P. Provencio, Langmuir 16 (2000) 9912.

[71] J.P. Wilcoxon, G.A. Samara, P.N. Provencio, Phys. Rev. B: Condens. Matter Mater. Phys. 60 (1999) 2704.

[72] J.G.C. Veinot, J. Galloro, L. Pugliese, R. Pestrin, W.J. Pietro, Chem. Mater. 11 (1999) 642.

[73] J.P. Wilcoxon, S.A. Craft, Nanostruct. Mater. 9 (1997) 85.

[74] T. Siebrands, M. Giersig, P. Mulvaney, C.-H. Fischer, Langmuir 9 (1993) 2297.

[75] D.F. Shriver, P. Atkins, C.H. Langford, Inorganic Chemistry, 2nd Edition, W. H. Freeman and Company, New York, 1994, p. 317.

[76] R.J. Hunter, Foundations of Colloid Science, Vol. 1, Oxford Univ. Press, New York, 1986.

[77] C.S. Hirtzel, R. Rajagopalan, Colloidal Phenomena: Advanced Topics, Noyes Publications, Park Ridge, N. J., 1985.

[78] A.J. Bard, L.R. Faulkner, Electrochemical Methods: Fundamentals and Applications, Wiley, New York, 1980.

[79] S. Özkar, R.G. Finke, "Nanocluster Formation and Stabilization Fundamental Studies: Ranking Commonly Employed Anionic Stabilizers via the Development, Then Application, of Five Comparative Criteria", in press.

[80] H. Liu, N. Toshima, J. Chem. Soc., Chem. Commun. (1992) 1095.

[81] A.C. Templeton, W.P. Wuelfing, R.W. Murray, Acc. Chem. Res. 33 (2000) 27.

[82] D.I. Gittins, F. Caruso, Angew. Chem. Int. Ed. 40 (2001) 3001.

[83] D. de Caro, J.S. Bradley, New J. Chem. 22 (1998) 1267.

[84] R.G. Finke, unpublished observations.

[85] G. Schmid, V. Maihack, F. Lantermann, S. Peschel, J. Chem. Soc., Dalton Trans. (1996) 589.

[86] J.J. van der Klink, H.B. Brom, Prog. Nucl. Magn. Reson. Spectrosc. 36 (2000) 89.

[87] K. Kimura, Mesosc. Mater. Clusters (1999) 153.

[88] J.S. Bradley, J.M. Millar, E.W. Hill, J. Am. Chem. Soc. 113 (1991) 4016.

[89] G. Schmid, Struct. Bonding 62 (1985) 51.

[90] J.P. Yesinowski, J. Am. Chem. Soc. 103 (1981) 6266.

[91] D. de Caro, J.S. Bradley, Langmuir 14 (1998) 245.

[92] D. de Caro, J.S. Bradley, Langmuir 13 (1997) 3067.

[93] A. Rodriguez, C. Amiens, B. Chaudret, M.-J. Casanove, P. Lecante, J.S. Bradley, Chem. Mater. 8 (1996) 1978.

[94] J.S. Bradley, E.W. Hill, B. Chaudret, A. Duteil, Langmuir 11 (1995) 693.

[95] C. Amiens, D. de Caro, B. Chaudret, J.S. Bradley, R. Mazel, C. Roucau, J. Am. Chem. Soc. 115 (1993) 11638.

[96] J.S. Bradley, J.M. Millar, E.W. Hill, S. Behal, J. Catal. 129 (1991) 530.

[97] M.A. Watzky, R.G. Finke, J. Am. Chem. Soc. 119 (1997) 10382.

[98] B.C. Gates, Catalytic Chemistry, Wiley, New York, 1992, pp. 396-403.

[99] J.P. Wilcoxon, R.L. Williamson, R. Baughman, J. Chem. Phys. 98 (1993) 9933.

[100] M.T. Reetz, R. Breinbauer, P. Wedemann, P. Binger, Tetrahedron 54 (1998) 1233.

[101] M.T. Reetz, E. Westermann, Angew. Chem., Int. Ed. 39 (2000) 165.

[102] J. Le Bars, U. Specht, J.S. Bradley, D.G. Blackmond, Langmuir 15 (1999) 7621.

[103] S. Klingelhöfer, W. Heitz, A. Greiner, S. Oestreich, S. Förster, M. Antonietti, J. Am. Chem. Soc. 119 (1997) 10116.

[104] M.T. Reetz, G. Lohmer, Chem. Commun. (1996) 1921.

[105] M.T. Reetz, R. Breinbauer, K. Wanninger, Tetrahedron Lett. 37 (1996) 4499.

[106] M. Beller, H. Fischer, K. Kühlein, C.-P. Reisinger, W.A. Herrmann, J. Organomet. Chem. 520 (1996) 257.

[107] M. Brust, M. Walker, D. Bethell, D.J. Schiffrin, R. Whyman, J. Chem. Soc., Chem. Commun. (1994) 801.

[108] A.C. Templeton, M.J. Hostetler, E.K. Warmoth, S. Chen, C.M. Hartshorn, V.J. Krishnamurthy, M.D.E. Forbes, R.W. Murray, J. Am. Chem. Soc. 120 (1998) 4845.

[109] A.C. Templeton, M.J. Hostetler, C.T. Kraft, R.W. Murray, J. Am. Chem. Soc. 120 (1998) 1906.

[110] M. Bartz, J. Küther, R. Seshadri, W. Tremel, Angew. Chem., Int. Ed. 37 (1998), 2466.

[111] H. Li, Y.-Y. Luk, M. Mrksich, Langmuir, 15 (1999) 4957.

[112] Y. Wang, H. Liu, Y. Jiang, J. Chem. Soc., Chem. Commun. (1989) 1878.

[113] P. Mulvaney, L.M. Liz-Marzán, M. Giersig, T. Ung, J. Mater. Chem. 10 (2000) 1259.

[114] L.M. Liz-Marzán, P. Mulvaney, Recent Res. Dev. Phys. Chem. 2 (1998) 1.

[115] L.M. Liz-Marzán, P. Mulvaney, New J. Chem. 22 (1998) 1285.

[116] L.M. Liz-Marzán, M. Giersig, P. Mulvaney, Langmuir 12 (1996) 4329.

[117] L.M. Liz-Marzán, M. Giersig, P. Mulvaney, Chem. Commun. (1996) 731.

[118] T. Ung, L.M. Liz-Marzan, P. Mulvaney, Langmuir 14 (1998) 3740.

[119] M. Giersig, L.M. Liz-Marzan, T. Ung, D. Su, P. Mulvaney, Ber. Bunsen-Ges. 101 (1997) 1617.

[120] M. Giersig, T. Ung, L.M. Liz-Marzan, P. Mulvaney, Adv. Mater. 9 (1997) 570.

[121] I.T. Horvath, Aqueous-Phase Organomet. Catal. (1998) 548.

[122] I.T. Horvath, G. Kiss, R.A. Cook, J.E. Bond, P.A. Stevens, J. Rabai, E.J. Mozeleski, J. Am. Chem. Soc. 120 (1998) 3133.

[123] I.T. Horvath, J. Rabai, Science 266 (1994) 72.

[124] J.A. Gladysz, Science 266 (1994) 55.

[125] K.T. Wan, M.E. Davis, Nature 370 (1994) 449.

[126] J.P. Arhancet, M.E. Davis, J.S. Merola, B.E. Hanson, Nature 339 (1989) 454.

[127] P.J. Dyson, D.J. Ellis, D.G. Parker, T. Welton, Chem. Commun. (1999) 25.

[128] J. Dupont, G.S. Fonseca, A.P. Umpierre, P.F.P. Fichtner, S.R. Teixeira, J. Am. Chem. Soc. 124 (2002) 4228.

[129] R.G. Finke, K.R. Seddon, experiments in progress.

[130] J.D. Aiken, III, R.G. Finke, J. Am. Chem. Soc. 121 (1999) 8803.

[131] J.E. Hamlin, K. Hirai, A. Millan, P.M. Maitlis, J. Mol. Catal. 7 (1980) 543.

[132] G.M. Whitesides, M. Hackett, R.L. Brainard, J.P.P.M. Lavalleye, A.F. Sowinski, A.N. Izumi, S.S. Moore, D.W. Brown, E.M. Staudt, Organometallics 4 (1985) 1819.

[133] P. Foley, R. DiCosimo, G.M. Whitesides, J. Am. Chem. Soc. 102 (1980) 6713.

[134] D.R. Anton, R.H. Crabtree, Organometallics 2 (1983) 855.

[135] R.H. Crabtree, M.F. Mellea, J.M. Mihelcic, J.M. Quirk, J. Am. Chem. Soc. 104 (1982) 107.

[136] R.H. Crabtree, J.M. Mihelcic, J.M. Quirk, J. Am. Chem. Soc. 101 (1979) 7738.

[137] J.P. Collman, K.M. Kosydar, M. Bressan, W. Lamanna, T. Garrett, J. Am. Chem. Soc. 106 (1984) 2569.

[138] L.N. Lewis, N. Lewis, J. Am. Chem. Soc. 108 (1986) 7228.

[139] L.N. Lewis, J. Am. Chem. Soc. 112 (1990) 5998.

[140] Y. Lin, R.G. Finke, Inorg. Chem. 33 (1994) 4891.

[141] Y. Lin, Ph.D. Dissertation, Department of Chemistry, University of Oregon, March 1994.

[142] J. Halpern, Inorg. Chim. Acta 50 (1981) 11.

[143] J. Halpern, T. Okamoto, A. Zakhariev, J. Mol. Catal. 2 (1977) 65.

[144] J. Blum, I. Amer, K.P.C. Vollhardt, H. Schwarz, G. Hoehne, J. Org. Chem. 52 (1987) 2804.

[145] J. Blum, I. Amer, A. Zoran, Y. Sasson, Tetrahedron Lett. 24 (1983) 4139.

[146] P.M. Maitlis, Acc. Chem. Res. 11 (1978) 301.

[147] M.J. Russell, C. White, P.M. Maitlis, J. Chem. Soc., Chem. Commun. (1977) 427.

[148] M. Bennett, Chemtech 10 (1980) 444.

[149] M.A. Bennett, T.-N. Huang, T.W. Turney, J. Chem. Soc., Chem. Commun. (1979) 312.

[150] G.M. Whitesides, M. Hackett, R.L. Brainard, J.P.P.M. Lavalleye, A.F. Sowinski, A.N. Izumi, S.S. Moore, D.W. Brown, E.M. Staudt, Organometallics 4 (1985) 1819.

[151] J.P. Ennett, Ph.D. Dissertation, Department of Chemistry, Australian National University, 1984.

[152] M.A. Bennett, J.P. Ennett, Inorg. Chim. Acta 198-200 (1992) 583.

[153] D.A. Tocher, R.O. Gould, T.A. Stephenson, M.A. Bennett, J.P. Ennett, T.W. Matheson, L. Sawyer, V.K. Shah, J. Chem. Soc., Dalton Trans. (1983) 1571.

[154] J.A. Widegren, M.A. Bennett, R.G. Finke, experiments in progress.

[155] R.A. Sheldon, M. Wallau, I.W.C.E. Arends, U. Schuchardt, Acc. Chem. Res. 31 (1998) 485.

[156] I.W.C.E. Arends, R.A. Sheldon, Appl. Catal., A 212 (2001) 175.

[157] I.W. Davies, L. Matty, D.L. Hughes, P.J. Reider, J. Am. Chem. Soc. 123 (2001) 10139.

[158] K.R. Januszkiewicz, H. Alper, Organometallics 2 (1983) 1055.

[159] J. Foise, R. Kershaw, K. Dwight, A. Wold, Mater. Res. Bull. 20 (1985) 147.

[160] Z. Duan, M.J. Hampden-Smith, A.P. Sylwester, Chem. Mater. 4 (1992) 1146.

[161] P. Drognat Landré, M. Lemaire, D. Richard, P. Gallezot, J. Mol. Catal. 78 (1993) 257.

[162] P. Drognat Landré, D. Richard, M. Draye, P. Gallezot, M. Lemaire, J. Catal. 147 (1994) 214.

[163] B.R. James, Y. Wang, T.Q. Hu, Chem. Ind. 68 (1996) 423.

[164] T.Q. Hu, B.R. James, S.J. Rettig, C.-L. Lee, Can. J. Chem. 75 (1997) 1234.

[165] J. Schulz, A. Roucoux, H. Patin, Chem. Commun. (1999) 535.

[166] J. Schulz, A. Roucoux, H. Patin, Chem.--Eur. J. 6 (2000) 618.

[167] R.J. Bonilla, P.G. Jessop, B.R. James, Chem. Commun. (2000) 941.

[168] J.A. Widegren, R.G. Finke, Inorg. Chem. 41 (2002) 1558.

[169] K.R. Januszkiewicz, H. Alper, Can. J. Chem. 62 (1984) 1031.

[170] G.C. Bond, Catalysis by Metals, Academic Press, New York, 1962.

[171] J.D. Aiken, III, R.G. Finke, Chem. Mater. 11 (1999) 1035.

[172] J.A. Widegren, R.G. Finke, unpublished experiments.

[173] H. Yang, H. Gao, R.J. Angelici, Organometallics 19 (2000) 622.

[174] H. Ahn, T.J. Marks, J. Am. Chem. Soc. 120 (1998) 13533.

[175] M. Bartók, Stereochemistry of Heterogeneous Metal Catalysis, Wiley, New York, 1985.

[176] V. Kogan, Z. Aizenshtat, R. Neumann, New J. Chem. 26 (2002) 272.

[177] U.K. Singh, M.A. Vannice, AIChE J. 45 (1999) 1059.

[178] J. Wang, Q. Li, J. Yao, Appl. Catal., A 184 (1999) 181.

[179] D. Franquin, S. Monteverdi, S. Molina, M.M. Bettahar, Y. Fort, J. Mater. Sci. 34 (1999) 4481.

[180] R. Molina, G. Poncelet, J. Catal. 199 (2001) 162.

[181] R. Raja, S. Hermans, D.S. Shephard, B.F.G. Johnson, G. Sankar, S. Bromley, J.M. Thomas, Chem. Commun. (1999) 1571.

[182] R. Raja, G. Sankar, S. Hermans, D.S. Shephard, S. Bromley, J.M. Thomas, B.F.G. Johnson, T. Maschmeyer, Chem. Commun. (1999) 2131.

CHAPTER III

A REVIEW OF THE PROBLEM OF DISTINGUISHING TRUE HOMOGENEOUS CATALYSIS FROM SOLUBLE-METAL-PARTICLE HETEROGENEOUS CATALYSIS UNDER REDUCING CONDITIONS

This dissertation chapter discusses the important, but difficult, problem of determining the nature of the true catalyst. The methods reviewed in this chapter are used in Chapter VI to investigate an arene hydrogenation catalyst based on the monometallic precatalyst Ru(II)(η^6-C_6Me_6)$(OAc)_2$. This chapter also has some relevance to Chapter V, in which a soluble nanocluster catalyst is used for arene hydrogenation.

This chapter, which has been submitted to the *Journal of Molecular Catalysis A: Chemical*, was written by J.A.W. and then lightly edited by R.G.F. in two sessions (8 hours total).

A review of the problem of distinguishing true homogeneous catalysis from soluble-metal-particle heterogeneous catalysis under reducing conditions

Jason A. Widegren and Richard G. Finke

Abstract

This review considers cases in which a discrete transition-metal complex is used as a precatalyst for reductive catalysis: it focuses on the problem of determining if the true catalyst is a metal-complex homogeneous catalyst or if it is a soluble-metal-particle heterogeneous catalyst. The various experiments that have been used to distinguish homogeneous and heterogeneous catalysis are outlined and critiqued. A more general method for making this distinction is then discussed. Next, the circumstances that make heterogeneous catalysis probable, and the telltale signs that a heterogeneous catalyst has formed, are outlined. Finally, catalytic systems requiring further study to determine if they are homogeneous or heterogeneous are listed. The major findings of this review are: (i) the *in situ* reduction of transition-metal complexes to form soluble-metal-particle heterogeneous catalysts is common; (ii) the formation of such a catalyst is easy to miss

because colloidal solutions often appear homogeneous to the naked eye; (iii) a variety of experiments have been used to distinguish homogeneous catalysis from heterogeneous catalysis, but there is no single definitive experiment for making this distinction; (iv) experiments that provide kinetic information are more useful than experiments that do not; and (v) a general approach for distinguishing homogeneous catalysis from heterogeneous catalysis has been developed. Additionally, (vi) the conditions under which a heterogeneous catalyst is likely to form include: (a) when easily reduced transition-metal complexes are used as precatalysts; (b) when forcing reaction conditions are employed; (c) when nanocluster stabilizers are present; and (d) when monocyclic arene hydrogenation is observed. Finally, (vii) the telltale signs of heterogeneous catalysis include the formation of dark reaction solutions, metallic precipitates, and the observation of induction periods and sigmoidal kinetics.

1. Introduction

The use of transition-metal complexes for reductive catalysis is widespread. In general, the transition-metal complex added to the reaction is not the true catalyst. Rather, the added complex is a precursor, or precatalyst, from which the true catalyst forms *in situ* [1]. The true catalyst *can be colloidal metal that forms from the precatalyst under reducing conditions, as well as bulk metal in the form of a film or powder.* In fact, the literature indicates that *in situ* formation of such metal-particle heterogeneous catalysts is much more prevalent than currently appreciated. This fact is the primary motivation for writing this review.

Distinguishing metal-complex homogeneous catalysis from metal-particle heterogeneous catalysis is not trivial [1]; it is a task which has caused considerable consternation in the literature. This problem is most difficult when a colloidal/nanocluster catalyst is involved, partly because colloidal solutions often appear homogeneous to the eye. Additionally, nanoclusters/colloids can be as small as ~1 nm in diameter, which makes them difficult to detect by some methods (*vide infra*). The literature in this area dates back to about 1980 and includes contributions from Maitlis [2], Whitesides [3], Crabtree [4,5,6], Collman [1,7], Lewis [8,9] and our group [10,11].

Although clear and useful distinctions between "colloids" and "nanoclusters" can be made [12], we will use both words synonymously herein to refer to soluble metal particles [13,14,15,16,17,18,19]. Conventionally, the criterion of solubility was used to categorize "homogeneous" and "heterogeneous" catalysts; however, we will follow Schwartz's modern definitions for homogeneous and heterogeneous catalysis [20]. Specifically, heterogeneous catalysts have multiple types of active sites and homogeneous catalysts have a single type of active site. Therefore, soluble nanoclusters are typically "soluble heterogeneous catalysts".

This review considers cases in which a transition-metal complex is added as a precatalyst for reductive catalysis (primarily hydrogenation catalysis); it focuses on the problem of determining if the true catalyst is a metal-complex homogeneous catalyst or if it is a soluble-metal-particle heterogeneous catalyst. First, the various experiments that have been used to distinguish homogenous and heterogeneous catalysis will be outlined and critiqued. Then, a more general method for making this distinction will be discussed. Next, we discuss the circumstances that make heterogeneous catalysis probable, and the

telltale signs that a heterogeneous catalyst has formed. Finally, we list literature catalyst systems that require further study to determine if their true catalysts are homogeneous or heterogeneous (see Table 3.1 of the Appendix for detailed information about each of these catalyst systems).

2. Description of the various experiments used to distinguish true homogeneous catalysis from soluble-metal-particle catalysis

A variety of experiments have been used to distinguish homogeneous catalysis from heterogeneous catalysis. However, it must be emphasized that *there is no single definitive experiment for making this distinction.* The most convincing studies [4,8,10,21,22,23,24] use a combination of experiments before arriving at a compelling conclusion. Additionally, some experiments cannot be used with certain catalyst systems; therefore, it is important to be aware of the experimental "toolkit" available and to know the strengths and weaknesses of each experimental "tool". A perusal of these experiments illustrates a few important points: first, experiments that provide information about kinetics are generally more powerful than experiments that do not;[1] second, it is best if one can perform control experiments using authentic heterogeneous catalysts or authentic homogeneous catalysts [10]; and third, the detection of small, soluble, nanocluster catalysts by some of the experimental techniques below is problematic.

---

[1] Transmission electron microscopy (TEM) is an illustrative example. TEM does not provide any kinetic information and, therefore, cannot identify the nature of the true catalyst in any compelling way. In contrast, some of the other experiments described in this section, notably catalyst formation kinetic studies and the quantitative catalyst poisoning experiment with CS_2 (or other ligands), do provide kinetic information and, hence, do provide compelling evidence for the nature of the true catalyst.

2.1. Reaction kinetics

Because catalysis is a wholly kinetic phenomenon [25,26], the most compelling evidence for the identity of the true catalyst will always be kinetic in nature.[1] Three observables related to reaction kinetics will be discussed in terms of how they help distinguish homogeneous from heterogeneous catalysis: (i) kinetic reproducibility; (ii) the observation of sigmoidal kinetics for the catalytic reaction; and (iii) comparison of the kinetics of the catalytic reaction with the kinetics of precatalyst decomposition.

It has been suggested that one can distinguish homogeneous from heterogeneous catalysis by whether or not the kinetics are reproducible—that is, homogeneous catalysis exhibits reproducible kinetics and heterogeneous catalysis exhibits irreproducible kinetics [27,28].[2] However, the recent discovery of highly reproducible catalytic systems involving nanocluster catalysts shows that such a distinction is not absolute [10,29]. In short, the observation of irreproducible kinetics is consistent with the *in situ* formation of a heterogeneous catalyst, but reproducible kinetics cannot be used to rule out a heterogeneous catalyst since soluble heterogeneous catalysts with ±15% kinetic reproducibility are now known [10].

The observation of a sigmoidal kinetic curve for the hydrogenation of substrate is powerful *prima facie* evidence for the *in situ* formation of a heterogeneous catalyst [10,21,24,30,31,32,33,34,35]. Sigmoidal kinetics results from an apparently general[3]

---

[1] For example, consider the quote provided elsewhere [27]: "Note also that a true homogeneous catalyst usually demonstrates a notably better reproducibility in the values of reaction rate than a catalyst whose activity arises from its decomposition into a colloidal metal. This difference in reproducibility can also be used to distinguish between the two types of catalysis." As noted in the text, this statement is not true, having been disproved in 1994 [10].

[3] This mechanism for transition-metal nanocluster formation under H_2 has been observed for at least nine different nanocluster systems and three different transition metals (Ir [10,30,31,32,34,35], Rh [21,33] and

mechanism for the formation of metal particles from transition-metal salts under H_2 [30,31]. This mechanism involves a pseudoelementary [30,31,36,37,38] nanocluster nucleation step ($A \rightarrow B$, rate constant k_1) followed by a pseudoelementary autocatalytic surface-growth step ($A + B \rightarrow 2B$, rate constant k_2). (A pseudo-elementary step is just the sum of multiple elementary steps which, however, can be treated kinetically as an elementary step [30,31].) Such a kinetic scheme results in a *characteristic sigmoidal curve* for both the nanocluster formation reaction and the catalytic hydrogenation reaction. Figure 3.1 shows an example of these kinetics for the hydrogenation of cyclohexene by an $Ir(0)_{\sim 300}$ nanocluster that forms *in situ* from an Ir(I) precatalyst [10,30,31,32]. The experimental data in Figure 3.1 are closely fit by the kinetic scheme $A \rightarrow B$ (rate constant k_1) and $A + B \rightarrow 2B$ (rate constant k_2) [30,31]. Given the prior literature [10,21,24,30,31,32,33,34,35], *such a kinetic curve and curvefit are as compelling a single piece of evidence as exists for the formation of a heterogeneous catalyst*, at least for hydrogenation catalysis. Unfortunately, the absence of sigmoidal reaction kinetics does not rule out heterogeneous catalysis: in order for the sigmoidal kinetics to be obvious, k_1 must be relatively small and k_2 must be relatively large; this results in a long induction period followed by a rapid increase in catalytic activity, that is, a sigmoidal curve. Sigmoidal kinetics are not expected if formation of the heterogeneous catalyst is complete before a significant amount of the substrate has been hydrogenated (i.e., if catalyst formation is fast relative to catalysis, or if the precatalyst is pretreated with reductant in the absence of substrate). No induction period is observed in such a

---

Ru [24,31]). In addition, autocatalysis is a more general kinetic scheme for growth processes (see the

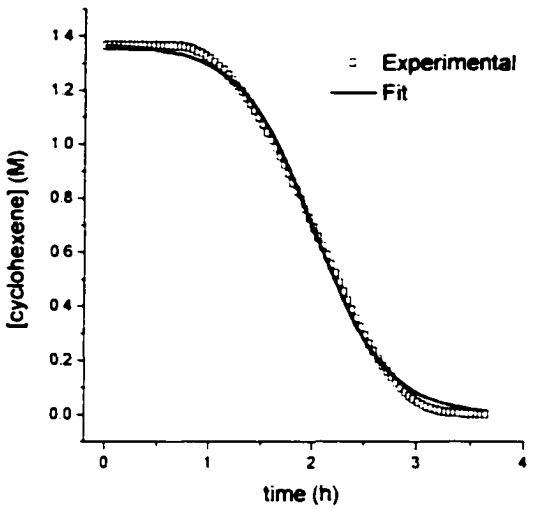

Figure 3.1. Typical cyclohexene concentration vs time curve for a cyclohexene hydrogenation reaction starting with the precatalyst $[Bu_4N]_5Na_3[(1,5\text{-}COD)Ir{\bullet}P_2W_{15}Nb_3O_{62}]$. Note the distinctive, sigmoidal, "autocatalytic" shape of the curve. The true catalyst in this system is a distribution of soluble $Ir(0)_{\sim 300}$ nanoclusters that forms *in situ* from the reduction of the Ir(I) precatalyst by H_2. The $Ir(0)_{\sim 300}$ nanoclusters form via a nucleation pseudoelementary [27] step ($A \rightarrow B$, rate constant k_1) followed by an autocatalytic surface-growth pseudoelementary step ($A + B \rightarrow 2B$, rate constant k_2). The kinetics of nanocluster formation is responsible for the observed sigmoidal kinetics of the cyclohexene hydrogenation reaction. In general, the observation of sigmoidal kinetics, at least for a catalytic hydrogenation reaction starting with a monometallic precatalyst, is *prima facie* evidence for the *in situ* formation of a metal-particle catalyst.

case. A second scenario obscuring sigmoidal kinetics is if the heterogeneous catalyst deactivates to a significant extent in comparison to its *in situ* rate of formation during the catalytic hydrogenation reaction. In this case, an induction period is still observed, but the reaction does not "turn on" in such a dramatic fashion due to the continual loss of activity.

---

references cited elsewhere [30]).

If one can show that the precatalyst is decomposing to form metal particles, then it is very useful to follow the kinetics of precatalyst decomposition [30,31,33,39,40,41]. If precatalyst decomposition and catalytic hydrogenation both occur with sigmoidal kinetics and identical induction periods, that is excellent *prima facie* evidence for a heterogeneous catalyst. In such a case it is also useful to show that catalytic activity is still observed after the precatalyst has been completely reduced to metal$(0)_n$.

Despite the central importance of reaction kinetics in determining the true nature of the catalyst (and for catalysis in general), the literature shows that it is quite common to ignore kinetics in catalytic studies. A common scenario involves introducing the precatalyst and substrate into a reactor, waiting for a given length of time, stopping the reaction, and analyzing the final reaction products. Clearly, the observation of an induction period or of sigmoidal kinetics is impossible in such an experiment. Furthermore, in cases where the catalytic reactions go to completion before any analysis, it is impossible to judge the kinetic reproducibility. Hence, it is crucial to follow the reaction progress vs time whenever possible.

2.2. Transmission electron microscopy (TEM)

Transmission electron microscopy is a sensitive technique for detecting the presence of nanoclusters deposited from reaction solutions [8,10]. A back-of-the-envelope calculation shows that TEM can detect nanoclusters in solutions where the concentration of colloidal metal is $\leq 10^{-12}$ M.[4] However, such sensitivity is potentially

---

[4] TEM samples are commonly prepared by simply depositing a drop of the reaction solution onto a carbon-coated TEM grid; the solvent evaporates, leaving the nanoclusters (and any other nonvolatile material) on the support film of the TEM grid. Let us assume that the drop size is 10 μL (which is reasonable, given the

deceiving since TEM does not provide evidence for the kinetic competence of the nanoclusters as catalysts. Put another way, TEM can show the presence of very low levels of nanocluster formation, but cannot show if the nanoclusters are responsible for the observed catalysis. Another problem with TEM is that small (<1 nm) nanoclusters and nanoclusters of lighter, first-row transition metals are difficult to image by TEM due to the inherently lower contrast of such species. Also, because of the nature of negative results, TEM cannot rule out the presence of a nanocluster catalyst—if nanoclusters are not seen by TEM, one cannot safely conclude that the catalyst is truly homogeneous. These limitations require that TEM be used in combination with other techniques in order to convincingly determine the nature of the true catalyst. However, if one understands its limitations, TEM is an excellent, if not first-choice, technique for scouting cases where a nanocluster catalyst is suspected. Upfront use of TEM is emphasized in a more general approach to distinguishing homogeneous vs heterogeneous catalysis [10].

2.3. Mercury poisoning

The ability of Hg(0) to poison metal-particle heterogeneous catalysts, by amalgamating the metal or adsorbing on the metal surface, has been known for >80 years [3,42] and is a widely used test [3,4,8,10,21,23,24,43,44,45]. This experiment is performed by adding Hg(0) to the reaction solution.[5,6] The suppression of catalysis by

---

size of normal TEM grids), that the drop contains 10 000 nanoclusters (which should be sufficient for finding and imaging the nanoclusters on the grid), and that the average nanocluster has 1000 metal atoms (which corresponds to a nanocluster with a diameter of a few nanometers). The concentration of colloidal metal in such a solution is 1.7×10^{-12} M.

[5] The Hg(0)-poisoning experiment is occasionally performed improperly. In one literature example a solution of precatalyst was stirred with Hg(0) for 1 h, the solution was filtered, and a catalytic hydrogenation reaction was then started [44]. The hydrogenation proceeded with the same catalytic activity as an experiment in which Hg(0) was never present, and this was used (erroneously) to rule out the

Hg(0) is evidence for a heterogeneous catalyst; if Hg(0) does not suppress catalysis, that is (negative) evidence for a homogeneous catalyst. The Hg(0)-poisoning experiment is easy to perform, *but is not definitive by itself and is not universally applicable.* Hg(0) can cause complicating side reactions [3] and is known to react with some single-metal complexes [3,23,46,47]. To avoid incomplete poisoning and erroneous conclusions, one must be able to ensure intimate contact of the Hg(0) bead with the entire reactor; hence, using a large excess of Hg(0) in a well stirred solution is key [10,21]. Hg(0) is probably most effective in poisoning metals that form an amalgam, such as Pt, Pd and Ni; metals that do not form amalgams with Hg(0), such as Ir, Rh and Ru are probably more difficult to poison with Hg(0) [3].[7] Hence, if the addition of Hg(0) to the reaction solution suppresses the catalytic activity, one should perform a control experiment showing that the precatalyst complex does not react with Hg(0); if Hg(0) does react with the precatalyst, then this test becomes ambiguous. Similarly, if the addition of Hg(0) to the reaction solution has little effect on the catalytic activity, one should perform a control experiment showing that an authentic heterogeneous catalyst of the same metal *is* poisoned under identical conditions.

---

presence of a nanocluster catalyst. The problem with this experiment is that the Hg(0) was removed by filtration *before the catalytic reaction was allowed to start* (i.e., before a heterogeneous catalyst could have formed). As performed, the experiment only shows that the precatalyst does not react with Hg(0), which is a nice control experiment, but not quite to the point. The Hg(0) should have remained in the reaction solution for the duration of the catalytic reaction or added after the catalytic reaction had already begun, as done elsewhere [10,21,24].

[6] For a hydrogenation reaction, the following protocol is recommended [10,21]. Allow the catalytic hydrogenation reaction to proceed to ~50% completion, release the H_2 pressure, add the (excess of) Hg(0) to the reaction solution, let the reaction solution stir so that the Hg(0) has a chance to contact any metal particles that may be present, re-pressurize the reactor with H_2, and check for catalytic activity [21].

[7] As evidence for this statement, experiments show that a large excess of Hg(0) is necessary to poison completely an authentic Rh(0)$_n$ nanocluster [21]. Hence, an improperly performed poisoning experiment

2.4. Quantitative CS_2 (or other ligand) poisoning

Though underutilized, poisoning experiments using added ligands, such as CS_2 PPh_3, and thiophene, can be powerful if performed quantitatively [10,11,23,24,48,49,50]. These poisons bind strongly to metal centers, thereby blocking access of the substrate to the active site. If a catalyst can be poisoned completely with <<1.0 equivalent of the added ligand (per metal atom), that is compelling (kinetic) evidence for a heterogeneous catalyst. The logic here is that in a heterogeneous catalyst only a fraction of the metal atoms are on the surface (e.g., about 50% of the Ir is on the surface of a 2 nm, $Ir(0)_{\sim 300}$ nanocluster [10,30,32]); hence, even if every surface atom is active, <<1.0 equivalent of ligand will be sufficient to poison the catalyst.[8] On the other hand, typically ≥1.0 equivalent of ligand is required to completely poison homogeneous, monometallic catalysts.[9] See elsewhere [10,11,48] for prototypical examples of this powerful but underutilized "fractional poisoning" experiment.

One limitation of this experiment is that it must be performed at <~50 °C because ligands such as CS_2 will begin to dissociate from a heterogeneous catalyst at higher temperatures [24,51,52,53]. For example, in a cyclohexene hydrogenation experiment 5 mol% CS_2 completely poisons an authentic $Rh(0)_n$ nanocluster at 25 °C; however, simply

---

(i.e., one in which a large excess of Hg(0) is not used) can lead to incorrect conclusions about the nature of the catalyst.

[8] Experimentally, 1–3 mol% CS_2 poisons >90% of the catalytic activity of ~4 nm, $Rh(0)_{\sim 2400}$ nanoclusters, which have about 30% of the Rh on the surface [48]. In that study it was also found that 3.5 mol% CS_2 completely poisons a commercial Rh/Al_2O_3 catalyst with an average metal-particle diameter of ~3.6 nm [48].

[9] This argument assumes a large equilibrium constant for the binding of the poison to the metal. Because of this assumption, we recommend using well-established poisons (such as CS_2) and performing appropriate control experiments with authentic homogeneous and heterogeneous catalysts. One such control experiment is to show that the added ligand is unable to disassemble authentic nanoclusters *of the same metal* into monometallic complexes: $M_n + (x \bullet n)L \rightarrow nML_x$. Metals with weaker M–M bonding (such as first row metals, Pd, and others) are most prone to such a process.

raising the reaction temperature *of that same, poisoned solution* to 100 °C results in rapid and complete hydrogenation of the substrate [24]. The development of poisons that bind irreversibly at higher temperatures is an important, but presently unfulfilled, goal in heterogeneous catalysis.

2.5. Crabtree's test (homogeneous catalyst poisoning)

Crabtree and co-workers discovered that dibenzo[*a,e*]cyclooctatetraene (DCT) poisons at least some homogeneous catalysts [4] by binding strongly to them. They found that 1.0 equivalent of DCT completely poisons homogeneous catalysts such as $RhCl(PPh_3)_3$. On the other hand, DCT has little or no effect on at least Rh colloids, Pd colloids and Pd/C heterogeneous catalysts [4]. Poisoning with DCT is in principle a nice complement to the mercury-poisoning experiment described earlier. If one equivalent of DCT completely inhibits catalysis, but Hg(0) has little effect on catalysis, that is compelling evidence for a homogeneous catalyst. Conversely, if DCT has little effect on catalysis, but Hg(0) acts as a poison, that is compelling evidence for a heterogeneous catalyst. One potential problem with using DCT is that the inhibition of homogeneous catalysis develops slowly in some cases, so DCT must to be stirred with the active catalyst species for hours [4]. Consequently, the active catalyst must be stable on that longer timescale in order to obtain meaningful results. Another potential limitation is that DCT is unlikely to bind to (and poison) all homogeneous catalysts [4] and, to date, has been tested with only a few complexes of Group VIII metals. A final difficulty is that DCT is not commercially available and its synthesis is unreliable [54]; hence, the

development of a better synthesis for DCT or of a generally applicable DCT replacement is needed.

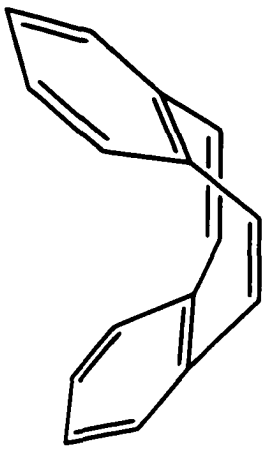

dibenzo[*a*,*e*]cyclooctatetraene (DCT)

2.6. Maitlis' test (filtration)

The filtration test relies on a comparison of catalytic activity before and after filtering the active catalyst solution [2,4,23,28,55,56]. In one version of this test, a high-surface-area filter aid such as powdered cellulose [2], Celite [4] or powdered graphite [56] is added to the active catalyst solution. The reaction solution is then filtered through a glass frit. The filter aid, along with any adhering metal particles, is washed with solvent and then returned to the (rinsed) reaction vessel. After adding fresh solvent and substrate, the catalytic activity of the filter aid (plus any adhering metal particles) is tested; any observed catalytic activity is attributed to heterogeneous catalysis. Ideally, the filtrate is also tested for catalytic activity, as this allows one to determine the relative amount of homogeneous vs heterogeneous catalysis (it also functions as a control experiment since the total catalytic activity of the filter aid and the filtrate should be approximately the same as the catalytic activity of the original reaction solution). This

test is probably most useful for determining if *bulk metal* is responsible for the catalysis. As pointed out in the original paper [2], it is not clear if this method will be capable of reliably testing for the presence of a nanocluster catalyst. One report in the literature indicates that this filtration method (using Celite) is unsuccessful at detecting a colloidal Rh catalyst [4], but another report (using powdered graphite) apparently detects a colloidal Rh catalyst [56].

A second version of the filtration test involves filtering the active catalyst solution through a small-pore membrane filter [22,28,55]. If filtration does not change the observed catalytic activity, the catalyst is assumed to be homogeneous. Unfortunately, membrane filters with pores small enough to exclude nanoclusters are slow and difficult to use [28], so this version of the filtration test is again best for determining if bulk metal is responsible for the catalysis.

Both versions of the filtration test share some drawbacks. In order for either filtration test to be convincing, control experiments with authentic homogeneous catalysts and authentic nanocluster catalysts are needed.[10] Also, the filtration tests do not address the problem of continued generation of heterogeneous species following the filtration [28]. Additionally, the physical manipulations involved in the filtration could lead the decomposition of a truly homogeneous catalyst, thereby leading to the erroneous conclusion that a heterogeneous catalyst is involved, and in the absence of additional, suitable control experiments [28].

2.7. Collman's test (hydrogenation of polymer-bound substrates)

Collman and co-workers described the use of polymer-bound substrates to distinguish homogeneous catalysts from heterogeneous catalysts that are >8 nm in diameter [1,7]. Homogeneous catalysts are believed to be more active for the hydrogenation of polymer-bound substrates, apparently due to the lack of mobility of the heterogeneous catalysts in the polymer matrix; however, the heterogeneous[11] Ziegler-type polymer hydrogenation catalyst based on nickel(II)octanoate and triethyl aluminum [50] appears to be a counter-example to the belief that heterogeneous catalysts are relatively inactive for polymer hydrogenation. The difference in activity between homogeneous and heterogeneous catalysts is then used to suggest the nature of the true catalyst. A nice feature of this method is that it is based on the reactivity of the active catalytic species and is not influenced by inactive components in the reaction solution. As pointed out in the original paper [7], though, only large (>8 nm in diameter) metal particles were used to verify this method, so it is not clear if it will work for smaller nanoclusters. It would be instructive to check this method with small, well-characterized, modern nanocluster catalysts as well as with soluble, heterogeneous, Ziegler-type catalysts [50].

2.8. Light scattering

Light scattering has been used to test for the presence of metal particles in catalyst solutions [4,8,22,28,45,57,58]. The detection limits are quite good for this technique.

---

[10] Note how the use of (often-ignored) controls with, for example, authentic nanoclusters is a recurring key to reliably distinguishing homogeneous from heterogeneous catalysts, a point first made elsewhere [10].

[11] The Ziegler-type catalyst based on nickel(II)octanoate and triethyl aluminum is believed to be "a colloidal suspension of small Ni clusters embedded in an amorphous organo-alumina soap" [50]. The

although not as good as TEM; Crabtree found that a solution of iridium colloids with 3×10^{11} particles/cm^3 (25 nm average radius) could easily be detected [5]. Light scattering can detect particles >1 nm in diameter [45]. An advantage of light scattering (compared to TEM) is that the analysis is done in solution (i.e., *in situ*). Like TEM, however, light scattering can detect nanoclusters, but cannot determine their kinetic competence as catalysts; hence, light scattering must be used in combination with other experiments to convincingly determine the nature of the true catalyst. One problem with light scattering is that the presence of dust or particles from abrasion of the reactor can lead to "false positives" [28]. Again, suitable control experiments are imperative.

2.9. Centrifugation

The centrifugation of nanoclusters has been known for many years [59,60,61,62,63], but is rarely used to test for nanocluster catalysts [64,65,66]. Metal particles have a high molecular weight and are relatively dense, so they are relatively easy to sediment from solution by centrifugation (i.e., compared to common transition-metal complexes). In principle, this powerful, non-invasive, solution technique allows the separation of soluble nanoclusters from lighter, soluble, transition-metal complexes.[12] To test for a soluble nanocluster catalyst, one would first spin a solution containing the active catalyst. Then, if sediment forms, it is separated from the supernatant and both are tested for catalytic activity. Catalytically active sediment and catalytically inactive

---

evidence for heterogeneity includes complete inhibition of catalysis by <<1 equiv of sulfur-containing poisons and EXAFS spectra showing intense Ni–Ni signals at distances comparable to bulk Ni [50].

[12] See elsewhere for an example of this type of experiment [10]. In that study, $Ir(0)_{\sim 900}$ nanoclusters were separated from $P_2W_{15}Nb_3O_{62}^{9-}$ by spinning at 20 000 rpm for less than 10 min. Under these conditions the

supernatant are consistent with a nanocluster catalyst. One problem with this experiment is that it is very difficult to achieve a quantitative separation of the sediment and the supernatant without using specialized, viscous gels; therefore, both will probably have some residual catalytic activity. Another problem is that this experiment will not work if the reaction is catalyzed by a low concentration of highly active nanoclusters since no visible sediment will form. Given these problems, centrifugation alone cannot be used to rule out a nanocluster catalyst. A final difficulty with this experiment is that small nanoclusters and nanoclusters of lighter elements are more difficult to sediment from solution, which leaves some question about the appropriate conditions for the experiment. In addition, control experiments with authentic samples of the nanoclusters, the homogeneous precatalyst, and the nanoclusters plus homogeneous precatalyst should be done when using this technique.

2.10. Reactivity patterns

The ability of a catalyst to promote certain reactions is occasionally used as an indication of the catalyst's identity. The idea is to choose a reaction that a heterogeneous catalyst will catalyze, but that a homogeneous catalyst will not (or vice versa). The problem with using reactivity patterns is that it is difficult to find a reaction that only works with heterogeneous catalysts (or only homogeneous catalysts). In practice, only two reactions have been widely used, hydrogenation of monocyclic arenes [7,21] and hydrogenation of aromatic nitro groups [4,22,23,45]. The lore of catalysis once held the belief that benzene hydrogenation could be used as a test for heterogeneous catalysis

---

$Ir(0)_{\sim 900}$ nanoclusters form a dark brown precipitate while (most of) the polyoxoanion remains in the

because only heterogeneous catalysts were capable of promoting the reaction [21]. However, there are now a *few* well-established examples of monometallic catalysts capable of monocyclic arene hydrogenation [67,68].[13,14] Additionally, not all heterogeneous catalysts are active catalysts for monocyclic arene hydrogenation. Consequently, the ability of a catalyst to hydrogenate monocyclic arenes is not definitive regarding the identity of the true catalyst. Essentially the same points can be made regarding the hydrogenation of aromatic nitro groups. In short, we do not recommend the use of these experiments.

3. A general approach to distinguishing homogeneous catalysis from heterogeneous catalysis

As mentioned earlier (and also emphasized elsewhere [4,10]), no single experiment is capable of answering the "homogeneous or heterogeneous" question for all systems. It should be clear from the discussion above that it is desirable to perform a series of experiments if one wants to convincingly determine the nature of the catalyst.

---

colorless supernatant.

[13] There are actually many claims of homogeneous arene hydrogenation catalysis in the literature [1,67,68]. However, few of these claims are based on solid evidence, and there is now evidence that several of these systems are actually heterogeneous [68]. This is certainly an area of catalysis that would benefit from further efforts to distinguish homogeneous from heterogeneous catalysis. So far, true homogeneous catalysts for monocyclic arene hydrogenation are rare.[14]

[14] The Nb^{V} and Ta^{V} hydrido aryloxide complexes, such as $[Ta\{OC_6H_3(C_6H_{11})_2\text{-}2,6\}_2(H)_3(PMe_2Ph)_2]$, developed by Rothwell and coworkers are well-established examples of monometallic catalysts capable of monocyclic arene hydrogenation based on the following evidence [67]: (i) the reduction of Nb^{V} or Ta^{V} to Nb(0) or Ta(0) metal particles by hydrogen is extremely unlikely under the reaction conditions; and (ii) the observed selectivity of the catalyst for the intramolecular hydrogenation of the aryloxide ligands is consistent with a homogeneous mononuclear catalyst, but difficult to explain if the true catalyst is heterogeneous (*ortho*-phenyl substituents on the aryloxide ligand are hydrogenated, while hydrogenation of phenyl rings *meta* or *para* to the aryloxide oxygen is not observed nor is hydrogenation of the phenoxide nucleus itself ever observed).

Along these lines, a more general approach has been developed for distinguishing homogeneous and heterogeneous catalysts [10]. This approach, which has been used successfully on several catalytic systems [10,21,24], is diagrammed in Figure 3.2. This

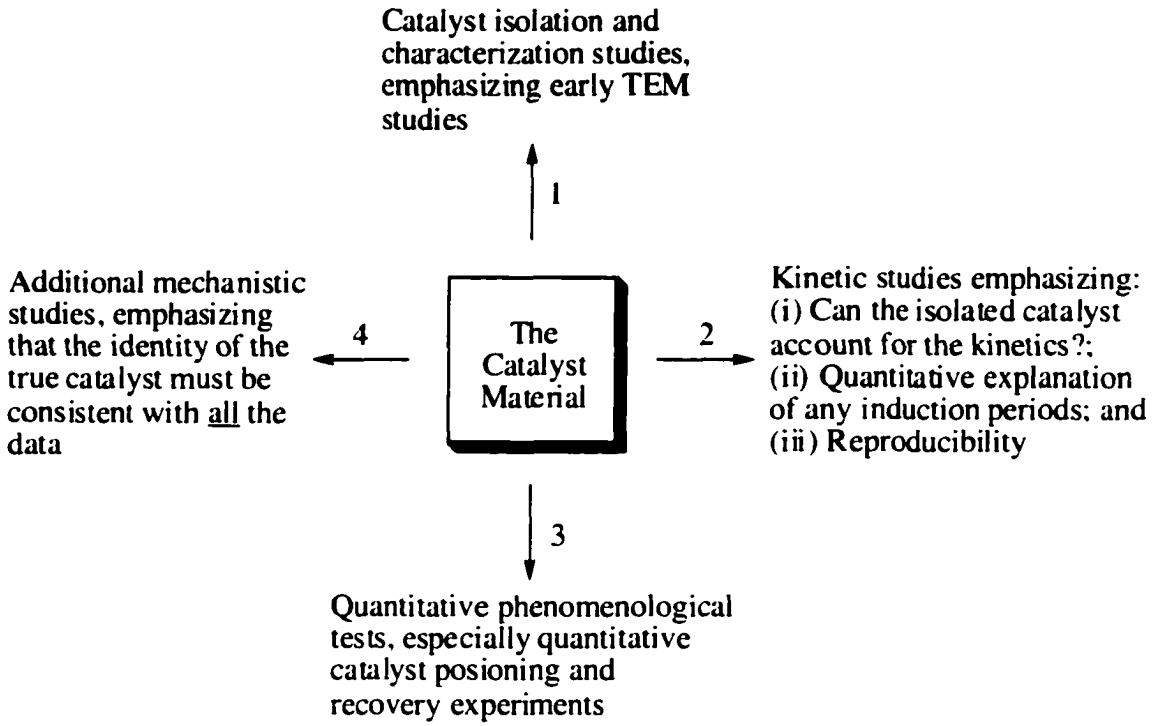

Figure 3.2. A more general approach to distinguishing between a metal-particle "heterogeneous" catalyst and a metal-complex "homogeneous" catalyst [10]. See Figure 5 elsewhere [10] for the expanded version of this figure.

more general approach emphasizes: (1) catalyst isolation and characterization, especially by initial TEM studies; (2) kinetic studies; (3) quantitative catalyst poisoning experiments; and (4) the perhaps obvious, but still important, concept that the identity of the true catalyst must be consistent with all the data.

3.1. Catalyst isolation and characterization

The first step in the general method for answering the "homogeneous or heterogeneous" question involves attempted isolation and characterization of the catalyst

material. These experiments are not intended to unequivocally identify the true catalyst; rather, they are intended as scouting experiments to give one a better idea what the possibilities are. Ideally, the first thing one would like to know is if metal particles form under catalytic conditions. The *in situ* formation of bulk metal is typically evidenced by the visible formation of a dark powder or metallic mirror; verification that such a precipitate is indeed bulk metal can be readily accomplished using XPS or XRD [24,39]. The formation of soluble nanoclusters is easier to miss because nanocluster solutions may appear homogeneous to the naked eye. Indeed, highly catalytic solutions of well-stabilized nanoclusters will remain completely soluble and apparently "homogeneous" [10,32,33,69]. For this reason, the use of TEM is suggested as the single most powerful and broadly applicable method for the detection of nanoclusters. Other techniques, such as light scattering and centrifugation, can also be used to detect soluble nanoclusters. If bulk metal or metal nanoclusters are detected in the isolated catalyst material, then one needs to turn to kinetic methods to determine if they are the true catalyst.

A point of note here: the ability to isolate a large percentage of the precatalyst complex (or some other soluble metal complex) following catalysis has been used as evidence of homogeneous catalysis [44,70,71,72,73]. *This is incorrect!* Such a result does not rule out the possibility that a small percentage of highly active colloids or bulk metal is responsible for the observed catalysis. See elsewhere for further discussion of this point [2,10].

3.2. Kinetic studies

The second step in the general method for answering the "homogeneous or heterogeneous" question involves kinetic studies. If an induction period is observed then the "catalyst" added to the reaction must actually be a *precatalyst*, which has to convert into the true catalyst before any catalysis occurs. Any time an induction period is observed in reductive catalysis, one should suspect the *in situ* formation of a heterogeneous catalyst. If the overall kinetics of a hydrogenation reaction is sigmoidal, that is excellent evidence—*indeed, the to-date kinetic signature* [10,21,24,30,31,32,33,34,35]—for the *in situ* formation of a heterogeneous catalyst (*vide supra*). Of course, pre-treatment of the "catalyst" with reductant may eliminate the induction period by allowing the true catalyst to form in the absence of substrate. If one is able to isolate the putative catalyst from a reaction solution, then one should check to see if the isolated material can account for the observed kinetics. Basically, one must show that the isolated catalyst, after adding fresh solvent and substrate, can catalyze the reaction at a kinetically competent rate without an induction period.

3.3. Catalyst poisoning experiments

The third step in the general method for answering the "homogeneous or heterogeneous" question emphasizes quantitative poisoning studies. Of the three poisoning methods discussed above (mercury, CS_2 and DCT), mercury poisoning is the least definitive because an excess of mercury must be used, so quantitative results cannot be obtained (*vide supra*). On the other hand, quantitative experiments are possible with CS_2, and other ligand-based poisons. As mentioned earlier, if one can show that $<<1$

equivalent of CS_2 completely poisons catalysis, that is compelling evidence for a heterogeneous catalyst because such a result is consistent with the geometric features of metal-particle catalysis.[8] but difficult to explain for homogeneous catalysis. It is advisable to try more than one type of poisoning experiment on each catalyst system. For example, the CS_2-poisoning and Hg(0)-poisoning experiments form a nice complement.

3.4. The identity of the true catalyst will be consistent with all the data

The fourth step in the general method for answering the "homogeneous or heterogeneous" question emphasizes the important concept that the identity of the true catalyst must be consistent with *all* the data. After performing multiple experiments a consistent picture should emerge regarding the true nature of the catalyst. However, a situation may arise in which some experimental results indicate a heterogeneous catalyst and others indicate a homogeneous catalyst. In such a circumstance, one should first make sure that the reaction conditions have not changed significantly from one experiment to the next since this can cause the nature of the catalyst to change [7,23,45]. Also, one should consider performing additional control experiments to ensure that the experiments are functioning as expected and that the interpretation of the data is not complicated in some unseen way.

4. An overview of when to suspect soluble-metal-particle heterogeneous catalysis

The formation of a soluble-metal-particle heterogeneous catalyst from a monometallic precatalyst is more likely under certain circumstances. It is important to be

familiar with those circumstances so that one can be on the lookout for the telltale signs of heterogeneous catalysis. Conditions under which a heterogeneous catalyst is likely to form include: (i) when easily reduced transition-metal complexes are used as precatalysts; (ii) when forcing reaction conditions are employed; (iii) when nanocluster stabilizers are present (anions such as halides or carboxylates, polar solvents, R_4N^+ counterions, etc. [34]); and (iv) when monocyclic arene hydrogenation is observed. The telltale signs of heterogeneous catalysis include (v) the formation of dark reaction solutions and metallic precipitates; and (vi) the observation of induction periods and sigmoidal kinetics. A key point regarding the observation of a metallic precipitate when starting with a single-metal precatalyst: *this demands that nanoclusters were formed en route to the metallic precipitate* (as there is no other known way to go from monometallic species to bulk metal [10]). Hence, in such cases nanoclusters as the true catalyst must be considered.

4.1. The use of easily reduced transition-metal complexes

The reduction of many late-transition-metal salts with H_2 is thermodynamically favorable under routine reaction conditions. Hence, whether or not metal particles form in such systems is simply a question of kinetics. To complicate matters, such metal particles are good catalysts for a variety of reactions, including hydrogenation. Consequently, the *in situ* formation of heterogeneous hydrogenation catalysts from late-transition-metal precatalysts is probably quite common (see section 4.4. for some examples). However, in some cases the oxidative-addition activation of H_2 by a M^{n+} precatalyst is not viable because it would require the formation of an energetically

prohibitive $M(H)_2^{n+2}$ oxidation state. In such cases reduction of the precatalyst can still occur via *heterolytic hydrogen activation* [1,74] if the needed base is present, since the $M^{n+} + H_2 + B: \rightarrow [M^{n+}–H]^{n-1} + B–H^+$ reaction causes no increase in the M^{n+} oxidation state. The literature reveals (i) that the key requirements for heterolytic hydrogen activation are a metal whose oxidation state is high enough that further oxidation is unfavorable, an available coordination site, and a way to stabilize the released proton (i.e., the presence of a base), especially in nonaqueous solvents; (ii) that amines, carboxylates, alkoxides and hydroxide are commonly used bases (the base can also be an internal M-R which undergoes a four-centered reaction with H_2, a second version of heterolytic hydrogen activation); and (iii) that the metals for which heterolytic hydrogen activation is to be expected (i.e., when a base is present) include Pd(II), Pt(IV), Ru(II), Ru(III), Rh(III), Ir(III), Ag(I), Au(III), Cu(I), and Cu(II) [31].

4.2. The use of forcing reaction conditions

The use of forcing reaction conditions (high temperature, high H_2 pressure, strong reducing agents) increases the probability that a heterogeneous catalyst will form. For example, hydrogenations with the precatalyst $[Rh(C_5Me_5)Cl_2]_2$ are apparently homogeneously catalyzed at ~5 atm H_2 and 50 °C, but develop a heterogeneous component at 50 atm H_2 and 50 °C [7]. As a second example, Wilkinson's catalyst, a well-know homogeneous catalyst under mild reaction conditions, develops a heterogeneous component after several hours at 130 °C and ~3.5 atm of H_2 [45]. Even subtle changes in reaction conditions can cause the nature of the catalyst to change. Homogeneous catalysis was observed with (N,N'-diaryl-

diiminoacenaphthene)Pd^0(alkene) as the precatalyst, THF as the solvent, and electron deficient alkenes as the substrate [23]. However, switching either the solvent to benzene or the substrate to cyclohexene caused a significant heterogeneous component to develop [23]. The lesson is that the nature of the true catalyst can change with the reaction conditions. An important point here is that the reaction $M_n + (x \bullet n)L \leftrightarrows nML_x$ appears to be exothermic in many cases (i.e., shifted to the left at higher reaction temperatures). Further studies of such equilibria are needed to verify or refute this point, however.

4.3. The presence of nanocluster stabilizers

Transition-metal nanoclusters, $M(0)_n$, are only kinetically stable because the formation of bulk metal is the thermodynamic minimum [12,75].[15] Therefore, nanoclusters that are freely dissolved in solution must be stabilized in a way that prevents the nanoclusters from diffusing together and coalescing [12], ultimately to bulk metal. Nanocluster stabilization is usually discussed in terms of two general categories of stabilization, electrostatic and steric [76,77]. Electrostatic stabilization is achieved by the coordination of anionic ligands, such as halides, carboxylates or polyoxoanions, to the coordinatively unsaturated metal atoms on the surface of the metal particles [76]. This results in the formation of an electrical double-layer (really a diffuse electrical multi-layer) [78], and results in coloumbic repulsion between individual nanoclusters with their coordinated anions. Steric stabilization is achieved by the presence of bulky, typically

---

[15] From the enthalpies of vaporization (i.e., ignoring solvation effects), one finds that the bulk metal is 133, 155 and 160 kcal/mol more stable than single Rh(0), Ru(0) and Ir(0) atoms, respectively [75]. Obviously, nanoclusters are more stable than isolated metal atoms because they have many metal–metal bonds, but they are still less stable than the thermodynamic sink of bulk metal, in which essentially every metal atom has the maximum possible number of metal–metal bonds.

organic materials that, due to their steric bulk, impede the nanocluster surfaces from touching and thereby agglomerating [76]. Polymers (particularly polyvinylpyrrolidone), dendrimers and large alkylammonium cations are examples of common organic steric stabilizers of nanoclusters and colloids.

The formation of highly active nanocluster catalysts is more likely if nanocluster stabilizers are present in the reaction solution. To illustrate this point, 2100 catalytic turnovers for cyclohexene hydrogenation are observed with [(1,5-COD)$Rh^{I}(CH_3CN)_2$][BF_4] as the precatalyst; however, due to the absence of nanocluster stabilizers, the catalyst quickly deactivates by forming low-surface-area bulk Rh metal [69]. On the other hand, cyclohexene hydrogenation with $[Bu_4N]_5Na_3$[(1,5-COD)Rh^{I}•$P_2W_{15}Nb_3O_{62}$] as the precatalyst yields an active and long-lived nanocluster catalyst capable of >190 000 catalytic turnovers because of the stabilizing effect of the polyoxoanion and tetrabutylammonium [33,39,69].

The solvent also plays a role in nanocluster stability. DLVO theory [76,77] of colloid stabilization predicts that the thickness of the stabilizer double layer will increase as the dielectric constant (ε) of the solvent increases; hence, theory predicts that colloid stability will be enhanced in high dielectric solvents. This prediction has not been carefully tested [34], but some data are available. Notably, Reetz and Lohmer found [79] that Pd nanoclusters are especially stable in propylene carbonate, for which $\varepsilon = 69$ (for comparison $\varepsilon = 20$ for acetone and $\varepsilon = 39$ for acetonitrile). These solvent- (and chloride- [14]) stabilized nanoclusters have the highest demonstrated thermal stability of any known soluble nanocluster, showing no visually observable formation of bulk metal even after several days at 140–155°C [79]. Reetz and Lohmer's nanoclusters were also shown

to catalyze Heck coupling reactions at temperatures as high as 160°C [79], a record reaction temperature for a soluble nanocluster catalyst. A recent report shows that nanoclusters might also be especially stable in ionic liquids [80]. In that work, chloride-stabilized Ir nanoclusters were found to be capable of >8400 catalytic turnovers for olefin hydrogenation at 70 °C and 4 atm of H_2 in the ionic liquid 1-butyl-3-methylimidazolium hexafluorophosphate [80].[16] A scrutiny of the literature reveals several probable, but unrecognized, cases of nanocluster catalysis in ionic liquids [81,82,83,84,85]. These are systems where more evidence is needed for or against nanoclusters as the true catalyst.

Another key here is that the use of lower concentrations [69] of nanoclusters has a significant stabilizing effect because it slows down the kinetics of bimolecular aggregation. Note the insidious nature of this effect in regards to determining the true catalyst: low concentrations of small, highly active nanoclusters can easily be the true, hard-to-detect catalyst!

4.4. The hydrogenation of monocyclic arenes

The hydrogenation of monocyclic arenes is a difficult reaction to catalyze [86,87,88]. Typically it is accomplished with heterogeneous catalysts of Group VIII metals, such as Rh/Al_2O_3 or Raney nickel [89]. There are several claims of metal-complex homogeneous catalysts capable of monocyclic arene hydrogenation [1,67,68]. However, (i) there is usually little evidence to support the hypothesis that the true catalyst in these systems is homogeneous;[14] (ii) two such catalyst have now been shown to be

---

[16] Autocatalytic kinetics, a mercury-poisoning experiment, TEM data, and catalyst isolation experiments leave little doubt that Ir nanoclusters are the true catalyst in this system.

heterogeneous, as the following examples and references illustrate; and (iii) there is at least some evidence that other systems are heterogeneous as well.

Perhaps the best example of an arene hydrogenation catalyst that was initially believed to be homogeneous, but where later evidence definitely shows that it is heterogeneous, is the important arene hydrogenation catalyst based on $RhCl_3$ and $[(C_8H_{17})_3NCH_3]Cl$ [90,91]. Initially, it was claimed that the $[(C_8H_{17})_3NCH_3]^+[RhCl_4]^-$ ion-pair was the true catalyst [90]. Later work using the more general approach to the "homogeneous or heterogeneous catalysis problem" [10] mentioned above, including TEM, Hg(0)-poisoning, and solution-phase kinetic studies demonstrating sigmoidal, $A \rightarrow B$, $A + B \rightarrow 2B$ kinetics, convincingly shows that the true catalyst is actually a distribution of Rh(0) colloids stabilized by Cl^- and $[(C_8H_{17})_3NCH_3]^+$ [21].

The second example involves the use of $Ru(\eta^6\text{-}C_6Me_6)(O_2CMe)_2$ for benzene hydrogenation [24,92,93,94]. Early catalytic studies [92,93] were unable to determine the nature of the true catalyst [92]; however, recent work including TEM, Hg(0)-poisoning, and kinetic studies showing characteristic sigmoidal kinetics, convincingly shows that the true catalyst is heterogeneous [24].

There is some evidence for the *in situ* formation of a heterogeneous catalyst in other arene hydrogenation systems that employ homogeneous precatalysts. One example involves the use of $[Rh(\eta^5\text{-}C_5Me_5)Cl_2]_2$ for arene hydrogenation [57,95]. The catalyst in this system was originally claimed to be homogeneous on the basis of light scattering experiments. However, later work [7] suggests that the true catalyst may be heterogeneous, though the evidence is not definitive—note here the problem caused in the initial study by relying solely on light scattering without, for example, kinetic studies.

Briefly, the evidence for heterogeneity includes (i) the observation of dark colored reaction solutions, (ii) the routine observation of 1–2 h induction periods, an observation characteristic of metal-particle formation [10,30,31], (iii) the deposition of Rh metal on the reactor walls, and (iv) the observation that the catalyst is much more active for the hydrogenation of benzene and cumene than it is for the hydrogenation of polystyrene [7]. This system is under further investigation [96].

Another example involves $Ru_2Cl_2(\mu\text{-}H)_2(\mu\text{-}Cl)(\eta^6\text{-}C_6Me_6)_2$ as a precatalyst for arene hydrogenation [97,98]. This catalyst was originally thought to be homogeneous; however, a later study shows that the catalyst is inactive in the presence of Hg(0) [99], implying that the true catalyst is heterogeneous [3,10].[17] These examples show that soluble nanoclusters are fairly pervasive in claimed "homogeneous" arene hydrogenation systems.

4.5 The formation of metallic precipitates and dark reaction solutions

Certain experimental observables can indicate the *in situ* formation of a heterogeneous catalyst. The most obvious of these is the formation of metallic precipitates during the course of the reaction in the form of a metal powder or mirror. Verification that such a precipitate is indeed bulk metal can be accomplished with XPS or XRD [24,39] as mentioned earlier. Since metal surfaces are good catalysts for a variety of reactions, one must strongly suspect heterogeneous catalysis in such systems. As

---

[17] Additionally, poisoning experiments reported in the original study [98] are, in hindsight, more consistent with the hypothesis that the catalyst is heterogeneous than with the hypothesis that it is homogeneous. For example, the presence of only 0.05 equivs of thiophene (per Ru atom) dramatically slows the turnover frequency (from 4.1 min^{-1} in an unpoisoned experiment to 0.3 min^{-1} with 0.05 equivs of thiophene) [98].

pointed out elsewhere [5], one cannot rule out heterogeneous catalysis by showing that the metallic precipitate is inactive, because the process in Eq. 1 may be occurring.

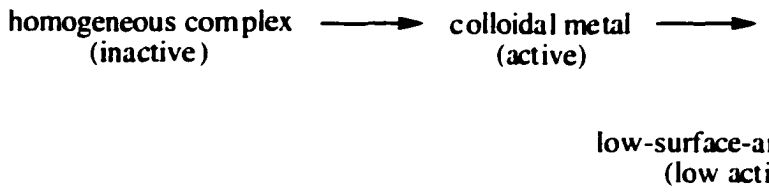

(1)

The *in situ* formation of a soluble nanocluster catalyst is difficult to impossible to detect visually because the reaction solutions typically appear homogeneous and may not precipitate bulk metal. Nevertheless, nanocluster solutions of transition metals are often dark brown or black, so a darkening reaction solution suggests the possibility that a nanocluster catalyst is forming.

4.6. The observation of induction periods and sigmoidal kinetics

The presence of an induction period is one consequence of the *in situ* formation of a heterogeneous catalyst from a monometallic precatalyst [30,31]. If the end of the induction period is accompanied by a darkening of the reaction solution or the formation of a metallic precipitate, that strongly suggests the *in situ* formation of a heterogeneous catalyst. However, an induction period may be too short to observe in some cases of heterogeneous catalysis. Additionally, if the precatalyst is pretreated with reductant in the absence of substrate [21,90], then no induction period is expected. If the end of the induction period is followed by an "autocatalytic burst" of activity, that is excellent

---

Such a result is difficult to explain for a homogeneous catalyst, but makes perfect sense for a heterogeneous

evidence for the *in situ* formation of a heterogeneous catalyst. At least for hydrogenation reactions, the prior literature shows that such sigmoidal, "autocatalytic" kinetics are characteristic of *in situ* nanocluster formation [10,21,24,30,31,32,33,34,35]. Note also the point made earlier: the observation of a metallic precipitate when beginning with a single-metal precatalyst *demands* that nanoclusters were formed [10].

4.7. The issue of the $M_n + (x \bullet n)L \leftrightarrows nML_x$ equilibrium

One key, presently poorly understood, issue is the position of the $M_n + (x \bullet n)L \leftrightarrows nML_x$ equilibrium as a function of metal, ligand type, amount of ligand, and temperature. The position of this equilibrium determines what species are present as potential catalysts. Relevant literature includes the fact that CO treatment of $Rh(0)_n$ rafts yields discrete $Rh(CO)_x^{0/+}$ species, a process that can be reversed [100,101]. Also, Union Carbide's study of $CO + H_2 \rightarrow CH_3OH + HOCH_2CH_2OH$ + other products, using Rh carbonyl cluster precatalysts, showed that these precatalysts are unstable because the Rh–Rh and Rh–CO bond energies are of similar strengths, with the Rh–CO bond being a bit stronger [102]. That makes the $M_n + (x \bullet n)L \leftrightarrows nML_x$ equilibrium exothermic, *meaning that nanocluster formation is thermodynamically favored at higher temperatures* in at least this system [102].

In other cases, it appears that the presence of strongly binding or chelating ligands may inhibit, perhaps completely, reduction to a $M(0)_n$ state. An example under investigation [103] is the interesting $[Ir(1,5\text{-}COD)Cl]_2$ / bidentate chiral phosphine catalyst system for imine hydrogenation at ~70 atm of H_2 [104,105]. In the absence of

---

catalyst where only a fraction of the total metal atoms are on the surface and active."

phosphine, $[Ir(1,5\text{-}COD)Cl]_2$ is readily reduced to $Ir(0)_n$ at only ~4 atm of H_2 [34]; however, presence of the bidentate phosphine ligand appears to inhibit reduction of the Ir^I(phosphine) complex even at ~70 atm of H_2, although this has not yet been conclusively demonstrated [103]. One available piece of evidence for the homogeneity of this system is that its high enantioselectivity is without good precedent in heterogeneous catalysis.

The case of Pd(0) complexes and nanoclusters provides another important example, making clear that the type of ligands, and the ligand to metal ratio, are important in determining the form of Pd(0) present. First, the commercially available complex $Pd(0)(PPh_3)_4$ reminds us that mononuclear, 18-electron complexes of Pd(0) are well-known and isolable. Second, in the absence of phosphine ligands $Pd(0)_n$ colloids are known to form in Pd-catalyzed C–C coupling reactions with $Pd(OAc)_2$ as the precatalyst [106,107]; however, the addition of four equivalents of PPh_3 (vs Pd) to this system completely inhibits colloid formation [106]. Third, the existence of Pd nanoclusters of *average* formulas such as $Pd_{\sim 560}phen_{\sim 60}(OAc)_{\sim 180}$ (phen = 1,10-phenanthroline), $Pd_{\sim 1400}phen_{\sim 60}O_{\sim 1100}$ and $Pd_{\sim 2000}phen_{\sim 80}O_{\sim 1600}$ [108] shows that the number and type of ligands are factors in determining the average size of the resultant distribution of nanoclusters.

Another important paper in this general regard is a very recent one showing $Au(0)_n + (m \bullet x)L \leftrightarrows Au(0)_{n-m} + mAuL_x$ [109], that is, the formation of smaller $Au(0)_{n-m}$ particles from larger ones in the presence of added ligands such as $RSH \geq RNH_2 \geq R_3P \geq RSiH_3$ (the ordering indicates the ligands qualitative ability to effect breakup of the $Au(0)_n$ nanoclusters). In short, not nearly enough is known about how the metal, ligand

type, amount of ligand, temperature, and other variables influence the $M_n + (x \bullet n)L \leftrightarrows nML_x$ equilibrium. Understanding these factors will be important to a better understanding of when to expect homogeneous vs heterogeneous catalysis.

Although we focus on hydrogenation catalysis in this review, the problem of distinguishing homogeneous and heterogeneous catalysis is not limited to hydrogenation reactions. *In situ* formation of heterogeneous catalysts has also been identified as an issue in hydrosilylation reactions [8,9,47,110], ring-opening polymerization catalysis [111], alkane activation [112], and C–C coupling reactions [106]. The pervasiveness of the "homogeneous or heterogeneous" problem in catalytic science is further illustrated by the identification of *homogeneous species* as the true catalysts for initially *heterogeneous* oxidation catalysts based on molecular sieves [113,114], and for carbonylation and Heck coupling catalysts where Pd/C and Pd/Al_2O_3 are the *precatalysts* [115].

5. Examples of catalyst systems of interest for further study

One of the aims of this review is to enable researchers to determine for themselves probable cases of heterogeneous catalysis. Since most catalyst systems in the literature have not been examined carefully in light of the "homogeneous or heterogeneous" question, a large number of systems are of interest for further study. To guide the reader, we reference a few such systems here. See Table 3.1 of the Appendix for detailed information about each of these catalyst systems. Systems that employ easily reduced transition-metal complexes as precatalysts can be found in references [66,81,82,106,107,116,117,118,119,120,121]. Systems employing forcing reaction

conditions can be found in references [44,64,65,73,82,83,84,104,106,107,116,118,119,122,123,124,125,126,127,128,129,130]. Systems in which known nanocluster stabilizers are present can be found in references [64,65,66,73,82,83,104,106,107,116,117,119,120,124,128,129,130]. Systems in which monocyclic arene hydrogenation is observed can be found in references [1,44,64,66,84,106,116,117,118,126,127,128,129,130,131]. Systems that form dark reaction solutions or metallic precipitates can be found in references [7,64,65,66,73,82,85,106,107,116,117,119,120,125,127,131]. Systems that exhibit induction periods or sigmoidal kinetics can be found in references [7,65,106,120,124,125,131]. Systems that meet at least four of the six criteria, that is, systems that very likely involve metal-particle catalysts, are found in references [64,65,66,82,106,107,116,117,119,120].

6. Summary and future outlook

The major findings of this review are:

• Catalysis under reducing conditions is often performed with a transition-metal complex as the precatalyst. *In situ* reduction of such a precatalyst to form a metal-particle heterogeneous catalyst is common.

• A variety of experiments can been used to help distinguish homogeneous catalysis from heterogeneous catalysis; however, there is no single definitive experiment for making this distinction.

• Distinguishing homogeneous catalysis from heterogeneous catalysis is most difficult when a nanocluster catalyst is involved, partly because nanocluster solutions appear homogeneous to the eye. Additionally, nanoclusters can be as small as ~1 nm in diameter, which makes them difficult to detect by some methods.

• Kinetic information is crucial to the determination of the true catalyst, catalysis being a "wholly kinetic phenomenon" [25,26].

• A general approach for distinguishing homogeneous catalysis from heterogeneous catalysis is available and involves the four components shown back in Figure 3.2.

• Conditions under which a heterogeneous catalyst is likely to form include: (i) when easily reduced transition-metal complexes are used as precatalysts; (ii) when forcing reaction conditions are employed; (iii) when nanocluster stabilizers are present [34]; and (iv) when monocyclic arene hydrogenation is observed.

• The telltale signs of heterogeneous catalysis include the formation of dark reaction solutions and metallic precipitates, plus the observation of induction periods and sigmoidal kinetics.

• Under conditions that favor nanocluster formation, the primary hypothesis to be disproven [132] is that nanoclusters are the true catalyst.

An obvious area for future research is to investigate more catalytic systems in terms of the "homogeneous or heterogeneous" question. Table 3.1 of the Appendix lists about 30 catalytic systems for which the *in situ* formation of a heterogeneous catalyst is worth investigating. Related to this, a few areas of catalysis warrant closer inspection:

• Further study of Pd-catalyzed C–C coupling reactions is of interest. It appears that Pd nanoclusters are commonly formed in such systems [82,106,107,119,133]. The role of such nanoclusters in catalysis needs to be clarified.

• The role of nanoclusters in Pt-catalyzed hydrosilylation reactions is much debated [8,9,47,110,120]. However, the central importance of kinetics in determining the nature of the true catalyst(s) in these systems has been largely ignored. Kinetic studies, including quantitative CS_2-poisoning experiments, are of interest for these systems.

• Precatalysts composed of transition-metal complexes with polymeric ligands are quite common [73,116,117,128,129,131]. Under reducing conditions, how common is the formation of a polymer-stabilized nanocluster catalyst?

• The *in situ* generation of a heterogeneous catalyst appears to be common for systems that are capable of monocyclic arene hydrogenation [68]. Hence, studying more of these systems by the more general method [10] for answering the "homogeneous or heterogeneous" question would be of interest.

Another general area for future research is the further development of methods for distinguishing homogeneous and heterogeneous catalysts. Some worthwhile problems include:

• A systematic study of the poisoning of transition-metal catalysts with mercury would be useful. For example, it would be valuable to know the poisoning properties of mercury vs temperature. It would also be useful to know which metals require a large excess of mercury, or other specialized conditions, for complete poisoning.

• Developing ligand-based poisons similar to CS_2, but which work at higher temperatures, would be quite valuable. Currently, the powerful, quantitative, ligand-

based poisoning experiment can only be performed for systems that operate near room temperature [48]. Many systems of interest, including many monocyclic arene hydrogenation catalysts, are active only at higher temperatures.

• An improved synthesis of DCT, further study of DCT, and DCT analogs or replacements are all of interest.

• Further investigation of Maitlis' filtration test using proven nanocluster catalysts is of interest. Can this test be used, perhaps under modified conditions, to detect nanocluster catalysts, or is it limited to the detection of catalysis by bulk metal precipitates?

• It would be instructive to check Collman's test with smaller, well-characterized, modern nanocluster catalysts, as well as with as with soluble, heterogeneous, Ziegler-type, polymer hydrogenation catalysts [50].

• And finally, more information is needed about the $M_n + (x \bullet m)L \leftrightarrows M_{n-m} + mML_x$ equilibrium and its impact on the "is it homogeneous or heterogeneous catalysis" problem.

Acknowledgments.

Financial support was provided by the Department of Energy, Chemical Sciences Division, Office of Basic Energy, grant DOE FG06-089ER13998.

References:

[1] J.P. Collman, L.S. Hegedus, J.R. Norton, R.G. Finke, Principles and Applications of Organotransition Metal Chemistry, Chap. 10, University Science Books, Mill Valley, 1987.

[2] J.E. Hamlin, K. Hirai, A. Millan, P.M. Maitlis, J. Mol. Catal. 7 (1980) 543.

[3] G.M. Whitesides, M. Hackett, R.L. Brainard, J.P.P.M. Lavalleye, A.F. Sowinski, A.N. Izumi, S.S. Moore, D.W. Brown, E.M. Staudt, Organometallics 4 (1985) 1819.

[4] D.R. Anton, R.H. Crabtree, Organometallics 2 (1983) 855.

[5] R.H. Crabtree, M.F. Mellea, J.M. Mihelcic, J.M. Quirk, J. Am. Chem. Soc. 104 (1982) 107.

[6] R.H. Crabtree, J.M. Mihelcic, J.M. Quirk, J. Am. Chem. Soc. 101 (1979) 7738.

[7] J.P. Collman, K.M. Kosydar, M. Bressan, W. Lamanna, T. Garrett, J. Am. Chem. Soc. 106 (1984) 2569.

[8] L.N. Lewis, N. Lewis, J. Am. Chem. Soc. 108 (1986) 7228.

[9] L.N. Lewis, J. Am. Chem. Soc. 112 (1990) 5998.

[10] Y. Lin, R.G. Finke, Inorg. Chem. 33 (1994) 4891.

[11] Y. Lin, Ph.D. Dissertation, Department of Chemistry, University of Oregon, March 1994.

[12] J.D. Aiken, III, Y. Lin, R.G. Finke, J. Mol. Catal. A: Chem. 114 (1996) 29.

[13] R.G. Finke, in: D.L. Feldheim, C.A. Foss, Jr. (Eds.), Metal Nanoparticles: Synthesis, Characterization, and Applications, Chap. 2, Marcel Dekker, Inc., New York, 2001.

[14] J.D. Aiken, III, R.G. Finke, J. Mol. Catal. A: Chem. 145 (1999) 1.

[15] H. Bönnemann, W. Brijoux, A.S. Tilling, K. Siepen, Top. Catal. 4 (1998) 217.

[16] J.S. Bradley, in: G. Schmid (Ed.), Clusters and Colloids: From Theory to Applications, VCH Publishers, New York, 1994, p. 459-544.

[17] L.N. Lewis, Chem. Rev. 93 (1993) 2693.

[18] G. Schmid, Chem. Rev. 92 (1992) 1709.

[19] G. Schmid, Endeavour 14 (1990) 172.

[20] J. Schwartz, Acc. Chem. Res. 18 (1985) 302.

[21] K.S. Weddle, J. D. Aiken III, R.G. Finke, J. Am. Chem. Soc. 120 (1998) 5653.

[22] R.H. Crabtree, M.F. Mellea, J.M. Mihelcic, J.M. Quirk, J. Am. Chem. Soc. 104 (1982) 107.

[23] R. van Asselt, C.J. Elsevier, J. Mol. Catal. 65 (1991) L13.

[24] J.A. Widegren, M.A. Bennett, R.G. Finke, "Is It Homogeneous or Heterogeneous Catalysis? Identification of Ruthenium Metal Particles as the True Catalyst in Benzene Hydrogenations Starting with the Monometallic Precursor, $Ru(II)(\eta^6\text{-}C_6Me_6)(OAc)_2$", submitted.

[25] J. Halpern, Inorg. Chim. Acta 50 (1981) 11.

[26] J. Halpern, T. Okamoto, A. Zakhariev, J. Mol. Catal. 2 (1977) 65.

[27] The Chemistry and Physics of Small Metallic Particles. Faraday Discuss. 92 (1991) 102.

[28] R.M. Laine, J. Mol. Catal. 14 (1982) 137.

[29] M.N. Vargaftik, I.I. Moiseev, D.I. Kochubey, K.I. Zamaraev, Faraday Discuss. 92 (1991) 13.

[30] M.A. Watzky, R.G. Finke, J. Am. Chem. Soc. 119 (1997) 10382.

[31] J.A. Widegren, J.D. Aiken, III, S. Özkar, R.G. Finke, Chem. Mater. 13 (2001) 312.

[32] Y. Lin, R.G. Finke, J. Am. Chem. Soc. 116 (1994) 8335.

[33] J.D. Aiken III, R.G. Finke, Chem. Mater. 11 (1999) 1035.

[34] S. Özkar, R.G. Finke, J. Am. Chem. Soc. 124 (2002) 5796.

[35] S. Özkar, R.G. Finke, manuscript in preparation.

[36] R.M. Noyes, R.J. Field, Acc. Chem. Res. 10 (1977) 273.

[37] R.J. Field, R.M. Noyes, Acc. Chem. Res. 10 (1977) 214.

[38] R.J. Field, R.M. Noyes, Nature 237 (1972) 390.

[39] J.A. Widegren, R.G. Finke, Inorg. Chem. 41 (2002) 1558.

[40] Z. Duan, M.J. Hampden-Smith, A.P. Sylwester, Chem. Mater. 4 (1992) 1146.

[41] J.S. Bradley, J. Am. Chem. Soc. 101 (1979) 7419.

[42] C. Paal, W. Hartmann, Chem. Ber. 51 (1918) 711.

[43] P. Foley, R. DiCosimo, G.M. Whitesides, J. Am. Chem. Soc. 102 (1980) 6713.

[44] G. Süss-Fink, M. Faure, T.R. Ward, Angew. Chem. Int. Ed. 41 (2002) 99.

[45] L.N. Lewis, J. Am. Chem. Soc. 108 (1986) 743.

[46] R.A. Jones, F.M. Real, G. Wilkinson, A.M.R. Galas, M.B. Hursthouse, J. Chem. Soc., Dalton Trans. (1981) 126.

[47] J. Stein, L.N. Lewis, Y. Gao, R.A. Scott, J. Am. Chem. Soc. 121 (1999) 3693.

[48] B.J. Hornstein, J.D. Aiken III, R.G. Finke, Inorg. Chem. 41 (2002) 1625.

[49] M.N. Vargaftik, V.P. Zagorodnikov, I.P. Stolyarov, I.I. Moiseev, D.I. Kochubey, V.A. Likholobov, A.L. Chuvilin, K.I. Zamaraev, J. Mol. Catal. 53 (1989) 315.

[50] K.A. Johnson, Polymer Preprints 41 (2000) 1525.

[51] L. Gonzalez-Tejuca, K. Aika, S. Namba, J. Turkevich, J. Phys. Chem. 81 (1977) 1399.

[52] R. Frety, P.N. Da Silva, M. Guenin, Catal. Lett. 3 (1989) 9.

[53] J.B. Butt, Catal. Sci. Technol. 6 (1987) 1.

[54] R.H. Crabtree, private communication.

[55] R.M. Laine, R.G. Rinker, P.C. Ford, J. Am. Chem. Soc. 99 (1977) 252.

[56] P. Drognat Landré, D. Richard, M. Draye, P. Gallezot, M. Lemaire, J. Catal. 147 (1994) 214.

[57] M.J. Russell, C. White, P.M. Maitlis, J. Chem. Soc., Chem. Commun. (1977) 427.

[58] R.H. Crabtree, J.M. Mihelcic, J.M. Quirk, J. Am. Chem. Soc. 101 (1979) 7738.

[59] T. Svedberg, H. Rinde, J. Am. Chem. Soc. 46 (1924) 2677.

[60] H. Cölfen, Critical Reviews of Optical Science and Technology CR69 (1997) 525.

[61] M.N. Vargaftik, V.P. Zagorodnikov, I.P. Stolyarov, I.I. Moiseev, D.I. Kochubey, V.A. Likholobov, A.L. Chuvilin, K.I. Zamaraev, J. Mol. Catal. 53 (1989) 315.

[62] G. Schmid, B. Morun, J.-O. Malm, Angew. Chem., Int. Ed. Engl. 28 (1989) 778.

[63] G. Schmid, A. Lehnert, Angew. Chem., Int. Ed. Engl. 28 (1989) 778.

[64] S.J. Lapporte, W.R. Schuett, J. Org. Chem. 28 (1963) 1947.

[65] A. Alvanipour, L.D. Kispert, J. Mol. Catal. 48 (1988) 277.

[66] E.N. Rasadkina, T.S. Kukhareva, I.D. Rozhdestvenskaya, I.V. Kalechits, Kinet. Katal. 16 (1975) 1465.

[67] I.P. Rothwell, Chem. Commun. (1997) 1331.

[68] J.A. Widegren, R.G. Finke, "A review of soluble transition-metal nanoclusters as arene hydrogenation catalysts", J. Mol. Catal. A: Chem., in press.

[69] J.D. Aiken, III, R.G. Finke, J. Am. Chem. Soc. 121 (1999) 8803.

[70] J.W. Johnson, E.L. Muetterties, J. Am. Chem. Soc. 99 (1977) 7395.

[71] E.L. Muetterties, J.R. Bleeke, Acc. Chem. Res. 12 (1979) 324.

[72] M.A. Bennett, T.-N. Huang, A.K. Smith, T.W. Turney, J. Chem. Soc., Chem. Commun. (1978) 582.

[73] D.E. Bergbreiter, R. Chandran, J. Am. Chem. Soc. 109 (1987) 174.

[74] P.J. Brothers, Prog. Inorg. Chem. 28 (1981) 1.

[75] D.F. Shriver, P. Atkins, C.H. Langford, Inorganic Chemistry, 2nd Edition, W. H. Freeman and Company, New York, 1994, p. 317.

[76] R.J. Hunter, Foundations of Colloid Science, Vol. 1, Oxford Univ. Press, New York, 1986.

[77] C.S. Hirtzel, R. Rajagopalan, Colloidal Phenomena: Advanced Topics, Noyes Publications, Park Ridge, N. J., 1985.

[78] A.J. Bard, L.R. Faulkner, Electrochemical Methods: Fundamentals and Applications, Wiley, New York, 1980.

[79] M.T. Reetz, G. Lohmer, Chem. Commun. (1996) 1921.

[80] J. Dupont, G.S. Fonseca, A.P. Umpierre, P.F.P. Fichtner, S.R. Teixeira, J. Am. Chem. Soc. 124 (2002) 4228.

[81] P.A.Z. Suarez, J.E.L. Dullius, S. Einloft, R.F. De Souza, J. Dupont, Polyhedron 15 (1996) 1217.

[82] D.E. Kaufmann, M. Nouroozian, H. Henze, Synlett (1996) 1091.

[83] J.F. Knifton, J. Am. Chem. Soc. 103 (1981) 3959.

[84] P.J. Dyson, D.J. Ellis, T. Welton, D.G. Parker, Chem. Commun. (1999) 25.

[85] Y. Chauvin, L. Mussmann, H. Olivier, Angew. Chem., Int. Ed. Engl. 34 (1996) 2698.

[86] J. March, Advanced Organic Chemistry: Reactions, Mechanisms, and Structure, 4th edition, Wiley-Interscience, New York, 1992, pp. 780.

[87] A. Stanislaus, B.H. Cooper, Catal. Rev. – Sci. Eng. 36 (1994) 75.

[88] R.J. Fessenden, J.S. Fessenden, Organic Chemistry, 5th edition, Chap. 11, Brooks/Cole Publishing Company, Pacific Grove, 1993.

[89] R.L. Augustine, Heterogeneous Catalysis for the Synthetic Chemist, Chap. 17, Marcel Dekker, New York, 1996.

[90] J. Blum, I. Amer, K.P.C. Vollhardt, H. Schwarz, G. Hoehne, J. Org. Chem. 52 (1987) 2804.

[91] J. Blum, I. Amer, A. Zoran, Y. Sasson, Tetrahedron Lett. 24 (1983) 4139.

[92] J.P. Ennett, Ph.D. Dissertation, Department of Chemistry, Australian National University, 1984.

[93] M.A. Bennett, J.P. Ennett, Inorg. Chim. Acta 198-200 (1992) 583.

[94] D.A. Tocher, R.O. Gould, T.A. Stephenson, M.A. Bennett, J.P. Ennett, T.W. Matheson, L. Sawyer, V.K. Shah, J. Chem. Soc., Dalton Trans. (1983) 1571.

[95] P.M. Maitlis, Acc. Chem. Res. 11 (1978) 301.

[96] C. Hagen, R.G. Finke, experiments in progress.

[97] M. Bennett, Chemtech 10 (1980) 444.

[98] M.A. Bennett, T.-N. Huang, T.W. Turney, J. Chem. Soc., Chem. Commun. (1979) 312.

[99] B.R. James, Y. Wang, C.S. Alexander, T.Q. Hu, Chem. Ind. 75 (1998) 233.

[100] H.F.J. van't Blik, J.B.A.D. van Zon, T. Huizinga, J.C. Vis, D.C. Koningsberger, R. Prins, J. Am. Chem. Soc. 107 (1985) 3139.

[101] H.H. Lamb, B.C. Gates, H. Knözinger, Angew. Chem. Int. Ed. Engl. 27 (1988) 1127.

[102] J.L. Vidal, W.E. Walker, Inorg. Chem. 19 (1980) 896.

[103] X. Zhang, C. Hagen, R.G. Finke, experiments in progress.

[104] D. Xiao, X. Zhang, Angew. Chem. Int. Ed. 40 (2001) 3425.

[105] D. Xiao, Z. Zhang, X. Zhang, Org. Lett. (1999) 1679.

[106] M.T. Reetz, E. Westermann, Angew. Chem., Int. Ed. 39 (2000) 165.

[107] F. Zhao, M. Shirai, M. Arai, J. Mol. Catal. A: Chem. 154 (2000) 39.

[108] I.I. Moiseev, R.I. Rudy, N.V. Cherkashina, L.K. Shubochkin, D.I. Kochubey, B.N. Novgorodov, G.A. Kryukova, V.N. Kolomiychuk, M.N. Vargaftik, Inorg. Chim. Acta 280 (1998) 339.

[109] B.L.V. Prasad, S.I. Stoeva, C.M. Sorensen, K.J. Klabunde, "Digestive Ripening Agents for Gold Nanoparticles: Alternatives to Thiols", submitted.

[110] L.N. Lewis, R.J. Uriarte, N. Lewis, J. Mol. Catal. 66 (1991) 105.

[111] K. Temple, F. Jäkle, J.B. Sheridan; I. Manners, J. Am. Chem. Soc. 123 (2001) 1355.

[112] R.H. Crabtree, Chem. Rev. 85 (1985) 245.

[113] R.A. Sheldon, M. Wallau, I.W.C.E. Arends, U. Schuchardt, Acc. Chem. Res. 31 (1998) 485.

[114] I.W.C.E. Arends, R.A. Sheldon, Appl. Catal., A 212 (2001) 175.

[115] I.W. Davies, L. Matty, D.L. Hughes, P.J. Reider, J. Am. Chem. Soc. 123 (2001) 10139.

[116] E.N. Rasadkina, T.V. Kuznetsova, A.T. Teleshev, I.D. Rozhdestvenskaya, I.V. Kalechits, Kinet. Katal. 15 (1974) 969.

[117] E.N. Rasadkina, I.D. Rozhdestvenskaya, I.V. Kalechits, Kinet. Katal. 17 (1976) 916.

[118] M. Onishi, K. Hiraki, M. Yamaguchi, J. Morishita, Inorg. Chim. Acta 195 (1992) 151.

[119] S. Mukhopadhyay, G. Rothenberg, D. Gitis, Y. Sasson, J. Org. Chem. 65 (2000) 3107.

[120] X. Coqueret, G. Wegner, Organometallics 10 (1991) 3139.

[121] J.A. Osborn, R.R. Schrock, J. Amer. Chem. Soc. 93 (1971) 3089.

[122] H. Chen, S. Schlecht, T.C. Semple, J.F. Hartwig, Science 287 (2000) 1995.

[123] P. Pertici, G. Vitulli, C. Bigelli, R. Lazzaroni, J. Organomet. Chem. 275 (1984) 113.

[124] E. Fache, F. Senocq, C. Santini, J.M. Basset, J. Chem. Soc., Chem. Commun. (1990) 1776.

[125] J.C. Tsai, K.M. Nicholas, J. Am. Chem. Soc. 114 (1992) 5117.

[126] E. Garcia Fidalgo, L. Plasseraud, G. Süss-Fink, J. Mol. Catal. A: Chem. 132 (1998) 5.

[127] L. Plasseraud, G. Süss-Fink, J. Organomet. Chem. 539 (1997) 163.

[128] P. Dini, D. Dones, S. Montelatici, N. Giordano, J. Catal. 30 (1973) 1.

[129] D.P. Harrison, H.F. Rase, Ind. Eng. Chem. Fundam. 6 (1967) 161.

[130] M.J. Russell, C. White, P.M. Maitlis, J. Chem. Soc., Chem. Commun. (1977) 427.

[131] R.A. Jones, M.H. Seeberger, J. Chem. Soc., Chem. Commun. (1985) 373.

[132] J.R. Platt, Science 146 (1964) 347.

[133] M. Beller, H. Fischer, K. Kühlein, C.-P. Reisinger, W.A. Herrmann, J. Organomet. Chem. 520 (1996) 257.

APPENDIX

A review of the problem of distinguishing true homogeneous catalysis from soluble-metal-particle heterogeneous catalysis under reducing conditions

Jason A. Widegren and Richard G. Finke

APPENDIX

Table 3.1. A list of catalyst systems for which the *in situ* formation of a metal-particle catalyst is likely

	Authors (date)	Catalyst system	Why *in situ* metal-particle formation is likely	Ref
1	G. Süss-Fink and co-workers (2002)	Triruthenium clusters are used as precatalysts for benzene hydrogenation at 60 atm of H_2 and 110 °C.	Forcing reaction conditions are used and monocyclic arene hydrogenation is observed. A mercury poisoning experiment was performed, but the mercury was (inappropriately) removed before the hydrogenation reaction was started.	[1]
2	D. Xiao, and X. Zhang (2001)	The precatalyst is formed in situ from $[Ir(COD)Cl]_2$ and a chelating phosphine ligand. This precatalyst is used for imine hydrogenation at room temperature and ~70 atm of H_2.	Forcing reaction conditions are used and a known nanocluster stabilizer is present (chloride). However, the presence of a chelating phosphine ligand may keep this catalyst homogeneous.	[2]
3	J.F. Hartwig and co-workers (2000)	$Cp^*Rh(\eta^4\text{-}C_6Me_6)$ is used as a precatalyst for alkane activation at 150 °C.	Forcing reaction conditions are used.	[3]
4	M.T. Reetz and E. Westermann (2000)	Palladium-catalyzed coupling reactions (Heck and Suzuki) are investigated using several different precatalysts.	In this important paper, using phosphane-free catalyst systems, the authors observe induction periods and sigmoidal kinetics (see Fig. 1 and 3). They also observe the presence of nanoclusters by TEM. These systems contain nanocluster stabilizers (acetate and tetrabutylammonium halide). Forcing conditions and easily reduced precatalysts like $Pd(OAc)_2$ are used. It is not clear from this study is if the Pd nanoclusters are directly involved in the catalytic cycle, or if they only serve as a reservoir for Pd in these systems.	[4]
5	Y. Sasson and co-workers (2000)	Palladium-catalyzed coupling reactions are investigated using a precatalyst of $PdCl_2$ / tetrahexylammonium chloride / AcOH / AcONa. The reactions were performed at 80–105 °C.	The formation of metallic precipitates is observed. This system contains nanocluster stabilizers (acetate and tetrahexylammonium chloride). Forcing conditions and an easily reduced precatalyst are employed.	[5]
6	M. Arai and co-workers (2000)	Palladium-catalyzed Heck reactions are investigated using a precatalyst of $Pd(OAc)_2$ / triethylamine / $NaCO_3$. The reactions were performed at 80–110 °C.	They observe the presence of nanoclusters by TEM, along with the formation of metallic precipitates. This system contains nanocluster stabilizers (acetate and carbonate). Forcing conditions and an easily reduced precatalyst are employed.	[6]

7	P.J. Dyson and co-workers (1999)	$[H_4Ru_4(\eta^6\text{-}C_6H_6)_4][BF_4]_2$ is used as the precatalyst for arene hydrogenation at 60 atm of H_2 and 90 °C.	Forcing reaction conditions are used and monocyclic arene hydrogenation is observed.	[7]
8	G. Süss-Fink and co-workers (1998)	$(\eta^6\text{-}C_6H_6)_2Ru_2Cl_4$ is used as a precatalyst for the hydrogenation of benzene derivatives at 60 atm of H_2 and 90 °C.	Forcing reaction conditions are used and monocyclic arene hydrogenation is observed. This system contains a nanocluster stabilizer (chloride).	[8]
9	A.M. Trzeciak and co-workers (1998)	$HRh[P(NC_4H_4)_3]_4$ and $HRh(CO)[P(NC_4H_4)_3]_3$ are used as the precatalysts for alkene and arene hydrogenation at 5 atm of H_2 and 80 °C.	Forcing reaction conditions are used and monocyclic arene hydrogenation is observed.	[9]
10	G. Süss-Fink and co-workers (1997)	$[(\eta^6\text{-}C_6H_6)_4Ru_4H_4]Cl_2$ is used as a precatalyst for the hydrogenation of benzene derivatives at 60 atm of H_2 and 90 °C.	Forcing reaction conditions are used and monocyclic arene hydrogenation is observed. After complete conversion of benzene, the formation of metallic Ru is observed. This system contains a nanocluster stabilizer (chloride).	[10]
11	R.F. De Souza and co-workers (1996)	$[Rh(COD)_2][BF_4]$ and other precatalysts are used for alkene hydrogenation at 10 atm of H_2 and 25 °C.	Somewhat forcing conditions (10 atm of H_2), and an easily reduced precatalyst are used.	[11]
12	D.E Kaufmann and co-workers (1996)	$Pd(OAc)_2$ and other precatalysts are used for Heck coupling reactions at 100 °C.	Forcing reaction conditions and easily reduced precatalysts are used. This system contains known nanocluster stabilizers (such as tetraalkylammonium bromide salts). Dark brown reaction solutions and metallic precipitates form.	[12]
13	Y. Chauvin and co-workers (1995)	$[Rh(norbornadiene)(PPh_3)_2][PF_6]$ and other precatalysts are used for alkene hydrogenation at 1 atm of H_2 and 30 °C.	The reaction solution turns from orange to brown upon exposure to hydrogen.	[13]
14	M. Onishi and co-workers (1992)	$[Rh(COD)(Ph_2PCH_2COO)]$ and $[Rh(CO)_2(Ph_2PCH_2COO)]$ are used as precatalysts for arene hydrogenation at 50 °C and 5–50 atm of H_2.	Forcing reaction conditions and easily reduced precatalysts are used. Plus, monocyclic arene hydrogenation and aromatic nitro group hydrogenation are observed.	[14]
15	J.C. Tsai and K.M. Nicholas (1992)	$[Rh(norbornadiene)(Pme_2Ph)_3][BF_4]$ is used as a precatalyst for the hydrogenation of carbon dioxide to formic acid at about 50 atm of H_2 and 40 °C.	Forcing reaction conditions are used. An induction period is observed unless the precatalyst is pretreated with H_2. Dark precipitate forms from the precatalyst under hydrogen.	[15]
16	X. Coqueret and G. Wegner (1991)	$PtCl_2$(diene) is used as the precatalyst for hydrosilylation at 25–60 °C.	Sigmoidal reaction kinetics are observed (see Figure 1 of the referenced paper). The reaction solution darkens (though only after the hydrosilylation reaction is complete). An easily reduced precatalyst is used and known nanocluster stabilizers are present (chloride).	[16]

17	J.-M. Basset and co-workers (1990)	$RuCl_2[(m\text{-}NaSO_3C_6H_4)_3P]_3$ and related complexes are used in conjuction with salts such as NaI. These precatalysts were used to hydrogenate propionaldehyde at 50 atm of H_2 and 100 °C.	Forcing reaction conditions are used. Induction periods are observed in the absence of added salt (see Fig. 1 of the referenced paper). Known nanocluster stabilizers (halides) are found to cause a "remarkable" increase in activity.	[17]
18	A. Alvanipour and L.D. Kispert (1988)	The catalyst was formed from the combination of triethyl aluminum and Co(stearate)$_2$. This catalyst was used in for naphthalene (and other bicyclic arene) hydrogenation at about 50 atm of H_2 and 22 °C.	Forcing reaction conditions and strong reducing agents are used. This system contains known nanocluster stabilizers (long-chain carboxylates). Induction periods are observed, as is the formation of black reaction solutions	[18]
19	J.P. Collman and co-workers (1987)	A number of "homogeneous" arene hydrogenation catalysts from the earlier literature are tabulated in Table 10.2 of this reference.	This reference discusses the possibility that at least some of these systems are heterogeneous.	[19]
20	D.E. Bergbreiter and R. Chandran (1987)	The precatalyst was formed by tethering Rh(I) complexes to functionalized ethylene oligomers via phosphine groups. This precatalyst was then used to hydrogenate alkenes at 1 atm of H_2 and 100 °C.	Forcing reaction conditions are used. Additionally, known nanocluster stabilizers (polymers) are present, and the catalyst solutions darken during the course of the reaction. However, most of the Rh(I) complex remains intact by ^{31}P NMR and Collman's polymer hydrogenation test appears to indicate a homogeneous catalyst (although Collman's test appears to be a poor choice for this system).	[20]
21	R.A. Jones and M.H. Seeberger (1985)	The precatalyst was formed by tethering Rh(COD) (or other) moieties to polystyrene beads via phosphido linkages. This precatalyst was then used to hydrogenate benzene at 1–3 atm of H_2 and 25–45 °C.	The polystyrene beads darken during the reaction. Additionally, induction periods and monocyclic arene hydrogenation is observed. However, no metal crystallites were observed by X-ray photoelectron spectroscopy or X-ray diffraction analysis.	[21]
22	P. Pertici and co-workers (1984)	Rh(η^6-arene)(η^4-COD) complexes are used as precatalysts for alkene hydrogenation at room temperature and 1–60 atm of H_2.	Forcing reaction conditions are used in some cases. Catalyst decomposition is observed under some conditions. However, benzene is not hydrogenated under these conditions.	[22]
23	J.F. Knifton (1981)	Ru(acac)$_3$ and other precatalysts are used to synthesize ethylene glycol from synthesis gas at 430 atm of CO/H_2 (1:1) and 220 °C.	Forcing reaction conditions are used and known nanocluster stabilizers (tetraalkylammonium bromide salts) are present. However, no metallic precipitates or higher hydrocarbons are formed.	[23]

24	P.M. Maitlis and co-workers (1977)	$[Rh(\eta^5\text{-}C_5Me_5)Cl_2]_2$ is the precatalyst for the hydrogenation of alkenes, alkynes, arenes and nitroaromatics at 50 atm of H_2 and 50 °C.	Forcing conditions are used, a known nanocluster stabilizer is present (choride), and monocyclic arene hydrogenation is observed. However, no metal particles were visible by light scattering. A second paper [24] using the same system reports (i) the observation of dark colored reaction solutions and the formation of metallic precipitates, (ii) the observation of 1–2 h induction periods, and (iv) the observation that the catalyst is much more active for the hydrogenation of benzene and cumene than it is for the hydrogenation of polystyrene.	[25]
25	E.N. Rasadkina and co-workers (1976)	The precatalyst was formed from the combination of a polyamide and a palladium or rhodium salt such as $RhCl_3 \bullet 3H_2O$. This precatalyst was used to hydrogenate alkenes, arenes and nitroaromatics at 1 atm of H_2 and 25 °C.	Easily reduced precatalysts are used and known nanocluster stabilizers (polymers) are present. Dark brown reaction solutions and metallic precipitates form. Monocyclic arene hydrogenation and nitro group hydrogenation are observed.	[26]
26	E.N. Rasadkina and co-workers (1975)	The precatalyst was formed from the combination of a polyamide and a platinum salt such as K_2PtCl_4. This precatalyst was used to hydrogenate alkenes, arenes and nitroaromatics at 1 atm of H_2 and 30 °C.	Easily reduced precatalysts are used and known nanocluster stabilizers (polymers) are present. Brown reaction solutions and metallic precipitates form. Monocyclic arene hydrogenation and nitro group hydrogenation are observed.	[27]
27	E.N. Rasadkina and co-workers (1974)	The precatalyst was formed from the combination of a polyamide and a Group VIII metal salt such as $RhCl_3 \bullet 3H_2O$. This precatalyst was dissolved and treated with H_2 at about 150 °C. It was then used to hydrogenate benzene at 1 atm of H_2 and 160 °C.	Forcing reaction conditions and easily reduced precatalysts are used. Known nanocluster stabilizers (polymers) are present and the dark brown reaction solutions form. Monocyclic arene hydrogenation is observed.	[28]
28	P. Dini and co-workers (1973)	Precatalysts were prepared by stirring a polyamide (such as Nylon-6) with an aqueous solution of a Pt compound (such as H_2PtCl_6), followed by drying in a vacuum oven. The dried material was then activated in a H_2 atmosphere at 160 °C for 7 h. These materials were used to hydrogenate benzene at 140–190 °C. The authors believe the true catalyst is "a chloride-containing platinum complex where the metal atom is coordinatively bound to two amide groups of the polymeric chain."	Forcing reaction conditions are used and known nanocluster stabilizers (polymers) are present. Monocyclic arene hydrogenation is observed. Additionally, H_2 chemisorption measurements show that only a fraction of the Pt atoms chemisorb H_2, suggestive evidence for the formation of nanoclusters. However, the authors conclude that no Pt(0), is forming because of the negative evidence that X-ray measurements failed to show characteristic Pt diffraction patterns.	[29]

29	J.A. Osborn and R.R. Schrock (1971)	$[Ir(COD)_2][PF_6]$ and similar complexes are used as hydrogenation catalysts at 30 °C and 1 atm of hydrogen.	Very easily reduced precatalysts are used. However, the selectivities (at least for COD hydrogenation) appear to be at odds with a metal particle catalyst.	[30]
30	D.P. Harrison and H.F. Rase (1967)	Precatalysts were prepared by stirring nylon fibers with an aqueous solution of H_2PtCl_6 at 100 °C, followed by drying in an oven at 120 °C. The dried material was then activated in a H_2 atmosphere at reaction temperature for >1 h. These materials were used to hydrogenate benzene at 205–425 °C.	Forcing reaction conditions are used and known nanocluster stabilizers (polymers) are present. Monocyclic arene hydrogenation is observed. However, the authors conclude that no $Pt(0)_x$ is forming on the basis of X-ray and IR measurements, and on the selectivity of the catalysts for partial benzene hydrogenation.	[31]
31	S.J. Lapporte and W.R. Schuett (1963)	The catalyst was formed from the combination of triethyl aluminum and nickel(II) 2-ethylhexanoate. This catalyst was used for arene hydrogenation at about 70 atm of H_2 and 150 °C.	Forcing reaction conditions and strong reducing agents are used. Known nanocluster stabilizers (long-chain carboxylates) are present. The formation of black reaction solutions and the hydrogenation of monocyclic arenes are observed.	[32]

References

[1] G. Süss-Fink, M. Faure, T.R. Ward, Angew. Chem. Int. Ed. 41 (2002) 99.

[2] D. Xiao, X. Zhang, Angew. Chem. Int. Ed. 40 (2001) 3425.

[3] H. Chen, S. Schlecht, T.C. Semple, J.F. Hartwig, Science 287 (2000) 1995.

[4] M.T. Reetz, E. Westermann, Angew. Chem., Int. Ed. 39 (2000) 165.

[5] S. Mukhopadhyay, G. Rothenberg, D. Gitis, Y. Sasson, J. Org. Chem. 65 (2000) 3107.

[6] F. Zhao, M. Shirai, M. Arai, J. Mol. Catal. A: Chem. 154 (2000) 39.

[7] P.J. Dyson, D.J. Ellis, T. Welton, D.G. Parker, Chem. Commun. (1999) 25.

[8] E. Garcia Fidalgo, L. Plasseraud, G. Süss-Fink, J. Mol. Catal. A: Chem. 132 (1998) 5.

[9] A.M. Trzeciak, T. Glowiak, J.J. Ziólkowski, J. Organomet. Chem. 552 (1998) 159.

[10] L. Plasseraud, G. Süss-Fink, J. Organomet. Chem. 539 (1997) 163.

[11] P.A.Z. Suarez, J.E.L. Dullius, S. Einloft, R.F. De Souza, J. Dupont, Polyhedron 15 (1996) 1217.

[12] D.E. Kaufmann, M. Nouroozian, H. Henze, Synlett (1996) 1091.

[13] Y. Chauvin, L. Mussmann, H. Olivier, Angew. Chem., Int. Ed. Engl. 34 (1995) 2698.
[14] M. Onishi, K. Hiraki, M. Yamaguchi, J. Morishita, Inorg. Chim. Acta 195 (1992) 151.
[15] J.C. Tsai, K.M. Nicholas, J. Am. Chem. Soc. 114 (1992) 5117.
[16] X. Coqueret, G. Wegner, Organometallics 10 (1991) 3139.
[17] E. Fache, F. Senocq, C. Santini, J.M. Basset, J. Chem. Soc., Chem. Commun. (1990) 1776.
[18] A. Alvanipour, L.D. Kispert, J. Mol. Catal. 48 (1988) 277.
[19] J.P. Collman, L.S. Hegedus, J.R. Norton, R.G. Finke, Principles and Applications of Organotransition Metal Chemistry, Chap. 10, University Science Books, Mill Valley, 1987.
[20] D.E. Bergbreiter, R. Chandran, J. Am. Chem. Soc. 109 (1987) 174.
[21] R.A. Jones, M.H. Seeberger, J. Chem. Soc., Chem. Commun. (1985) 373.
[22] P. Pertici, G. Vitulli, C. Bigelli, R. Lazzaroni, J. Organomet. Chem. 275 (1984) 113.
[23] J.F. Knifton, J. Am. Chem. Soc. 103 (1981) 3959.

[24] J.P. Collman, K.M. Kosydar, M. Bressan, W. Lamanna, T. Garrett, J. Am. Chem. Soc. 106 (1984) 2569.
[25] M.J. Russell, C. White, P.M. Maitlis, J. Chem. Soc., Chem. Commun. (1977) 427.
[26] E.N. Rasadkina, I.D. Rozhdestvenskaya, I.V. Kalechits, Kinet. Katal. 17 (1976) 916.
[27] E.N. Rasadkina, T.S. Kukhareva, I.D. Rozhdestvenskaya, I.V. Kalechits, Kinet. Katal. 16 (1975) 1465.
[28] E.N. Rasadkina, T.V. Kuznetsova, A.T. Teleshev, I.D. Rozhdestvenskaya, I.V. Kalechits, Kinet. Katal. 15 (1974) 969.
[29] P. Dini, D. Dones, S. Montelatici, N. Giordano, J. Catal. 30 (1973) 1.
[30] J.A. Osborn, R.R. Schrock, J. Amer. Chem. Soc. 93 (1971) 3089.
[31] D.P. Harrison, H.F. Rase, Ind. Eng. Chem. Fundam. 6 (1967) 161.
[32] S.J. Lapporte, W.R. Schuett, J. Org. Chem. 28 (1963) 1947.

CHAPTER IV

ADDITIONAL INVESTIGATIONS OF A NEW KINETIC METHOD TO FOLLOW TRANSITION-METAL NANOCLUSTER FORMATION, INCLUDING THE DISCOVERY OF HETEROLYTIC HYDROGEN ACTIVATION IN NANOCLUSTER NUCLEATION REACTIONS

This dissertation chapter contains the manuscript of a full paper published in *Chemistry of Materials*, and describes the development and testing of a new kinetic method for following transition-metal nanocluster formation under hydrogen. Use of this new kinetic method led the discovery that heterolytic hydrogen activation is important for nanocluster nucleation when the nanocluster precursors contain metals in high oxidation states. The new kinetic method is also used in Chapters V and VI to follow the *in situ* formation of $Rh(0)_n$ and $Ru(0)_n$ catalysts for arene hydrogenation.

Two of the experiments described in this chapter were *not* performed by J.A.W. The hydrogen uptake experiment (Figure 4.4) was performed by J.D.A. and the solvent vapor pressure experiment (Figure 4.6) was performed by S.Ö. The manuscript was prepared by J.A.W. with assistance and editing (about 50 hours total) by R.G.F.

Additional Investigations of a New Kinetic Method to Follow Transition-Metal Nanocluster Formation, Including the Discovery of Heterolytic Hydrogen Activation in Nanocluster Nucleation Reactions

Jason A. Widegren, John D. Aiken III, Saim Özkar and Richard G. Finke

Abstract

A few years ago we developed a new kinetic method for following transition metal nanocluster formation in which the resultant nanocluster's catalytic activity was used as a reporter reaction via the pseudoelementary step concept. This method in turn yielded insights into a new, broadly applicable mechanism of nanocluster formation under H_2 consisting of (a) slow, continuous nucleation, A —> B, followed by (b) fast autocatalytic surface growth , A + B —> 2B (A = the nanocluster precursor, $[Bu_4N]_5Na_3[(1,5\text{-}COD)Ir{\bullet}P_2W_{15}Nb_3O_{62}]$. B = the resultant nanocluster's surface metal atoms), in which the nanocluster behaves as a "living metal polymer". Herein this new kinetic method is investigated and tested further: (i) by following the $Ir(0)_{\sim 300}$ nanocluster's kinetics of formation more directly via the H_2 uptake reaction of the $[Bu_4N]_5Na_3[(1,5\text{-}COD)Ir{\bullet}P_2W_{15}Nb_3O_{62}]$ precursor—does this also show an autocatalytic H_2 uptake curve?; (ii) by seeing if the predicted initially small, then larger (past the induction period) sizes of

the nanoclusters are verifiable directly by TEM; (iii) by testing commercial non-linear least squares software (Microcal's ORIGIN) in the kinetic analysis and with the goal of making the new kinetic method readily available to others; (iv) by showing when it is necessary to correct for the solvent vapor pressure, and how to do so, in the H_2 pressure-loss measurements when more volatile solvents such as acetone are used in the nanocluster formation reaction; (v) by showing whether or not the new kinetic method can be successfully used in other nanocluster formation reactions of different metals and for more difficult reactions such as arene hydrogenation; and (v) by numerical integration simulations of the first 45 or so steps in the nanocluster formation reaction—does this atomically detailed mechanism show autocatalysis or not, and if so can it be fit by the A —> B, A + B —> 2B mechanism? Tests of each of the issues (i)–(v) are reported in the present contribution. Finally, (vi) the new kinetic method has been exploited to yield insights into higher valent metals that undergo nucleation under H_2, namely to discover and report for the first time the significance of heterolytic hydrogenation activation, with its requirement for added base in the nanocluster formation reactions of higher valent, electrophilic metals such as Pd(II), Pt(IV), Ru(III), Rh(III), Ag(I), Au(III), Cu(II) and Ir(III).

Introduction

Nanoparticles[1] are an important, very active area of modern materials science. Of special interest is the synthesis of near-monodisperse (i.e., $\leq \pm 15\%$)[2] nanoclusters where their size, size-distribution, composition and shape are controlled via designed, rational syntheses. Hindering accomplishment of this important objective, however, is the relative dearth of kinetic and mechanistic information on the formation pathway(s) of modern, compositionally well-defined transition-metal nanoclusters.[3,4] Our recent nanocluster reviews[2] reveal three main reasons for this dearth of kinetic and mechanistic studies: (i) only recently have the first examples of modern, *compositionally fully defined*, prototype

transition-metal nanoclusters appeared, that is, ones suitable for in-depth kinetic and mechanistic studies.[1,2b,5] An example is the $P_2W_{15}Nb_3O_{62}^{9-}$ polyoxoanion- and Bu_4N^+ -stabilized, 20 ± 3 Å $Ir(0)_{\sim 190-450}$ (hereafter $Ir(0)_{\sim 300}$)[2-5] nanoclusters that we first reported in 1994, Figure 4.1, nanoclusters which are synthesized from the well-established precatalyst,[6] $[Bu_4N]_5Na_3[(1,5\text{-COD})Ir{\bullet}P_2W_{15}Nb_3O_{62}]$ by reduction under H_2. Second, (ii) the available ways to monitor the formation of nanoclusters in real time are limited[7]; and hence (iii) only more recently have mechanistic chemists begun to tackle this area.[4]

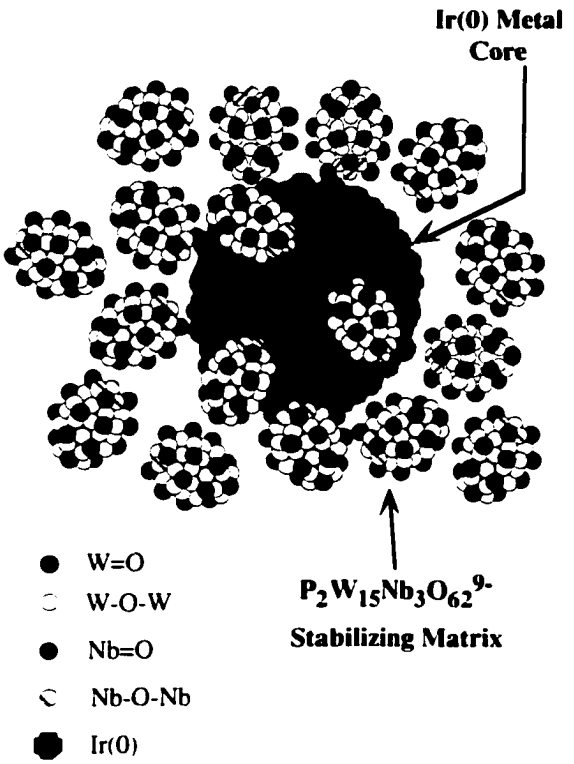

Figure 4.1. Idealized, roughly-to-scale representation of a $P_2W_{15}Nb_3O_{62}^{9-}$ polyoxoanion and Bu_4N^+ stabilized $Ir(0)_{\sim 300}$ nanocluster, $[Ir(0)_{\sim 300}(P_4W_{30}Nb_6O_{123}^{16-})_{\sim 33}](Bu_4N)_{\sim 300}Na_{\sim 228}$. The Ir(0) atoms are known (by electron diffraction) to be cubic-close packed as shown.[5] For the sake of clarity, only 17 polyoxoanions are shown, the polyoxoanion is shown in its monomeric, $P_2W_{15}Nb_3O_{62}^{9-}$ form (and not as its Nb-O-Nb bridged, anhydride, $P_4W_{30}Nb_6O_{123}^{16-}$ form that is known to be present[5]), and the ~300 Bu_4N^+ and ~228 Na^+ cations have been deliberately omitted. The highly catalytically active, bottleable the redissolvable $Ir(0)_{\sim 300}$ nanoclusters[2,5,8] have been extensively characterized by TEM, electron diffraction, electrophoresis, elemental analysis, ultracentrifugation MW determination, and IR and UV-visible spectroscopy.[2-5] The polyoxoanion component of our nanoclusters is without precedent in any previous type of nanocluster or colloid, a point that is fortified by the knowledge that the required type of basic polyoxoanion (i.e., with surface oxygen basicity) is new.[2]

In 1997 we reported[8] the development of an indirect—but continuous, easy, highly quantitative and thus powerful—method to monitor the formation, eq. 1, of the Ir(0) transition-metal nanoclusters in Figure 4.1 via their catalytic hydrogenation (H_2 uptake) activity, Figure 4.2. The new method exploited the concept of *pseudoelementary*[9] reaction

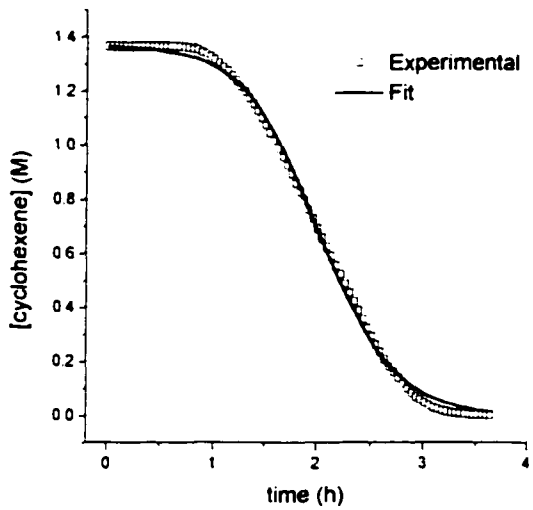

Figure 4.2. Typical cyclohexene loss vs time curve and curvefit demonstrating the generally excellent fit to the nucleation plus autocatalysis, then hydrogenation, three-step kinetic model in eqs. 2(a-c). The first ca. 30 minutes of the pressure data was back extrapolated to remove the rise seen due to the acetone solvent's vapor pressure re-equilibration; see the section that follows on this topic for further details. The observed data points do not show error bars from the high-precision pressure transducer measurement of the H_2 consumption since they are ± 0.01 psig (which translates to ± 0.001 M cyclohexene) and thus are too small to depict (i.e., are smaller than the width of the line shown). The error bars on the rate constants k_1 and k_2 that result from the kinetic analysis and curvefits, *vide infra*, are typically 10-15%. The deviation of the curvefit from the data late in the reaction is also understood, being due to cyclohexene concentration nearing zero and the resultant failure of step 2c to be faster than steps 2a and 2b, *vide infra* (i.e., the expected failure at low [cyclohexene] of the pseudoelementary concept used to follow the nanocluster formation reaction, *vide infra*). Note that these kinetic curves and their underlying nucleation and autocatalytic growth are sensitive functions of the exact water content and purity / source of the acetone solvent,[5h] the H_2 pressure, the temperature, the presence of additional $[P_2W_{15}Nb_3O_{62}]^{9-}$ polyoxoanion, trace O_2, and other variables,[8] factors that must be considered when comparing individual kinetic curves and their k_1 and k_2 rate constants (*vide infra*).

steps, eqs 2a-d. (where **A** in eqs. 2(a-d) is the precatalyst, $[Bu_4N]_5Na_3[(1,5\text{-}COD)Ir{\bullet}P_2W_{15}Nb_3O_{62}]$, and **B** is the catalyst composed of the Ir(0) surface sites on the near-monodisperse[2] distribution of developing nanoclusters, *vide infra*).

$$300\,[(1,5\text{-COD})Ir{\bullet}P_2W_{15}Nb_3O_{62}]^{8-} + 750\,H_2 \rightarrow Ir(0)_{\sim 300}{\bullet}(P_2W_{15}Nb_3O_{62}^{9-})_{\sim 66} + 300\ \text{cyclooctane} + 300\,H^+ + \sim 234\,[P_2W_{15}Nb_3O_{62}]^{9-} \quad (1)$$

$$x \left[A \xrightarrow[H_2]{k_1} B \right] \quad (2)a$$

$$1\text{-}x \left[A + B \xrightarrow[H_2]{k_2} 2\,B \right] \quad (2)b$$

$$\sim 1400 \left[B + \text{cyclohex}\textit{ene} + H_2 \xrightarrow{k_3} B + \text{cyclohex}\textit{ane} \right] \quad (2)c$$

$$\underline{\text{SUM:}} \quad A + \sim 1400\ \text{cyclohex}\textit{ene} + \sim 1400\,H_2 \xrightarrow{k_{obs}} B + \sim 1400\ \text{cyclohex}\textit{ane} \quad (2)d$$

A consideration of eq. 2d, the reaction obtained by summing the three steps outlined in eqs. 2a-2c, reveals that 2d is an illustrative example of the concept that Noyes has termed a pseudoelementary step.[9] If the third step, 2c, is fast on the timescale of the first and second steps, then the kinetics of the overall reaction, 2d, will be those of steps 1 and 2 only—*the desired nanocluster formation reactions*. This is shown in a perhaps more intuitive way in Figure 4.3. In other words, step 2d can then be treated and used kinetically as equivalent to an elementary step, even though step 2d is obviously not elementary—but is pseudoelementary—since it is composed of the three steps shown, 2(a-c).

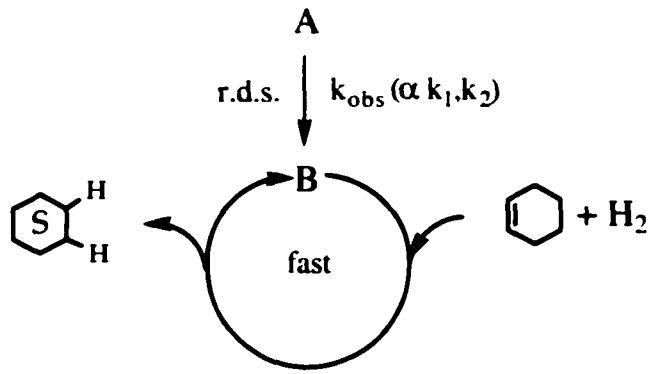

Figure 4.3. Simplified illustration of how transition-metal nanocluster formation is monitored via the fast, follow-up catalytic reaction of cyclohexene hydrogenation. As before, **A** is the precatalyst, $[Bu_4N]_5Na_3[(1,5\text{-COD})Ir{\bullet}P_2W_{15}Nb_3O_{62}]$, and **B** is the growing $Ir(0)_n$ nanocluster catalyst.

Experimentally, the excellent fit to the data using equations 2a-2c requires that the third step, 2c, be fast in comparison to the first two steps, 2a and 2b. In addition, we have confirmed experimentally the prediction that rate constants k_1 and k_2 for the nucleation and autocatalytic surface growth pseudo-elementary steps are *zero-order* with respect to cyclohexene concentration under the reaction conditions—that is, equation 2c involving cyclohexene has been shown to be fast as required to follow the growth of the nanoclusters via the pseudoelementary step, 2d.[8.10]

Note also that *only* if an autocatalytic step, A + B → 2B, specifically eq. 2b, is included, have we been able to come even close to fitting the observed kinetic data, Figure 4.2, as explained in greater detail elsewhere.[8.11] This result is intuitive as well in that we know of no other kinetic function which will allow a reaction to sit seemingly "dormant" for an hour, but then "turn on" and go to completion in a mere additional 2 hours, Figure 4.2. Confirming the apparent uniqueness of autocatalysis in explaining the kinetic data in Figure 4.2, we have also demonstrated (using numerical integration methods) that we were unable to find empirically any function other than autocatalysis that even comes close to fitting the observed kinetic curves.[11]

Our 1997 kinetic and mechanistic investigation of transition-metal nanocluster formation under H_2 also confirmed, by a second more direct (albeit less convenient and less precise) GLC method, that the use of the pseudo-elementary step method indeed works, and does so quantitatively giving the exact same rate constants k_1 and k_2 within experimental error as the pseudo-elementary step method. The details of the GLC data analysis include verification of the mathematically required stoichiometry factor (the 1400 in eq. 2c) and how to handle the changing fraction of surface atoms on the nanocluster (the "scaling factor", $(1 + x_{growth}) / 2$, shown in part B of Scheme 4.1, i.e., the mathematics needed to correct for the fact that the true growth reaction is not exactly A + B —> 2B but, instead, involves n —> n + 1 for $A + Ir(0)_n$ —> $Ir(0)_{n+1}$).[8] These important details are available both in the Supporting Information to the present paper, as well as in our 1997 paper[8] for the convenience of the interested reader.

The end result of our kinetic and mechanistic studies is a more quantitative, more exact mechanistic description of nanocluster formation as summarized schematically in the minimal, Occam's Razor mechanism shown in Scheme 4.1. Independent evidence for a diffusive, agglomerative growth step in competition with the autocatalytic surface growth (i.e., and as a function of H_2 pressure as the mechanism in Scheme 4.1 predicts) has also been published.[12] The availability for the first time of a convenient, facile method for following nanocluster formation allowed us to determine the effects on nanocluster nucleation (k_1) and growth (k_2) of reagents such as H_2O, H^+, added polyoxoanion, and changes in temperature.[8] Application of the new kinetic method also yielded a mechanistic basis for how and why "magic number" nanoclusters tend to form (as a natural consequence of autocatalytic surface growth[13]), insights into the concept of "living metal polymer" growth of nanoclusters and all its implications for size-and shape control[13]; and the first rational prescription for the synthesis of all possible geometric isomers of onion-shell, bi-, tri- and higher multimetallic nanoclusters.[13]

A) Nucleation (slow, continuous, homogeneous)

$$A \xrightarrow[H_2]{k_1} B$$

$$\leq 15\ Ir^{(I)} \xrightarrow[H_2]{k_1} Ir(0)_{\leq 15} \equiv$$ 

(Critical Nucleus)

B) Autocatalytic Surface Growth

$$A + B \xrightarrow[H_2]{k_2\ (obsd)} 2\ B$$

(This is the step repeated ≥ 300 times to yield $Ir(0)_{\sim 300}$)

$$Ir(0)_n + Ir^{(I)} \xrightarrow[H_2]{k_2\ (obsd)} Ir(0)_{n+1} \equiv$$ 

$$\text{Where } k_2\ (obsd) = k_2\left[\frac{1 + x_{growth}}{2}\right]$$

C) Diffusive Agglomerative Growth

$$Ir(0)_n + Ir(0)_m \xrightarrow{k_3} Ir(0)_{n+m}$$

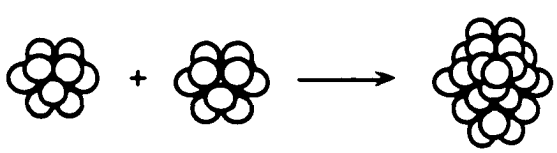

Scheme 4.1. Pictorial view of the proposed, minimum mechanism of formation of the Ir(0) and other transition-metal nanoclusters prepared under H_2.[8]

Despite the considerable success of the kinetic and mechanistic studies summarized above, several important questions remained unanswered, questions which require experimental scrutiny. Can one follow the nanocluster formation reaction directly in the absence of cyclohexene substrate, and by a method which yields precise kinetic data? If so, does that method also produce a sigmoidal kinetic curve? Can a curve directly monitoring of the conversion of $[Bu_4N]_5Na_3[(1,5\text{-COD})Ir{\bullet}P_2W_{15}Nb_3O_{62}]$ under H_2 into nanoclusters

be fit by the nucleation and autocatalytic growth mechanism with its k_1 and k_2 rate constants? Can the nanocluster sizes implied by the mechanism in Scheme 4.1 be verified directly by transmission electron microscopy (TEM) studies, namely smaller nanoclusters initially, then larger nanoclusters as time passes and as the autocatalytic surface growth mechanism operates? Is there commercial software that can be used to do the non-linear least-squares curve-fitting of the data in, for example, Figure 4.2, thereby making this new kinetic method more convenient to use for others (and if so does it verify the rate constants obtained by the programs we in part wrote and used initially)? Does a control experiment fully support our past back-extrapolation treatment of the initial pressure rise seen experimentally in the induction period and attributed to the volatile acetone solvent's vapor pressure? Can we show that the pseudo-elementary step method for following nanocluster growth works for other, more difficult and slower reactions[14] and with metals other than Ir (e.g., the Rh catalyzed arene hydrogenations that we are investigating[15])? Can we show that a computer numerical integration kinetic simulation of the more detailed mechanism implied by Scheme 4.1, consisting of the first 50 or so truly elementary mechanistic steps, produces a sigmoidal curve as expected? If so, can such a simulated curve be fit by our A —> B, A + B —> 2B (rate constants k_1 and k_2) model, thereby offering further support for the mechanism in Scheme 4.1 and its implied more detailed version? (Or, if not, what needs to be added or changed in the minimalistic, Occam's Razor mechanism in Scheme 4.1?) And, finally, what else can we learn about the mechanism in Scheme 4.1 if we examine additional metals such as Ru(II) under H_2 and en route to its corresponding nanoclusters? It is exactly these previously unanswered questions which are experimentally investigated herein and in the order presented above.

Results and Discussion

Verification of the Kinetic Method and the H_2 Uptake Stoichiometry in eq. 1: Hydrogen Uptake of the Precatalyst in the Absence of Cyclohexene and in Propylene Carbonate Solvent. The new kinetic method presented herein uses the convenient but indirect means of cyclohexene hydrogenation activity to follow nanocluster growth. When possible, it is best to verify such indirect methods by direct techniques. We were able to do just that by following the reduction of the precatalyst **A** in the absence of substrate. The experiment was performed on a high vacuum line with a high-precision pressure transducer capable of detecting ±0.1 torr (i.e., ± 0.002 psig) pressure changes—that is, a transducer 5 times more sensitive than our standard hydrogenation system for monitoring nanocluster formation via cyclohexene hydrogenation.[8] Initially, we attempted to use our standard solvent of acetone[5,8] to performed the desired H_2 uptake experiment. However, it was discovered using this more sensitive detector that, at least in the absence of the more readily hydrogenated cyclohexene, the $Ir(0)_n$ nanoclusters slowly hydrogenate the acetone solvent to form 2-propanol. (The formation of 2-propanol was verified by GLC and ^1H NMR, as shown in Figures 4.G, 4.H and 4.I of the Supporting Information.) Hence, acetone proved unsuitable for H_2 uptake experiments monitoring the reduction of **A** alone (but not for nanocluster studies followed by the much faster cyclohexene hydrogenation and where the net H_2 consumption due to solvent hydrogenation is negligible).

A search for suitable solvents revealed that propylene carbonate is *not* hydrogenated under the conditions of the H_2 uptake experiments and even at the detection limits of the high-precision pressure transducer. Accordingly, the hydrogen uptake due to the reduction of $[Bu_4N]_5Na_3[(1,5\text{-COD})Ir{\bullet}P_2W_{15}Nb_3O_{62}]$, **A**, alone was followed vs. time and to ±0.1 torr in an experiment in which 0.103 g **A** was dissolved in 2.0 mL propylene carbonate at 22.5 °C and with an initial H_2 pressure of 263.3 torr (5.091 psi). Note that these conditions

are necessarily at a lower H_2 pressure, as well as a different solvent, in comparison to our 40 psig H_2 (ca. 52 psi at our mile-high altitude where atmospheric pressure is ca. 640 torr) and acetone "standard conditions" used in our previous kinetic studies employing the pseudoelementary step method.[8]

Despite the necessarily different reaction conditions, the resulting hydrogen uptake curve, Figure 4.4, still has the expected sigmoidal shape; the associated induction period is about 30 min and the complete reaction time is about 4 h. As Figure 4.4 also shows, the resultant H_2 uptake curve can be closely fit by the identical analytic kinetic equations used previously (eqs. 2a and 2b above).[8] Note that the curve in Figure 4.4 is now closely fit even at the end of the reaction (*cf.* to the poorer fit in Figure 4.2 for this part of the curve), as it should be since there is no cyclohexene hydrogenation reporter reaction (no use of the pseudoelementary step concept) in the experiment recorded in Figure 4.4. The resultant rate constants under the specified conditions of propylene carbonate solvent, 22.5 °C, and 5.091

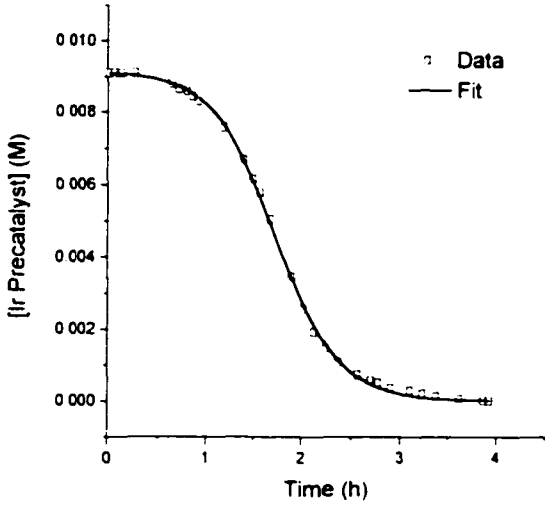

Figure 4.4. Plot of the loss of Ir precatalyst A (or, equivalently by eq. 1 the H_2 uptake) vs time due to the reduction of A by H_2 and in the absence of added cyclohexene. As shown, the sigmoidal curve is fit almost exactly by the identical analytic kinetic equations, corresponding to eqs. 2a and 2b (*vide supra*), which were used in our earlier work to fit kinetic curves such as the one back in Figure 4.2.

psi H_2 are $k_1 = 0.017\ h^{-1}$ and $k_{2(fit)} = 330\ M^{-1}h^{-1}$ (no correction has been made to $k_{2(fit)}$ for the *net* 3.5 H_2 to 1.0 **A** stoichiometry, nor were any other stoichiometry or scaling factors applied—see the Supporting Information for details).[16] The main conclusion from the H_2-uptake kinetic experiments, then, is the unequivocal demonstration that the reduction of **A** occurs in an autocatalytic manner. This experiment, in turn, provides strong support for the validity of our pseudo-elementary step kinetic method as a viable means for following nanocluster growth using the cyclohexene hydrogenation activity indirect assay.

Also of interest from the H_2 uptake experiment is the net stoichiometry in comparison to the predicted 2.5 H_2 to 1.0 **A** stoichiometry given back in eq. 1 in which the 1.0 additional equivalent of H_2 has been subtracted for the established reduction of the $P_2W_{15}Nb_3O_{62}^{9-}$ polyoxoanion to its 2 electron reduced "heteropolyblue",[5,8] $P_2W_{15}Nb_3O_{62}^{9-} + H_2 \longrightarrow P_2W_{15}Nb_3O_{62}^{11-} + 2\ H^+$. Experimentally, and as expected, 3.6 ± 0.4 equiv of hydrogen (i.e., 2.5 + 1.0 = 3.5 equiv) was consumed per equivalent of **A** in the experiment shown in Figure 4.4. Also, the expected 1.0 equiv of cyclooctane product were evolved within experimental error (experimentally 1.2 ± 0.2 equiv.), as confirmed by quantitative GLC for the experiment shown in Figure 4.4, verifying that part of eq. 1 as well. As has been noted elsewhere, such quantitative studies of nanocluster formation reactions leading to complete equations which include mass and charge balance, are unfortunately a rarity in all of the nanocluster formation literature.[2d] Such balanced equations are, however and of course, *a prerequisite* to meaningful mechanistic studies.

A Second Verification of the Kinetic Method and Its Implied Nanocluster Formation Mechanism in Figure 4.3: Nanocluster Size vs Time as Determined by TEM.

Nanocluster growth can also be followed directly by monitoring nanocluster sizes by TEM throughout a nanocluster formation reaction[7,17]—a powerful, direct way to follow nanocluster growth, at least *in principle*. In practice, the usefulness of TEM for kinetic

studies of nanocluster growth in real time is greatly restricted by the time required to prepare the sample and to obtain even a single data point. In addition, the intrinsic TEM error limits of ±2 Å for non-HR-TEM microscopes propagate to an experimental error approaching ±5 Å in our experience,[13] a distance equivalent to plus or minus an entire shell of Ir(0) metal atoms. In short, a size difference of >10 Å between two TEM "kinetic data points" is required to assure that the sizes are experimentally distinguishable. Despite these drawbacks, we felt it was important to verify by TEM the predicted features of nucleation and autocatalytic growth in the mechanism in Scheme 4.1: that one expects not to be able to see the small (<10Å) nanoclusters during the induction period,[18] that one expects relatively small nanoclusters to be visible directly following the induction period, and that one expects nanoclusters of increasing size as the reaction continues to completion.

Two experiments were done to test these predictions. In the first experiment, a normal cyclohexene hydrogenation was started and then a sample was removed for TEM analysis after 30 min under hydrogen, a time which was still within, but approaching the end of, the induction period. No nanoclusters were seen by TEM in this sample, as expected, indicating that they are <10 Å or so in size. Since in the strictest sense this is a negative result, the control was done of confirming by TEM that in this particular reaction, after going to completion (20 h under hydrogen pressure), 23 (± 4) Å nanoclusters were in fact formed (68 nanoclusters were measured; the reported error is ±1σ). It should also be noted that the hydrogen uptake curve (Figure 4.C of the Supporting Information) for this experiment is very similar to that in Figure 4.5, and exhibits the characteristic sigmoidal shape.

In the second experiment a normal cyclohexene hydrogenation experiment was started and a sample was removed for TEM analysis, but now after 50 min under hydrogen pressure and, hence, soon after the end of the induction period, Figure 4.5. The sample from the hydrogenation in Figure 4.5 contained 16 (± 3) Å nanoclusters by TEM (180 nanoclusters were measured). Another TEM sample was then harvested *from this same*

hydrogenation experiment, only now after 20 hours of reaction under hydrogen, a time at which all of the precursor **A** is known to be converted into nanoclusters.[8] This 20 h sample contained 27 (± 4) Å nanoclusters (207 nanoclusters were measured). In short, and as the new kinetic method and its resultant minimal mechanism (Figure 4.3) predict, the nanoclusters are <10 Å, 16 (± 3) Å, and 27 (± 4) Å as their sigmoidal formation curve, Figure 4.5, proceeds.

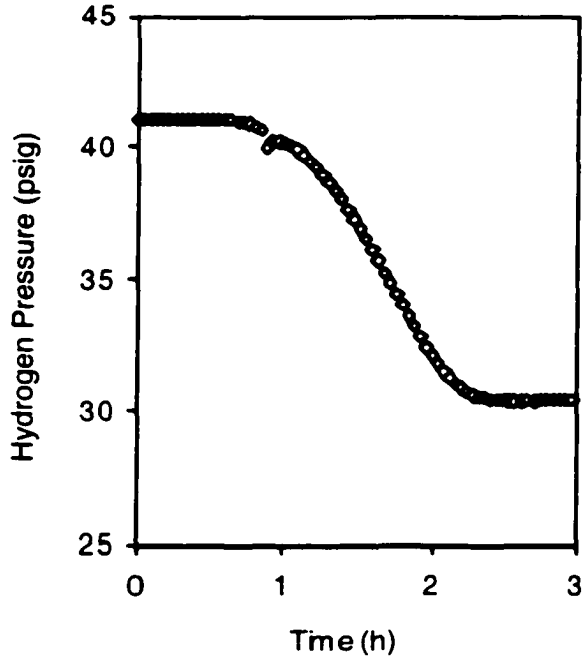

Figure 4.5. Hydrogen uptake curve in which a sample was removed for TEM analysis at 50 min. The temporary discontinuity in the curve at 50 min is due to the deliberate removal of a sample for TEM analysis. The first ca. 30 minutes of the pressure data was back extrapolated to remove the rise seen due to the acetone solvent's vapor pressure re-equilibration; see the section that follows on this topic for further details.

The Use of a Commercial Software Package for the Curvefit Data Analysis.

Previously, curve-fitting of the H_2 pressure (or, equivalently, the cyclohexene concentration) vs. time data was performed using a non-linear regression subroutine (RLIN),[8] available in the IMSL Statistical Library, a subroutine which uses a modified

Levenberg-Marquardt algorithm.[19] Calculations were done on an IBM/AIX workstation. A FORTRAN program was written which reads the list of input data points, defines the analytical expression to be used in the curvefit, asks for initial guesses of the variables (k_1 and k_2), and calls the appropriate RLIN subroutine.

Despite the full documentation of the above programs available elesewhere,[8] it seemed clear that the use of commercially available software that would run on a PC would aid the use of the new kinetic method detailed herein. Hence, we searched for generally available commercial packages that we could then test. As detailed below, the well-documented, commercial, non-linear least-squares curve-fitting package Microcal Origin works well (we used version 3.5.4). Origin also uses a Levenberg-Marquardt algorithm to generate the non-linear least-squares curvefit.

Two types of control experiments were done to assure that the values of the Origin-determined k_1 and k_2 are accurate. First, we calculated a "mock" set of data choosing k_1 = 0.005 h^{-1}, k_2 = 1 $M^{-1}h^{-1}$, $[A]_0$ = 1.2 M, and using a time interval of 2.5 min (typical data as well as the same time interval that we use for a typical hydrogenation experiment). Fitting the first 110 data points in the calculated, mock data set, Origin found the same values (and produced the error bars) of: $k_1 = 0.0050 \pm (6 \times 10^{-9})$ h^{-1} and $k_2 = 1.0 \pm (3 \times 10^{-7})$ $M^{-1}h^{-1}$, obviously identical to the input k_1 and k_2 values. This curvefit is available in the Supporting Information as Figure 4.D.

Second, an experimental data set from a hydrogenation experiment starting with the precursor **A** was curve-fit using our previous curve-fitting routine.[8] The resulting values of k_1 and k_2 were 0.0042 and 5.29, respectively. Next, the *exact same data points* were fit with Origin, resulting in k_1 and k_2 values of 0.0042 ± 0.0003 and 5.30 ± 0.06 (the error bars, again, are those determined by Origin). Again, the k_1 and k_2 values are identical within the error limits of the fit.

These results: (i) identify a readily available, commercial curve-fitting package; (ii) validate the accuracy of that package for the present situation and curvefits, and (iii) also serve as a quantitative verification of the numbers from our previous curve-fitting program.

Control Experiments Examining Two Different Ways to Correct for Solvent Vapor Pressure, and the Effect on the Resultant k_1 and k_2 Values from the Curvefit.

As detailed in the Experimental section, the protocol for hydrogenation experiments with cyclohexene involves filling a Fischer-Porter (hereafter, F-P) pressure bottle with acetone solvent, cyclohexene and the precatalyst **A**, all done in an N_2 atmosphere drybox. Then the F-P bottle is removed from the drybox, and attached to the hydrogenation line via Swagelok TFE-sealed quick-connects (a full drawing of the apparatus is available elsewhere[5b]). Next, the N_2 in the F-P bottle is flushed out and replaced with 40 psig H_2. This is accomplished with 13–15 purge cycles (which consist of pressurizing the F-P bottle to ca. 40 psig H_2, then releasing the pressure from the vent valve) before the final pressurization to 40 psig H_2. During the purging cycles solvent vapor is also unavoidably swept out of the F-P bottle. Over the initial part of the hydrogenation experiment (ca. 1/2 hr) the solvent vapor pressure returns to equilibrium, resulting in an initial *increase* in pressure being seen (as in Figure 4.6a). Our past treatment of this pressure increase[8,12,13,20] has been to simply back-extrapolate the data from the linear part of the induction period (and for induction periods longer than ca. 1/2 hour, *vide infra*), thereby removing this experimental artifact. This back-extrapolation was performed on the data shown in Figures 4.2 and 4.5, for example.

To test the validity of the back-extrapolation treatment of the data we did a control experiment where we measured pressure vs time data for the vapor pressure increase of the acetone (plus its dissolved cyclohexene) following a standard cycle of purges. We then used that data to correct, point-by-point, the original data (i.e., before the back-extrapolation)

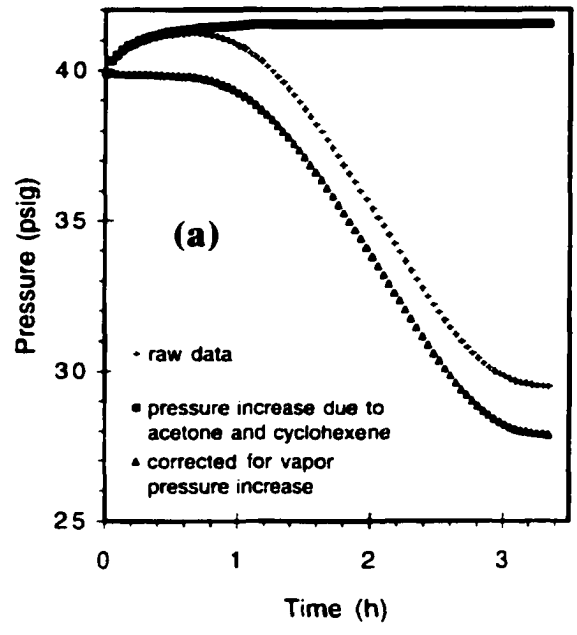

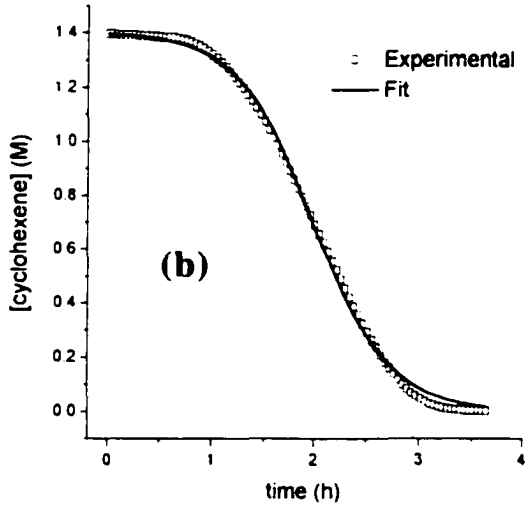

Figure 4.6. (a) Pressure vs time plot showing the raw data from the hydrogenation experiment shown in Figure 4.2 (note the initial increase in pressure due to solvent vapor pressure equilibration), the measured pressure vs time data for the vapor pressure increase of the acetone (plus its dissolved cyclohexene) following a standard cycle of purges in our apparatus, and the experimentally corrected hydrogen uptake curve. (b) The curvefit of experimentally corrected hydrogen uptake curve yields k_1 and k_2 values that are the same (within experimental error) as for the back-extrapolated (normal treatment) data. A comparison of Figure 4.6b with Figure 4.2 shows the similarity of the two curves and the two curvefits.

from the cyclohexene hydrogenation experiment shown in Figure 4.2. Those curves are shown in Figure 4.6a. The experimentally corrected data were then curve-fit, Figure 4.6b. The k_1 and k_2 values for the experimental vapor pressure corrected data are $k_1 = 0.013\ h^{-1}$ and $k_{2(hydrogenation\ corrected} = 3.4 \times 10^3\ M^{-1}h^{-1}$, compared to $k_1 = 0.010\ h^{-1}$ and $k_{2(hydrogenation\ corrected} = 3.6 \times 10^3\ M^{-1}h^{-1}$ for the back-extrapolated data (normal treatment of the data).

An analysis of the data shows: (i) that, indeed, it is the acetone solvent vapor pressure that causes most of the initial rise in pressure seen in the first ca. 1/2 hour of the induction period; (ii) that the experimentally corrected data may give a marginally better fit; but (iii) that the two treatments give k_1 and k_2 within experimental error (±15%) of each other; so (iv) that the more easily used, back-extrapolation method is what we recommend and what we will continue to use *so long as the induction period is ≥ca. 1/2 hour.* In addition, (v) that no such problem exists in cases where a less volatile solvent can be used (as in the use of propylene carbonate in Figure 4.4; note the lack of an initial pressure rise in that curve), but, correspondingly, the use of a more volatile solvent, substrate or product will require correction for their vapor pressure—that is, this is a subtle but important design feature in using the new method detailed herein. A derivation of the associated, simple pressure equations needed to understand exactly the underlying kinetics and mathematics of this vapor pressure correction to the kinetic experiments is provided in the Supporting Information.

Evidence for the New Method Being Applicable to Other Metals and Reactions: the Case of Rh(0) Nanoclusters in Olefin *and* Arene Hydrogenation. We have recently used the new kinetic and pseudoelementary step method herein to follow the formation of 40 ± 6 Å *Rh(0)* nanoclusters from hydrogenation of the precursor, $[Bu_4N]_5Na_3[(1,5\text{-COD})Rh{\bullet}P_2W_{15}Nb_3O_{62}]$, and in the presence of cyclohexene.[20] In an experiment directly analogous to that with the Ir congener, **A**, the Rh precursor yielded a sigmoidal hydrogen uptake curve, one closely fit by the kinetic equations 2a-2d, as shown in

Figure 6 of reference 19. This shows that the method is applicable to at least Rh, Ir and, by implication, probably other transition metals as well. (See a later section for the application of the new method to Ru(0) nanocluster formation and the interesting findings which resulted.)

We wanted to see if we could change reactions, specifically to a more difficult, slower reactions such as arene hydrogenation,[21] but then still use the new kinetic method to follow nanocluster formation.[22] Indeed, we have successfully done such an experiment using the Rh(0) nanocluster precursor, $[Bu_4N]_5Na_3[(1,5\text{-COD})Rh{\bullet}P_2W_{15}Nb_3O_{62}]$, and benzene as the substrate.[15] We have been able to use the new kinetic method herein to follow nanocluster formation for a second case of arene hydrogenation. Specifically, elsewhere[22] we have shown that the true catalysts, when beginning from the ion-pair precursor $[(C_8H_{17})_3NCH_3]^+[RhCl_4]^-$, are the Rh(0) nanoclusters that are shown to be present by TEM, *not* the discrete, monometallic ion-pair as previously believed (see the references provided elsewhere[22]). The data demonstrate that the $[(C_8H_{17})_3NCH_3]^+[RhCl_4]^-$) precursor cannot be the catalyst to within the $\leq \pm 15\%$ error limits of the $A \rightarrow B$, $A + B \rightarrow 2B$ curvefits to the (in that case) mildly sigmoidal kinetic data[22]—that is, A can only be a catalyst precursor. The important point is that this is another example of the value of the new kinetic method and its ability to monitor nanocluster nucleation and growth.

Computer Kinetic (Numerical Integration) Modeling of Autocatalytic Surface Growth. In order to verify the general mechanism in Figure 4.3, we wanted to see if we could simulate, via numerical integration, the first 50 or so elementary steps implied by the pseudoelementary steps in Figure 4.3. In addition, we wanted to explicitly account for the range of nanoclusters of different sizes that are generated over the full course of the reaction, accounting explicitly and individually for the changing fraction of nanocluster surface atoms[23]—that is, to do this in a cluster-by-cluster way. The treatment of the (changing) fraction of surface atoms is important since only the surface atoms can

participate in at least most common types of catalysis (i.e., and since we are not considering materials like metal oxides where bulk oxide can participate in oxidation catalysis, for example). Specifically, we wanted to answer the questions: does a more "realistic" mechanism for nanocluster growth give the same type of sigmoidal olefin hydrogenation curve as predicted by eqs. 2(a-d) and as seen in Figures 4.2, 4.5, 4.6 and 4.8. If so, can that curve be fit by the pseudo-elementary step model of eqs. 2(a-d)? Computer numerical integration kinetic modeling was used to answer these questions.

The kinetic model is shown in Scheme 4.2. The model first describes a $H_{2(gas)}$ to $H_{2(soln)}$ equilibrium. Then the nucleation [$\mathbf{A} \rightarrow M(0)_1$] and growth [$\mathbf{A} + M(0)_1 \rightarrow M(0)_2$ through $\mathbf{A} + M(0)_{44} \rightarrow M(0)_{45}$] steps follow. Lastly, the alkene hydrogenation steps are shown. The rate constants and initial concentrations used for the kinetic model were made to correspond to a standard hydrogenation experiment as much as possible; see the Experimental for a detailed discussion. Note that the rate constants in Scheme 4.2 are distinguished from other rate constants in the text by the addition of a "prime", for example k_1', k_2' and so on. The kinetic model in Scheme 4.2 assumes that the rate of olefin hydrogenation and the rate of reaction of **A** with the growing nanoclusters are structure insensitive[24] (i.e., that there is no particle size dependence, and every surface atom is assumed to have equal catalytic activity). The model also assumes that the nanoclusters grow in an "ideal" manner where each $M(0)_x$ corresponds to a single species[25] and where each shell of atoms becomes complete before growth occurs on the next shell. Nanocluster agglomeration is not accounted for in this model. The changing fraction of nanocluster surface atoms is explicitly taken into account by the choice of the rate constants k_2'–k_{90}'; full details are available in the Supporting Information. The nanoclusters were grown computationally to maximum size of $M(0)_{45}$ because this represents the limit of the kinetic modeling software employed—MacKinetics version 0.9.1b, which has a limit of 50 chemical species. The actual kinetic scheme, as it was typed into the MacKinetics program, is available in the Supporting Information.

$H_{2(gas)} \rightarrow H_{2(soln)}$	$k_f' = 1 \times 10^9$
$H_{2(soln)} \rightarrow H_{2(gas)}$	$k_r' = 4 \times 10^{11}$
$A \rightarrow M(0)_1$	$k_1' = 0.002$
$A + M(0)_1 \rightarrow M(0)_2$	$k_2' = 200$
$A + M(0)_2 \rightarrow M(0)_3$	$k_3' = 383$
$A + M(0)_3 \rightarrow M(0)_4$	$k_4' = 567$
•	•
•	•
•	•
$A + M(0)_{44} \rightarrow M(0)_{45}$	$k_{45}' = 6829$
$M(0)_1 + \text{alkene} + H_{2(soln)} \rightarrow M(0)_1 + \text{alkane}$	$k_{46}' = 4.00 \times 10^5$
$M(0)_2 + \text{alkene} + H_{2(soln)} \rightarrow M(0)_2 + \text{alkane}$	$k_{47}' = 7.67 \times 10^5$
$M(0)_3 + \text{alkene} + H_{2(soln)} \rightarrow M(0)_3 + \text{alkane}$	$k_{48}' = 11.3 \times 10^5$
•	•
•	•
•	•
$M(0)_{45} + \text{alkene} + H_{2(soln)} \rightarrow M(0)_{45} + \text{alkane}$	$k_{90}' = 139 \times 10^5$

Scheme 4.2. The kinetic model used to account for the production of nanoclusters of different sizes and for the effects of surface area. The time units in this Scheme are in hours and the concentration units are in molarity.

The results of this kinetic model are shown in Figure 4.7. Note that *the kinetic model does indeed produce a sigmoidal curve.* Furthermore, the curve produced *is closely fit (Figure 4.7) by the identical analytic kinetic equations used to analyze the experimental hydrogenation curves.* Hence, this more detailed mechanism for nanocluster growth does indeed give the same type of sigmoidal olefin hydrogenation curve as predicted by equations 2(a-d) and as seen experimentally in Figure 4.2. The values of the rate constants yielded by the curvefit in Figure 4.7 are $k_1 = 0.027\ h^{-1}$ and $k_{2(\text{hydrogenation corrected})} = 300\ M^{-1}h^{-1}$ ($k_{2(\text{hydrogenation corrected})}$ is the value of k_2 after correcting for both the scaling and the stoichiometry factors—see the Supporting Information for details). One might be tempted to compare the values of k_1 and $k_{2(\text{hydrogenation corrected})}$ to the individual rate constants k_1' and k_2' from Scheme 4.2. However, k_1 and $k_{2(\text{hydrogenation corrected})}$ are not elementary step rate constants, and are not solely dependant on values chosen for k_1' and k_2'. For example, k_1

and $k_{2(hydrogenation)corrected}$ both become larger as rate constant values for the olefin hydrogenation steps (k_{46}'–k_{90}') are increased. As a final note, additional simulations demonstrate that a sigmoidal olefin hydrogenation curve is also produced if one requires a "critical nucleus" to form before olefin hydrogenation activity can begin (see Figure 4.E of the Supporting Information for the case where the nanoclusters were required to be ≥ $M(0)_{13}$ before they became active olefin hydrogenation catalysts). On the basis of the fraction of cyclooctane evolution vs. time in our previous work, a critical nucleus size of ≤15 Ir(0) atoms has been estimated.[8]

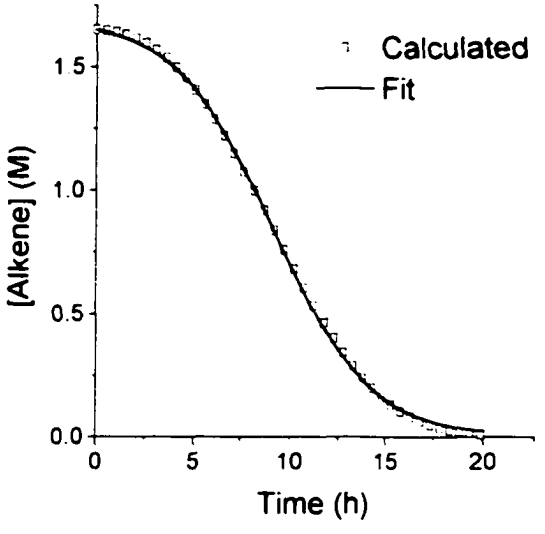

Figure 4.7. Results of the kinetic model showing that a sigmoidal curve is indeed produced. The "Calculated" points from the kinetic model produce a curve that is closely fit by the identical analytic kinetic equations used to analyze the experimental hydrogenation curves.

The Discovery of the Importance of Heterolytic Hydrogenation Activation—and the Need to Add Base to Initiate Nanocluster Formation—for Cationic Metals Such as Ru(II) That Do Not Undergo Ready *cis*-Oxidative Addition of H_2.

As part of our extension to other metals, we investigated the hydrogen uptake curves of a Ru(II) system based on the precatalyst $[Bu_4N][Ru(1,5\text{-}COD)(CH_3CN)(P_3O_9)]$, with cyclohexene present and using the pseudo-elementary step reporter method to monitor nanocluster formation. Not unexpectedly, we found that under H_2 alone, nanoclusters did not form (Figure 4.8a) even at times 5–10 fold longer than needed to form the Rh or Ir nanoclusters. We reasoned that oxidative-addition activation of H_2 by the present Ru(II) precursor to yield $Ru^{IV}(H)_2$ is energetically prohibitive. We further reasoned that heterolytic hydrogen activation[26] is required to initiate the formation of Ru(0) nanoclusters; hence, the addition of a base is crucial as can be seen by the general stoichiometry for heterolytic hydrogen activation, eq. 3. Note that depending upon the strength of the base and the pK_a of the resultant M–H, the required stoichiometry can be between 1 equiv of base (eq. 3a) and 2 equiv of base (eq. 3b and 3c).

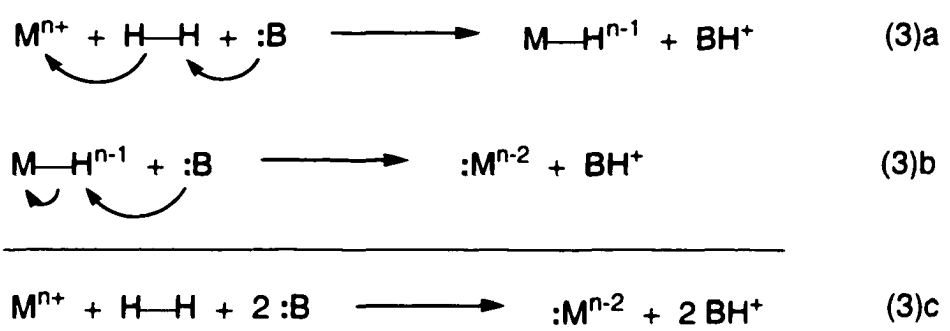

As Figure 4.8b shows, the addition of 1.0 equiv of tetrabutylammonium hydroxide ($Bu_4N^+OH^-$) does indeed "turn on" the formation of nanoclusters from this divalent metal precursor: the induction period for nanocluster formation (as monitored by their catalytic activity using the methodology reported herein) drops from >13 hours to about 10 minutes

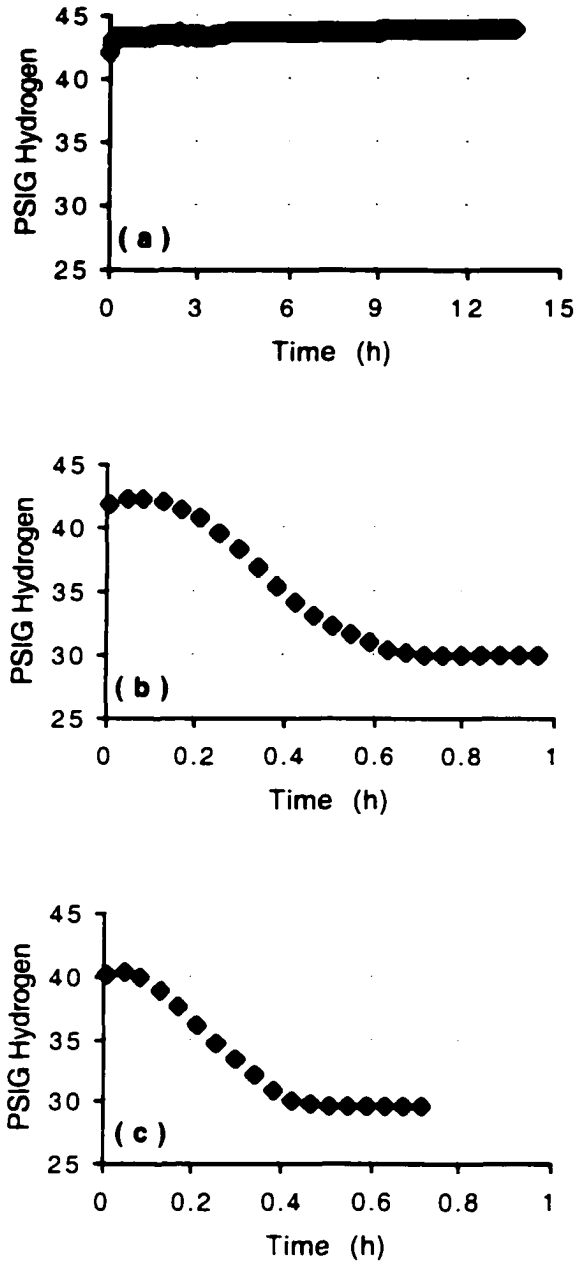

Figure 4.8. Hydrogen uptake curves produced by the Ru(II) precatalyst $[Bu_4N][Ru(1,5\text{-}COD)(CH_3CN)(P_3O_9)]$ in (a) the absence of base, with (b) 1.0 equiv of $Bu_4N^+OH^-$ added, and with (c) 2.0 equiv of $Bu_4N^+OH^-$ added. Not unexpectedly, we found that in the absence of added base (i.e., under H_2 alone), nanoclusters did not form even after >13 hours. The addition of 1.0 equiv of $Bu_4N^+OH^-$ does indeed "turn on" the formation of nanoclusters, shortening the induction period for nanocluster formation to about 10 minutes. The addition of a second equivalent of $Bu_4N^+OH^-$ shortens the induction period by a further factor of two to about 5 minutes.

for the Ru(II) precursor, a rate increase of >78 fold. Figure 4.8c shows that the addition of a second equivalent of strong base shortens the induction period by (only) an additional factor of two to about 5 minutes.

A search of the heterolytic hydrogen activation literature[26] revealed (i) that the key requirements for heterolytic hydrogenation are a metal whose oxidation state is high enough that further oxidation is unfavorable, an available coordination site and a way to stabilize the released proton (i.e, the presence of a base), especially in nonaqueous solvents; (ii) that amines, carboxylates, alkoxides and hydroxide are commonly used bases (the base can also be an internal M-R which undergoes a four-centered reaction with H_2 that is a second version of heterolytic hydrogen activation[26a]); and (iii) that it is difficult to distinguish mechanistically true heterolytic hydrogenation activation from the two-step sequence of oxidative addition followed by deprotonation of the metal hydride by the added base. Nevertheless, (iv) practically speaking the metals which undergo the net reaction stoichiometry of eq. 3, *where the presence of base may generally be required to initiate nanocluster formation, include Pd(II), Pt(IV), Ru(II), Ru(III), Rh(III), Ir(III), Ag(I), Au(III), Cu(I), and Cu(II).* Note that the added base is required only for the *nucleation step* back in Scheme 4.1; once $M(0)_n$ nanoclusters of the critical nucleus size (or larger) are formed they can then activate H_2 by *cis*-oxidative addition on the $M(0)_n$ surface and then grow by the autocatalytic surface-growth mechanism, Scheme 4.1. In fact, we recommend that the use of coordinating vs non-coordinating bases (e.g., a prototype non-coordinating base being Proton Sponge, 1,8-bis(dimethylamino)naphthalene) be a design consideration in the synthesis of nanoclusters of the above metals and under H_2, along with thoughts about whether or not more than 1 equivalent of a coordinating base should be used (excess base being a good ligand and, hence, a poison for nanocluster surface sites, thereby inhibiting subsequent surface-based, *autocatalytic* growth).

We wondered whether or not literature nanocluster formation reactions under hydrogen beginning with Pd(II),[27,28,29,30,31,32,33,34,35,36] Pt(IV),[28,35,36,37,38,39]

Ru(III),[35,40,41,42] Rh(III),[35,36,40,43,44,45,41,46,42] Ag(I),[28,29] Au(III),[28,29] Cu(II)[47,29] and Ir(III)[35,36] require the presence of added base. That is, has this very fundamental key to producing nanoclusters from metals in higher oxidation states been missed previously as we suspected? Has the availability of our new method for easily monitoring nanocluster growth allowed us to discover a key to the rational synthesis of nanoclusters from electrophilic metals placed under H_2?

In fact, a search of the nanocluster and colloid literature reveals that M(0) nanoclusters prepared from metal salts or organometallic complexes of Pd(II), Pt(IV), Ru(III), Rh(III), Ag(I), Au(III), Cu(II) and Ir(III) with hydrogen as the reductant have commonly been prepared *in the presence of a base*. Bases such as alkylammines,[35,40,41,42,43,44,45,46] ammonia,[47] carboxylates,[27,28,29,31,32,34] and alkoxides[30] have been used. It is also common for the base to be coordinated to the metal (e.g., palladium(II)acetate is often used as a precursor to Pd(0) nanoclusters when hydrogen is used as the reductant[27,31,32]). Interestingly, there appears to be only one prior example in the nanocluster synthesis literature where the necessity of the base was recognized.[47] However, even in that work the possible generality of heterolytic hydrogen activation for nanocluster formation from electrophilic metals went unrecognized.[47] Importantly, there are cases where nanocluster formation is not seen, even when forcing conditions are used, *but in the absence of base*.[48]

The lack of an easily applied method to follow nanocluster formation reactions in real time is probably what has delayed the discovery of heterolytic hydrogen activation in nanocluster formation until now. The present first recognition of the importance of heterolytic hydrogen activation in nanocluster nucleation reactions from higher valent metals placed under H_2, a discovery made possible by the new kinetic method presented in this paper, promises to be a valuable insight for the rational synthesis of nanoclusters of metals such as Pd(II), Pt(IV), Ru(III), Rh(III), Ag(I), Au(III), Cu(II) and Ir(III).

Summary and Conclusions

To summarize, our new indirect but continuous, easy, quantitative and powerful way to monitor transition metal nanocluster formation under H_2 has been developed in greater detail and with an eye towards making it as easy as possible for other researchers to use. The method has been further investigated, improved and documented: (i) by showing that direct monitoring of the nanocluster formation (by following the H_2 uptake due only to the nanocluster formation reaction or by following nanocluster size by TEM) gives the predicted sigmoidal kinetic curve and nanocluster size-dependencies vs time, respectively; (ii) by finding and testing for accuracy a commercial non-linear least-squares curve-fitting package that should be readily available and easily implemented by others; (iii) by doing key control experiments to document how to handle volatile solvents or substrates; (iv) by showing that nanocluster formation can be successfully monitored for other metals and more difficult reactions, such as Rh catalyzed arene hydrogenation; (v) by showing that computer kinetic simulations provide strong support for the more detailed mechanism implied by the Occam's razor mechanism in Scheme 4.1; and significantly (vi) by discovering, via the new kinetic method, heterolytic hydrogen activation with its requirement for ≥1 equivalent of added base in the nanocluster nucleation steps of certain higher valent, electrophilic metals. This last finding adds eqs. 3(a-c) as an important variant on the nucleation steps back in the generalized mechanism in Scheme 4.1. In fact, heterolytic hydrogen activation can now be added to the list of other findings noted in the Introduction and which were discovered using the new kinetic methodology presented herein (i.e., implications for shape and size control via the living metal polymer concept[13]; the first mechanistic explanation for why magic number sized nanoclusters tend to form[13]; how to make onion-skin geometry bi- tri- and higher multimetallic nanoclusters,[13] and now the importance of heterolytic hydrogen activation in the formation of nanoclusters under H_2 from higher valent M^{n+} precursors).

It is our hope that the present studies, plus our earlier work,[5,8,12,13,20,22] will allow others to use this new methodology to monitor their nanocluster formation reactions under reductive conditions. We are certainly continuing to use this methodology to monitor a wide range of nanocluster formation reactions in our own laboratories. Also planned are additional studies to see if the methods herein can be extended to a range of other reductants besides H_2, to a range of other metals whose nanoclusters are of interest, and to the important cases of particle-size-sensitive (i.e., "structure-sensitive") reactions.

Experimental

Materials. Acetone was purchased from Burdick & Jackson (water content < 0.2%) and stored in a Vacuum Atmospheres drybox. The source, purity and water content of the acetone or other solvents are known to be important in the nanocluster formation reaction.[5,8] Cyclohexene (Aldrich, 99%) was purified by distillation from Na under argon and stored in the drybox. Propylene carbonate (Aldrich, 99.7%, anhydrous, packaged under N_2) was transferred into the drybox and used as received. Ethanol (95 vol %) was prepared by mixing 19 mL of anhydrous ethanol (Pharmco) with 1.0 mL of "nano-pure" water (distilled water filtered through a Barnstead filtration system). Tetrabutylammonium hydroxide ($Bu_4N^+OH^-$) was purchased from Aldrich as a 1.0 M aqueous solution. A 0.5 M solution of $Bu_4N^+OH^-$ was made by diluting the 1.0 M solution with nano-pure water. The iridium nanocluster precursor complex $[Bu_4N]_5Na_3[(1,5\text{-COD})Ir{\bullet}P_2W_{15}Nb_3O_{62}]$ (**A**)[6a] was prepared from $[Bu_4N]_9[P_2W_{15}Nb_3O_{62}]$ made by our most recent method[6b] [and using $NbCl_5$ as the Nb source, as detailed in footnote 20 of reference 6b (this footnote has a typographical error—a 0.5% solution of H_2O_2 is used, *not* a 5% solution)] and was stored in the drybox. The ruthenium precatalyst $[Bu_4N][Ru(1,5\text{-COD})(CH_3CN)(P_1O_9)]$ was prepared following literature procedures[49] and was stored in the drybox.

Hydrogenations. These were generally done as before; see the Experimental Section elsewhere[8] under the identical heading, "Hydrogenations". Briefly, in the drybox 20 ± 1 mg of **A** was dissolved in 2.5 mL of acetone and 0.5 mL of cyclohexene. This bright yellow solution was transferred into a new 22 × 175 mm Pyrex culture tube containing a 5/8" × 5/16" stir bar. The culture tube was placed in a Fischer-Porter (F-P) pressure bottle modified with Swagelock TFE-sealed Quick-Connects. The F-P bottle was then sealed, brought out of the drybox, placed in a 22.0 °C temperature controlled water bath and connected to a H_2 line via the Quick-Connects. The F-P bottle was then purged 15 times (waiting 15 s between purges) with 40 psig H_2. Following the purges the F-P bottle was pressurized to 40 (± 1) psig H_2. During the purging (and during the hydrogenation reaction) the reaction solution was vortex-stirred. Five minutes after the beginning of the purges was designated $t = 0$, and at this time data collection was initiated using an Omega PX-621 pressure transducer interfaced to a PC.

Hydrogen Uptake from the Precatalyst Alone (i.e., in the Absence of Cyclohexene). A drawing of the gas-uptake apparatus used for this experiment is given in Supporting Information. It consists of the following major pieces: a high vacuum line (≤ 10^{-4} torr, as continuously monitored by a Varian 524-2 Cold Cathode Gauge); a 50 mL Pyrex reaction flask of known volume; and a MKS Type 122A Baratron pressure transducer (+999 torr maximum pressure; ±0.1 Torr), also of known volume.

While in a nitrogen atmosphere drybox, **A** (103.4 mg, 1.82×10^{-5} mol) was weighed into a two-dram vial. Propylene carbonate (2.0 mL) was then added via gas-tight syringe to yield a dark, orange-amber, homogeneous solution. This solution was transferred via disposable polyethylene pipet into the reaction flask (which also contained a 1 mm × 3 mm Teflon-coated magnetic stir bar). The flask was sealed, brought out of the drybox, and attached to the gas-uptake apparatus. Next, the reaction solution was degassed (to < 10^{-4} torr) via three freeze-pump-thaw cycles at liquid nitrogen temperature. On final thawing the reaction solution was warmed to room temperature (22.5 °C), vortex stirring was initiated,

and hydrogen was introduced into the vacuum line. Then the part of the vacuum line containing the reaction flask and the pressure transducer was isolated at an initial pressure of 263.0 torr H_2. Hydrogen uptake was observed after an induction period of approximately 30 minutes. No further hydrogen uptake was observed after 4 h of reaction, at which time the pressure had decreased to 249.9 torr H_2 (which corresponds to an uptake of 3.6 ± 0.4 equivalents of hydrogen per mole of **A**). During the course of the reaction the solution became a dark blue-black color as expected for the precedented formation of the 2 e– reduced, heteropolyblue-blue, $H_2[P_2W^{VI}_{13}W^{V}_{2}Nb_3O_{62}]^{9-}$.[5] Quantitative GLC confirmed that 1.2 ± 0.2 equiv of cyclooctane had evolved during the reaction, indicating complete reduction of **A**.

TEM Size Determination of the Ir(0) Nanoclusters vs the Extent of Their Formation Reaction. These experiments were started as "Standard Conditions" cyclohexene hydrogenations (see the section entitled "Hydrogenations"). At a predetermined time during the hydrogenation reaction (and as shown by the discontinuity in the data in Figure 4.5), a sample was withdrawn from the F-P bottle by first opening the F-P bottle up to the H_2 line, then opening the top (purge) valve on the F-P bottle. This arrangement provided a constant flow of H_2 out of the F-P bottle and thus protected the contents from O_2. An 18-inch, stainless steel needle (attached to a 1-mL plastic syringe) was threaded down into the F-P bottle and a 0.3 mL sample of the reaction solution was removed. (The needle and syringe were both purged with H_2 prior to insertion into the F-P bottle.) The sample was syringed into a disposable one-dram glass vial, which was capped immediately. The vent valve on the F-P bottle was then closed, the F-P bottle was repressurized to the pressure present just before the pressure release (see the discontinuity point in Figure 4.5), and the hydrogenation reaction was allowed to continue. A disposable syringe needle was then pushed through the cap of the sample vial before placing the sample into the antechamber of the drybox. After evacuation of the antechamber the sample (which was dry by this time) was brought into the drybox. The entire sampling procedure

took about 2 min, including repressurizing the F-P bottle and placing the sample in the antechamber.

After 20 h under hydrogen the hydrogenation reaction was stopped and TEM samples were prepared from the final reaction solution as described in a section available elsewhere[8] labeled "(G) Transmission Electron Microscopy (TEM)". Briefly, the F-P bottle was brought back into the drybox and the reaction solution (a dark suspension) was transferred into a glass vial. The polyoxoanion-stabilized nanoclusters were allowed to separate before removing the colorless supernatant with a pipet. The precipitate was then dried and sent as a solid to the University of Oregon for TEM analyses, performed there as before[8] by Dr. Eric Schabtach. The samples removed during the hydrogenation reaction (taken at 30 and 50 min in separate experiments) were also sent as solids to the University of Oregon for TEM.

The Use of a Commercial Software Package for the Curvefit Data Analysis. When making initial guesses in Origin for the values of k_1 and k_2 it was found that, in order for the subroutine to converge, one must guess a value of k_1 that is within about four orders of magnitude of the "real" value. Initial guesses for k_2 are simpler to make since the subroutine will almost always converge if the value guessed is *smaller* than the real value, even if the guess is 20 to 30 orders of magnitude smaller! However, guessing values of k_2 that are as little as 5 to 10 times larger than the real value can cause failure to converge. One advantage of using Origin is that it is not necessary to pick a wide range of empirical initial guesses to avoid local minima because one can watch as the curvefit approaches the data (i.e., Origin displays and continually updates its calculated curvefit for comparison to the actual data).

As with all numerical integration methods, it is important to choose the right units for the time data when curve-fitting in Origin. If the induction period is a big number in whatever time units chosen, then the value of k_1 is small with dimensions of those units^{-1}. As the value of k_1 becomes very small, the relative error in the curvefit generally becomes

larger (plus getting the program to converge if k_1 is very small seems to be more difficult). Hence, we recommend picking the time units (seconds, hours, days, etc) so that the induction period is about 10 of those units or less.

Computer Kinetic Modeling (Numerical Integration) of Autocatalytic Surface Growth. The initial concentrations used for the kinetic model (Scheme 4.2) were made to correspond to a standard hydrogenation experiment as much as possible. The initial concentrations of precatalyst and alkene used for the model were $[A]_0 = 0.0012$ M and $[\text{alkene}]_0 = 1.65$ M. MacKinetics cannot tolerate more than one kind of concentration unit (i.e., all concentrations must be in terms of molarity, pressure, or other appropriate units). Since a gas, H_2, is included in the kinetic model, the previously developed concept of a "hydrogen reservoir",[8,50] which converts the hydrogen pressure into a mathematically equivalent "molarity", needed to be employed. Put another way, the "hydrogen reservoir" is a way to treat pressures as if they were molar concentrations, but in a way that maintains the experimentally correct (known) amount of H_2 in solution for a given solvent and at a specified pressure. Using the "hydrogen reservoir" concept and using the conditions of the experiment shown in Figure 4.2 (except for the H_2 pressure, for which 40 psi was assumed) gives an $[H_2(\text{reservoir})]_i$ of 3.6 M (see page 144 of reference 50), and this is the initial value used for the concentration of $H_{2(gas)}$ in Scheme 4.2. The concentrations of all the other species is zero at $t = 0$.

The rate constants used for the kinetic model shown in Scheme 4.2 were chosen in following way. (All of the rate constants in Scheme 4.2 have time units of hours and concentration units of molarity.) The values of k_f' and k_r' were made large in comparison to the other rate constants in order to avoid H_2 gas-to-solution "mass transfer" limitations[12] (our cyclohexene hydrogenation experiments are purposefully run under conditions that avoid mass transfer limitations[12]). The ratio of k_f' to k_r' was determined by the "hydrogen reservoir"[8,50] concept which takes into account the known solubility of hydrogen in acetone.[51] The value of k_1' (in h^{-1}) was made small relative to $k_2'[A]$ (also in h^{-1}) because

autocatalytic surface growth is known to be faster than nucleation. The values of k_1' and k_2' were also adjusted to avoid a significant amount of $M(0)_{45}$ formation within the time required to hydrogenate all of the cyclohexene. (The formation of $M(0)_{45}$ is undesirable because it obscures the desired autocatalytic nature of the kinetic model; recall that the $M(0)_{45}$ species cannot grow any larger in this model, so autocatalytic surface growth can no longer take place for this species.) The values of k_1' and k_2' used in Scheme 4.2 lead to the formation of only a small amount of $M(0)_{45}$ near the end of the alkene hydrogenation (see Figure 4.F of the Supporting Information). The value of k_{46}', the rate constant for the first alkene hydrogenation reaction, was made large relative to k_2' because alkene hydrogenation is being used as a fast reporter reaction for nanocluster growth. The values of k_3'–k_{45}' and k_{47}'–k_{90}' were determined relative to k_2' and k_{46}', respectively, as described in detail in the Supporting Information (i.e., by taking into account the changing fraction of surface atoms).

The alkene hydrogenation curves resulting from the numerical integration were curve-fit in exactly the same way as our experimental data (shown in Figure 4.2, for example). The curves were imported into Origin and only the first half of the alkene loss was used for the curvefit. Also, the reported values for $k_{2(hydrogenation,corrected)}$ have been corrected for the stoichiometry factor and for the scaling factor (see the Supporting Information or our original treatment elsewhere[8]).

The Discovery of the Importance of Heterolytic Hydrogenation Activation—and the Need to Add Base to Initiate Nanocluster Formation—from Cationic Metals Such as Ru(II). The hydrogenation experiments with the precatalyst $[Bu_4N][Ru(1,5\text{-}COD)(CH_3CN)(P_3O_9)]$ were performed in the same manner as the hydrogenation experiments described above in the section labeled "Hydrogenations". In the drybox 5.4 (± 0.1) mg of $[Bu_4N][Ru(1,5\text{-}COD)(CH_3CN)(P_3O_9)]$ was dissolved in 2.5 mL of 95% ethanol and 0.5 mL of cyclohexene, forming a clear, pale yellow solution. The $Bu_4N^+OH^-$ base was added at this point with a 50 μL syringe. For the experiment with 2.0 equivalents of base, 15 μL of 1.0 M $Bu_4N^+OH^-$ was added. For the experiment with 1.0

equivalent of base, 15 μL of 0.5 M $Bu_4N^+OH^-$ was added. Addition of base caused no noticeable change in the solution's appearance. The pale yellow solution was transferred into a new 22 × 175 mm Pyrex culture tube containing a 5/8" × 5/16" stir bar. The culture tube was placed in a Fischer-Porter pressure bottle modified with Swagelock TFE-sealed Quick-Connects. The pressure bottle was then sealed, brought out of the drybox, placed in a 50 °C temperature controlled water bath and connected to a H_2 line via the Quick-Connects. The pressure bottle was then purged 15 times (waiting 15 s between purges) with 40 psig H_2. Following the purges the pressure bottle was pressurized to 40 ± 1 psig H_2. During the purging (and during the hydrogenation reaction) the reaction solution was vortex-stirred. Five minutes after the beginning of the purges was designated $t = 0$, and at this time data collection was initiated using an Omega PX-621 pressure transducer interfaced to a PC.

During the hydrogenation experiment with $[Bu_4N][Ru(1,5\text{-}COD)(CH_3CN)(P_3O_9)]$ in the absence of base the reaction solution remains clear and pale yellow. For the experiments with added base, the reaction solution became cloudy and brown and yielded an insoluble dark colored precipitate. A TEM of the experiment with 2.0 equivalents of base showed the presence of micrometer scale particles, presumably bulk metal (see Figure 4.K of the Supporting Information).

Acknowledgments.

The TEMs for this work were obtained with the expert assistance of Dr. Eric Schabtach at the University of Oregon's Microscopy Center. Dr. Nicola E. Brasch is acknowledged for her advice concerning commercial non-linear least-squares curve-fitting software. We also wish to thank Professor Steven H. Strauss at Colorado State University for allowing us to use his high-vacuum line for the H_2 uptake experiments. Financial

support was provided by the Department of Energy, Chemical Sciences Division, Office of Basic Energy, grant DOE FG06-089ER13998.

Supporting Information Available: Text describing a key control experiment demonstrating that the more direct monitoring of Ir(0) nanocluster formation by the GLC-determined evolution of cyclooctane gives identical rate constants, k_1 and k_2, within experimental error. Text describing the data analysis for cyclohexene hydrogenation experiments and how the changing fraction of nanocluster surface atoms is handled (i.e., the "scaling factor"). Figure 4.A showing a detailed schematic of the high-vacuum gas-uptake apparatus used to measure H_2 uptake from the reduction of **A** in the absence of substrate. Figure 4.B showing a histogram of nanocluster sizes when isolated after 50 min under H_2 and after 20 h under H_2. Figure 4.C showing the hydrogen uptake curve for the "standard conditions" cyclohexene hydrogenation experiment where a TEM sample was removed after 30 min. Figure 4.D showing the curvefit generated in Origin to a "mock" data set. Text describing, in the kinetic modeling, the "Treatment of the Changing Fraction of Surface Atoms by the Relative Values of k_2'–k_{90}'", plus the actual program used for the kinetic modeling experiment in MacKinetics. Figure 4.E showing the results of the kinetic modeling program if a "critical nucleus" size of $M(0)_{13}$ is used. Figure 4.F showing the concentration vs time curves for several $M(0)_x$ species in the kinetic modeling experiment. Figures 4.G, 4.H and 4.I showing GLC and ^1H NMR confirmation that the acetone solvent is hydrogenated by the Ir(0) nanoclusters to form isopropanol. Text showing a mathematical treatment of the solvent vapor pressure correction. Figure 4.J showing the sigmoidal hydrogen uptake curve for the hydrogenation of benzene with $TBA_5Na_3(COD)Rh{\bullet}P_2W_{15}Nb_3O_{62}$ as the precatalyst. Figure 4.K showing a TEM of the reaction solution following a cyclohexene hydrogenation with the precatalyst $[Bu_4N][Ru(COD)(CH_3CN)(P_2O_9)]$ in the presence of 2 equiv of TBA^+OH^-.

References:

[1] Reviews on nanoclusters; see also our own reviews elsewhere[2]: (a) Jena, P.; Rao B. K.; Khanna, S. N. *Physics and Chemistry of Small Clusters*; Plenum: New York, 1987; (b) Andres, R. P.; Averback, R. S.; Brown, W. L.; Brus, L. E.; Goddard, W. A., III; Kaldor, A.; Louie S. G.; Moscovits, M.; Peercy, P. S.; Riley, S. J.; Siegel, R. W.; Spaepen, F.; Wang, Y. *J. Mater. Res.* **1989**, *4*, 704. This is a Panel Report from the United States Department of Energy, Council on Materials Science on "Research Opportunities on Clusters and Cluster-assembled Materials"; (c) Thomas, J. M. *Pure Appl. Chem.* **1988**, *60*, 1517; (d) Henglein, A. *Chem. Rev.* **1989**, *89*, 1861; (e) A superb series of papers, complete with a record of the insightful comments by the experts attending the conference, is available in: *Faraday Discussions* **1991**, *92*, 1-300; (f) Bradley, J. S. in *Clusters and Colloids. From Theory to Applications*; Schmid, G., Ed.; VCH: New York, 1994; p. 459-544; (g) Schmid, G. in *Aspects of Homogeneous Catalysis*; Ugo, R., Ed.; Kluwer: Dordrecht, 1990; Chapter 1. (h) Bönnemann, H.; Braun, G.; Brijoux, W.; Brinkmann, R.; Tilling, A. S.; Seevogel, K.; Siepen, K. *J. Organomet. Chem.* **1996**, *520*, 143-162 and the collection of "key publications" cited as references 2-61 therein. (i) Raithby, P. R. *Platinum Metals Rev.* **1998**, *42*, 146. (j) Schmid, G.; Bäumle, M.; Geerkens, M.; Heim, I.; Osemann, C.; Sawitowski, T. *Chem. Soc. Rev.* **1999**, *28*, 179.

[2] (a) See elsewhere for a review of nanocluster catalysis which includes necessary key terms and definitions of:[2b] nanoclusters; traditional colloids; monodisperse and near-monodisperse nanoparticles; "magic number" (i.e., full shell and thus enhanced stability) nanoclusters; Schwartz's updated definition of homogeneous vs. heterogeneous catalysts; inorganic ("charge") and organic ("steric") stabilization mechanisms for colloids and nanoparticles; plus a review of the Bu_4N^+ and polyoxoanion-stabilized $Ir(0)_{\sim 300}$ nanoclusters discussed herein. A review focusing on nanocluster catalysis is also available,[2c] as is a recent review emphasizing the important components of nano-*molecular* chemistry and its advantages over nano-colloidal or nano-materials chemistry:[2d] (b) Aiken, J. D. III; Lin, Y.; Finke, R. G. *J. Mol. Catal. A: Chem.* **1996**, *114*, 29-51. (c) Aiken, J. D., III; Finke, R. G. *J. Mol. Catal. A: Chem.* **1999**, *145*, 1. (d) Finke, R. G. in "Metal Nanoparticles: Synthesis, Characterization and Applications", Feldheim, D. L.; Foss Jr., C. A., Eds.; Marcel Dekker, Inc.: New York, 2001, in press ("Transition-Metal Nanoclusters: Solution-Phase Synthesis, then Characterization and Mechanism of Formation, of Polyoxoanion- and Tetrabutylammonium-Stabilized Nanoclusters").

[3] Classic papers on nanocluster formation: (a) LaMer's mechanism of sulfur sol formation, consisting of homogeneous nucleation from supersaturated solution followed by diffusive, agglomerative growth (a mechanism quite different than that discovered for transition metal nanocluster formation via the kinetic methods reported herein and as summarized elsewhere[8]): LaMer, V.K.; Dinegar, R.H. *J. Am. Chem. Soc.* **1950**, *72*, 4847; LaMer, V. K. *Ind. Eng. Chem.* **1952**, *44*, 1270. (b) Turkevich's mechanistic studies: Turkevich, J.; Stevenson, P.C.; Hillier, J. *Faraday Discuss. Chem. Soc.* **1951**, *11*, 55. (c) Reiss, H. *J. Chem. Phys.* **1951**, *19*, 482. (d) A comprehensive list of the 19 prior papers since 1950, plus the 6 pulse radiolysis papers cited below,[3f-i] which provide mechanistic data on colloid or nanocluster formation has been compiled in Table A of the Supporting Information elsewhere[8] for the interested reader, along with brief summaries covering the contents of each paper. (e) Listed in references 3f-i below are studies of pulse radiolysis reduction of Ag^+ to $Ag(0)_n$ nanoclusters. These studies[3f-i] (which are somewhat buried in the pulse radiolysis and Ag photographic process literature) were not noted previously,[8] only because they were not uncovered via our earlier literature search of nanocluster formation kinetic and mechanistic studies.[8] These Ag^+ reduction studies are, however, relevant to the present and

our earlier kinetic and mechanistic work,[8] even though: (i) Ag^+ and Ag(0) are not, strictly speaking, transition metals (do not have *partially filled* d or f shells), (ii) the pulsed reduction nature of the pulse radiolysis method bears little resemblance to a continuous reduction method such as the use of H_2 herein; and (iii) the pulse radiolysis method suffers from not producing useful quantities of isolable nanoclusters (and thus uncharacterized are the nanocluster product's composition, size dispersion, and so on). In addition, and although autocatalysis is occasionally mentioned therein,[3f-i] (iv) there is no unequivocal, compelling kinetic evidence for autocatalysis (nor identification or semi-quantitative treatment of issues such as the fraction of surface atoms). Nevertheless, the following proposed steps in the Ag(0) and our Ir(0) systems are formally analogous mechanistically as surface-growth processes: $Ag(0)_n + Ag^+ + SPV^{\bullet} \longrightarrow Ag(0)_{n+1} + SPV$ (where SPV = sulfonato-propylviologen); and $Ir(0)_n + [(1,5\text{-COD})Ir^{I}\bullet P_2W_{15}Nb_3O_{62}]^{8-} + 2.5\ H_2 \longrightarrow Ir(0)_{n+1} + \text{cyclooctane} + H^+ + [P_2W_{15}Nb_3O_{62}]^{9-}$. Note that the reduction of Ag^+ is proposed to occur only after formation of $Ag(0)_n\bullet Ag^+$ (i.e., after coordination of Ag^+ to the $Ag(0)_n$ surface), which differs from the $Ir(0)_n$ case only in that activation of xH_2 on the $Ir(0)_n$ surface to give $Ir(0)_n\bullet(H)_{2x}$ probably occurs first, that is, prior to the reaction of the resultant $Ir(0)_n\bullet(H)_{2x}$ with $[(1,5\text{-COD})Ir^{I}(\text{solvent})]^+$ and / or $[(1,5\text{-COD})Ir^{I}\bullet P_2W_{15}Nb_3O_{62}]^{8-}$. (f) Mostafavi, M.; Marignier, J. L.; Amblard, J.; Belloni, J. *Radiat. Phys. Chem.* **1989**, *34*, 605. Mostafavi, M.; Marignier, J. L.; Amblard, J.; Belloni, J. *Z. Phys. D-Atoms, Molecules and Cluster* **1989**, *12*, 31. Belloni, J.; Amblard, J.; Marignier, J. L.; Mostafavi, M. in *Clusters of Atoms and Molecules, II: Solvation and Chemistry of Free Clusters, and Embedded, Supported and Compressed Clusters*; Haberland, H., Ed.; Springer-Verlag: Berlin, 1994; Vol. 2, p 290. (g) Henglein, A.; Tausch-Treml, R. *J. Colloidal and Interfacial Science* **1981**, *80*, 84. (h) Ershov, B. G.; Kartashev, N. I. *Russ. Chem. Bull.* **1995**, *44*, 29. (i) Rabani, J.; Fessenden, R. W.; Sassoon, R. E. *J. Phys. Chem.* **1988**, *92*, 2379.

[4] More recent mechanistic investigations of transition-metal nanocluster formation are the following: (a) Our 1997 study[8]; (b) Petroski, J. M.; Wang, Z. L.; Green, T. C.; El-Sayed, M. A. *J. Phys. Chem. B* **1998**, *102*, 3316. (c) Henglein, A.; Giersig, M. *J. Phys. Chem. B* **2000**, *104*, 6767. Note that this paper misquotes our 1997 paper[8] when it says: "It seems probable that reduction by H_2 does not proceed through intermediate *free atoms* (i.e., via naked Ir(0)), as has been postulated.[8] (The parenthetical comment, and the italics, have been added. Reference 8 is to our 1997 mechanistic paper, which just happens to also be reference 8 herein.[8]) In fact, we specifically worried about the high, unstable energetics of Ir(0) formation in footnotes 10, 43a, 44, and 45 of our paper. We concluded that *highly ligated, and thus stabilized, $Ir(0)L_y$*,—not naked Ir(0) atoms as (mis)quoted above[4c]—is what our evidence suggests. Also made elsewhere in footnote 43d is the point that in general and energetically speaking, one wants Ir-Ir bond formation to proceed reduction to $Ir(0)_x\bullet L_y$ whenever possible.[8] Note that our published data is compelling in requiring the formation of $Ir(0)L_y$ or $Ir(0)_x\bullet L_y$ species *somewhere along the reaction coordinate.* Nevertheless, Henglein's intuition, that there may need to be intermediates other than $Ir(0)L_y$ prior to $Ir(0)_x\bullet L_y$ along the reaction pathway, may well be right. The one intriguing possibility that we have been able to come up with for such an intermediate is under investigation. (d) See also the related topic of the mechanisms of formation of semiconductor nanocrystals: Peng, X.; Wickham, J.; Alivisatos, A. P. *J. Am. Chem. Soc.* **1998**, *120*, 5343. Chen, C.-C.; Herhold, A. B.; Johnson, C. S.; Alivisatos, A. P. *Science* **1997**, *276*, 398.

[5] (a) Lin, Y.; Finke, R. G. *J. Am. Chem. Soc.* **1994**, *116*, 8335. (b) Lin, Y.; Finke, R. G. *Inorg. Chem.* **1994**, *33*, 4891. (c) The *average* composition of the $Ir(0)_{\sim 300}$ and $Ir(0)_{\sim 900}$ nanoclusters were demonstrated to be $[Ir(0)_{\sim 300}(P_4W_{30}Nb_6O_{123}^{16-})_{\sim 33}](Bu_4N)_{\sim 300}Na_{\sim 228}$ and $[Ir(0)_{\sim 900}(P_4W_{30}Nb_6O_{123}^{16-})_{\sim 60}](Bu_4N)_{\sim 660}Na_{\sim 300}$, respectively. Note that the $P_2W_{15}Nb_3O_{62}^{9-}$ has formed its anhydride, in the presence of the one equivalent of H^+

produced in the nanocluster formation reaction, via the reaction: 2 $P_2W_{15}Nb_3O_{62}^{9-}$ + $2H^+$ --> H_2O + $[(P_2W_{15}Nb_3O_{61})_2\text{–}O]^{16-}$ (see elsewhere for additional discussion of this point).[5a,b] (d) Additional characterization studies of the $Ir(0)_{\sim 300}$ nanoclusters by HR-TEM, HR-TEM of nanoclusters deposited on SiO_2 spheres, STM and, if possible, mass spectroscopy are nearing completion and will be reported in due course, Aiken, John D. III; Finke, R. G., unpublished results. (e) The present paper is Part VII in a series of papers focusing on the kinetics and mechanism of nanocluster formation reactions.[5,8,12,13,20,22]

[6] (a) Pohl, M.; Lyon, D. K.; Mizuno, N.; Nomiya, K.; Finke R. G. *Inorg. Chem.* **1995**, *34*, 1413; (b) Weiner, H.; Aiken, J. D. III; Finke, R. G. *Inorg. Chem.* **1996**, *35*, 7905.

[7] (a) The detection of nanocluster sizes and size-distributitions is most commonly done by TEM (transmission electron microscopy), although reports of changes induced by the TEM beam are fairly frequent;[1] additional lead references of TEM-induced changes of nanoclusters are provided in reference 18 elsewhere.[5a] One might believe that light scattering is the method of choice for size-distribution monitoring, but this is really only 100% true *if* a single-size, monodispersed nanocluster is present.[7b] (b) Briefly, the reason that light scattering is not the method of choice when a distribution of nanocluster sizes is present is that it involves a fit to a multiexponential function (i.e., instead of a single exponential or function), and then a non-linear least-squares fit. Hence, the resulting solution cannot be guaranteed to be the true global minimum for the problem. We thank Dr. Jess Wilcoxon of Sandia National Labs for his expert discussions on this point.

[8] Watzky, M. A.; Finke, R. G. *J. Am. Chem. Soc.* **1997**, *119*, 10382.

[9] A *pseudoelementary step* is a term invented by Professor Richard Noyes, at the University of Oregon, for dealing with complex (oscillating) reactions. For an introduction to the concept of pseudoelementary reactions, a concept created for and often necessary with the kinetics of more complex systems, see the pioneering work of Professor Noyes and co-workers: (a) Noyes, R. M.; Field, R. J. *Acc. Chem. Res.* **1977**, *10*, 214; (b) Noyes, R. M.; Field, R. J. *Acc. Chem. Res.* **1977**, *10*, 273; (c) Field, R. J.; Noyes, R. M. *Nature* **1972**, *237*, 390.

[10] Note also that implicit in the kinetic treatment is the *approximation* that all Ir(0) surface atoms on the growing, and thus temporally different size, nanoclusters react at the same rate. This approximation: (i) is fully consistent with the literature of olefin hydrogenation being a structure-insensitive reaction, (ii) is further supported by the direct monitoring of the Ir(0) formation by its cyclooctane evolution reaction (since the two methods yield the same rate constants within experimental error; this requires that there is not, as expected, a detectable particle size dependence *difference* between cyclohexene and cyclooctadiene hydrogenation), and (iii) in any event is a necessary approximation in these *first studies* since a range of different particle sizes is only now becoming available to see if this approximation holds in nanocluster catalysis. We note, however, that an obvious goal of future studies is to determine independently the particle-size effects in, especially, nanocluster catalyzed structure-sensitive reactions, and then to see if the same particle-size effects can be deconvoluted out of kinetic curves analogous to those in Figures 4.2, 4.4, 4.5 and 4.6.

[11] Lyon, D. K.; Finke, R. G. *Inorg. Chem.* **1990**, *29*, 1787.

[12] Aiken, J. D. III; Finke, R. G.; *J. Am. Chem. Soc.* **1998**, *120*, 9545.

[13] Watzky, M. A.; Finke, R. G. *Chem. Mater.* **1997**, *9*, 3083.

[14] (a) Arene hydrogenation is, like simple olefin hydrogenation a so-called "structure-insensitive" (i.e., largely particle-size-insensitive—see reference 24 below) reaction. Eventually it will be important to look at highly particle-size sensitive, structure-sensitive reactions as well, as then the k_1(apparent) and k_2(appparent) will contain valuable information about that size-sensitivity.

[15] Widegren, J. A.; Finke, R. G. unpublished results and experiments in progress. One such arene hydrogenation experiment has been reproduced in Figure 4.J of the Supporting Information for the interested reader. In this experiment the Rh nanocluster precursor, $[Bu_4N]_5Na_3[(1,5\text{-COD})Rh{\bullet}P_2W_{15}Nb_3O_{62}]$, is reduced in the presence of the more difficult substrate benzene (experimental conditions: 50 °C, 40 psig H_2, and propylene carbonate solvent). A sigmoidal hydrogen uptake curve results, characteristic of the nucleation and autocatalytic surface growth mechanism as summarized in Scheme 4.1, one which could be fit to the usual analytic equations for the reactions in eqs. 2a and 2b.

[16] Since we know, in the presence of cyclohexene, that there is an olefin dependence to k_2, and probably also one to k_1 at lower olefin concentrations (see the top and bottom plots in Figure 6 elsewhere[8]), we expect a comparison of the above rate constants to those under our rather different, "standard conditions"[8] (of acetone solvent, 1.65 M cyclohexene, 22 °C and 40 psig of H_2) to reveal that the rate "constants" from these two different experiments are, simply, different (i.e., that k_1 and k_2 are really the pseudo-first and pseudo-second order rate constants k_1(obsd) and k_2(obsd)). In fact, a comparison of the rate constants from the curvefit in Figure 4.2 and where standard conditions were used, $k_1 = 0.010\ h^{-1}$ and $k_{2(hydrogenation)corrected} = 3.6 \times 10^3\ M^{-1}h^{-1}$, to those given above confirms this prediction: they are different. (Note that $k_{2(hydrogenation)corrected}$ is the value of k_2 after correcting for both the scaling and the stoichiometry factors—see the Supporting Information for details.)

[17] An excellent example of the use of TEM to follow nanocluster growth is provided by El-Sayed and co-workers 1998 paper.[4b]

[18] That is, one would not expect to see nanoclusters during the induction period as long as the size of the critical nucleus is too small to be visualized by TEM. For this system the critical nucleus size has been estimated at $\leq Ir(0)_{\sim 15}$,[8] which is too small to be seen by the microscope used in the present studies.

[19] Press, W. H.; Flannery, B. P.; Teukolsky, S. A.; Vetterling, W. T. *Numerical Recipes*; Cambridge University: Cambridge, 1989.

[20] Aiken, J. D. III; Finke, R. G. *Chem. Mater.* **1999,** *11,* 1035.

[21] A few lead references on arene hydrogenation include: (a) Collman, J. P.; Hegedus, L. S.; Norton, J. R.; Finke, R. G. *Principles and Applications of Organotransition Metal Chemistry*; University Science Books: Mill Valley, CA, 1987; pp 549-556; (b) Linn, D. E., Jr; Halpern, J. *J. Am. Chem. Soc.* **1987**, *109*, 2969; (c) Rothwell, I. P. *Chem. Commun.* **1997**, 1331; (d) Gao, H.; Angelici, R. J.; *J. Am. Chem. Soc.* **1997**, *119*, 6937; (e) Ahn, H.; Marks, T. J. *J. Am. Chem. Soc.* **1998**, *120*, 13533; (f) Adams, C. J.; Earle, M. J.; Seddon, K. R. *Chem. Commun.* **1999**, 1043.

[22] Weddle, K. S.; Aiken, J. D. III; Finke, R. G. *J. Am. Chem. Soc.* **1998,** *120,* 5653.

[23] For experimental kinetic data, the changing fraction of surface atoms throughout a nanocluster formation reaction has been treated for the first time, and in an in a quantitative but average way, using the "scaling factor" described originally elsewhere[8] as well as in the Supporting Information accompanying the present paper. For example, $k_2(\text{hydrogenation})_{\text{corrected}} = k_2(\text{hydrogenation})/0.8$, and (in the Supporting Information) $k_2(\text{GLC})_{\text{corrected}} = k_2(\text{GLC})/0.7$. Note that in footnote 38b elsewhere[8] there is a typographical error in both this latter equation (it was inverted) and in the scaling factor (the previous 0.51 is in error).

[24] Lead references and further discussion of structure sensitive or insensitive reactions are available in footnote 52 elsewhere.[5b] (b) Note, however, that ethylene hydrogenation on $Pt(0)_n$ particles supported on SiO_2 is a stucture-insensitive reaction only to an *apparent* factor of ≤ 3; see Figure 9 p. 110 of Che, M.; Bennett, C. O. *Adv. Catal.* ***1989***, *36*, 55-172. Note that we say apparent since one cannot rule out, on the basis of only the data in Figure 9 of the Che and Bennett paper, a SiO_2 effect on the hydrogenation rate that is somehow also a function of the $Pt(0)_n$ particle size (i.e., rather than an intrinsic rate effect due solely to the metal particle size and completely independent of the SiO_2). This example illustrates why we believe nanoclusters will prove valuable in testing such often cited, but still too phenomenology-based, mechanistic concepts of heterogeneous catalysis.

[25] In reality a large number of nanocluster geometries are possible for each $M(0)_x$, with surface irregularities (roughness; facets) and a more fluid-like surface structure probably being much more common than is generally recognized: (a) Uppenbrink, J.; Wales, D. J. *J. Chem. Phys.* **1992**, *96*, 8520. (b) Doye, J. P. K.; Wales, D. J. *New J. Chem.* **1998**, 733. (c) Soler, J. M.; Beltrán, M. R.; Michaelian, K.; Garzón, I. L.; Ordejón, P.; Sánchez-Portal, D.; Artacho E. *Phys. Rev. B* **2000**, *61*, 5771. (d) Lewis, L. J., Jensen, P.; Barrat, J.-L. *Phys. Rev. B* **1997**, *56*, 2248. (e) Dassenoy, F.; Casanove, M.-J.; Lecante, P.; Verelst, M.; Snoeck, E.; Mosset, A.; Ely, T. O.; Amiens, C.; Chadret, B. *J. Chem. Phys.* **2000**, *112*, 8137. (f) See the quote on p. 719 elsewhere[1b] that calculations "have shown that there are many metastable (structural) configurations in a 0.1 eV range above the equilibrium state, and that their number increases significantly with the cluster size". (g) For Si_n nanoclusters: Ballone, P.; Andreoni, W.; Car, R.; Parrinello, M. *Phys. Rev. Let.* **1988**, *60*, 271.

[26] (a) Collman, J. P.; Hegedus, L. S.; Norton, J. R.; Finke, R. G. *Principles and Applications of Organotransition Metal Chemistry*; University Science Books: Mill Valley, CA, 1987; pp 291-293; (b) Brothers, P. J. *Prog. Inorg. Chem.* **1981**, *28*, 1.

[27] Bönnemann, H.; Brinkmann, R.; Neiteler, P. *Appl. Organomet. Chem.* **1994**, *8*, 361.

[28] Clay, R. T.; Cohen, R. E. *Supramol. Sci.* **1995**, *2*, 183.

[29] Clay, R. T.; Cohen, R. E. *Supramol. Sci.* **1997**, *4*, 113.

[30] Fukuoka, A.; Sato, A.; Kodama, K.-Y.; Hirano, M; Komiya, S. *Inorg. Chim. Acta* **1999**, *294*, 266.

[31] Schmid, G.; Harms, M.; Malm, J.-O.; Bovin, J.-O.; Ruitenbeck, J. v.; Zandbergen, H. W.; Fu, W. T. *J. Am. Chem. Soc.* **1993**, *115*, 2046.

[32] Vargaftik, M. N.; Zagorodnikov, V. P.; Stolarov, I. P.; Moiseev, I. I.; Kochubey, D. I.; Likholobov, V. A.; Chuvilin, A. L.; Zamaraev, K. I. *J. Mol. Cat.* **1989**, *53*, 315.

[33] Ciebien, J. F.; Cohen, R. E.; Duran, A. *Supramol. Sci.* **1998**, *5*, 31.

[34] Henglein, A. *J. Phys. Chem. B* **2000**, *104*, 6683.

[35] Landré, P. D.; Richard, D.; Draye, M.; Gallezot, P.; Lemaire, M. *J. Catal.* **1994**, *147*, 214.

[36] Boutonnet, M.; Kizling, J.; Stenius, P.; Maire, G. *Colloids and Surfaces* **1982**, *5*, 209.

[37] Toshima, N.; Takahashi, T.; Hirai, H. *Chem. Lett.* **1985**, 1245.

[38] Meguro, K.; Torizuka, M.; Esumi, K. *Bull. Chem. Soc. Jpn.* **1988**, *61*, 341.

[39] Toshima, N.; Takahashi, T. *Bull. Chem. Soc. Jpn.* **1992**, *65*, 400.

[40] Bönnemann, H.; Braun, G.; Brijoux, W.; Brinkmann, R.; Schulze Tilling, A.; Seevogel, K.; Siepen, K. *J. Organomet. Chem.* **1996**, *520*, 143.

[41] Fache, F.; Lehuede, S.; Lemaire, M. *Tetrahedron Lett.* **1995**, *36*, 885.

[42] James, B. R.; Wang, Y.; Alexander, C. S.; Hu, T. Q. *Can. Chem. Ind.* **1998**, *75*, 233.

[43] Yonezawa, T.; Tominaga, T.; Richard D. *J. Chem. Soc., Dalton Trans.* **1996**, 783.

[44] Landré, P. D.; Lemaire, M.; Richard, D.; Gallezot, P. *J. Mol. Cat.* **1993**, *78*, 257.

[45] Nasar, K.; Fache, F.; Lemaire, M.; Béziat, J.-C.; Besson, M.; Gallezot, P. *J. Mol. Cat.* **1994**, *87*, 107.

[46] Weddle, K. S.; Aiken, J. D., III; Finke, R. G. *J. Am. Chem. Soc.* **1998**, *120*, 5653.

[47] Kanda, S.; Kori, T.; Kida, S. *J. Solid State Chem.* **1994**, *108*, 299.

[48] An illustrative example comes from a 1994 paper.[27] Those workers attempted to make Pd(0) colloids from four similar Pd(II) precursors ($[N(octyl)_4]_2PdBr_4$, $[N(octyl)_4]_2PdCl_4$, $[N(octyl)_4]_2PdCl_2Br_2$, and Pd(acetate)$_2$ / $[N(dodecyl)_4]Br$) and using H_2 as the reductant. The $[N(octyl)_4]_2PdBr_4$ could not be reduced (even under 50 bar H_2), $[N(octyl)_4]_2PdCl_4$ gave only a precipitate, $[N(octyl)_4]_2PdCl_2Br_2$ was reduced very slowly (after 14 days!) under 1 atmosphere of H_2, yet Pd(acetate)$_2$ / $[N(dodecyl)_4]Br$ was reduced in 16 hours (a factor of > 21 faster) under the same conditions.[27] Those workers correctly made the phenomenological conclusion that "the anion of the palladium salt is crucial for the success of the colloid synthesis",[27] but failed to have any fundamental insights as to why the anion is key. We can now offer a very likely if not compelling hypothesis: that the presence of a base (acetate) is allowing the Pd(acetate)$_2$ / $[N(dodecyl)_4]Br$ precursor to be reduced *initially* by a heterolytic hydrogen activation pathway. None of the other three precursors contained a base, and therefore have a large kinetic barrier to the nucleation of their nanocluster formation reactions.

[49] Attanasio, D.; Bachechi, F; Suber, L. *J. Chem. Soc., Dalton Trans.* **1993**, 2373.

[50] Lyon, D. K. Ph.D. Dissertation, University of Oregon, 1990; see pp 142-145.

[51] The solubility data for H_2 in acetone is from *The Matheson Unabridged Gas Book: Hydrogen*; Matheson: East Rutherford, NJ, 1974.

SUPPORTING INFORMATION

Additional Investigations of a New Kinetic Method to Follow Transition-Metal Nanocluster Formation, Including the Discovery of Heterolytic Hydrogen Activation in Nanocluster Nucleation Reactions

Jason A. Widegren, John D. Aiken III, Saim Özkar and Richard G. Finke

Key Control Demonstrating that the More Direct Monitoring of the Nanocluster $Ir(0)_n$ Formation by the GLC Determined Evolution of Cyclooctane Gives Identical Rate Constants, k_1 and k_2, within Experimental Error.

The details and data for this key control experiment is available elsewhere for the interested reader.[1] The key results are that the kinetic curve from the GLC data is sigmoidal as expected, is well-fit by the same equations, and it *yields the same rate constants as obtained previously within experimental error* as the pseudoelementary step-monitored reaction.[1] The fact that the mathematically required correction factors are needed to get agreement between the rate constants[2]: $k_{1(GLC)} = 2.8\ (\pm\ 1.8) \times 10^{-3}\ h^{-1}$; $k_{2(GLC\ corrected} = 2.4\ (\pm\ 0.2) \times 10^{3}\ M^{-1}h^{-1}$ (from the cyclooctane data and curve-fit), while $k_{1(hydrogenation)} = 1.8\ (\pm\ 0.2) \times 10^{-3}\ h^{-1}$ and $k_{2(hydrogenation\ corrected} = 2.2\ (\pm\ 0.3) \times 10^{3}\ M^{-1}h^{-1}$.[1] The large error bar on the GLC-derived k_1 rate constant is due to the fewer—and lower, ± 10%, precision—data available by the GLC method compared to the hydrogenation method [i.e., and the hydrogenation method's ≥ 300 points of ± 0.01 psig pressure transducer-obtained data which is, therefore, of a 100 fold higher, ± 0.1% precision (calculated as follows: ±0.01 psig / ca.14 psig H_2 total pressure loss = ± 0.1%)].

The important result is that the identical resultant k_1 and k_2 values offer *compelling evidence that the two methods are monitoring the same process*, $Ir(0)_n$ nanocluster formation. Further details are available elsewhere.[1]

A Closer Look at the Data Analysis, and How the Changing Fraction of Nanocluster Surface Atoms is Handled (the Fraction of Surface Atoms "Scaling Factor"). The differential and integrated rate equations used to analyze the kinetic data, and corresponding to the mechanism of eqs. 2(a-d), have been provided earlier[1] as Appendix A and Appendix B; they are reporduced here for the convenience of the reader and to have as much of the key information needed to use the new kinetic method gathered in one place. The key differential equation is A.5 below (where the equation numbers are

those retained from the earlier Appendix A[1] to avoid confusion, i.e., the preceding eqs. A.1 through A.4 in the earlier Appendix A[1] are not reproduced before eq. A.5 below):

A.5 $$\frac{-d[\bigcirc]}{dt} = k_1[\bigcirc]_t + \frac{k_2}{1400}[\bigcirc]_t\left([\bigcirc]_0 - [\bigcirc]_t\right)$$

Equation A.5 is the differential form of the integrated rate equation, A.6 below, that we actually use for the curvefits (eq. A.6 is identical to eq. 4 in our earlier paper[1]):

A.6 $$[A]_t = \frac{\frac{k_1}{k_2} + [A]_0}{1 + \frac{k_1}{k_2[A]_0} * \exp(k_1 + k_2[A]_0)\, t}$$

Note that a comparison of these two equations reveals that $k_{1(curvefit)} = k_1$, but $k_{2(curvefit)} = \frac{k_2}{1400}$ or $1400\, k_{2(curvefit)} = k_2$. This factor of 1400 is, therefore, the mathematically required "stoichiometry correction factor"[1] in eqs. 2c and 2d and that is introduced by the pseudoelementary step method of following the hydrogenation reaction of 1400 equivalents of cyclohexene as shown in Figure 4.2 of the main text.

Scaling Factor for the Rate Constant k_2. (The treatment below follows that provided elsewhere,[1] but where the eq. 3 series below is replaced by the eq. C series in the Appendix C elsewhere.[1])

If one is to apply rigorously the autocatalytic model:

3.1(a) $$A \xrightarrow{k_1} B$$

3.1(b) $$A + B \xrightarrow{k_2} 2\,B$$

where the sum reaction is:

3.1(c) $$2\,A \rightarrow 2\,B$$

to the formation of nanoclusters:

3.2(a) $$n\,Ir(0) \rightarrow Ir(0)_n \qquad \text{(nucleation)}$$

3.2(b) "Ir(0)" + $Ir(0)_n \rightarrow Ir(0)_{n+1}$ (growth)

then one needs to express eqs. 3.2(a,b) as in eqs. 3.3(a,b), since the catalytic species B corresponds to active surface atoms on the nanocluster:

3.3(a) n $Ir(0) \rightarrow Ir(0)_{n(\text{surface atoms})}$

3.3(b) "Ir(0)" + $Ir(0)_{n(\text{surface atoms})} \rightarrow Ir(0)_{n+1(\text{surface atoms})}$

Let us now define $x_{(\text{nucleation or growth})}$ as the fraction of surface atoms gained in a reaction step (of nucleation or growth), eq. C3.4(a):

3.4(a) $$x_{(\text{nucleation or growth})} = \frac{\text{increase in number of surface atoms}}{\text{increase in total number of atoms}};$$

Alternatively, and while noting that atom packing begins about a single, central atom one can define and then use a $x_{(\text{average})}$ as defined in C 3.4(b)

C 3.4(b) $$x_{(\text{average})} = \frac{1 + \text{no. surface atoms}}{1 + \text{total no. atoms}}$$

The autocatalysis model in eq. 3.1 can then be rewritten more precisely, for the present case of nanocluster formation, as eqs. 3.5(a,b):

3.5(a) $A \xrightarrow{k_1} x_{\text{nucleation}}\ B$

3.5(b) $A + x_{\text{nucleation}}\ B \xrightarrow{k_2} (x_{\text{nucleation}}+x_{\text{growth}})\ B$

where the sum reaction is:

3.5(c) $2\ A \rightarrow (x_{\text{nucleation}}+x_{\text{growth}})\ B$

At the end of the induction period, which also marks the end of the nucleation step (or at least most of it), less than 5% of the total amount of cyclooctane has evolved (see Figure 7 elsewhere),[3] indicating that the nucleus size should be less than 15 atoms (and if one makes the crude assumption that the size increase is a linear function of time, undoubtedly a very rough approximation to the size-dependence of the nanoclusters with their sigmoidal-shaped kinetic curves). In this size range, the value of $x_{(\text{nucleation or growth})}$ is ≥ 0.92 (see the list of estimated Scaling Factors below). Hence, we can approximate $x_{\text{nucleation}}$ as ≈ 1, from which we obtain:

3.6(a) $$-\frac{1}{2}\frac{d[A]}{dt} = \frac{1}{1+x_{\text{growth}}}\frac{d[B]}{dt}$$

3.6(b) $\frac{d[B]}{dt} = -\frac{1+x_{growth}}{2}\frac{d[A]}{dt}$

3.6(c) $[B]_t = \frac{1+x_{growth}}{2}([A]_0-[A]_t)$

so that the rate equation becomes:

3.7(a) $-\frac{d[A]}{dt} = k_1[A] + k_2[A][B]$

3.7(b) $-\frac{d[A]}{dt} = k_1[A] + k_2\frac{1+x_{growth}}{2}[A]([A]_0-[A]_t)$

Hence, the value of k_2 obtained from curvefits is really $k_{2(curvefit)} = k_2(x)$, that is, it contains a mathematically required "scaling factor"[1] correction of $x = \frac{1+x_{growth}}{2}$. Note that in this "zeroth-order" treatment, x_{growth} is assumed to be a constant, while rigorously it is a function of time. The ≤15-25% error introduced by this approximation will be discussed in the next section but is, however, quite tolerable, relative to the inherent ±10-15% error in k_2, *vide infra.*

Estimation of the Scaling Factors. As explained above, the steps of nucleation (n Ir(0) → $Ir(0)_n$) and growth ($Ir(0)_n$ + "Ir(0)" → $Ir(0)_{n+1}$) can be summarized by "2A → $(1+x_{growth})$B", where x_{growth} is the fraction of active surface atoms gained in the growth step. The value of x_{growth} is thus given by the ratio of the increase in the number of surface atoms divided by the increase in the total number of atoms.

As also detailed above, the rate equation for "2A → $(1+x_{growth})$B" is given by $-d[A]/dt = k_1[A] + k_2\left(\frac{1+x_{growth}}{2}\right)[A]([A]_0-[A])$. The calculated value of k_2 (obtained from curvefitting, then corrected by the stoichiometry factor), is thus really $k_{2(curve\text{-}fit)corrected} = k_2\left(\frac{1+x_{growth}}{2}\right)$. This becomes relevant when comparing values of $k_{2(curve\text{-}fit)corrected}$ in which values of the "scaling factor" $\left(x = \frac{1+x_{growth}}{2}\right)$ vary. An average value of the factor x_{growth} can be calculated for the addition of one atomic shell to a full-shell nanocluster (the formula for the number of atoms added to the nth shell of a nanocluster is $10n^2+2$ (and is the same for ccp, hcp and at least some other packing geometries).[4]

shell #	# surface atoms	total # atoms	x_{growth}	$x_{average}$	$\frac{1+x_{growth}}{2}$
0→1	1→12	1→13	0.92	0.92	0.96
1→2	12→42	13→55	0.71	0.72	0.86
2→3	42→92	55→147	0.54	0.60	0.77
3→4	92→162	147→309	0.43	0.51	0.72
4→5	162→252	309→561	0.36	0.44	0.68
5→6	252→359	561→920	0.30	0.38	0.65

For curvefitting purposes of the hydrogenation data such as in Figure 4.2 of the main text, only the data prior to the consumption of half the initial cyclohexene concentration is included. At that time only 23 ± 7% of the initial amount of Ir(I) has been reduced to Ir(0) (i.e. only 23 ± 7% of the total equivalent of cyclooctane has evolved, see Figure 7 elsewhere),[3] indicating that the average cluster size is roughly 70 ± 20 atoms (this again makes the crude assumption that the cluster size-increase is linear). However, the value of the scaling factor, $x = \frac{1+x_{growth}}{2}$, can be seen from the last entry in the above list to be somewhat insensitive to size for the range up to $Ir(0)_{\sim 300}$ nanoclusters and, overall, is estimated as close to 0.8 (previously[1] ≥0.72).

For the GLC data monitoring nanocluster formation and which is available elsewhere,[1] the nanocluster formation is monitored over a different, much larger ca. 80% fraction of the nanocluster growth. Nanoclusters in the estimated $Ir(0)_{\sim 260\text{-}300}$ size range should be formed, with a corresponding scaling factor x = ca. 0.7 [our earlier estimate[1] of this as 0.51 is in error (was actually x_{growth} and not the desired $(1 + x_{growth})/2$].

The above treatment shows that the scaling factor, x, is constant to within 0.9 ± 0.1 or ≤11% over the time course that hydrogenation data is collected and to where ca.

$Ir(0)_{\sim 70 \pm 20}$ is estimated to be formed. In addition, x is constant to better than 0.8 ± 0.2 or 25% for the full size range of $Ir(0)_{\sim 13\text{-}920}$ nanoclusters we've investigated to date.

The result, then, is that the above,"zeroth-order", treatment of the issue of the changing number of surface atoms, and for a reaction that was chosen to be insensitive to particle size (i.e., olefin hydrogenation, a structure-insensitive reaction) introduces an error that is comparable, and thus quite tolerable (albeit perhaps a significant component of), the observed ± 10–15% error in k_2.

Lastly, while one can envisage more exact treatments of x_{growth} in which it is treated as a time-dependent variable (e.g., see the section in the Experimental entitled "Computer Kinetic (Numerical Integration) Modeling of Autocatalytic Surface Growth"), it is worth noting that the present case is the first time that the changing fraction of surface atoms has even been considered explicitly much less treated semi-quantitatively. The agreement it yields when comparing $k_{2(GLC)corrected} = 2.4\ (\pm 0.2) \times 10^3\ M^{-1}h^{-1}$ vs the $k_{2(hydrogenation)corrected} = 2.2\ (\pm 0.3) \times 10^3\ M^{-1}h^{-1}$ is pleasing and supports the treatment of the data at the observed as well as estimated error limits of ± 15%. Hence, the present method seems likely to work for most cases, especially where ± 10-15% GLC or NMR data may be the case, and also given the sizable effects on the k_1 and k_2 values for nanocluster formation reactions of the variables studied elsewhere such as water, anions, cations, and H^+.[1,3]

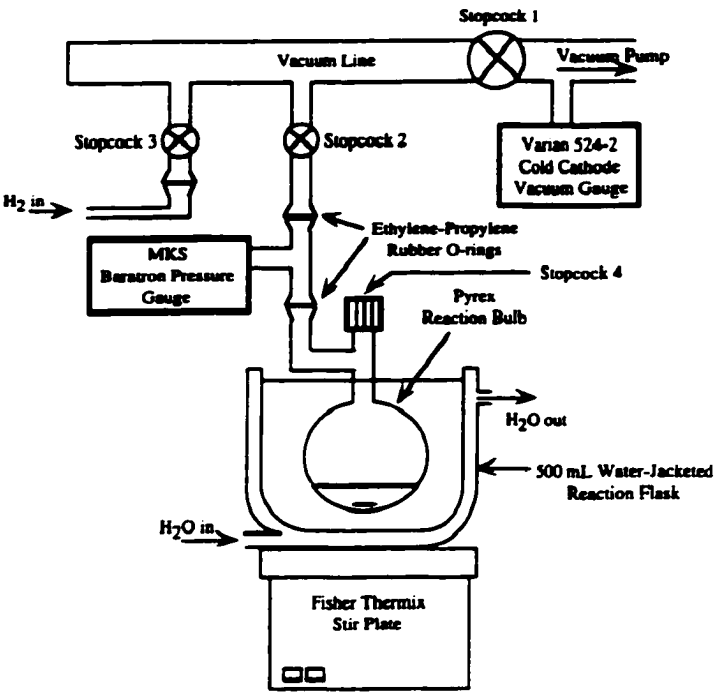

Figure 4.A. Detailed schematic of the hydrogen-uptake apparatus used in the present study.

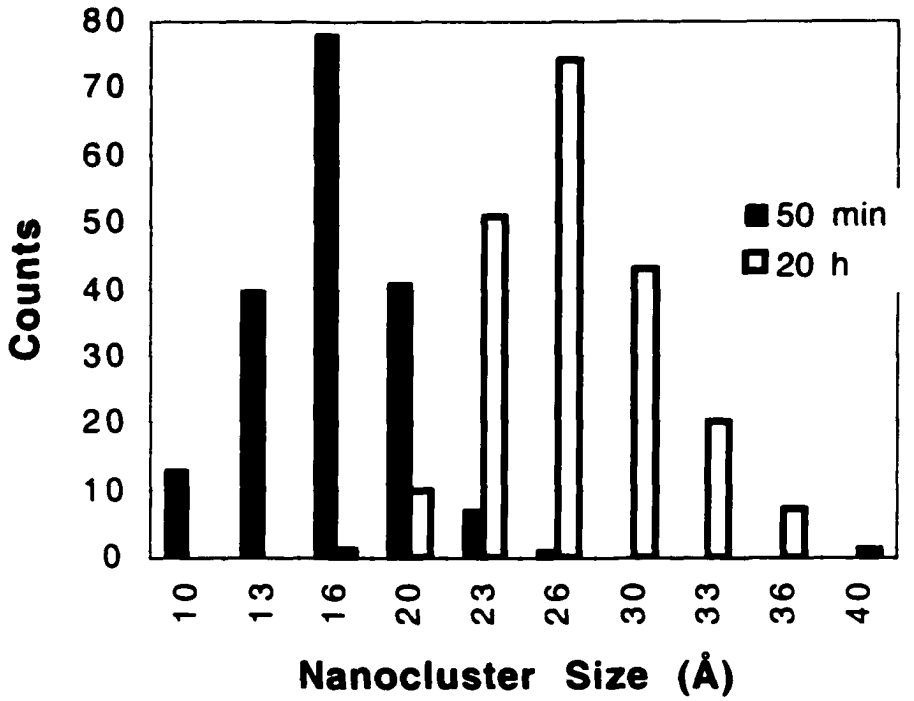

Figure 4.B. Histogram of nanocluster sizes after 50 min and after 20 h for the same cyclohexene hydrogenation experiment starting with the nanocluster precursor **A**. At 50 min the nanoclusters were found to be 16 (± 3) Å in diameter (n=180). At 20 h (i.e., after complete reduction of **A**) the nanoclusters were found to be 27 (± 4) Å in diameter (n=207).

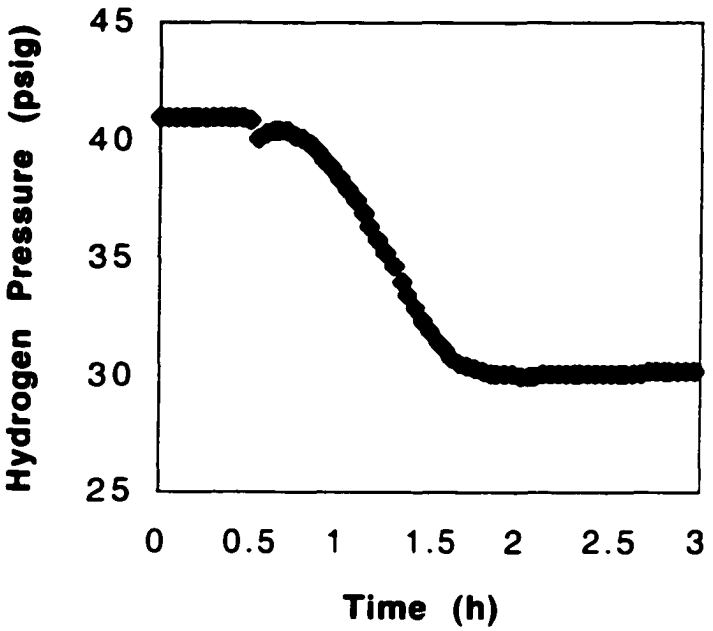

Figure 4.C. Hydrogen uptake curve for a cyclohexene hydrogenation experiment starting with the nanocluster precursor **A**. A sample was removed for TEM analysis at 30 min (near the end of the induction period). *No* nanoclusters were seen in the micrographs of the 30 min sample. The discontinuity in the curve is due to the sampling procedure.

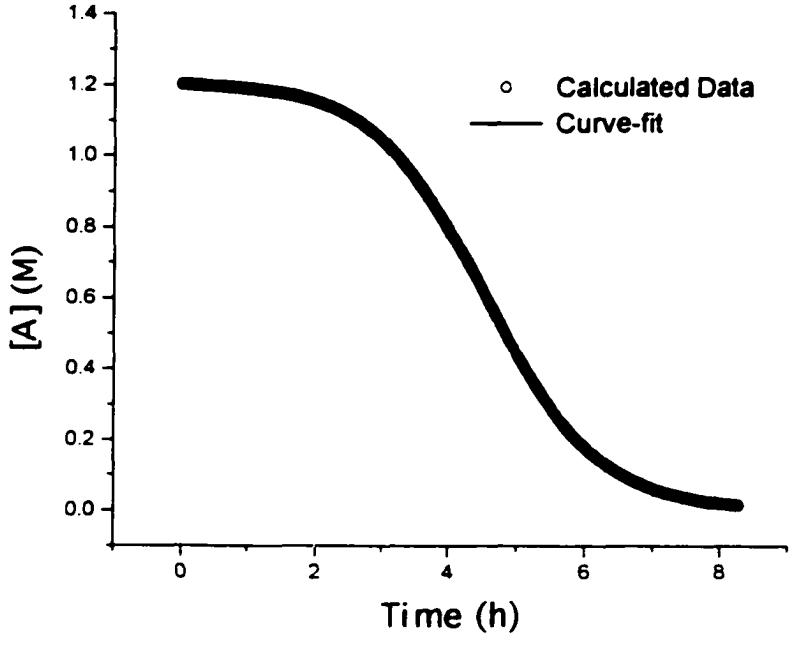

Figure 4.D. A "mock" set of data calculated for the autocatalytic mechanism presented in the main text ($A \rightarrow B$ and $A + B \rightarrow 2B$, rate constants k_1 and k_2, respectively). This "mock" data was calculated using time intervals of 2.5 min, $k_1 = 0.005\ h^{-1}$, $k_2 = 1\ M^{-1}h^{-1}$, and $[A]_0 = 1.2$ M. This calculated curve was fit using Microcal Origin. The curve-fit line is visible in the center of the curve. Origin set the values (and the error bars) of k_1 at $0.005 \pm (6 \times 10^{-9})\ h^{-1}$ and k_2 at $1 \pm (3 \times 10^{-7})\ M^{-1}h^{-1}$.

Treatment of the Changing Fraction of Surface Atoms by the Relative Values of k_2'–k_{90}'. The kinetic model shown in Scheme 4.2 was designed to account for the generation of nanoclusters of different sizes and to allow for autocatalytic surface growth where the changing fraction of nanocluster surface atoms is taken into account. Simply treating each $M(0)_x$ as a separate species allows for nanoclusters of different sizes. The autocatalytic surface growth and the changing fraction of surface atoms are accounted for in the choice of the rate constants k_2'–k_{90}'. For example, there are three metal atoms on the surface of $M(0)_3$, so there are three possible sites for a reaction to take place, compared to only one for $M(0)_1$. As a first approximation, then, the reaction corresponding to k_4' should be three times faster than reaction corresponding to k_2' (assuming equal concentrations), and this is accomplished by making k_4' about three times larger than k_2'. Note that k_4' is actually a little less than three times larger than k_2', and this is due to the way the changing fraction of nanocluster surface atoms is handled, which is discussed next.

As a nanocluster begins to grow, the first shell of metal atoms packs around the central metal atom until the central atom becomes "hidden" in the core of the nanocluster. In a close packed structure the first shell consists of 12 atoms packed around the central atom. If we make all the assumptions listed above (that all surface atoms are equally active, that the reaction is structure-insensitive, etc.), then $M(0)_{13}$, with its twelve surface atoms, should react only twelve times as fast as $M(0)_1$.[5] The loss of this surface atom during the growth of the first shell is accomplished "fractionally" in the kinetic model in Scheme 4.2; specifically, each metal atom added to the nanocluster from $M(0)_2$ to $M(0)_{13}$ is counted as the addition of only 11/12 of a reactive site for the purposes of assigning the statistically correct rate constant. As the nanocluster adds a second shell of metal atoms [i.e., goes from $M(0)_{13}$ to $M(0)_{55}$] the first shell starts to be covered up. To complete the second shell, 42 atoms have to be added and they cover up the 12 atoms in the first shell. On average, then, two atoms are covered for every seven atoms that are added. Hence, again for the purposes of

determining the appropriate rate constants, each atom added to the second shell was counted as the addition of only 5/7 of a reactive site.

Kinetic Modeling of Autocatalytic Surface Growth. The following is the complete kinetic modeling program as it was typed into MacKinetics. Comments about the program (indicated by the symbol, #) are included as an aid to the reader.

```
reset                                   # resets all values to zero

reactions                               # a list of all the reactions follows

H2gas -> H2soln, kf=1E9                 # hydrogen gas-to-soln rxn
H2soln -> H2gas, kr=4E11          # hydrogen soln-to-gas rxn

A -> B, k1=.002                         # the "nucleation" reaction

A + B -> C, k2=200                      # the "autocatalytic growth" reaction
A + C -> D, k3=383                      # C has 2 M(0) atoms so rate is ~2X as big
A + D -> E, k4=567                      # (And so on).
A + E -> F, k5=750
A + F -> G, k6=933
A + G -> H, k7=1117
A + H -> I, k8=1300
A + I -> J, k9=1483
A + J -> K, k10=1667
A + K -> L, k11=1850
A + L -> M, k12=2033
A + M -> N, k13=2217
A + N -> O, k14=2400
A + O -> P, k15=2543
A + P -> Q, k16=2686
A + Q -> R, k17=2829
A + R -> S, k18=2971
A + S -> T, k19=3114
A + T -> U, k20=3257
A + U -> V, K21=3400
A + V -> W, k22=3543
A + W -> X, k23=3686
A + X -> Y, k24=3829
A + Y -> Z, k25=3971
A + Z -> BB, k26=4114
A + BB -> CC, k27=4257
A + CC -> DD, k28=4400
A + DD -> EE, k29=4543
A + EE -> FF, k30=4686
A + FF -> GG, k31=4829
A + GG -> HH, k32=4971
A + HH -> II, k33=5114
A + II -> JJ, k34=5257
A + JJ -> KK, k35=5400
A + KK -> LL, k36=5543
A + LL -> MM, k37=5686
A + MM -> NN, k38=5829
```

```
A + NN -> OO, k39=5971
A + OO -> PP, k40=6114
A + PP -> QQ, k41=6257
A + QQ -> RR, k42=6400
A + RR -> SS, k43=6543
A + SS -> TT, k44=6686
A + TT -> UU, k45=6829

B + alkene + H2soln -> B + alkane, k51=4E5          # catalytic reporter reaction
C + alkene + H2soln -> C + alkane, k52=7.67E5   # C has 2 M(0) atoms so the
D + alkene + H2soln -> D + alkane, k53=11.3E5       # rate constant is ~2X as big
E + alkene + H2soln -> E + alkane, k54=15E5         # (And so on)
F + alkene + H2soln -> F + alkane, k55=18.7E5
G + alkene + H2soln -> G + alkane, k56=22.3E5
H + alkene + H2soln -> H + alkane, k57=26E5
I + alkene + H2soln -> I + alkane, k58=29.7E5
J + alkene + H2soln -> J + alkane, k59=33.3E5
K + alkene + H2soln -> K + alkane, k60=37E5
L + alkene + H2soln -> L + alkane, k61=40.7E5
M + alkene + H2soln -> M + alkane, k62=44.3E5
N + alkene + H2soln -> N + alkane, k63=48E5
O + alkene + H2soln -> O + alkane, k64=50.9E5
P + alkene + H2soln -> P + alkane, k65=53.7E5
Q + alkene + H2soln -> Q + alkane, k66=56.6E5
R + alkene + H2soln -> R + alkane, k67=59.4E5
S + alkene + H2soln -> S + alkane, k68=62.3E5
T + alkene + H2soln -> T + alkane, k69=65.1E5
U + alkene + H2soln -> U + alkane, k70=68E5
V + alkene + H2soln -> V + alkane, k71=70.9E5
W + alkene + H2soln -> W + alkane, k72=73.7E5
X + alkene + H2soln -> X + alkane, k73=76.6E5
Y + alkene + H2soln -> Y + alkane, k74=79.4E5
Z + alkene + H2soln -> Z + alkane, k75=82.3E5
BB + alkene + H2soln -> BB + alkane, k76=85.1E5
CC + alkene + H2soln -> CC + alkane, k77=88E5
DD + alkene + H2soln -> DD + alkane, k78=90.9E5
EE + alkene + H2soln -> EE + alkane, k79=93.7E5
FF + alkene + H2soln -> FF + alkane, k80=96.6E5
GG + alkene + H2soln -> GG + alkane, k81=99.4E5
HH + alkene + H2soln -> HH + alkane, k82=102E5
II + alkene + H2soln -> II + alkane, k83=105E5
JJ + alkene + H2soln -> JJ + alkane, k84=108E5
KK + alkene + H2soln -> KK + alkane, k85=111E5
LL + alkene + H2soln -> LL + alkane, k86=114E5
MM + alkene + H2soln -> MM + alkane, k87=117E5
NN + alkene + H2soln -> NN + alkane, k88=119E5
OO + alkene + H2soln -> OO + alkane, k89=122E5
PP + alkene + H2soln -> PP + alkane, k90=125E5
QQ + alkene + H2soln -> QQ + alkane, k91=128E5
RR + alkene + H2soln -> RR + alkane, k92=131E5
SS + alkene + H2soln -> SS + alkane, k93=134E5
TT + alkene + H2soln -> TT + alkane, k94=137E5
UU + alkene + H2soln -> UU + alkane, k95=139E5
```

```
end                     # this command means no more reactions

integrate 0 25 50       # integrates from 0-25 h giving 50 data pts
A .0012                 # the initial concentration of 'A' is 1.2 mM
alkene 1.65             # the initial concentration of cyclohexene is 1.65 M
H2gas 3.6               # the "virtual" concentration of hydrogen is 3.6 M

go                      # this makes the integration begin

plot alkene             # this tells the program to graph [alkene] vs time
plot B UU               # this tells the program to graph [B] and [UU] vs time
print alkene            # this prints out a list of 50 data pts for [alkene] vs time
```

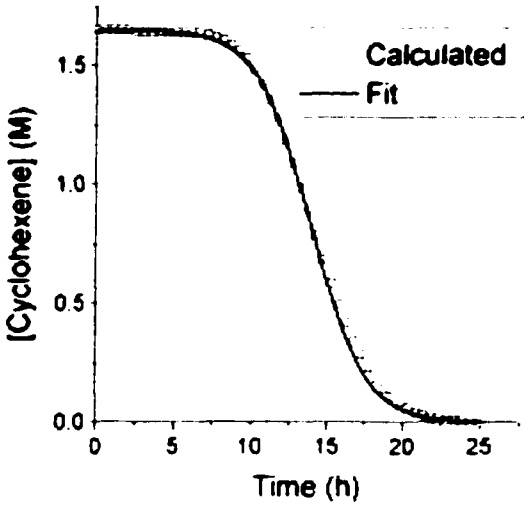

Figure 4.E. Plot of the alkene hydrogenation curve generated by computer modeling of the kinetic equations in Scheme 4.2 (main text), except that the equations corresponding to k_{46}'–k_{57}' have been removed (i.e., the alkene hydrogenation reactions for the species $M(0)_1$–$M(0)_{12}$ were removed from the model). This means that a "critical nucleus" of $M(0)_{13}$ must be reached before the nanoclusters are active olefin hydrogenation catalysts. The plot of the cyclohexene concentration vs time is sigmoidal and well fit by eqs. 2a-d (main text). The rate constants resulting from the fit are $k_{1(fit)} = 2.3 \times 10^{-4}\ h^{-1}$ and $k_{2(fit,corrected)} = 540\ M^{-1}h^{-1}$.

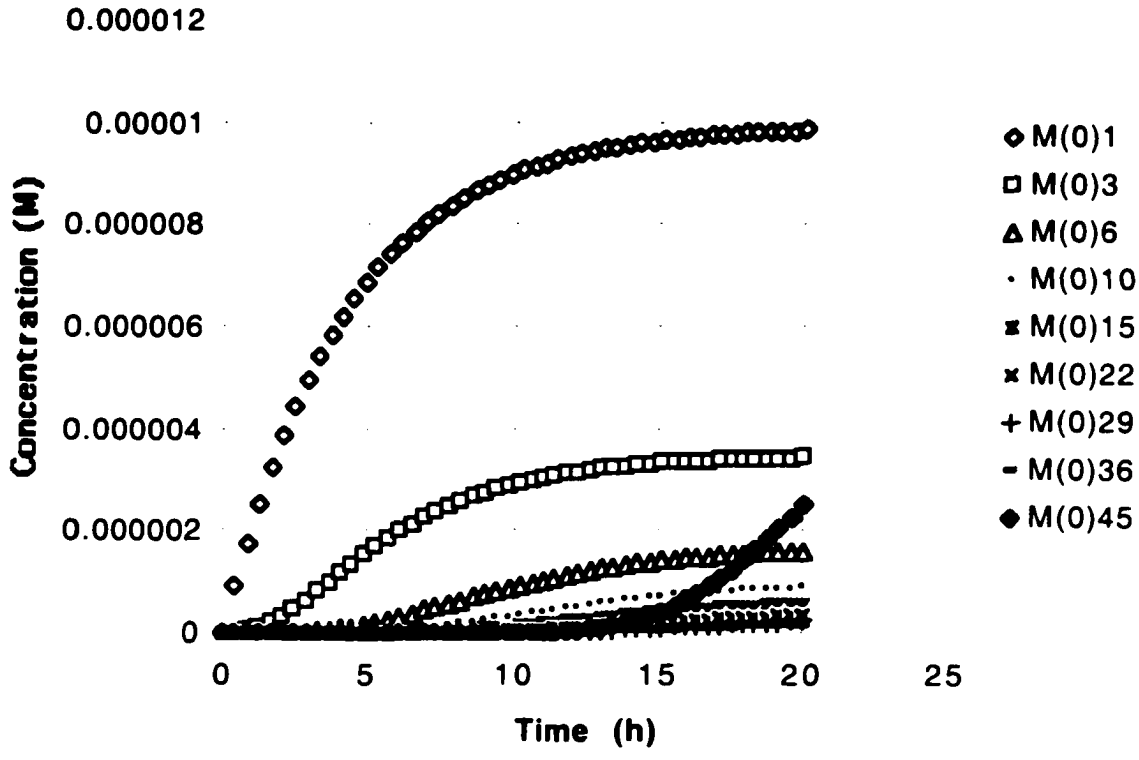

Figure 4.F. Plot of the concentrations of (selected) nanocluster species produced over the course of a numerical integration using the mathematical model shown in Scheme 4.2 (main text). The concentration of $M(0)_{45}$ is of special interest because $M(0)_{45}$ cannot undergo autocatalytic surface growth in this model. Consequently, it is undesirable for the concentration of $M(0)_{45}$ to become relatively large during the time when alkene hydrogenation occurs. The plot clearly shows that the concentration of $M(0)_{45}$ is almost zero until about 15 hours, at which time the hydrogenation of alkene is already almost complete (see Figure 4.7 of the main text).

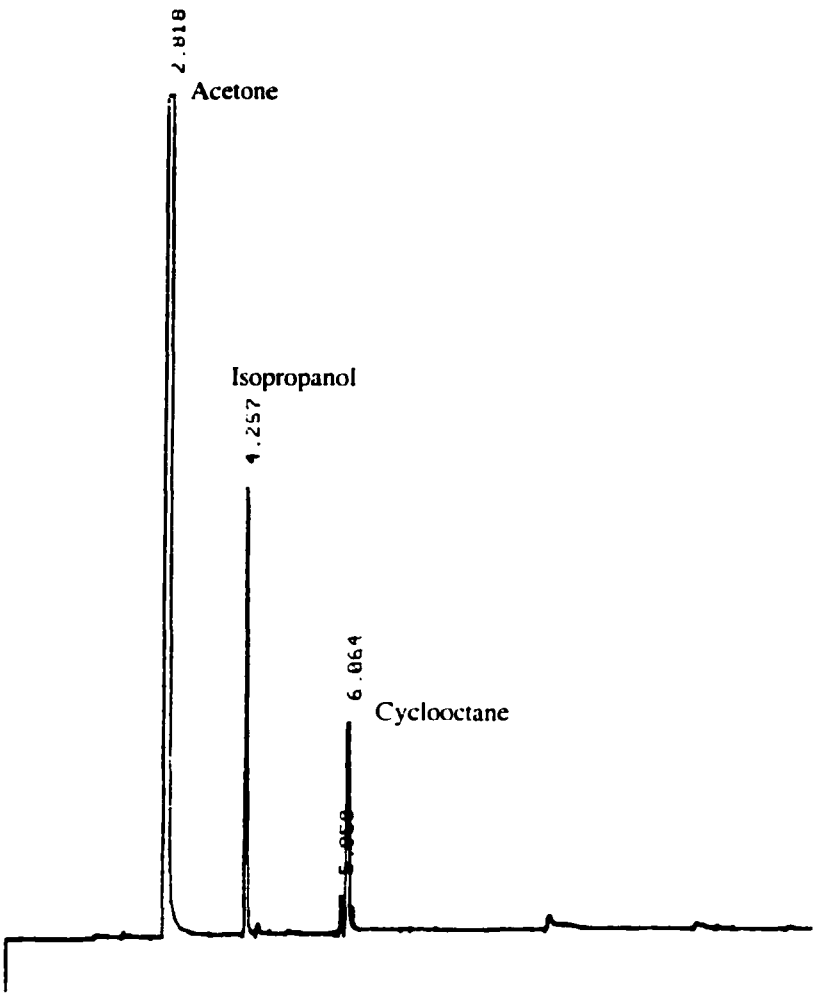

Figure 4.G. GLC of the reaction mixture from the H_2 gas-uptake experiment beginning with 151.2 mg **1** in 5.0 mL acetone-d_6. The reaction was quenched after 28.5 hrs. GLC shows acetone, cyclooctane, and isopropanol, present from the hydrogenation of acetone-d_6 by the Ir(0) nanoclusters. Quantitative GLC shows that 1.1 ± 0.1 equiv cyclooctane is produced. GLC conditions: T_1 = 50 °C, t_1 = 3 min, ramp = 10 °C/min, T_2 = 150 °C, t_2 = 16 min, Supelcowax 10 column, 4 μL injection.

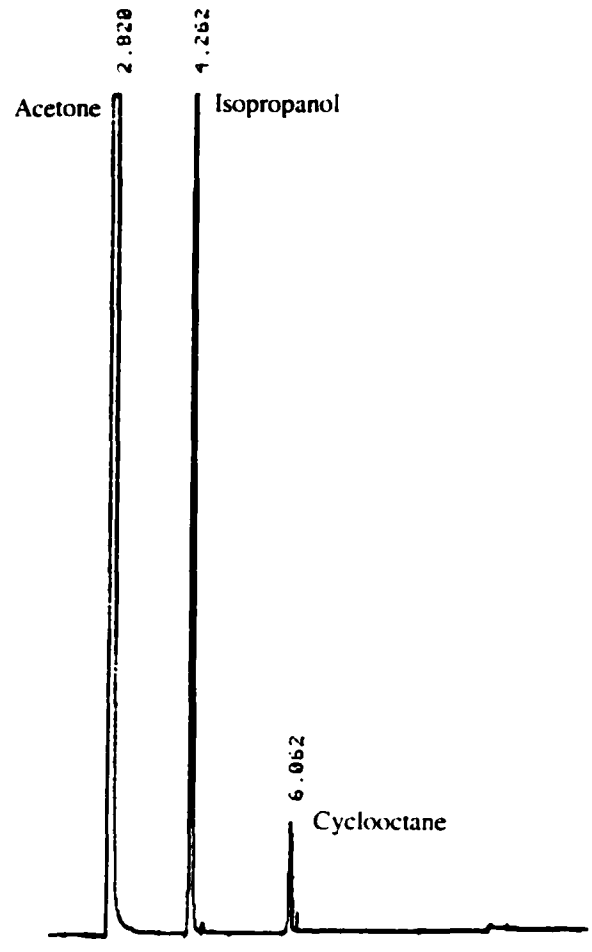

Figure 4.H. GLC of the reaction mixture from the H_2 gas-uptake experiment beginning with 152.7 mg **1** in 10.0 mL acetone-d_6. The reaction was stopped after more than 99 hrs, after which time all of the H_2 had been consumed (ca. 40 equiv). GLC shows acetone, cyclooctane, and isopropanol, present from the hydrogenation of acetone-d_6 by the Ir(0) nanoclusters. Quantitative GLC shows that 0.9 ± 0.1 equiv cyclooctane is produced. GLC conditions: T_1 = 50 °C, t_1 = 3 min, ramp = 10 °C/min, T_2 = 150 °C, t_2 = 16 min, Supelcowax 10 column, 4 μL injection.

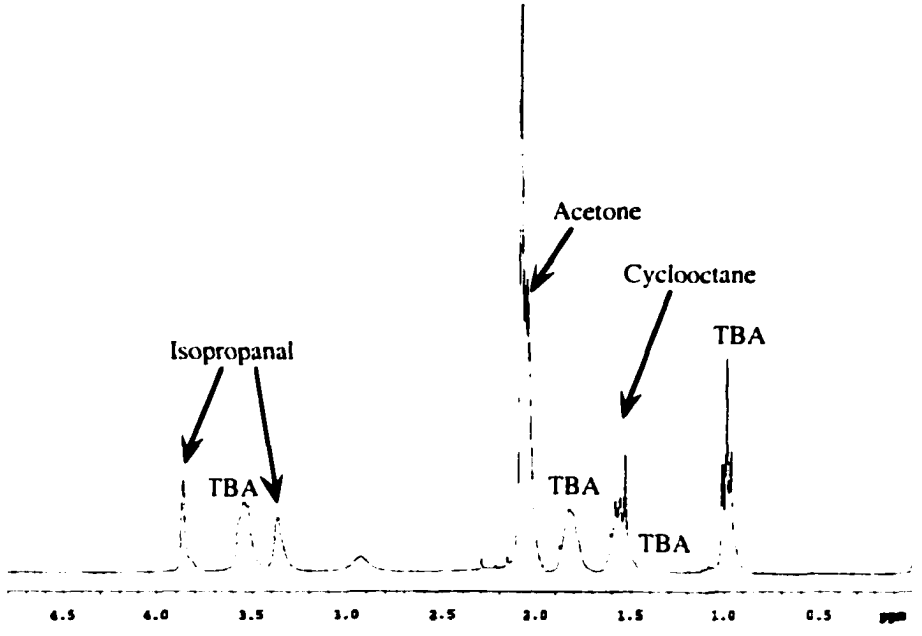

Figure 4.I. ^{1}H NMR of the neat reaction mixture from the H_2 gas-uptake experiment beginning with 152.7 mg **1** in 10.0 mL acetone-d_6. The reaction was stopped after more than 99 hrs, after which time all of the H_2 had been consumed (ca. 40 equiv). Resonances are seen for the tetrabutylammonium cations, cyclooctane, acetone (residual), and isopropanol, present hydrogenation of acetone-d_6 by the Ir(0) nanoclusters.

The Mathematics Behind the Treatment of the Solvent Vapor Pressure Correction to the Hydrogen Pressure Loss Measurement During a Hydrogenation Experiment.

The treatment below shows that, to correct for the solvent vapor pressure, either of the following needs to be true: (i) that it ($P_{solvent}$) needs to remain constant throughout the hydrogen pressure loss, or (ii) that the H_2 pressure loss data needs to be corrected point-by-point for the solvent vapor pressure and using an experimentally determined solvent vapor pressure curve.

(i) Beginning with equations 2(a-d) from the main text:

$$x \left[\; A \xrightarrow{k_1} B \; \right] \qquad (2)a$$

$$1\text{-}x \left[\; A + B \xrightarrow{k_2} 2\,B \; \right] \qquad (2)b$$

$$\sim 1400 \left[\; B + \text{cyclohex}\textit{ene} + H_2 \xrightarrow{k_3} B + \text{cyclohex}\textit{ane} \; \right] \qquad (2)c$$

$$\underline{\text{SUM:}} \quad A + \sim 1400\ \text{cyclohex}\textit{ene} + \sim 1400\ H_2 \xrightarrow{k_{obs}} B + \sim 1400\ \text{cyclohex}\textit{ane} \qquad (2)d$$

(ii) We want to measure $\left. \dfrac{-d[H_2]}{dt} \right/_{1400} = \dfrac{-d[A]}{dt} = \dfrac{+d[B]}{dt}$

(iii) We actually measure P_{total} vs time.

(iv) where, assuming ideal gasses,

$$P_{total} = \sum_i P_i = P_{hydrogen} + P_{acetone} + P_{cyclohexene} + P_{cyclohexane}$$

(v) Hence, $P_{hydrogen} = P_{total} - P_{acetone} - P_{cyclohexene} - P_{cyclohexane}$

Note that even $P_{acetone}$, the largest of the three vapor pressures, is only ca. 190 torr at 22 °C, compared to 40 psig H_2 (i.e., ca. 2700 torr H_2). $P_{cyclohexene} \approx P_{cyclohexane} \approx 80$ torr at 22 °C.

It then follows that:

$$P_{hydrogen} \approx P_{total} - P_{constant}$$

if the pressure change at the beginning of the hydrogenation, and due primarily to the acetone, is removed.

(vi) Differentiating, one sees that:

$$\frac{d[P_{hydrogen}]}{dt} = \frac{d[P_{total}]}{dt} - \frac{d[P_{constant}]}{dt}, \text{ but } \frac{d[P_{constant}]}{dt} = 0$$

These simple considerations show: (i) that we need to correct for the initial rise in the P_{total} data seen in, for example, Figure 4.6a in the main text (this can be done by either the point-by-point method or by the back extrapolation discussed in the main text), and (ii) the solvent and other vapor pressures need to be constant with time after that (i.e., and as they are after the initial rise to reach equilibrium as seen in the total pressure vs time curves in, for example, Figure 4.6a of the main text).

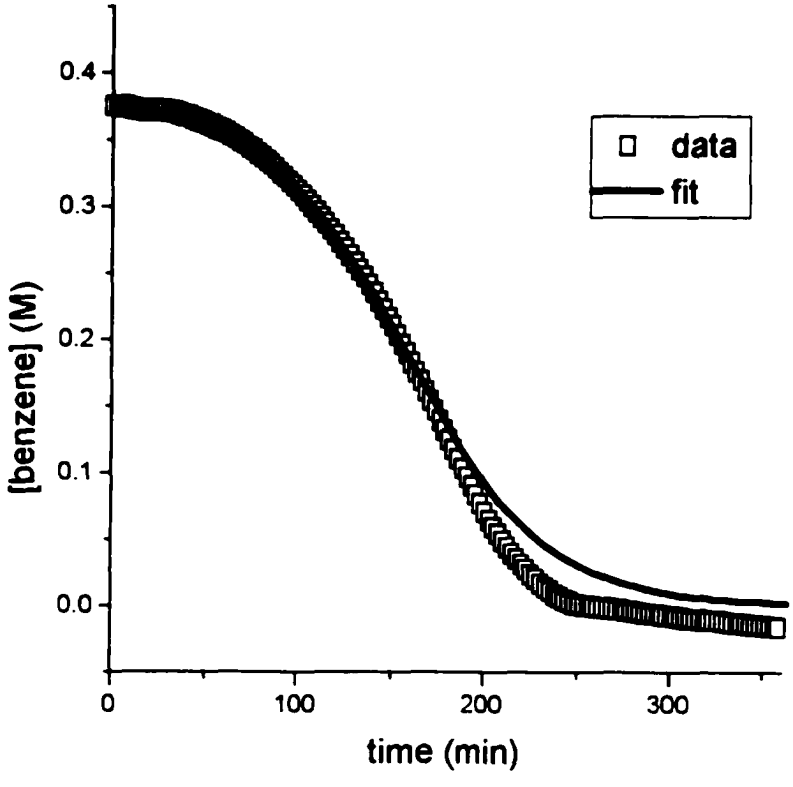

Figure 4.J. Curvefit of the loss of benzene over time when using $TBA_5Na_3(COD)Rh{\bullet}P_2W_{15}Nb_3O_{62}$ as the precatalyst. The conditions of the experiment were as follows: 20.3 mg precatalyst, 2.9 mL propylene carbonate, 0.1 mL benzene, 50 °C, 40 psig H_2 initial pressure. Note that the fit to the data is generally quite good. [The deviation in the fit at the end of the run (near 200 minutes) is both expected and understood, being due to the lack of sufficient benzene at this point to support the excess benzene conditions required by the pseudo-elementary step reporter methodology.] The curve-fit rate constants for the A → B nucleation, then A + B → 2B autocatalytic surface-growth mechanism are $k_1 = 1.6\ (\pm\ 0.2) * 10^{-3}\ min^{-1}$ and $k_{2(hydrogenation)} = 20\ (\pm\ 1)\ M^{-1}\ min^{-1}$ ($k_{2(hydrogenation)}$ has been corrected for the stoichiometry factor). In this experiment about 300 total turnovers of benzene hydrogenation are seen.

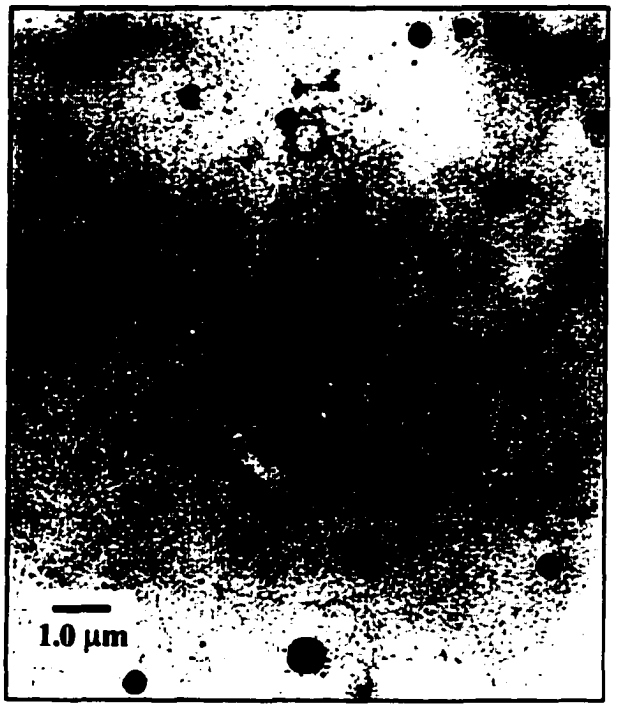

Figure 4.K. TEM of the reaction solution for a hydrogenation with the precatalyst $[Bu_4N][Ru(COD)(CH_3CN)(P_3O_9)]$. The reaction conditions included 5.5 mg of precatalyst, 2.5 mL of 95% EtOH, 0.5 mL of cyclohexene, 40 psig initial H_2 pressure and 50 °C reaction temperature. Note the presence of micrometer-size particles of bulk metal. Such large particles are an indication of nanocluster agglomeration, and show that the Ru(0) nanoclusters are not well-stabilized by the $P_3O_9^{3-}$ anion under these conditions.

References:

[1] Watzky, M. A.; Finke, R. G. *J. Am. Chem. Soc.* **1997**, *119*, 10382.

[2] (a) Note that, as detailed elsewhere,[1] the hydrogenation curve-fit k_2 (i.e., $k_{2(hydrogenation)}$) is corrected by a mathematically required stoichiometry factor, $k_{2(hydrogenation)} = 1400\, k_{2(fit)}$. (b) Both $k_{2(hydrogenation)}$ and $k_{2(GLC)}$ need to be, and thus are, corrected by a scaling factor introduced by the changing number of surface to total Ir(0) atoms (see the derivations and further details available in this Supporting Information as well as elsewhere[1]): $k_{2(hydrogenation)corrected} = k_{2(hydrogenation)}/0.8$, and $k_{2(GLC)corrected} = k_{2(GLC)}/0.7$ (Note that in footnote 38b elsewhere[1] there is a typographical error in both this latter equation (it was inverted) and in the scaling factor (the previous 0.51 is in error).

[3] Lin, Y.; Finke, R. G. *Inorg. Chem.* **1994**, *33*, 4891.

[4] Teo, B. K.; Sloane, N. J. A. *Inorg. Chem.* **1985**, *24*, 4545.

[5] (a) Note this kinetic model necessarily assumes that there is no size-dependence to the intrinsic rates of the nanoclusters, a point that is surely wrong given that an Ir(0) atom for example is 159 kcals/mol[5b] more energetic—and thus surely also more reactive—than is bulk $Ir(0)_n$ metal; also note that this assumption will be necessary until and unless a way to correct for the intrinsic $\Delta G_{formation}$ and associated reactivity of the nanoclusters becomes available. (b) Shriver, D. F.; Atkins, P.; Langford, C. H. *Inorganic Chemistry*, 2nd ed.; W. H. Freeman and Company: New York, 1994; p 317.

CHAPTER V

ANISOLE HYDROGENATION WITH WELL-CHARACTERIZED POLYOXOANION- AND TETRABUTYLAMMONIUM-STABILIZED Rh(0) NANOCLUSTERS: THE EFFECTS OF ADDED WATER AND ACID, PLUS ENHANCED CATALYTIC RATE, LIFETIME AND PARTIAL HYDROGENATION SELECTIVITY

This dissertation chapter contains the manuscript of a full paper published in *Inorganic Chemistry*, and describes the use of polyoxoanion- and tetrabutylammonium-stabilized Rh(0) nanoclusters for anisole (i.e., methoxybenzene) hydrogenation. Among soluble nanocluster catalysts, these Rh(0) nanoclusters have a record catalytic lifetime for monocyclic arene hydrogenation and an unprecedented selectivity for the partial hydrogenation of arenes. The work herein probes the effects of proton donors, such as water and tetrafluoroboric acid, on arene hydrogenation catalysis. Finally, the catalytic properties of soluble polyoxoanion-stabilized Rh(0) nanoclusters are compared to a prototype heterogeneous metal-particle catalyst, Rh/Al_2O_3.

The experiments described in this chapter were performed by J.A.W. The manuscript was prepared by J.A.W. with editing (about 20 hours total) by R.G.F.

Anisole Hydrogenation with Well-Characterized Polyoxoanion- and Tetrabutylammonium-Stabilized Rh(0) Nanoclusters: The Effects of Added Water and Acid, Plus Enhanced Catalytic Rate, Lifetime and Partial Hydrogenation Selectivity

Jason A. Widegren and Richard G. Finke

Abstract

Following a comprehensive look at the arene hydrogenation literature by soluble nanocluster catalysts (see Table 2.1), six key, unfulfilled goals in nanocluster arene hydrogenation catalysis are identified. To begin to address those six goals, well-characterized polyoxoanion- and tetrabutylammonium-stabilized Rh(0) nanoclusters have been synthesized by the reduction of the precisely defined precatalyst $[Bu_4N]_5Na_3[(1,5\text{-}COD)Rh{\bullet}P_2W_{15}Nb_3O_{62}]$ with H_2 in propylene carbonate solvent. These Rh(0) nanoclusters are characterized by their stoichiometry of formation, transmission electron microscopy, and the two rate constants which characterize their mechanism of formation; previous studies in our laboratories have provided additional characterization of polyoxoanion-stabilized Rh(0) nanoclusters. Propylene carbonate solutions of the Rh(0) nanoclusters catalyze the hydrogenation of anisole (methoxybenzene) under mild conditions

(22–78 °C, 30–40 psig H_2). Proton donors such as water or $HBF_4 \bullet Et_2O$ are discovered to affect both nanocluster formation and nanocluster arene hydrogenation catalysis. Under identical conditions the Rh(0) nanoclusters are 10-fold more active than a commercially available, oxide-supported 5% Rh/Al_2O_3 catalyst of the same average metal-particle size. A series of lifetime experiments shows that the Rh(0) nanoclusters are capable of at least 2600 total turnovers (TTO), a lifetime significantly longer than the ~100 TTO often seen for nanocluster arene hydrogenation catalysts, and a lifetime slightly better than the prior record of 2000 TTO for a literature nanocluster system. The present polyoxoanion-stabilized Rh(0) nanoclusters also display a record, albeit modest, 30% selectivity for the partial hydrogenation of anisole to 1-methoxycyclohexene with an overall yield of up to 8% at higher temperatures. In comparison to the 5% Rh/Al_2O_3 catalyst, the polyoxoanion-stabilized nanoclusters yield a 4.7-fold higher maximum yield of 1-methoxycyclohexene. The Summary and Conclusion section lists the seven main findings of the present work, including how they address five of the aforementioned six main goals in nanocluster arene hydrogenation.

Introduction

Arene hydrogenation is an active area of modern research,[1,2,3,4,5,6,7] the origins of which can be traced back to the catalytic hydrogenation of benzene one century ago using finely divided nickel as the catalyst.[8,9] The production of substituted cyclohexanes from the corresponding substituted arenes is the goal of much of this research.[10,11,12,13] The hydrogenation of benzene to cyclohexane is probably the most important industrially practiced arene hydrogenation reaction, the resultant cyclohexane being used primarily in the production of the nylon precursor, adipic acid.[14,15] Partial arene hydrogenation to cyclohex*enes* is also an active area of research,[1,16,17] the industrially practiced partial

hydrogenation of benzene to cyclohexene by Asahi Chemical Industry in Japan[18] being a noteworthy example.

Arene hydrogenation has also garnered current interest due to the demand for cleaner-burning, low-aromatic-content diesel fuels,[4] interest stimulated by the recent discovery that diesel exhaust particles contain powerful carcinogens,[19] particles which also contribute to the prevalence of asthma and nasal allergies.[20,21] The chemically demanding problem of hydrogenating aromatic polymers is also of current interest since the resultant polymers can have dramatically improved thermal and oxidative stability: for example, hydrogenation of aromatic rings in the biopolymer, lignin, has been suggested as a way to inhibit the yellowing of paper made from mechanical pulps.[22,23,24,25] Another example of the importance of aromatic polymer hydrogenation is the conversion of polystyrene to poly(cyclohexylethylene), a process which Dow Plastics is attempting to commercialize for use in optical media applications such as digital versatile discs (DVDs).[26] In short, arene hydrogenation remains a very important area of research in catalysis.

Traditionally, most arene hydrogenation has been done with classical heterogeneous catalysts. However, the use of soluble transition-metal nanoclusters[27,28,29,30,31,32,33,34,35,36,37,38,39,40,41,42] for arene hydrogenation has increased dramatically in recent years[10,11,12,22,23,43,44,45,46,47,48,49,50,51,52,53,54] (see Table 2.1 for a complete list, plus a brief description, of each paper dealing with monocyclic arene hydrogenation by soluble nanocluster catalysts). Soluble nanocluster catalysts have some advantages over traditional heterogeneous catalysts: first, they are often more active under mild conditions than the corresponding traditional heterogeneous catalysts,[11,47] and the present work will quantify that reactivity in the case of our polyoxoanion-stabilized nanoclusters. This enhanced reactivity is important when the substrate is temperature sensitive, for example. Second, soluble nanocluster catalysts are also more selective than the corresponding traditional heterogeneous catalysts for some reactions,[28] for example the larger cis/trans ratio for di-substituted benzene hydrogenation products seen for

nanoclusters.[47] Third, perhaps the most important advantage of soluble nanocluster catalysts is that they are easier to study because of their solubility and lack of a solid support; therefore, it is expected that they will be easier to optimize than traditional heterogeneous catalysts. Disadvantages of soluble nanocluster catalysts exist as well, of course, and in comparison to traditional heterogeneous catalysts: two of note are poorer stability towards bulk metal formation and the greater difficulty of catalyst/product separations over the simple filtration that is a hallmark advantage of traditional heterogeneous catalysts.

Much of the work using soluble nanocluster arene hydrogenation catalysts follows a seminal paper in 1983 by Januszkiewicz and Alper[43] which performed hydrogenations under biphasic, aqueous/organic reaction conditions using $[RhCl(1,5\text{-hexadiene})]_2$ as the precatalyst, and tetraalkylammonium hydrogen sulfate or tetraalkylammonium bromide as the phase transfer agent and nanocluster stabilizer (halide and tetraalkylammonium salts are well known, widely used nanocluster stabilizers[28,29,34,36,37]). The colloidal nature of the catalyst was actually not known at the time, but these authors insightfully suggest a year later in 1984 that the actual catalyst is "a highly active form of colloidal rhodium",[55] and subsequent studies by others on very similar systems identify colloidal Rh as the true arene hydrogenation catalyst in such systems.[23,49,51] Using mild reaction conditions (room temperature, 1 atm H_2), Januszkiewicz and Alper demonstrated up to 100 total turnovers for a variety of arenes (TTO, calculated by dividing the moles of hydrogenated arene by the moles of Rh present).[43] Unfortunately, no reaction times were given, so the catalytic activity (the turnover frequency, TOF) is unknown; providing a TOF for comparison to the literature and heterogeneous Rh catalysts is one of multiple goals, therefore, of the present work.

A perusal of the literature studies of soluble nanocluster arene hydrogenation catalysis in Table 2.1 demonstrates the following points: first, most studies use Rh(0) as the active metal, Rh also being the most active metal in the heterogeneous catalysis arene

hydrogenation literature.[56] Second, Ru(0) nanoclusters are the second most common catalyst in this literature, again paralleling the extensive use of Ru in the heterogeneous catalysis of arene hydrogenation. Third, the three most commonly used nanocluster precursor compounds are $[RhCl(diene)]_2$, $RhCl_3 \bullet 3H_2O$ and $RuCl_3 \bullet 3H_2O$, and most soluble nanocluster arene hydrogenation catalysts use tetraalkylammonium salts to stabilize the nanoclusters against agglomeration. Fourth, the reaction conditions are typically mild (approximately room temperature and 1 atm H_2) and often biphasic (aqueous/organic). Fifth, the best soluble nanocluster arene hydrogenation catalyst in the previous literature, in terms of catalytic activity and lifetime, is the one developed in 1999–2000 by Roucoux and coworkers[52,53] involving water-soluble nanocluster catalysts formed by $NaBH_4$ reduction of $RhCl_3 \bullet 3H_2O$ in aqueous solutions of hydroxyalkylammonium bromide salts. Using mild (room temperature, 1 atm H_2), aqueous/organic biphasic reaction conditions they demonstrate a record 2000 TTO in 37 hours for the hydrogenation of anisole (methoxybenzene).[53] It is not stated if their catalyst is still active after 2000 TTO.

More to the point of the present work, our comprehensive survey of the relevant literature (Table 2.1) reveals that the following are important, unfulfilled goals in the area of nanocluster arene hydrogenation: (i) the use of a nanocluster system in which the nanoclusters have been well characterized (so that one can use the relatively well-defined composition and nature of nanocluster metal-particle catalysts to understand better the observed catalysis); (ii) the use of nanoclusters stabilized by the anion which has a record stabilizing effect[57] and which yields nanoclusters with a record catalytic lifetime in solution for at least simple olefin hydrogenation,[58] the $P_2W_{15}Nb_3O_{62}^{9-}$ polyoxoanion; (iii) the development of a nanocluster arene hydrogenation system that is not aqueous/organic biphasic so that the commonly observed effects of water in arene hydrogenation systems can be tested and better understood—an important component of the present work, vide infra; (iv) the extension of the catalytic lifetime beyond the normally observed ~100 TTO in a well-defined system and, ideally, far beyond the current record of 2000 TTO[53]; (v) the

attainment of high yields of the valuable, partially hydrogenated, cyclohex*ene* products of arene hydrogenation, and with a better-defined, prototype nanocluster system; and (vi) the completion of a kinetic and mechanistic study.

Herein we describe studies that address the issues (i)-(vi) described above. Specifically, in the present work we describe the use of polyoxoanion- and tetrabutylammonium-stabilized Rh(0) nanoclusters[58,59,60] for the hydrogenation of anisole. Polyoxoanion-stabilized Rh(0) nanoclusters have been prepared and well characterized in our prior work.[58,59,60] In addition, the Rh(0) nanoclusters made under the specific anisole hydrogenation conditions utilized herein have been independently characterized by (a) confirmation of the expected stoichiometry of nanocluster formation, (b) transmission electron microscopy (TEM), and (c) a determination of the two rate constants that have been shown to characterize unequivocally the kinetics and mechanism of nanocluster formation under H_2.[61,62] The Rh(0) nanoclusters are shown to hydrogenate anisole under mild conditions (22–78 °C, 30–40 psig H_2) in a single phase using propylene carbonate as the solvent and compare well with the best literature nanocluster catalysts in terms of activity and lifetime. The effects on catalytic performance of added water and of added $HBF_4 \bullet Et_2O$ are tested and, among soluble nanocluster catalysts in the literature, the polyoxoanion-stabilized Rh(0) nanoclusters display an unprecedented, albeit modest, selectivity for the partial hydrogenation of anisole to 1-methoxycyclohexene.

Results and Discussion

I. The Synthesis and Characterization of Polyoxoanion-Stabilized Rh(0) Nanoclusters Formed under Anisole Hydrogenation Conditions. Since we have previously prepared and characterized polyoxoanion-stabilized 40 ± 6 Å Rh(0) nanoclusters under *cyclohexene* hydrogenation conditions,[58,59,60] all that is needed here is to detail our choice of anisole as a substrate, our Standard Conditions for its hydrogenation, and to

characterize the Rh(0) nanoclusters made under *anisole* hydrogenation conditions so that, with our earlier work,[58,59,60] the resultant Rh(0) nanoclusters qualify as well-characterized nanoclusters.

a. Choice of Anisole and Standard Conditions for Its Hydrogenation. Anisole was chosen as the substrate for four main reasons: (i) it has a high boiling point (154 °C), which minimizes evaporative loss during the hydrogenation experiments and subsequent work-up; (ii) the methyl group protons provide an excellent ^{1}H NMR handle; and (iii) the methoxy substituent makes anisole relatively easy to partially hydrogenate, compared to benzene, and also allows determination of the selectivity for hydrogenation over hydrogenolysis ($Ph–OCH_3 + H_2 \rightarrow Ph–H + CH_3OH$). Also, significantly, (iv) most papers dealing with soluble nanocluster catalysts for arene hydrogenation have used anisole or a substituted anisole as a substrate (see Table 2.1); hence, comparisons of the literature with the work herein are greatly facilitated by the choice of anisole as the substrate.

The Standard Conditions for anisole hydrogenation developed and used herein are 2.9 mL of propylene carbonate, 0.14 mL of anisole (1.3×10^{-3} mol), 20 ($\pm$ 0.5) mg of precatalyst, $[Bu_4N]_5Na_3[(1,5\text{-COD})Rh{\bullet}P_2W_{15}Nb_3O_{62}]$, **A** ($3.6 \times 10^{-6}$ mol), 22 °C and 40 ($\pm$ 1) psig initial H_2 pressure (ca. 3.7 atm), Scheme 5.1; these conditions allow for a maximum of 360 total turnovers at a maximum pressure loss at complete conversion of 11 psig in our apparatus, a value which will be used in the interpretation of several experiments which follow.

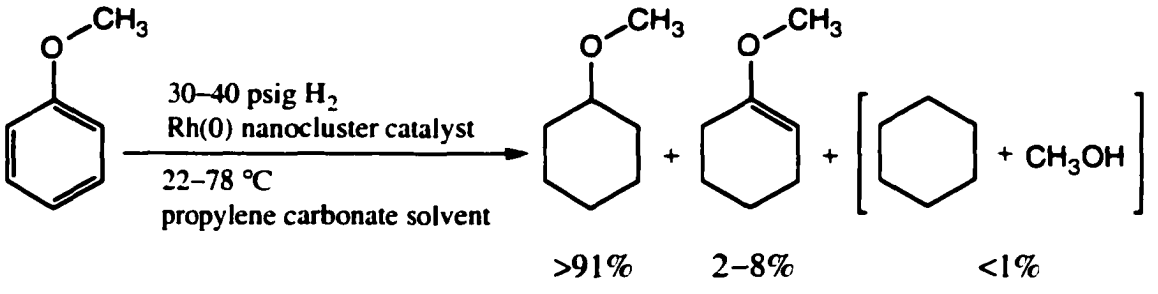

Scheme 5.1. The reaction products observed, plus the range of conditions used, for anisole hydrogenation. In every case the fully hydrogenated compound, methoxycyclohexane, was the major product. Maximum yields of the partially hydrogenated intermediate, 1-methoxycyclohexene, were in the ~2–8% range (see Table 5.2). The hydrogenolysis products, cyclohexane and methanol, were observed in trace amounts (<1%). Most hydrogenations were done at 22 °C, but a few were run at temperatures as high as 78 °C, experiments which show that increasing the temperature leads to an increase in the maximum yield of 1-methoxycyclohexene.

b. Formation of the Active, Polyoxoanion-Stabilized Rh(0) Nanocluster Catalyst in Anisole. The in situ reduction of **A**, to form polyoxoanion-stabilized Rh(0) nanoclusters was monitored as before[59] by measuring the H_2 pressure loss with a high-precision pressure transducer in an anisole hydrogenation under Standard Conditions; the resulting H_2 pressure vs time data are shown in Figure 5.1. At the end of the induction period the solution begins to darken giving the expected[59] clear, dark brown, completely soluble nanocluster solution after ca. 1.0 h under Standard Conditions. Judging from the pressure loss, the anisole hydrogenation reaction is ~20% complete after 22 h (~70 TTO) with a maximum rate of hydrogen uptake of 0.16 psig/h (a TOF of 5.2 turnovers/h). The rate of hydrogen uptake has slowed considerably after 20 h, as Figure 5.1 shows, and even though the conversion was only ca. 20%. A control experiment was done with the more easily reduced substrate cyclohexene to be sure that fully active Rh(0) nanoclusters were being formed; the observation of *H_2 mass-transfer-limited rates* of cyclohexene reduction (37.0 psig/h initial rate; Figure 5.A of the Supporting Information) confirms: (a) that very

active nanoclusters are being formed and, therefore, (b) that anisole hydrogenation is just, as expected, a significantly more difficult reaction.

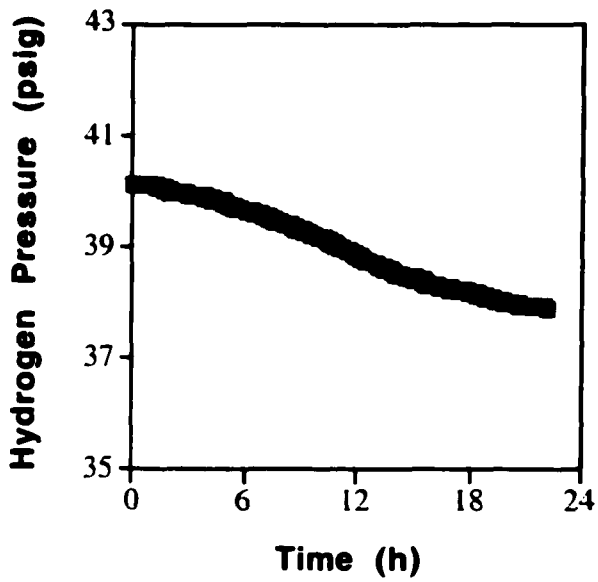

Figure 5.1. H_2 pressure vs time for a Standard Conditions anisole hydrogenation with $[Bu_4N]_5Na_3[(1,5\text{-COD})Rh{\bullet}P_2W_{15}Nb_3O_{62}]$, **A**, as the precatalyst. The conditions for the hydrogenation include 2.9 mL of propylene carbonate, 0.14 mL of anisole (1.3×10^{-3} mol), 20 ($\pm$ 0.5) mg of **A** (3.6×10^{-6} mol) and 22 °C. The total change in H_2 pressure for this experiment (about 2 psig) indicates that the reaction is only about 20% complete after 22 h, yet the rate of hydrogen uptake has already slowed considerably due to deactivation of the Rh(0) nanocluster catalyst.

c. Characterization of the Resultant Polyoxoanion-Stabilized Rh(0) Nanoclusters.

The polyoxoanion-stabilized Rh(0) nanoclusters formed under anisole hydrogenation conditions were characterized by (i) their precedented[59] stoichiometry of formation, Scheme 5.2, (ii) TEM of the resultant unagglomerated nanoclusters, Figure 5.2, (iii) X-ray photoelectron spectroscopy (XPS) to confirm the expected[59,63] intimate presence of the polyoxoanion surrounding the Rh(0) nanocluster, and (iv) demonstration of the characteristic autocatalytic kinetics of formation, Figure 5.3, in a cyclooctane evolution experiment (described below). Briefly, quantitative GLC analysis confirms that the

expected, 1.0 (± 0.1) equivs of cyclooctane evolve during the nanocluster formation reaction; the stoichiometry in Scheme 5.2 is further established by a hydrogen gas-uptake experiment reported elsewhere[59] showing that the precatalyst, **A**, dissolved in propylene carbonate and reduced by hydrogen in the absence of substrate, consumes the expected 2.5 equivs of H_2, plus 1.0 equiv of H_2 for the reduction of the polyoxoanion to its corresponding W(V)• containing heteropoly blue; see the discussion provided elsewhere.[59] XPS on a sample of the polyoxoanion- and tetrabutylammonium-stabilized Rh(0) nanoclusters confirmed the presence of the polyoxoanion stabilizer (W, Nb, and O peaks) as well as the expected, but still interesting, *lack* of a Rh(0) signal, consistent with the Rh(0) nanoclusters being buried under a ≥15 Å sheath of the large (12 Å × 15 Å) $P_2W_{15}Nb_3O_{62}^{9-}$ polyoxoanion stabilizer, Figure 5.K(a) of the Supporting Information).

$$n\ \{\ [(1,5\text{-COD})Rh^{I}\bullet P_2W_{15}Nb_3O_{62}]^{8-} + 2.5\ H_2 \longrightarrow$$

$$1/n\ Rh(0)_n + \text{cyclooctane} + H^+ + P_2W_{15}Nb_3O_{62}^{9-}\ \} \qquad (1)$$

$$n/2\ \{\ 2\ P_2W_{15}Nb_3O_{62}^{9-} + 2\ H^+ \longrightarrow$$

$$P_2W_{15}O_{61}Nb_3\text{-}O\text{-}Nb_3O_{61}W_{15}P_2^{16-} + H_2O\ \} \qquad (2)$$

Scheme 5.2. Stoichiometry of reduction for the precatalyst $[Bu_4N]_5Na_3[(1,5\text{-COD})Rh\bullet P_2W_{15}Nb_3O_{62}]$, **A**, under H_2. The evolution of 1.0 equiv of cyclooctane is a valuable GLC handle for monitoring the nanocluster formation reaction and its kinetics. Note also that the precedented[59,63] formation of the anhydride dimer of the polyoxoanion in the presence of acid produces 0.5 equivs of H_2O.

TEM analysis of the final reaction solution of a Standard Conditions anisole hydrogenation, Figure 5.2, shows nanoclusters with an average diameter of 5.3 (± 1.0) nm (these and all subsequent TEM error bars are one standard deviation (±1σ) for >135

nanoclusters counted). Assuming that the nanoclusters are spherical and that they have the same density as bulk Rh metal, one can calculate (see footnote 29 elsewhere[63]) that the Rh(0) nanoclusters with a diameter of 5.3 nm contain on average ~5700 Rh atoms, $Rh(0)_{\sim 5700}$. The TEM in Figure 5.2 showing *unagglomerated* nanoclusters at the end of the anisole hydrogenation under Standard Conditions yields another important conclusion: the catalytic deactivation noted earlier is not due to nanocluster agglomeration or instability (consistent with this the reaction solution remained clear, with no visible bulk metal or other precipitate throughout the anisole hydrogenation experiment). Hence, a surface deactivation phenomenon is most likely responsible for the observed deactivation.[64,65,66,67,68]

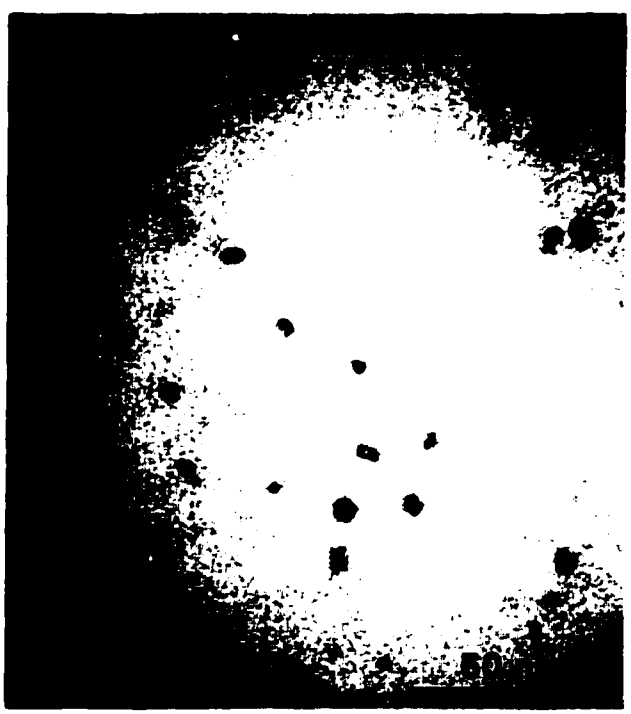

Figure 5.2. Transmission electron micrograph of polyoxoanion- and tetrabutylammonium-stabilized Rh(0) nanoclusters prepared under H_2 from $[Bu_4N]_5Na_3[(1,5\text{-COD})Rh{\bullet}P_2W_{15}Nb_3O_{62}]$ at 22 °C in 2.9 mL of propylene carbonate and 0.14 mL of anisole. Sample preparation involved removal of the propylene carbonate solvent via ether precipitation, as described in the Experimental. From 15 micrographs, including the one above, the size distribution of the resultant nanoclusters was found to be 5.3 (± 1.0) nm (where the error bars are $\pm 1\sigma$ for a sample size of n = 155), corresponding to an average nanocluster size of $Rh_{\sim 5700}$.

d. Characterization of the Nanocluster Formation Kinetics via the Evolution of Cyclooctane. Previously, we developed novel methods[61,62] to follow the kinetics of nanocluster nucleation and growth using the concept of a pseudoelementary mechanistic step.[69,70,71] The mechanism we uncovered, and which is proving general for the formation of transition-metal nanoclusters by the reduction of metal salts under H_2,[61] consists of two pseudo-elementary steps and their associated rate constants: slow continuous nucleation, $A \rightarrow B$ (rate constant k_1), followed by fast autocatalytic surface growth $A + B \rightarrow 2B$ (rate constant k_2), where **A** is the nanocluster precursor $[Bu_4N]_5Na_3[(1,5\text{-COD})Rh{\bullet}P_2W_{15}Nb_3O_{62}]$ as before, and B is the catalytically active surface Rh(0) metal. Characterization of the nanoclusters by showing this mechanism applies, plus measurement of the two rate constants k_1 and k_2, is actually one of the more important characterization tools for transition-metal nanoclusters since a high k_2/k_1 ratio correlates with increasing nanocluster size, an increasing tendency to near-monodispersity ($\leq$15% size distribution[29]) and, in general, reveals whether or not the nanoclusters are formed under a high degree of kinetic control.

The Rh(0) nanocluster formation reaction was monitored by removing aliquots of the reaction solution for GLC analysis to follow the evolution of the 1.0 equiv of cyclooctane that accompanies the conversion of the precursor, **A**, into Rh(0) nanoclusters under H_2, Scheme 5.2.[61,62] (The more precise and larger-data-set-generating method of monitoring the hydrogen uptake curve,[61,62] in this case for anisole hydrogenation, Figure 5.1, could not be used due to catalyst deactivation.) The cyclooctane evolution experiment was carried out using the Standard Conditions described above (except that the H_2 pressure was kept at a constant 40 ($\pm$ 1) psig, see the Experimental for further details). The loss of **A**, as measured by its 1:1 cyclooctane evolution stoichiometry (Scheme 5.2), has the expected, sigmoidal, autocatalytic[61,62] shape, Figure 5.3, with an induction period of about 1 h, followed by complete reduction of precatalyst in about 7 h. The experimental data are

well fit by the slow continuous nucleation, then fast autocatalytic surface growth mechanism and associated kinetic equations, A → B (rate constant k_1) and A + B → 2B (rate constant k_2).[61,62] The rate constants determined from the curve-fit are $k_{1(GLC)} = 3.4 \times 10^{-2}\ h^{-1}$ and $k_{2(GLC)} = 1.1 \times 10^{3}\ M^{-1}h^{-1}$ (no correction has been made to $k_{2(GLC)}$ for the "scaling factor",[61,62,72] that is, for the changing number of Rh atoms on the nanocluster surface). Significantly, the ratio of k_2 to k_1 is quite large (>10^4), a desirable feature indicating that the

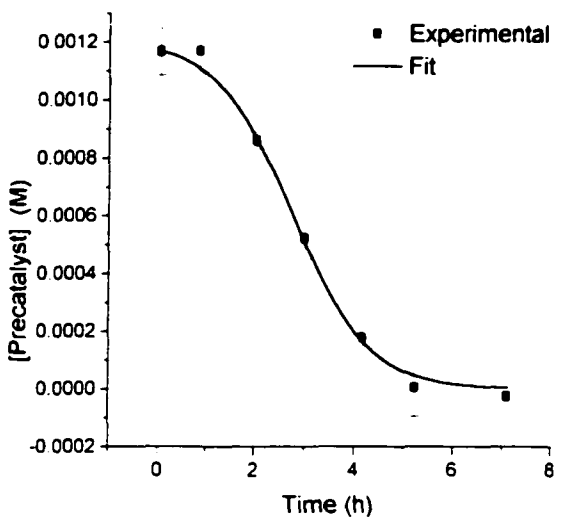

Figure 5.3. Loss of the Rh(0) nanocluster precatalyst $[Bu_4N]_5Na_3[(1,5\text{-}COD)Rh{\bullet}P_2W_{15}Nb_3O_{62}]$, **A**, as monitored by its GLC-determined evolution of 1.0 equiv of cyclooctane (according to eq. 1 of Scheme 5.2). The expected[61,62] sigmoidal experimental data has been fit to the kinetic equations A → B (rate constant k_1) and A + B → 2B (rate constant k_2), indicative of the nucleation and autocatalytic surface-growth mechanism.[61,62] The resulting, GLC-determined rate constants are $k_{1(GLC)} = 3.4 \times 10^{-2}\ h^{-1}$ and $k_{2(GLC)} = 1.1 \times 10^{3}\ M^{-1}h^{-1}$.

nanoclusters are formed in a kinetically controlled manner which generally leads to narrow size dispersion since nucleation (k_1) and growth (k_2) are well separated in time.[73] The sigmoidal shape of the curve in Figure 5.3, and the good curve-fit to the A → B and A + B → 2B kinetic scheme, provide excellent evidence that nanocluster formation occurs with the

same nucleation, then autocatalytic surface-growth mechanism that has been previously elucidated for transition-metal nanocluster formation under H_2.[61,62,72] Significantly, the curve-fit also shows that there is no detectable deactivation in the autocatalytic surface growth, at least for the time-scale of nanocluster formation in this experiment (i.e., in the first ~7 hours, compared to the 22 h of arene hydrogenation in the previous section and where deactivation is observed). The above results are notable even for their simple proof of when the nanoclusters are completely formed (i.e., so that they are not harvested too early or late); most papers in the nanocluster area fail to follow their reactions in any manner that allows this simple but important insight. Also notable is the quantitative fit to an established mechanism of formation done above, an important measurement we routinely do for our nanoclusters.

II. The Effects of Added Water on Anisole Hydrogenation. Arene hydrogenation with soluble nanocluster catalysts has been performed in biphasic (aqueous/organic) solvent systems in 12 of 17 prior studies, Table 2.1. There are only five reports in the literature where "water-free" hydrogenations were attempted.[11,12,24,51,74,75] In every case these "water-free" experiments exhibited either decreased hydrogenation activity or a complete lack of hydrogenation activity. Two studies report deuterium-labeling experiments showing the incorporation of hydrogen from water into the hydrogenated product.[51,74] It was suggested that the rate enhancing effect of water "could involve a favored cleavage of a Rh–C bond [i.e., the Rh–arene bond] by protonation (to give hydrogenated product) rather than reductive elimination of product from a hydrido-aryl species [H–Rh–Ar]".[51] In short, water is a key, but still ill-understood, component of arene hydrogenation with nanoclusters.

By design, our system allowed us to study the effects of water on the catalytic activity and lifetime of polyoxoanion- and tetrabutylammonium-stabilized nanoclusters. Studying the effects of water necessitated that we control all sources, and the absolute amount, of water present; we accomplished this by using carefully dried glassware, solvents

and reagents (see the Experimental for details). Our accounting for the water present includes the 0.5 equivs of water per $P_2W_{15}Nb_3O_{62}^{9-}$ generated during the reaction by the well-documented formation of the anhydride of the polyoxoanion, 2 $P_2W_{15}Nb_3O_{62}^{9-}$ + 2 H^+ → $[P_2W_{15}O_{61}Nb_3{-}O{-}Nb_3O_{61}W_{15}P_2]^{16-}$ + 1 H_2O, Scheme 5.2.[59,63]

The effects of H_2O on the Rh(0) nanoclusters were determined in a series of anisole hydrogenation experiments identical to the Standard Conditions anisole hydrogenation described earlier, except that 8–465 equivs of H_2O (vs Rh) was added. (A plot of the H_2 pressure vs time for each of these experiments is available as Figures 5.B–5.G in the Supporting Information.) Note that H_2O is present *during the formation of the nanoclusters*. Figure 5.4(a) shows a plot of maximum H_2 uptake rate vs the amount of H_2O added for this series of experiments. The maximum rate of H_2 uptake increases with added H_2O up to 60 equivs, Figure 5.4(a). With 60 equivs of H_2O added the maximum rate of H_2 uptake was 1.4 psig/h, almost 10-fold faster than the Standard Conditions experiment described earlier (i.e., with no H_2O added). If >60 equivs of H_2O are added, the rate of hydrogenation begins to decrease, Figure 5.4(a).

Figure 5.4(b) shows the same trend for the total H_2 uptake (which is proportional to the number of catalytic turnovers) in the first 24 h of each experiment—the total H_2 uptake reaches a peak for the experiment where 60 equivs of H_2O was added. Complete reduction of the precatalyst (i.e., complete nanocluster formation) was confirmed at the end of each of these experiments by quantitating the evolved cyclooctane with GLC. A black precipitate formed within the first 24 h for experiments with ≥60 equivs of H_2O added. The precipitate was unequivocally identified as bulk Rh(0) metal by XPS analysis (see Figure 5.K(b) of the Supporting Information).[76]

These results are of fundamental importance as they show for the first time: (i) a sharp maximum vs the amount of H_2O added, and (ii) nanocluster destabilization and precipitation in the presence of H_2O—that is, these results show that excess H_2O beyond a critical maximum has deleterious effects, at least for $P_2W_{15}Nb_3O_{62}^{9-}$-stabilized nanoclusters.

Similar behavior is expected, but untested, for other anionic, Brønsted basic, nanocluster stabilizers.

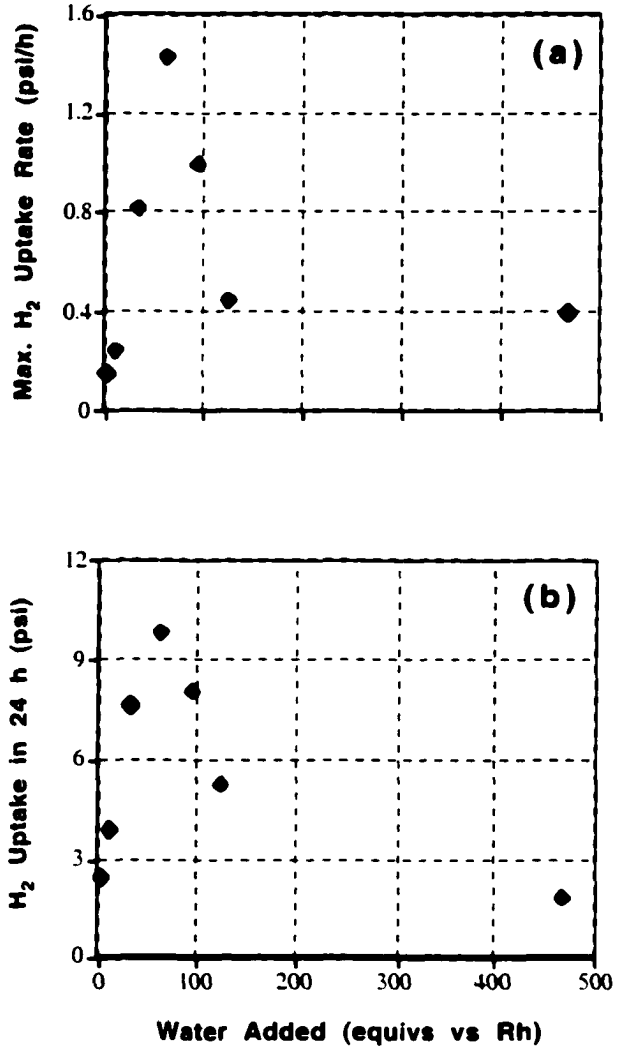

Figure 5.4. The effect of added H_2O on (a) the maximum rate of hydrogen uptake (i.e., the maximum rate of hydrogenation), and on (b) the total H_2 uptake (proportional to the total number of catalytic turnovers) observed over a 24-hour period. Both graphs reach a maximum at 60 equivs added H_2O. For the experiments with ≥60 equivs of H_2O a dark colored precipitate formed during the reaction, bulk metallic Rh(0) by XPS analysis.

We also tested the effect of H_2O on the activity of Rh(0) nanoclusters that were *formed in the absence of H_2O*. First, the nanoclusters were formed in the absence of substrate under what are otherwise essentially Standard Conditions (20 mg of **A** in 3.0 mL of propylene carbonate, 22 °C and 40 psig constant H_2 pressure). After 16 h under hydrogen, ample time for the complete reduction of the precatalyst **A**, 360 equivs of anisole (vs Rh) was added. The subsequent H_2 uptake rate is similar to the maximum H_2 uptake rate observed under Standard Conditions (0.094 psig/h and 0.16 psig/h, respectively), but TEM analysis of the resultant nanoclusters shows they are 6.2 (± 1.5) nm in diameter, corresponding to ca. $Rh(0)_{\sim 9100}$, and hence a bit larger on average than the 5.3 nm nanoclusters formed in the presence of substrate, a precedented, largely understood observation.[77]

After 5 h of anisole hydrogenation, at which point the anisole hydrogenation was about 4% complete, 60 equivs of H_2O (vs Rh) was added to the reaction solution, 60 equivs being chosen since it corresponds to the maximum in Figures 5.4a and 5.4b. (A plot of the hydrogen uptake curve for this experiment is available as Figure 5.H of the Supporting Information.) After adding H_2O the H_2 uptake rate was about twice as fast as before the H_2O was added (0.22 psig/h vs 0.094 psig/h). This experiment shows that H_2O increases the rate of hydrogenation, even for fully formed Rh(0) nanoclusters, *but only by 20% of the rate enhancement observed if H_2O is present while the nanoclusters are forming*. TEM measurements show no change beyond experimental error in average nanocluster diameter with added H_2O[78]—certainly nothing like the 10-fold change seen in the H_2 uptake rates with 60 equivs of H_2O present. Therefore, the effect of H_2O on nanocluster formation must be more subtle than a simply a change in total surface area.[79,80,81] These results, too, are of *fundamental significance as they suggest a previously missed effect of H_2O on the nanocluster formation reaction* in addition to its effect on arene hydrogenation catalysis.

The remaining hypotheses are that the rate enhancing effect of H_2O is caused by water acting as an acid, either protonating the basic polyoxoanion, $P_4W_{30}Nb_6O_{123}^{16-} + H_2O$

$\rightarrow HP_4W_{30}Nb_6O_{123}^{15-} + OH^-$ (which would effectively replace the $P_4W_{30}Nb_6O_{123}^{16-}$ with OH^-, a ligand that we previously demonstrated to be less stabilizing than the polyoxoanion[63]), or cleaving of the Rh–Ar bond by protonation to form the product, as suggested in the literature discussed earlier.[51] If it is the acidity of H_2O that is important for the rate enhancement, as the last two hypotheses suggest, then the addition of a different, stronger acid should have even larger effects then H_2O. Just such an experiment is described in the next section.

III. The Effects of Added $HBF_4 \bullet Et_2O$ on Anisole Hydrogenation. The hypothesis that H_2O is acting as a Brønsted acid was tested by seeing if a different acid, $HBF_4 \bullet Et_2O$, had any effect. $HBF_4 \bullet Et_2O$ was chosen because (i) it can be purchased anhydrous, which eliminates any interfering effects of water, (ii) it is a very strong acid, so any effect due to Brønsted acidity should be magnified, and (iii) the weakly coordinating anion BF_4^- has been shown not ligate or otherwise interfere with the stabilization of the nanoclusters by the much more basic and coordinating $P_2W_{15}Nb_3O_{62}^{9-}$.[57]

Given the issue of the *timing* of H_2O or other H^+ addition (before or after nanocluster formation), an experiment was performed in which fully *preformed* Rh(0) nanoclusters were prepared (as detailed in the Experimental section). Then 360 equivs of anisole (vs Rh) was added and the H_2 uptake rate was measured. Finally, 10 equivs of $HBF_4 \bullet Et_2O$ (vs Rh) was added and the H_2 uptake rate was measured again. The H_2 uptake rate was *about 6-fold faster* after the $HBF_4 \bullet Et_2O$ was added (0.63 psig/h; see Figure 5.I of the Supporting Information for the hydrogen uptake curve). This experiment shows that $HBF_4 \bullet Et_2O$ increases the catalytic activity of fully formed Rh(0) nanoclusters.

The effects or acid or water are consistent with either (or a combination of both) of the hypotheses noted above: an H^+-assisted cleavage of the Rh–Ar bond (we are accumulating evidence that H^+-assisted reductive elimination of nanocluster M–C bonds is a more general phenomenon[82]), and/or protonation of the polyoxoanion, thereby removing it from the surface of the nanocluster and yielding both a more active, and a less stable,

nanocluster. The observation of a metal precipitate when excess H^+ or H_2O is added requires that some of the observed effects must be due to the interaction of H^+ or H_2O with the basic $P_2W_{15}Nb_3O_{62}^{9-}$ polyoxoanion (pKa ~12; see the Supporting Materials elsewhere[83]).

IV. A Comparison of the Surface-Area-Corrected TOF for Two Rh(0) Nanocluster Catalysts and 5% Rh/Al_2O_3. By definition, TOF [(moles product) × (moles active site)$^{-1}$ × (time)$^{-1}$] should include corrections for the true number of active sites.[84] A first approximation way to estimate the number of active sites is to correct the TOF for the calculated number of surface atoms on an average nanocluster.[85] For example, in Roucoux's 2.1 nm average diameter nanoclusters[53] about 50% of the Rh(0) atoms are on the surface of the nanocluster.[79] Hence, dividing the uncorrected average TOF for Roucoux's catalyst of 54 turnovers/h (i.e., 2000 TTO ÷ 37 h reaction time) by 0.5 gives a corrected TOF of about 110 turnovers/(h·mol exposed Rh).

A TEM of the polyoxoanion-stabilized Rh(0) nanoclusters taken after 24 h in an experiment using Standard TTO Conditions (see Table 5.1) reveals 3.7 (± 0.6) nm diameter nanoclusters, corresponding to an average size of $Rh(0)_{\sim 1900}$ in which ca. 30% of the Rh(0) atoms are on the surface of the nanocluster.[79] Using the data in Table 5.1 for the Standard TTO Conditions experiment and dividing the apparent TOF by 0.3, one calculates a corrected TOF of 42 turnovers/(h·mol exposed Rh), *about half that of Roucoux's catalyst.*

For comparison, using the data in Table 5.1 for the 5% Rh/Al_2O_3 and dividing by a correction factor of[86] 0.3 one calculates a corrected TOF of 4 turnovers/(h·mol exposed Rh). These simple calculations yield another important insight, one fortified by an analogous finding in our catalyst poisoning work[84]: *the Rh(0) nanoclusters are at least 10-fold more active per exposed metal atom than their oxide-supported analogs.*

V. Anisole Hydrogenation Catalytic Lifetime Experiments with Polyoxoanion-Stabilized Rh(0) Nanoclusters and Their Comparison to Known Literature Catalysts. Practical catalytic applications, as well as mechanistic studies of

meaningful catalysts, both require a reasonable catalyst lifetime. To date, most of the literature systems using soluble (i.e., unsupported) nanoclusters as arene hydrogenation catalysts have had modest lifetimes at best, generally in the range of ≤100 TTO as Table 2.1 documents. The longest catalytic lifetime reported in the literature for such a system is the recent work by Roucoux and coworkers mentioned in the Introduction: under biphasic conditions, and using an aqueous solution Rh(0) nanoclusters stabilized by N-alkyl-N-(2-hydroxyethyl)ammonium bromide salts, they demonstrated 2000 TTO for anisole hydrogenation in 37 h at 20 °C and 1 atm of H_2.[53]

We tested the catalytic lifetime of our polyoxoanion- and tetrabutylammonium-stabilized Rh(0) nanoclusters for anisole hydrogenation in propylene carbonate, Table 5.1, first without, and then with, added H_2O or $HBF_4 \bullet Et_2O$, and under conditions which allow for a maximum of 2600 TTO. We also tested the 5% Rh/Al_2O_3 catalyst under the same conditions as a valuable comparison point.

The essence of the results, as summarized in Table 5.1, are that: (i) under Standard TTO Conditions, 1500 TTO are seen, but they require a rather long time, 120 h, and yield a small amount of black precipitate at the end of the reaction; (ii) with 30 equivs of H_2O added 2600 TTO are observed, a value higher than any reported in the literature (cf. Table 2.1), but a long time of 215 h is required and, again, a small amount of black precipitate is visible at the end of the reaction; (iii) 60 equivs of H_2O (the amount of water corresponding to the maximum in rate in Figure 5.4) does not improve the TTO beyond 1500 TTO due to the effects of water destabilizing the nanoclusters with more black precipitate being visible at the end of this experiment than for either of the previous two experiments (the reaction was stopped at 120 h); and (iv) 10 equivs of $HBF_4 \bullet Et_2O$ is more effective in that it gives 2600 TTO in a shorter, 144 h time. (An interesting organic side product, dodecahydrotriphenylene, precipitated from solution during the reaction with $HBF_4 \bullet Et_2O$; see the Supporting Information for the unequivocal characterization, as well as two possible mechanisms of formation, of this product from acid-catalyzed condensation of the partial

hydrogenation product 1-methoxycyclohexene.) Other key findings from the data in Table 5.1 are: (v) acetone is clearly an inferior solvent to propylene carbonate,[87] giving only 130 TTO plus more precipitate after only 95 h (when the reaction was stopped) than in any of the experiments in propylene carbonate; and (vi) the commercial 5% Rh/Al_2O_3 catalyst is very inferior compared to the Rh(0) nanoclusters and at the same level of Rh loading and same general particle size,[86] giving only 34 (± 2) TTO after 25 hours, and (in the same experiment) only 55 (± 4) TTO after 48 hours. This result is consistent with literature reports of relatively low activities of supported Rh catalysts for arene hydrogenation under similar conditions.[47,53,88]

Table 5.1. Total turnover experiments with Rh(0) nanoclusters or 5% Rh/Al_2O_3

Experimental Details	TTO Demonstrated	Reaction Time
Standard TTO Conditions[a]	1500 ± 100	120 h[e]
30 Equivs of H_2O Added	2600[b]	215 h[e]
60 Equivs of H_2O Added	1500 ± 100	120 h[e]
10 Equivs of HBF_4•Et_2O Added	2600[b]	144 h[e]
Acetone Solvent[c]	130 ± 10	95 h[f]
7.4 mg of 5% Rh/Al_2O_3[d]	55 ± 4	48 h

[a] The standard conditions for TTO experiments included 20.0 (± 0.5) mg $[Bu_4N]_5Na_3[(1,5\text{-}COD)Rh{\bullet}P_2W_{15}Nb_3O_{62}]$ (3.6×10^{-6} mol), 2.0 mL propylene carbonate, 1.0 mL anisole (9.2×10^{-3} mol; 2600 equivs vs the total Rh present), constant 40 psig H_2 and 22 °C. Changes or additions to the standard conditions are noted in the "Experimental Details" column above.

[b] Complete conversion of the substrate was observed in this experiment.

[c] The acetone used for this experiment is fairly "wet", containing 0.26% H_2O (compared to <0.005% H_2O for the propylene carbonate); for this experiment the acetone solvent contains 64 equivs of H_2O vs Rh.

[d] This amount of catalyst was chosen because 7.4 mg of 5% Rh/Al_2O_3 contains 3.6×10^{-6} mol of Rh, the same as the other TTO experiments.

[e] A small amount of black precipitate was visible at the end of the reaction.

[f] A large amount of precipitate was visible at the end of the reaction.

These lifetime experiments show that the polyoxoanion- and tetrabutylammonium-stabilized Rh(0) nanoclusters are reasonably long-lived catalysts for anisole hydrogenation, at least in comparison to the present state-of-the-art. In fact, the catalytic lifetime of ~2600 TTO (*in 144 h* with 10 equiv HBF_4•Et_2O added) is the longest demonstrated lifetime for any soluble nanocluster arene hydrogenation catalyst in the literature. However, recall that the Rh nanocluster catalyst developed by Roucoux and co-workers is capable of 2000 TTO

in 37 h,[53] and we suspect it may be capable of even greater TTO values. The additional suggestion here, which is unproven but quite plausible, is that the weakly basic and non-chelating Br^- stabilizer used in the Roucoux catalyst binds less strongly to the nanocluster surface, affording a higher TOF (vide supra), but a shorter lifetime, vs the $P_2W_{15}Nb_3O_{62}^{9-}$ polyoxoanion. Obviously, additional studies of the rate and lifetime (and selectivity, vide infra) of arene hydrogenation vs the X^- stabilizer[57] are warranted.

VI. The Observation of Partial Hydrogenation Products in the Hydrogenation of Anisole. Despite the widespread use of anisole as a substrate in arene hydrogenation studies with many types of catalysts (i.e., not just soluble nanocluster catalysts), its partial hydrogenation has been observed in only four cases.[89,90,91,92] The highest yield of 1-methoxycyclohexene with any of these catalysts is 20% using a heterogeneous 5% Ru/charcoal catalyst.[89] Even though anisole or some other aryl ether is used as a substrate in fourteen of the references in Table 2.1, the partial hydrogenation of an aryl ether has never been observed with a soluble nanocluster catalyst (see the documentation of this claim in the Supporting Information). Consequently, the yields of 1-methoxycyclohexene as high as 8% observed in the present anisole hydrogenation experiments are significant.

Figure 5.5 shows the percent yield of 1-methoxycyclohexene for an anisole hydrogenation experiment done at 40 °C; the identity of 1-methoxycyclohexene was unequivocally established by gas chromatography-mass spectrometry (GC-MS) and verified by the GLC retention time vs authentic 1-methoxycyclohexene. Quantitation of the amount of 1-methoxycyclohexene was accomplished by GLC using the established concept of "effective carbon number" and the accuracy of the quantitation was verified by ^{1}H NMR (see the Supporting Information for details). The concentration of 1-methoxycyclohexene vs time, Figure 5.5, is typical of, and quite well fit by, a classic A → B → C kinetic scheme,[93] the intermediate 1-methoxycyclohex*ene*, B, growing in and then being completely

converted to the final product, methoxycyclohex*ane*, C, in hydrogenations that were allowed to go to completion.

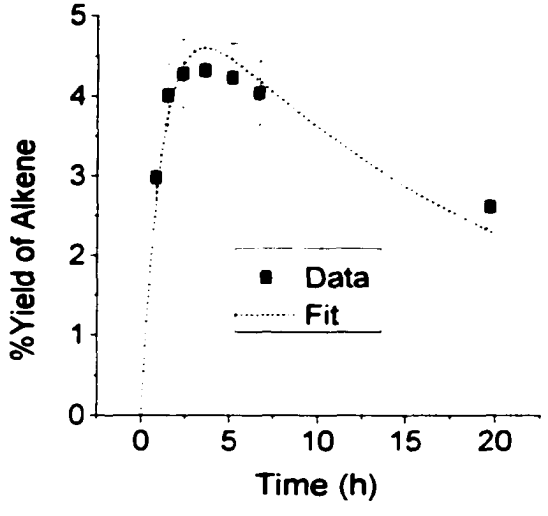

Figure 5.5. Percent yield of 1-methoxycyclohexene (determined by GLC) vs time for an anisole hydrogenation with polyoxoanion- and tetrabutylammonium-stabilized Rh(0) nanoclusters. The conditions were 2.9 mL of propylene carbonate, 0.14 mL of anisole, 20 mg of $[Bu_4N]_5Na_3[(1,5\text{-COD})Rh{\bullet}P_2W_{15}Nb_3O_{62}]$, 40 °C and 40 psig H_2 pressure. The maximum yield of 1-methoxycyclohexene for this experiment was 4.3%, which occurred at 65% conversion of anisole. The data are fit to an A → B → C kinetic scheme[93] (the dotted line), where B is the intermediate, 1-methoxycyclohexene.

Methoxycyclohexane and 1-methoxycyclohexene are the only *major* products detected by GLC in these experiments, Scheme 5.1. For example, see Figure 5.J(b) of the Supporting Information for the GLC trace for the reaction solution of an anisole hydrogenation run at 78 °C. Hydrogenolysis of the ether linkage to yield cyclohexane and methanol, Scheme 5.1, was detected, but occurred at trace levels (<1% yield).

Table 5.2 shows a list of experiments for which the selectivity to 1-methoxycyclohexene was quantitated. Using Standard Conditions, the initial selectivity to 1-methoxycyclohexene was 30 (± 2)% and the maximum yield of 1-methoxycyclohexene was 2.1 (± 0.2)%, which occurred at about 70% conversion. Increasing the temperature of

the reaction to 78 °C does not significantly change the initial selectivity, but it has a fairly dramatic effect on the maximum yield of 1-methoxycyclohexene: the maximum yield doubles on going from 22 °C to 40 °C, and doubles again on going from 40 °C to 78 °C. The 78 °C experiment had a maximum yield of 8.1 (± 0.8)% at 41% conversion, at which point the catalyst had lost all activity (although no precipitate was visible to the eye at this point). Complete deactivation occurred within about 1 h in the 78 °C experiment. By TEM these deactivated nanoclusters were found to be 5.7 (± 1.0) nm in diameter, the same size within experimental error as the 5.3 (±1.0) nm nanoclusters formed at 22 °C. It follows that a surface deactivation, and not an agglomeration, process must have inactivated the nanoclusters.

Table 5.2. GLC-determined selectivity for the catalytic hydrogenation of anisole to 1-methoxycyclohexene under various conditions

Experimental Details	Initial Selectivity (%)[b]	Maximum Yield (%)[c]	% Conversion at Max. Yield[d]
Standard Conditions (22 °C)[a]	30 ± 2	2.1 ± 0.2	70 ± 14
40 °C	31 ± 2	4.2 ± 0.4	64 ± 7
78 °C	33 ± 2	*8.1 ± 0.8*[e]	41 ± 2[e]
1.05 Equivs of $(Bu_4N)_9P_2W_{15}Nb_3O_{62}$ Added	30 ± 2	2.8 ± 0.3	39 ± 9
2.01 Equivs of $(Bu_4N)_9P_2W_{15}Nb_3O_{62}$ Added	27 ± 2	1.8 ± 0.2	29 ± 3
60 Equivs of H_2O Added	31 ± 2	2.6 ± 0.3	62 ± 12
Acetone Solvent	32 ± 2	1.7 ± 0.2	21 ± 8
7.4 mg of 5% Rh/Al_2O_3[f] at 22 °C	38 ± 3	1.7 ± 0.2[e]	8 ± 1[e]
7.4 mg of 5% Rh/Al_2O_3[f] at 78 °C	22 ± 2	1.4 ± 0.1[e]	6 ± 1[e]

[a] The Standard Conditions for these experiments included 20.0 (± 0.5) mg $[Bu_4N]_5Na_3[(1,5\text{-}COD)Rh{\bullet}P_2W_{15}Nb_3O_{62}]$ (3.6×10^{-6} mol), 2.9 mL propylene carbonate, 0.14 mL anisole (1.3×10^{-3} mol), constant 40 psig H_2 and 22 °C. Changes or additions to the standard conditions are noted in the "Experimental Details" column above.

[b] The initial selectivity is defined as [mol alkene/(mol alkene + mol alkane)]×100. The initial selectivity was determined at ≤ ~10 TTO. Error bars of ±7% have been assigned, which encompasses the maximum variation in nine repeat experiments under various conditions.

[c] The yield is defined as [mol alkene/(mol alkene + mol alkane + mol arene)]×100. Error bars of ±10% have been assigned, ±10% being twice the maximum variation in three repeat experiments at 40 °C.

[d] The % conversion is defined as [(mol alkene + mol alkane)/(mol alkene + mole alkane + mol arene)]×100. The error bars were determined by the frequency of sampling relative to the reaction progress.

[e] Deactivation stopped the hydrogenation at this point.

[f] This amount of catalyst was chosen because 7.4 mg of 5% Rh/Al_2O_3 contains 3.6×10^{-6} mol of Rh, the same as the other experiments.

The most obvious explanation for the relatively high selectivity in our system and for the partially hydrogenated product, 1-methoxycyclohexene, is the presence of the surface-attached[59,62,63] $P_2W_{15}Nb_3O_{62}^{9-}$; hence, we undertook experiments designed to probe the effect of the presence of the $P_2W_{15}Nb_3O_{62}^{9-}$ polyoxoanion. The addition of 1.0 equivs of the parent polyoxoanion, $(Bu_4N)_9P_2W_{15}Nb_3O_{62}$, to an otherwise Standard Conditions experiment (i.e., and in which 1.0 equivs $P_2W_{15}Nb_3O_{62}^{9-}$ per Rh atom is already present) gave no change in the initial selectivity but did lead to a small, probably significant increase in the maximum yield of alkene (compared to the Standard Conditions experiment). Interestingly, the reaction profile changed with added $(Bu_4N)_9P_2W_{15}Nb_3O_{62}$—the maximum yield of alkene occurred at about 39% conversion, sooner than for the Standard Conditions experiment. When 2.05 equivs of $(Bu_4N)_9P_2W_{15}Nb_3O_{62}$ was added to an otherwise Standard Conditions experiment the rate of catalytic hydrogenation was severely depressed and the maximum yield of alkene actually went back down to the level of the Standard Conditions experiment. Control experiments were also done which rule out the possible effects of H_2O[94] or solvent[95] on the observed, high selectivities; control experiments with the 5% Rh/Al_2O_3 catalyst were also performed.[96] The important implication is *that the $P_2W_{15}Nb_3O_{62}^{9-}$ is at least partially, and perhaps predominantly, responsible for the observed—and desired—selectivity*. Such demonstrations that nanocluster surface ligands can alter selectivity[97] are quite important, pointing to future directions of nanocluster research that promise to be productive. Figure 5.L in the Supporting Information shows how, in a general way, surface adsorbed polyoxoanions or other ligands can alter selectivity to the monoene by increasing the K(desorption) equilibrium constant for the monoene intermediate and in the classic Horiuti–Polanyi mechanism for catalytic hydrogenation on metal surfaces.

The important points, then, are: (i) partial hydrogenation of an aryl ether to the substituted cyclohexene using a nanocluster catalyst has been observed for the first time; (ii) a similar average particle size,[86] and thus surface area, 5% Rh/Al_2O_3 catalyst has a similar

selectivity at low temperature, but poorer selectivity at higher temperature, than the nanoclusters, and (iii) hence nanocluster catalyst provides the highest yield of 1-methoxycyclohexene. Overall, then, an important finding is that the polyoxoanion-stabilized nanoclusters (iv) behave as soluble analogs of heterogeneous catalysts[29]—but ones with improved selectivity, at least in this one particular reaction and under the conditions employed. This discovery also makes the present catalyst system an intriguing one for the further study of the many important variables in the partial hydrogenation of arenes with metal particle catalysts[1,17,98] and studies of the deactivation processes in those catalysts. Looking at the practical effects of polyoxoanions on functioning arene hydrogenation heterogeneous catalysts is also an important avenue of research suggested by our experiments.

Summary and Conclusions

Six key goals in the area of nanocluster arene hydrogenation were delineated in the Introduction from our analysis of the prior literature, namely the goals of: (i) the use of a nanocluster system in which the nanoclusters have been well characterized; (ii) the use of nanoclusters stabilized by the most effective anionic stabilizer currently known,[57] $P_2W_{15}Nb_3O_{62}^{9-}$; (iii) the development of a nanocluster arene hydrogenation system that is not aqueous/organic biphasic so that the effects of water can be tested, and so that kinetic and mechanistic studies can be more easily performed and interpreted; (iv) the extension of the catalytic lifetime beyond the normally observed ~100 TTO, and ideally even beyond the current record lifetime of 2000 TTO[53]; (v) the attainment of high yields of the valuable, partially hydrogenated, cyclohex*ene* products of arene hydrogenation; and ideally also (vi) the completion of a kinetic and mechanistic study of the best, prototype nanocluster arene hydrogenation system. The following list summarizes our efforts in achieving the first five of these six goals:

(1) The Rh(0) nanoclusters used in this study are well characterized and well understood, especially if one considers our previous work with such nanoclusters.[58,59,60] Herein the nanoclusters are characterized by confirmation of their expected stoichiometry formation, by TEM, and via a determination of their nanocluster formation rate constants.

(2) In situ reduction of the well-defined precatalyst, $[Bu_4N]_5Na_3[(1,5\text{-}COD)Rh{\bullet}P_2W_{15}Nb_3O_{62}]$, with H_2 ensures that the $P_2W_{15}Nb_3O_{62}^{9-}$ polyoxoanion is the only anionic stabilizer present.

(3) The Rh(0) nanoclusters are soluble and active in monophasic propylene carbonate (or other polar aprotic organic solvents). This allowed us to discover that proton donors such as water and $HBF_4{\bullet}Et_2O$ affect both the nanocluster formation reaction and the nanocluster arene hydrogenation catalytic reaction. As Figure 5.4 shows, the plot of activity vs added water has a sharp, heretofore unappreciated maximum at ca. 60 equivs of water per Rh present, at least for polyoxoanion-stabilized nanoclusters.

(4) A series of lifetime experiments showed that the Rh(0) nanoclusters are 10-fold more active than their traditional oxide-supported analog, 5% Rh/Al_2O_3. The lifetime experiments also shows that the Rh(0) nanoclusters are capable of at least 2600 TTO, the longest demonstrated lifetime for any soluble nanocluster arene hydrogenation catalyst reported in the literature, albeit over a relatively long 144 hours. Hence, the development of even more active, *longer-lived* nanocluster catalysts remains an important goal in this area.

(5) The polyoxoanion-stabilized Rh(0) nanoclusters display a modest, albeit a record, selectivity for nanocluster partial hydrogenation of anisole to 1-methoxycyclohexene with yields up to 8% at the relatively mild, maximum temperature examined of 78 °C. Obviously, higher yields of the alkene product are desirable; however, polyoxoanion-stabilized nanoclusters display sufficient selectivity to make them of interest as a model

system for further studies of the many important variables in the partial hydrogenation of arenes using metal particle catalysts.

(6) The polyoxoanion-stabilized nanoclusters provide both a higher yield of 1-methoxycyclohexene, and a longer lifetime prior to deactivation, than does a traditional 5% Rh/Al_2O_3 heterogeneous catalyst. This improved performance appears to be due to the presence of the polyoxoanion, results which suggest that the polyoxoanion is an interesting additive to study with other arene hydrogenation catalysts.

(7) The mechanistic study of nanocluster-catalyzed arene hydrogenation was only touched upon in this study, but even here we have an interesting result. We uncovered further evidence that H^+-assisted reductive elimination of nanocluster M–C bonds is a general phenomenon.[82]

Experimental

Materials. Propylene carbonate (Aldrich, 99.7%, anhydrous, packaged under N_2) was transferred into the drybox, evacuated for ≥1 h and stored over 5 Å molecular sieves activated in the drybox by heating at 105 °C under vacuum for 8 h. Anisole (Aldrich, 99.7%, anhydrous, packaged under N_2) was transferred into the drybox and evacuated for ≥1 h before use. Cyclohexene (Aldrich, 99%) was distilled from Na under argon and stored in the drybox. Acetone (Burdick and Jackson, 0.26% H_2O) was purged with Ar for 30 min before being transferred into the drybox. Methoxycyclohexane (Sigma-Aldrich Library of Rare Chemicals, about 80% pure by GLC) was used as received. A sample of 1-methoxycyclohexene (about 60% pure by GLC) was generously given to us by Professor Yian Shi's research group (the synthetic procedure for 1-methoxycyclohexene is available elsewhere[99]). Sealed ampules (1g) of CD_2Cl_2 were purchased from Cambridge Isotope Laboratories, Inc. "Nanopure" water (distilled water filtered through a Barnstead filtration system) was used for the hydrogenation experiments where water was added.

Tetrafluoroboric acid (Aldrich, 54 wt. % solution in diethyl ether) was transferred into the drybox and used as received.

The 5% Rh/Al_2O_3 (preactivated under H_2 by the manufacturer) was purchased from Strem. H_2 and CO chemisorption analysis shows that about 33% of the Rh atoms in this catalyst are exposed.[84] TEM analysis of this catalyst shows the Rh(0) particles are 3.6 (± 1.8) nm in diameter, and thus in the same general size range as our Rh(0) nanoclusters.[84] A control experiment described in the Supporting Information shows that this 5% Rh/Al_2O_3, after being evacuated at room temperature overnight and transferred into the drybox, has a high activity and long lifetime for the hydrogenation of cyclohexene, as we have found previously.[58] Nevertheless, we found that re-activating the catalyst under hydrogen had a beneficial effect on the anisole hydrogenation activity. Before re-activation the 5% Rh/Al_2O_3 gave only 13 (± 1) TTO in 24 h, compared to 34 (± 2) TTO in 25 h following re-activation. The 5% Rh/Al_2O_3 was re-activated by heating it to 130 °C for 1.5 h in a constant flow of H_2.[89] All of the anisole hydrogenation experiments with 5% Rh/Al_2O_3 reported herein were performed using the re-activated material.

The rhodium nanocluster precursor complex $[Bu_4N]_5Na_3[(1,5\text{-}COD)Rh{\bullet}P_2W_{15}Nb_3O_{62}]$, **A**, was prepared by literature methods[100] from $(Bu_4N)_9P_2W_{15}Nb_3O_{62}$ made by our most recent method[83] (using $K_7HNb_6O_{19}$ as the Nb source) and stored in the drybox. ^{31}P NMR showed **A** to be 94% pure. Analysis for **A**, calc (found): C 18.93 (18.73); H 3.47 (3.61); N 1.25 (1.28). ^{19}F NMR showed that 98% of the $[Bu_4N]BF_4$ generated during the support reaction, in which $[(1,5\text{-}COD)Rh(CH_3CN)_2]BF_4$ is added to $(Bu_4N)_9P_2W_{15}Nb_3O_{62}$, had been removed by the ethyl acetate/acetonitrile precipitations (the 2% $[Bu_4N]BF_4$ which remained, is 0.08 equivs vs Rh).

General Procedures. All of the glassware, except for the syringes, was dried for at least overnight in a 160 °C drying oven before being transferred into the drybox while still hot. The syringes used to measure and transfer propylene carbonate and anisole were dried overnight at 100 °C in a vacuum oven before being transferred into the drybox while still

hot. All catalyst reaction solutions were prepared under oxygen- and moisture-free conditions in a Vacuum Atmospheres drybox (<2 ppm of O_2 as continuously monitored by a Vacuum Atmospheres O_2-level monitor).

Analytical Procedures. Gas-liquid chromatography (GLC) was performed using a Hewlett-Packard 5890 series II instrument with a FID detector. The instrument was equipped with a 30 m × 0.25 mm Supelcowax-10 column and was coupled to a Hewlett-Packard 3395 integrator. Parameters were as follows: initial temperature, 50 °C; initial time, 3 min; ramp, 10 °C/min; final temperature, 250 °C; final time, 1 min; injector port temperature, 250 °C; detector temperature, 250 °C; injection volume, 4 μL.

Nuclear magnetic resonance (NMR) spectra were obtained as CD_2Cl_2 solutions in Spectra Tech NMR tubes (5 mm o.d.) at 25 °C on a Varian Inova 300 MHz instrument. Chemical shifts were referenced to the residual solvent impurity at 5.32 ppm. Spectral parameters for ^1H NMR (300 MHz) include: tip angle, 30° (pulse width, 2.9 μsec); acquisition time, 2.667 s; relaxation delay, 0.0 s; sweep width, 6000 Hz. An integration error of 5% was assumed in the error propagation for lifetime experiments followed by ^1H NMR.

Gas chromatography-mass spectrometry (GC-MS) was performed using a Hewlett-Packard 5890 series II GC with an MSD 5970 B. The GC was equipped with a 30 m (0.25 mm i.d., 0.25 μm film thickness) Supelco SPB-1 column. The ionizing voltage was 70 eV. The GC parameters were as follows: initial temperature, 50 °C; initial time, 3 min; solvent delay, 2 min; temperature ramp, 10 °C/min; final temperature, 270 °C; final time, 5 min; injector port temperature, 280 °C; detector temperature, 290 °C; injection volume, 0.1 μL. The mass marker calibration of the GC-MS was performed using perfluorotributylamine.

X-ray photoelectron spectroscopy (XPS) was performed using a Physical Electronics 5800 spectrometer equipped with a hemispherical analyzer and using monochromatic Al Kα radiation (1486.6 eV, the x-ray tube working at 15 kV and 350 W)

and a pass energy of 23.5 eV. Peaks were referenced to the C 1s line at 284.8 eV to account for sample charging. Good quality survey spectra were obtained with a single scan. High-resolution spectra were integrated over 5–20 scans depending of the intensity of the spectral region of interest. Two XPS samples were prepared. The sample for nanoclusters generated in a Standard Conditions anisole hydrogenation was prepared exactly as described below for TEM samples (i.e., the nanoclusters were twice precipitated with diethyl ether and then dried under vacuum; a piece of glass coated with the residue was used as the XPS sample). The sample of the black precipitate (i.e., the precipitate that formed in hydrogenations with ≥60 equivs of water added) was prepared from the stir bar used in the experiment in which 60 equivs of water was added. In the drybox the stir bar, which was coated with a film of the black precipitate, was removed from the reaction solution. The stir bar was thoroughly rinsed, first with acetonitrile and then with acetone, neither of which noticeably dissolved the precipitate. The stir bar was then dried under vacuum while still in the drybox. Both samples were briefly exposed to air when they were introduced into the spectrometer.

Transmission electron microscopy analysis was performed as before[62,63] at the University of Oregon with the expert assistance of Dr. Eric Schabtach. As described previously, micrographs of the nanoclusters were obtained with a Philips CM-12 microscope (with a 2.0 Å point-to-point resolution) operating at 100 KeV.[62,63] Size measurements were obtained from micrographs with magnifications of 430 K. Each size distribution was determined by measuring 136–165 nanoclusters. A control experiment published elsewhere[60] shows that Rh(0) nanoclusters do not form from the nanocluster precursor **A** under the electron beam.

We have experienced problems when using propylene carbonate solutions of nanoclusters to prepare TEM grids. The samples tend to charge in the electron beam, with consequent instability and destruction of the support films. This is probably due the presence of substantial amounts of (non-conducting) propylene carbonate, even on "dry"

TEM grids (propylene carbonate has a high boiling point and is difficult to remove by evaporation). Additionally, the nanoclusters on TEM grids prepared from propylene carbonate solutions tend to be in large clumps. Due to our difficulties preparing good TEM samples in the presence of propylene carbonate, we first isolated the nanoclusters from propylene carbonate by precipitating them twice in the following manner. In the drybox 0.25 mL of reaction solution was measured into a glass scintillation vial with a 1-mL plastic syringe. Then 10 mL of ethyl ether was added with a polyethylene pipet while swirling the contents of the vial. The solution turned cloudy after the addition of about 2 mL of ether. Following the addition of ether the cloudy solution was agitated for a few seconds with the polyethylene pipet. Then the vial was capped and sealed with parafilm. The sealed vial was brought out of the drybox and the fine precipitate was separated by centrifugation (1 h at 1200 rpm in a swinging-bucket centrifuge with a radius of 20 cm). The vial was transferred back into the drybox where the clear, colorless supernatant was decanted, leaving a small amount of dark colored oily solid in the bottom of the vial. This solid readily dissolved when 0.5 mL of acetonitrile was added with a 1-mL plastic syringe. Then 12 mL of ethyl ether was added with a polyethylene pipet while swirling the contents of the vial. The solution turned cloudy after the addition of about 4 mL of ether. Following the addition of ether the cloudy solution was agitated for a few seconds with the polyethylene pipet. Then the vial was once again capped and sealed with parafilm. The sealed vial was brought out of the drybox and centrifuged again. The vial was transferred back into the drybox where the clear, colorless supernatant was decanted, leaving a small amount of dark colored oily solid in the bottom of the vial. The vial was evacuated for 30 min, leaving a dark colored residue on the bottom of the vial. This TEM sample was sealed with parafilm, double-bottled and sent as a solid to Dr. Eric Schabtach at the University of Oregon. Dr. Schabtach dissolved the TEM samples in 0.5 mL of acetonitrile, placed a drop of the solution onto a carbon-coated copper TEM grid, and blotted off the excess liquid with a piece of filter paper.

A control experiment was performed to see if isolating the nanoclusters from propylene carbonate affects the nanocluster size distributions in the TEM samples. This experiment was performed using the reaction solution from an experiment in which the Rh(0) nanoclusters were formed in the absence of substrate. A small amount of the reaction solution was diluted 60:1 with acetonitrile; the TEM grid was prepared from the diluted solution. Electron micrographs of that grid showed a size distribution of 6.0 (± 1.2) nm (only 62 nanoclusters were measured due to the difficulties described above), compared to a size distribution of 6.2 (± 1.5) nm for such nanoclusters after being isolated from propylene carbonate using the precipitations described above. Hence, the precipitations do not affect the nanocluster size within experimental error.

Standard Conditions Anisole Hydrogenation Experiment. This experiment was done in a manner analogous to the cyclohexene hydrogenation experiments that we have been performing for some time now.[59,62,63] A schematic of the hydrogenation apparatus used is available in Figure 6 elsewhere.[101] In the drybox 20 (± 0.5) mg of $[Bu_4N]_5Na_3[(1,5\text{-COD})Rh{\bullet}P_2W_{15}Nb_3O_{62}]$, **A**, ($3.6 \times 10^{-6}$ mol) was weighed into a 2-dram glass vial. Then 2.9 mL of propylene carbonate was added to the vial with a 5-mL gastight syringe, followed by the addition of 0.14 mL of anisole (1.3×10^{-3} mol) with a 1-mL gastight syringe. This mixture was briefly agitated with a disposable polyethylene pipet until **A** dissolved completely. Using the same pipet, the bright yellow solution of **A** was then transferred into a new 22 × 175 mm Pyrex culture tube containing a 5/8 × 5/16 in. Teflon-coated stir bar. The culture tube was placed in a Fischer–Porter (hereafter, F–P) pressure bottle modified with Swagelock TFE-sealed Quick-Connects. The F–P bottle was then sealed, brought out of the drybox, placed in a 22.0 (± 0.1) °C temperature-controlled water bath and connected to a H_2 line via the Quick-Connects. Using the top (purge) valve, the F–P bottle was then purged 15 times (waiting 15 s between purges) with 40 psig H_2. Following the purges, the F–P bottle was pressurized to 40 (± 1) psig H_2 and then isolated (by closing the valve to the H_2 line). During the purging (and during the hydrogenation

reaction) the reaction solution was vortex-stirred (at >600 rpm). Five minutes after the beginning of the purges was designated $t = 0$, and at this time data collection (H_2 pressure vs time) was initiated using an Omega PX-621 pressure transducer (manufacturer specifications for the transducer include ±0.005 psig precision and ±0.15 psig accuracy) interfaced to a PC. The final reaction solution (after 24 h under H_2) was clear and dark brown with no visible precipitate.

Control Experiment Comparing the Rate of Anisole Hydrogenation with the Rate of Cyclohexene Hydrogenation. This experiment is described in the Supporting Information.

Monitoring Nanocluster Formation via the Evolution of Cyclooctane. This experiment was started in exactly the same way as the Standard Conditions anisole hydrogenation, except that the F–P bottle was left open to the H_2 line, which maintains the H_2 pressure at 40 (± 1) psig (this was done because the pressure must be released each time a sample is removed for GLC analysis). At regular intervals the purge valve on the F–P bottle was opened and a GLC sample removed. The GLC sample was obtained by threading an oven-dried, H_2-purged, 12-inch, stainless steel needle through the purge valve into the culture tube. A 0.05-mL aliquot of the reaction solution was removed with a disposable 1-mL syringe (which was attached to the needle). The purge valve was then closed so that the F–P bottle could re-pressurize to 40 psig. During the sampling procedure the constant flow of H_2 out of the F–P bottle protects the atmosphere inside it. The evolved equivalents of cyclooctane were determined by directly injecting the reaction solution into a calibrated gas chromatograph using a 10 μL gastight syringe.

The Addition of Water to Anisole Hydrogenation Experiments. Water was added to many of the reaction solutions. Unless otherwise noted, the water was added immediately after **A** had been dissolved in propylene carbonate and anisole (i.e., before the reaction solution was transferred to the culture tube and while still in the inert-atmosphere glovebox). The water was added to the solution with a syringe. For volumes <1.0 μL a

Hamilton 1.0 μL syringe with a Cheney adapter was used. For volumes from 1.0–10 μL a Hamilton gastight 10 μL syringe was used. For volumes >10 μL a Hamilton 50 μL syringe was used. The addition of water to the reaction solution did not cause a visible change in appearance.

The Effect of Water on the Anisole Hydrogenation Activity of Rh(0) Nanoclusters Preformed in the Absence of Substrate. For this experiment the nanoclusters were formed in exactly the same way as in the section titled "Control Experiment Comparing the Rate of Anisole Hydrogenation with the Rate of Cyclohexene Hydrogenation". Briefly, the nanoclusters were formed from 20 mg of **A** in 3.0 mL of propylene carbonate at 22 °C and 40 psig constant H_2 pressure. After 16 h under hydrogen, the F–P bottle was sealed, removed from the H_2 line and brought into the drybox. Then 0.14 mL of anisole (1.3×10^{-3} mol) was added to the culture tube with a 1-mL gastight syringe. The F–P bottle was then sealed, brought out of the drybox, placed in a 22.0 (± 0.1) °C temperature-controlled water bath and connected to a H_2 line via the Quick-Connects. Using the top (purge) valve, the F–P bottle was then purged 15 times (waiting 15 s between purges) with 40 psig H_2. Following the purges, the F–P bottle was pressurized to 40 (± 1) psig H_2 and then isolated (by closing the valve to the H_2 line). During the purging (and during the hydrogenation reaction) the reaction solution was vortex-stirred. Immediately after the F–P bottle was pressurized to 40 (± 1) psig H_2, data collection (H_2 pressure vs time) was initiated using an Omega PX-621 pressure transducer interfaced to a PC. After about 5 h of anisole hydrogenation the F–P bottle was once again sealed and brought into the drybox. Then 4.0 μL of H_2O (60 equivs vs Rh) was added to the culture tube with a 10 μL gas-tight syringe. The F–P bottle was then attached to the H_2 line in the same way it was done after the anisole had been added. For a plot of the hydrogen uptake curve for this experiment see Figure 5.H of the Supporting Information. The reported H_2 uptake rates for anisole hydrogenation in this experiment were determined in exactly the

same way as in the section titled "Control Experiment Comparing the Rate of Anisole Hydrogenation with the Rate of Cyclohexene Hydrogenation".

The Effect of $HBF_4 \bullet Et_2O$ on the Anisole Hydrogenation Activity of Rh(0) Nanoclusters Preformed in the Absence of Substrate. This experiment was performed exactly like the experiment described in the section titled "The Effect of Water on the Anisole Hydrogenation Activity of Rh(0) Nanoclusters Preformed in the Absence of Substrate", except that the initial anisole hydrogenation was only allowed to proceed for about 3 h (instead of 5 h) and 5.0 μL of $HBF_4 \bullet Et_2O$ (10 equivs vs Rh) was added (instead of 4.0 μL H_2O). Following the addition of $HBF_4 \bullet Et_2O$, the clear brown reaction solution turned deep blue immediately after the F–P bottle was pressurized with H_2. For a plot of the hydrogen uptake curve for this experiment see Figure 5.I of the Supporting Information.

Anisole Hydrogenation Catalytic Lifetime Experiments. Lifetime experiments with precatalyst **A** were set up in a manner analogous to Standard Conditions anisole hydrogenations (*vide supra*), except as follows: 2.0 mL of propylene carbonate and 1.0 mL of anisole (9.2×10^{-3} mol) were used to dissolve the 20 (± 0.5) mg of precatalyst (this allows for a maximum of 2600 TTO); the F–P bottle was left open to the H_2 line, which maintained the H_2 pressure at 40 (± 1) psig; and the reaction was monitored by periodically withdrawing aliquots of the reaction solution for ^1H NMR spectroscopy.

Aliquots were removed for ^1H NMR analysis as follows. First, the F–P pressure bottle was sealed, removed from the hydrogenation line and brought into the drybox. In the drybox the F–P bottle was opened and a couple drops of the reaction solution were removed with a polyethylene pipet. The F–P bottle was then re-sealed, brought back out of the drybox, attached to the hydrogenation line, purged 15 times with H_2 in the normal manner and the reaction allowed to continue at 40 (± 1) psig H_2. This sampling procedure takes about 30 min, which is insignificant on the time-scale of the lifetime experiments. The aliquot removed for ^1H NMR was placed in a NMR tube and dissolved in 1 g of CD_2Cl_2. The TTO were determined using the integrals of the peaks for the methyl-group protons of

anisole and methoxycyclohexane (the peaks are at δ 3.8 and 3.3, respectively). The intermediate, 1-methoxycyclohexene, was ignored in the determination of TTO by ^{1}H NMR because it was present in quantities ≤5%.

The lifetime experiment with $HBF_4 \bullet Et_2O$ added was started in the manner described above. After 16 h under hydrogen, the F–P bottle was sealed and brought into the drybox. In the drybox 5.0 μL of $HBF_4 \bullet Et_2O$ (10 equivs vs Rh) was added using a 10-μL gastight syringe. The F–P bottle was then resealed, brought out of the drybox, attached to the hydrogenation line, purged with H_2 in the normal manner and re-pressurized to 40 (± 1) psig H_2.

The lifetime experiment with 5% Rh/Al_2O_3 as the catalyst was performed just like lifetime experiments with **A**, except that 7.4 mg of 5% Rh/Al_2O_3 (3.6×10^{-6} mol Rh) was used instead of 20 mg of **A** (3.6×10^{-6} mol Rh). A total of 2600 TTO are possible in this experiment.

Control Experiment Showing the Activity and Lifetime of the 5% Rh/Al_2O_3 for Cyclohexene Hydrogenation. This experiment is described in the Supporting Information.

The Observation of Partial Hydrogenation Products in the Hydrogenation of Anisole. These experiments were performed in the same general manner as the experiment described in the section titled "Monitoring Nanocluster Formation via the Evolution of Cyclooctane". The F–P bottle was left open to the H_2 line, which maintains the H_2 pressure at 40 (± 1) psig. At regular intervals the purge valve on the F–P bottle was opened and a GLC sample was removed using the procedure described in the section titled "Monitoring Nanocluster Formation via the Evolution of Cyclooctane". No GLC samples were removed until after the end of the induction period, as judged by a noticeable darkening in the reaction solution. This precautionary measure assures that the sampling procedure will have as little effect as possible on the nanocluster nucleation process. For each GLC data point the relative amounts of anisole, 1-methoxycyclohexene and

methoxycyclohexane were quantified. The identities of the analyte peaks in the GLC traces were established by the retention times of authentic compounds. Additionally, the identities of anisole, 1-methoxycyclohexene and methoxycyclohexane were verified by GC-MS.

Table 5.2 shows a list of experiments for which the amount of 1-methoxycyclohexene was quantified. The experiment in Table 5.2 described as Standard Conditions was performed exactly like the experiment described in the section titled "Monitoring Nanocluster Formation via the Evolution of Cyclooctane". The experiment with 60 equivs of H_2O added (Table 5.2) only differed in that 4.0 μL of H_2O was added to the reaction solution with a 10-μL gastight syringe while still in the drybox. The experiments with 1.05 and 2.01 equivs of $(Bu_4N)_9P_2W_{15}Nb_3O_{62}$ added (Table 5.2) were performed exactly like the Standard Conditions experiment, except that 24.1 mg and 45.4 mg of $(Bu_4N)_9P_2W_{15}Nb_3O_{62}$, respectively, were weighed into the same vial as the precatalyst **A** while in the drybox. The experiments at 40 and 78 °C (Table 5.2) were performed exactly like the Standard Conditions experiment, except that the temperature of the water bath was adjusted to 40 and 78 °C, respectively. The experiment with acetone solvent (Table 5.2) was performed exactly like the Standard Conditions experiment, except that 2.9 mL of acetone was used instead of 2.9 mL of propylene carbonate. The experiments using 7.4 mg of 5% Rh/Al_2O_3 (Table 5.2) were performed exactly like the experiments with **A**, except that 7.4 mg of 5% Rh/Al_2O_3 was used instead of 20 mg of **A**.

The "initial selectivity" (i.e., the initial ratio of 1-methoxycyclohexene to methoxycyclohexane) was determined from direct injection of the first GLC sample. It was calculated by dividing the area of the 1-methoxycyclohexene peak by the sum of the areas for the 1-methoxycyclohexene and methoxycyclohexane peaks. This calculation makes use of the concept of "effective carbon number" (see the Supporting Information). In order to determine the percent yield of 1-methoxycyclohexene the GLC sample was diluted 20:1 with propylene carbonate. This dilution was necessary to keep the concentrations of anisole, 1-methoxycyclohexene and methoxycyclohexane in the range of linear FID

response. The percent yield of 1-methoxycyclohexene was calculated by dividing the area of the 1-methoxycyclohexene peak by the sum of the areas for the 1-methoxycyclohexene, methoxycyclohexane and anisole peaks.

The curve-fit shown in Figure 5.5 was generated by Microcal Origin, a commercial software package that we have previously validated for generating non-linear curve-fits.[61] The data in Figure 5.5 were fit to the analytic kinetic equation for the concentration of "B" in an A $\rightarrow$ B $\rightarrow$ C kinetic scheme (see equation 4-6 elsewhere[93]).

Use of Effective Carbon Number (ECN) for GLC Quantitation. See the Supporting Information for details.

Acknowledgments.

The TEM data for this study were expertly obtained by Dr. Eric Schabtach at the University of Oregon's Microscopy Center; it is a pleasure to acknowledge Dr. Schabtach's expertise and continued collaboration. The GC-MS work was expertly performed by staff scientist Donald Dick at the Colorado State University Central Instrument Facility. The XPS work was expertly performed by research associate Keri L. Williams at the Colorado State University Central Instrument Facility. We also thank Professor Robert M. Williams for useful discussions regarding the mechanism of formation of the dodecahydrotriphenylene byproduct. Financial support was provided by the Department of Energy, Chemical Sciences Division, Office of Basic Energy, grant DOE FG06-089ER13998.

Supporting Information Available: Figure 5.A, a plot of the H_2 pressure vs time for an experiment where both anisole and cyclohexene are hydrogenated with the same batch of polyoxoanion- and tetrabutylammonium-stabilized Rh(0) nanoclusters; a textual section titled "Control Experiment Comparing the Rate of Anisole Hydrogenation with the Rate of Cyclohexene Hydrogenation"; Figures 5.B–5.G, plots of hydrogen pressure vs time for

anisole hydrogenation experiments with 8, 30, 60, 90, 120 and 470 equivs of water added; Figure5.H, a plot of the H_2 pressure vs time for an experiment where anisole is hydrogenated under anhydrous conditions to begin with, and then with 60 equivs of H_2O added, using the same batch of polyoxoanion- and tetrabutylammonium-stabilized Rh(0) nanoclusters; Figure 5.I, a plot of the H_2 pressure vs time for an experiment where anisole is hydrogenated without acid to begin with, and then with 10 equivs of $HBF_4 \bullet Et_2O$ added, using the same batch of polyoxoanion- and tetrabutylammonium-stabilized Rh(0) nanoclusters; Figure 5.J, (a) a ^1H NMR spectrum and (b) a GLC trace of the reaction solution for an anisole hydrogenation at 78 °C, demonstrating the validity of the "effective carbon number" (ECN) approximation for this system; a textual section titled "Use of Effective Carbon Number (ECN) for GLC Quantitation"; Figure 5.K(a), an X-ray photoelectron spectrum of the polyoxoanion- and tetrabutylammonium-stabilized nanoclusters from a Standard Conditions anisole hydrogenation; Figure 5.K (b), an X-ray photoelectron spectrum of the black precipitate from an anisole hydrogenation with 60 equivalents of H_2O added; a textual section titled "Is the Selectivity of the Polyoxoanion- and Tetrabutylammonium-Stabilized Nanoclusters Unique?"; a textual section titled "Discussion of the Horiuti–Polanyi Mechanism for the Hydrogenation of Monocyclic Arenes with Group VIII Heterogeneous Metal Catalysts"; Figure 5.L, an adapted Horiuti-Polanyi mechanism for the catalytic hydrogenation of arenes on group VIII metals; a textual section titled "Control Experiment Showing the Activity and Lifetime of the 5% Rh/Al_2O_3 for Cyclohexene Hydrogenation"; a textual section titled "Identification of the White Precipitate in the Total Turnovers Experiment with $HBF_4 \bullet Et_2O$ Added"; Scheme 5.A, an arrow-pushing mechanism for the formation of dodecahydrotriphenylene from the acid-catalyzed condensation of 1-methoxycyclohexene; Figure 5.M, a GLC trace of the reaction solution from the total turnovers experiment with 10 equivs $HBF_4 \bullet Et_2O$ added.

References:

(1) Hu, S.-C.; Chen, Y.-W. *J. Chin. Inst. Chem. Eng.* **1998**, *29*, 387.

(2) Rothwell, I. P. *Chem. Commun.* **1997**, 1331.

(3) Harman, W. D. *Chem. Rev.* **1997**, *97*, 1953.

(4) Stanislaus, A.; Cooper, B. H. *Catal. Rev. - Sci. Eng.* **1994**, *36*, 75.

(5) Bennett, M. *Chemtech* **1980**, *10*, 444.

(6) Muetterties, E. L.; Bleeke, J. R. *Acc. Chem. Res.* **1979**, *12*, 324.

(7) Maitlis, P. M. *Acc. Chem. Res.* **1978**, *11*, 301.

(8) Sabatier, P. *Ind. Eng. Chem.* **1926**, *18*, 1004.

(9) Sabatier, P.; Senderens, J.-B. *Compt. Rend.* **1901**, *132*, 210.

(10) Albach, R.-W.; Jautelat, M. In *Ger. Offen.*; (Bayer A.-G., Germany).: DE, 1999; p 8 pp.

(11) Fache, F.; Lehuede, S.; Lemaire, M. *Tetrahedron Lett.* **1995**, *36*, 885.

(12) Nasar, K.; Fache, F.; Lemaire, M.; Beziat, J. C.; Besson, M.; Gallezot, P. *J. Mol. Catal.* **1994**, *87*, 107.

(13) Rylander, P. N. *Catalytic Hydrogenation in Organic Synthesis*; Academic Press: New York, 1979.

(14) Weissermel, K.; Arpe, H.-J. *Industrial Organic Chemistry*; 2nd ed.; VCH: New York, 1993.

(15) Parshall, G. W.; Ittel, S. D. *Homogeneous Catalysis, 2nd Edition. The Applications and Chemistry of Catalysis by Soluble Transition Metal Complexes*; Wiley: New York, 1992.

(16) Struijk, J.; Moene, R.; Van der Kamp, T.; Scholten, J. J. F. *Appl. Catal., A* **1992**, *89*, 77.

(17) Struijk, J.; D'Angremond, M.; Lucas-De Regt, W. J. M.; Scholten, J. J. F. *Appl. Catal., A* **1992**, *83*, 263.

(18) In *Chem. Engr.*, 1990; Vol. 97, December 20, p 25.

(19) Enya, T.; Suzuki, H.; Watanabe, T.; Hirayama, T.; Hisamatsu, Y. *Environ. Sci. Technol.* **1997**, *31*, 2772.

(20) Casillas, A. M.; Hiura, T.; Li, N.; Nel, A. E. *Ann. Allergy, Asthma, Immunol.* **1999**, *83*, 624.

(21) Nel, A. E.; Diaz-Sanchez, D.; Ng, D.; Hiura, T.; Saxon, A. *J. Allergy Clin. Immunol.* **1998**, *102*, 539.

(22) Hu, T. Q.; James, B. R.; Lee, C. L. *J. Pulp Pap. Sci.* **1997**, *23*, J200.

(23) Hu, T. Q.; James, B. R.; Lee, C. L. *J. Pulp Pap. Sci.* **1997**, *23*, J153.

(24) Hu, T. Q.; James, B. R.; Wang, Y. *J. Pulp Pap. Sci.* **1999**, *25*, 312.

(25) Hu, T. Q.; James, B. R. *J. Pulp Pap. Sci.* **2000**, *26*, 173.

(26) Tullo, A. In *Chemical and Engineering News*, 1999; pp 14-15.

(27) Puddephatt, R. J. *Met. Clusters Chem.* **1999**, *2*, 605.

(28) Aiken, J. D., III; Finke, R. G. *J. Mol. Catal. A: Chem.* **1999**, *145*, 1.

(29) Aiken, J. D., III; Lin, Y.; Finke, R. G. *J. Mol. Catal. A: Chem.* **1996**, *114*, 29.

(30) Schmid, G.; Baumle, M.; Geerkens, M.; Heim, I.; Osemann, C.; Sawitowski, T. *Chem. Soc. Rev.* **1999**, *28*, 179.

(31) Vargaftik, M. N.; Kozitsyna, N. Y.; Cherkashina, N. V.; Rudyi, R. I.; Kochubei, D. I.; Novgorodov, B. N.; Moiseev, I. I. *Kinet. Catal.* **1998**, *39*, 740.

(32) Herron, N.; Thorn, D. L. *Adv. Mater.* **1998**, *10*, 1173.

(33) Bradley, J. S. *Schr. Forschungszent. Juelich, Mater. Mater.* **1998**, *1*, D6.1.

(34) Bonnemann, H.; Brijoux, W.; Tilling, A. S.; Siepen, K. *Top. Catal.* **1998**, *4*, 217.

(35) Schmid, G. Ligand-Stabilized Clusters and Colloids. In *Appl. Homogeneous Catal. Organomet. Compd.*; Cornils, B., Wolfgang, H. A., Eds.; VCH: New York, 1996; Vol. 2, pp 636-644.

(36) Boennemann, H.; Brijoux, W. *Adv. Catal. Nanostruct. Mater.* **1996**, 165.

(37) Boennemann, H.; Braun, G.; Brijoux, G. B.; Brinkman, R.; Tilling, A. S.; Seevogel, K.; Siepen, K. *J. Organomet. Chem.* **1996**, *520*, 143.

(38) Schmid, G.; Maihack, V.; Lantermann, F.; Peschel, S. *J. Chem. Soc., Dalton Trans.* **1996**, 589.

(39) Bradley, J. S. The Chemistry of Transition Metal Colloids. In *Clusters and Colloids*, 1994; pp 459-544.

(40) Lewis, L. N. *Chem. Rev.* **1993**, *93*, 2693.

(41) Schmid, G. *Chem. Rev.* **1992**, *92*, 1709.

(42) Schmid, G. *Endeavour* **1990**, *14*, 172.

(43) Januszkiewicz, K. R.; Alper, H. *Organometallics* **1983**, *2*, 1055.

(44) Foise, J.; Kershaw, R.; Dwight, K.; Wold, A. *Mater. Res. Bull.* **1985**, *20*, 147.

(45) Duan, Z.; Hampden-Smith, M. J.; Sylwester, A. P. *Chem. Mater.* **1992**, *4*, 1146.

(46) Landre, P. D.; Lemaire, M.; Richard, D.; Gallezot, P. *J. Mol. Catal.* **1993**, *78*, 257.

(47) Landre, P. D.; Richard, D.; Draye, M.; Gallezot, P.; Lemaire, M. *J. Catal.* **1994**, *147*, 214.

(48) James, B. R.; Wang, Y.; Hu, T. Q. *Chem. Ind.* **1996**, *68*, 423.

(49) Hu, T. Q.; James, B. R.; Rettig, S. J.; Lee, C.-L. *Can. J. Chem.* **1997**, *75*, 1234.

(50) Weddle, K. S.; Aiken, J. D., III; Finke, R. G. *J. Am. Chem. Soc.* **1998**, *120*, 5653.

(51) James, B. R.; Wang, Y.; Alexander, C. S.; Hu, T. Q. *Chem. Ind.* **1998**, *75*, 233.

(52) Schulz, J.; Roucoux, A.; Patin, H. *Chem. Commun.* **1999**, 535.

(53) Schulz, J.; Roucoux, A.; Patin, H. *Chem.--Eur. J.* **2000**, *6*, 618.

(54) Bonilla, R. J.; Jessop, P. G.; James, B. R. *Chem. Commun.* **2000**, 941.

(55) Januszkiewicz, K. R.; Alper, H. *Can. J. Chem.* **1984**, *62*, 1031.

(56) Bond, G. C. *Catalysis by Metals*; Academic Press: New York, 1962.

(57) Özkar, S.; Finke, R. G. "A Comparison of the Nanocluster-Stabilizing Abilities of Commonly Employed Anions vs the $P_2W_{15}Nb_3O_{62}^{9-}$ Polyoxoanion "Gold Standard", submitted.

(58) Aiken, J. D., III; Finke, R. G. *J. Am. Chem. Soc.* **1999**, *121*, 8803.

(59) Aiken, J. D., III; Finke, R. G. *Chem. Mater.* **1999**, *11*, 1035.

(60) Aiken, J. D., III; Finke, R. G. *J. Am. Chem. Soc.* **1998**, *120*, 9545.

(61) Widegren, J. A.; Aiken, J. D., III; Özkar, S.; Finke, R. G. *Chem. Mater.* **2001**, *13*, 312.

(62) Watzky, M. A.; Finke, R. G. *J. Am. Chem. Soc.* **1997**, *119*, 10382.

(63) Lin, Y.; Finke, R. G. *J. Am. Chem. Soc.* **1994**, *116*, 8335.

(64) The formation of inactive spectator species, such as alkylidenes and alkylidynes, on the surface of metals is well known from single-crystal surface science.[65,66] In addition, Bradley and coworkers have concluded that colloidal metals formed under mild conditions generally have highly defected surfaces based on CO addition then IR studies.[67] Hence, another possibility is that the observed deactivation is due to a slow surface rearrangement or "annealing" process which results in nanoclusters that are more thermodynamically stable, but less catalytically active.

(65) Somorjai, G. A. *J. Phys. Chem. B* **2000**, *104*, 2969.

(66) Ponec, V. *J. Mol. Catal. A: Chem.* **1998**, *133*, 221.

(67) de Caro, D.; Bradley, J. S. *New J. Chem.* **1998**, *22*, 1267.

(68) Jacobs, P. W.; Somorjai, G. A. *J. Mol. Catal. A: Chem.* **1998**, *131*, 5.

(69) Noyes, R. M.; Field, R. J. *Acc. Chem. Res.* **1977**, *10*, 273.

(70) Field, R. J.; Noyes, R. M. *Acc. Chem. Res.* **1977**, *10*, 214.

(71) Field, R. J.; Noyes, R. M. *Nature* **1972**, *237*, 390.

(72) Watzky, M. A.; Finke, R. G. *Chem. Mater.* **1997**, *9*, 3083.

(73) Özkar, S.; Finke, R. G. manuscript in preparation.

(74) Blum, J.; Amer, I.; Vollhardt, K. P. C.; Schwarz, H.; Hoehne, G. *J. Org. Chem.* **1987**, *52*, 2804.

(75) The true arene hydrogenation catalyst in the important system developed by Blum et al.[74] was later found to be nanocolloidal: Weddle, K. S.; Aiken, J. D., III; Finke, R. G. *J. Am. Chem. Soc.* **1998**, *120*, 5653.

(76) Since it is important for the interpretation of the data, we verified that the black precipitate from one of the hydrogenations is actually bulk Rh metal. Since it was coated with the black precipitate, the stir bar from the experiment with 60 equivs of added water was used as the XPS sample (see the Experimental for details). The XPS survey spectrum shows the expected Rh(0) peaks (see Figure 5.K(b) of the Supporting Information), and, importantly, shows the absence of polyoxoanion stabilizer (compare to Figure 5.K(a) of the Supporting Information).

(77) The same trend has been observed before with polyoxoanion- and tetrabutylammonium-stabilized Ir(0) nanoclusters: those formed in the absence of cyclohexene substrate are 3.0 (± 0.4) nm, while those formed in the presence of cyclohexene are 2.0 (± 0.3).[63] This effect is readily explained by cyclohexene either increasing k_1 or slowing k_2 in the mechanism of formation of the nanoclusters (i.e., decreasing the k_2/k_1 ratio which predicts nanocluster size).[62,72]

(78) The presence of nanoclusters was confirmed by TEM for all of the "water-added" experiments, but size distributions were only determined for solutions with no visible precipitate. Of course, it is difficult to get a representative sample from an inhomogeneous reaction mixture; a reliable size distribution by TEM is generally not possible from a solution that also contains a precipitate.

(79) Teo, B. K.; Sloane, N. J. A. *Inorg. Chem.* **1985**, *24*, 4545.

(80) The hypothesis that the rate enhancing effect of H_2O is in part due to an effect of H_2O on nanocluster formation was tested by determining the nanocluster size distribution by TEM for the experiments with 8 and 30 equivs of water added. The experiment with 8 equivs of H_2O added gives a size distribution of 5.3 (± 0.9) nm, while the experiment with 30 equivs of H_2O added gives a size distribution of 4.6 (± 0.7) nm. It is conceivable, but

perhaps unlikely, that the rate-enhancing effect of H_2O changes dramatically as a function of nanocluster size, with the rate enhancement being greater for the smaller, developing nanoclusters than it is for the larger, preformed nanoclusters. This is a difficult hypothesis to test since it requires that one have access to preformed nanoclusters of a wide range of sizes.

(81) Rather dramatic changes in catalytic rate are observed when small amounts of water are added to the anisole hydrogenation experiments, as demonstrated in Figure 5.4. The change in the maximum hydrogen uptake rate (see Figure 5.4a) in going from the experiment with no water added to the experiment with 30 equivs of water added is about a factor of five. The change in total hydrogen uptake in 24 h (see Figure 5.4b) in going from the experiment with no water added to the experiment with 30 equivs of water added is about a factor of three. The following argument details why these rate changes cannot be entirely explained by a change in nanocluster surface area. A "magic number" (i.e., full shell) nanocluster with 12 complete shells has 6525 atoms[79] with 22% of the atoms on the surface of the nanocluster. A "magic number" nanocluster with 9 complete shells has 2869 atoms[79] with 28% of the atoms on the surface of the nanocluster. Note that the change in surface area between these full shell clusters is *less than a factor of 1.5*, even though the size difference between them is *greater* than the experimentally determined size difference in question (i.e., the size difference between the nanoclusters with no water added and the nanoclusters with 30 equivs of water added). Therefore, surface area alone cannot account for the 3-fold to 5-fold difference in catalytic rate between the two experiments with and without added water.

(82) Hornstein, B. J.; Lyon, D. K.; Aiken, J. D., III; Finke, R. G. unpublished results.

(83) Weiner, H.; Aiken, J. D., III; Finke, R. G. *Inorg. Chem.* **1996**, *35*, 7905.

(84) A paper developing the CS_2 poisoning method to determine the number of nanocluster active sites, and thus nanocluster TOFs, has been accepted for publication: Hornstein, B. J.; Aiken, J. D., III; Finke, R. G. "Nanoclusters in Catalysis: A Comparison of CS_2 Catalyst Poisoning of Polyoxoanion- and Tetrabutylammonium-Stabilized Rh(0) Nanoclusters to 5% Rh/Al_2O_3", *Inorg. Chem.*, **2001**, in press. As noted in this paper, the 3.6 ($\pm\geq$1.8) nm particle size for the 5% Rh/Al_2O_3 catalyst carries $\pm \geq 1.8$ nm error bars due to the heterogeneity of, and thus sampling problem with, the 5% Rh/Al_2O_3 catalyst.

(85) When correcting the TTO and the TOF for the number of surface atoms, one of the assumptions is that the number of metal atoms on the surface does not change during the course of the reaction. This assumption cannot hold true for our lifetime experiments because the observed agglomeration (i.e., bulk metal formation) at long reaction times means that the total surface area is decreasing during the course of the reaction. Nevertheless, by taking a TEM sample early in the reaction, an upper limit on the surface area can be established.

(86) TEM analysis of the 5% Rh/Al_2O_3 catalyst shows the Rh(0) particles are 3.6 ($\pm \geq 1.8$) nm in diameter[84]—almost exactly the same average size as the Rh(0) nanoclusters in the TTO experiment. Additionally, H_2 and CO chemisorption studies of the 5% Rh/Al_2O_3 show that about 33% of the Rh atoms are exposed, which is in good agreement with the TEM data.[84] Consequently, the TOF for the 5% Rh/Al_2O_3 was divided by 0.3 to correct for average number of surface Rh(0) atoms in this heterogeneous catalyst.

(87) Reetz, M. T.; Lohmer, G. *Chem. Commun.* **1996**, 1921.

(88) DeCanio, S. J.; Kirlin, P. S.; Foley, H. C.; Dybowski, C.; Gates, B. C. *Langmuir* **1985**, *1*, 243.

(89) Kluson, P.; Cerveny, L. *J. Mol. Catal. A: Chem.* **1996**, *108*, 107.

(90) Onishi, M.; Hiraki, K.; Yamaguchi, M.; Morishita, J. *Inorg. Chim. Acta* **1992**, *195*, 151.

(91) Russell, M. J.; White, C.; Maitlis, P. M. *J. Chem. Soc., Chem. Commun.* **1977**, 427.

(92) Drinkard, W. C., Jr. In *Ger. Offen.*; (du Pont de Nemours, E. I., and Co.).: DE, 1972; p 53 pp.

(93) Espenson, J. H. *Chemical Kinetics and Reaction Mechanisms*; McGraw-Hill: New York, 1981.

(94) A control experiment was done to rule out possible effects of H_2O as the explanation for the relatively high selectivity in our system for the partially hydrogenated 1-methoxycyclohexene. However, the addition of 60 equivs (4 μL) of H_2O to an otherwise Standard Conditions experiment had no effect on the selectivity to alkene within experimental error, Table 5.2. Therefore the presence (or absence) of H_2O does not seem to be responsible for the observed selectivity, at least for our current system.

(95) To determine if the solvent is responsible for the observed selectivity, a hydrogenation experiment was done using acetone as the solvent instead of propylene carbonate. However, the initial selectivity in acetone is the same as it is in propylene carbonate, so there is no evidence for a solvent effect. (The nanoclusters are not as soluble in acetone as they are in propylene carbonate, which leads to their precipitation from the acetone solution and causes the rate of catalytic hydrogenation to be severely depressed. Consequently, only the initial selectivity can be safely compared with the Standard Conditions experiment.)

(96) Control experiments examining the selectivity of the 5% Rh/Al_2O_3 catalyst at 22 and 78 °C were also performed and proved interesting. Using 7.4 mg of 5% Rh/Al_2O_3 (3.6×10^{-6} mol of Rh) instead of 3.6×10^{-6} mol of A yielded the following results: at 22 °C this typical heterogeneous catalyst displays a comparable (to slightly better) initial selectivity for the alkene intermediate, 38 (± 3)% vs 30 (± 2)% for the nanoclusters, Table 5.2, but this selectivity is *not* increased at the higher, 78 °C temperature. These results, as well as the product vs time curves at both temperatures (not shown), reveal deactivation of the 5% Rh/Al_2O_3 catalyst is occurring—complete deactivation occurs after only 1 h at 78 °C, similar to the polyoxoanion-stabilized nanoclusters (vide supra). Nevertheless, the polyoxoanion-stabilized nanoclusters win the test of the maximum yield of alkene—8.1 (± 0.8)% for the nanocluster vs 1.7 (± 0.2)% for the 5% Rh/Al_2O_3 catalyst.

(97) For an important paper showing the dramatic effects that ligands can have on nanocluster catalytic selectivities, see: Schmid, G.; Maihack, V.; Lantermann, F.; Peschel, S. *J. Chem. Soc., Dalton Trans.* **1996**, 589.

(98) Struijk, J.; Scholten, J. J. F. *Appl. Catal., A* **1992**, *82*, 277.

(99) Crivello, J. V.; Yoo, T. *J. M. S.—Pure Appl. Chem.* **1996**, *A33*, 717.

(100) Nomiya, K.; Pohl, M.; Mizuno, N.; Lyon, D. K.; Finke, R. G. *Inorg. Synth.* **1997**, *31*, 186.

(101) Lin, Y.; Finke, R. G. *Inorg. Chem.* **1994**, *33*, 4891.

SUPPORTING INFORMATION

Anisole Hydrogenation with Well-Characterized Polyoxoanion- and Tetrabutylammonium-Stabilized Rh(0) Nanoclusters: The Effects of Added Water and Acid Plus Enhanced Catalytic Rate, Lifetime and Partial Hydrogenation Selectivity

Jason A. Widegren and Richard G. Finke

Control Experiment Comparing the Rate of Anisole Hydrogenation with the Rate of Cyclohexene Hydrogenation.

A control experiment was performed where both anisole and cyclohexene were hydrogenated by the same batch of nanoclusters. In the drybox 20 (± 0.5) mg of **A** (3.6×10^{-6} mol) was weighed into a 2-dram glass vial. Then 3.0 mL of propylene carbonate was added to the vial with a 5-mL gastight syringe. This mixture was briefly agitated with a disposable polyethylene pipet until **A** dissolved completely. Using the same pipet the bright yellow solution of **A** was then transferred into a new 22 × 175 mm Pyrex culture tube containing a 5/8 × 5/16 in. Teflon-coated stir bar. The culture tube was placed in a Fischer–Porter (F–P) pressure bottle modified with Swagelock TFE-sealed Quick-Connects. The F–P bottle was then sealed, brought out of the drybox, placed in a 22.0 (± 0.1) °C temperature-controlled water bath and connected to a H_2 line via the Quick-Connects. Using the top (purge) valve, the F–P bottle was then purged 15 times (waiting 15 s between purges) with 40 psig H_2. Following the purges, the F–P bottle was pressurized to 40 (± 1) psig H_2 and maintained at that pressure for the next 16 h by leaving the F–P bottle open to the H_2 line. During the purging (and during the subsequent hydrogenation) the reaction solution was vortex-stirred. After 16 h under hydrogen, the F–P bottle was sealed, removed from the H_2 line and brought into the drybox. Then of 0.14 mL of anisole (1.3×10^{-3} mol) was added with a 1-mL gastight syringe to the clear, dark brown solution of Rh(0) nanoclusters in the culture tube. The F–P bottle was then sealed, brought out of the drybox, placed in a 22.0 (± 0.1) °C temperature-controlled water bath and connected to a H_2 line via the Quick-Connects. Using the top (purge) valve, the F–P bottle was then purged 15 times (waiting 15 s between purges) with 40 psig H_2. Following the purges, the F–P bottle was pressurized to 40 (± 1) psig H_2 and then isolated (by closing the valve to the H_2 line). During the purging (and during the hydrogenation reaction) the reaction solution was vortex-stirred. Immediately after the F–P bottle was pressurized to 40 (± 1) psig H_2, data collection (H_2 pressure vs time) was initiated using an Omega PX-621 pressure transducer interfaced to a PC. After 4 h of anisole hydrogenation the F–P bottle was once again sealed and brought into the drybox. Then 0.5 mL of cyclohexene (4.94×10^{-3} mol) was added with a 5.0-mL gastight syringe to the clear, dark brown reaction solution in the culture tube. The F–P bottle was then attached to the H_2 line in the same way it was done after the anisole had been added. For a plot of the hydrogen uptake curve for this experiment see Figure 5.A. The final reaction solution was clear and dark brown with no visible precipitate.

The reported H_2 uptake rate for anisole hydrogenation was determined in the following way. The first 30 min of H_2 pressure vs time data was ignored—this allows the solvent vapor pressure and the temperature of the apparatus to come to equilibrium.[1] Normally this would not be necessary since the pressure change due to these variables is small in this system (about 0.2 psig for a 22 °C experiment). However, the rate of anisole hydrogenation is slow enough that the overall H_2 uptake from the catalytic reaction is not much larger than the pressure change due to the experimental artifacts. By removing the first 30 min of data the pressure changes due to experimental artifacts are effectively

eliminated.[1] The H_2 uptake rate was obtained from the hour of data immediately following the first 30 min of ignored data (the H_2 uptake is quite linear on this timescale). As a final precaution, we verified that the percent conversion predicted by the reported H_2 uptake rate matched the percent conversion seen by ^1H NMR (the H_2 uptake rate predicted 4.0% conversion after 4 h while a ^1H NMR spectrum of the reaction solution showed 3.1% conversion after 4 h, equivalent results within experimental error). The reported H_2 uptake rate for the cyclohexene hydrogenation was determined simply by fitting the first few data points of the H_2 uptake curve. Since the pressure change due to catalysis is relatively large for this part of the experiment, the pressure change due to experimental artifacts is not significant.

Reference:

(1) Widegren, J. A.; Aiken, J. D., III; Özkar, S.; Finke, R. G. *Chem. Mater.* **2001**, *13*, 312.

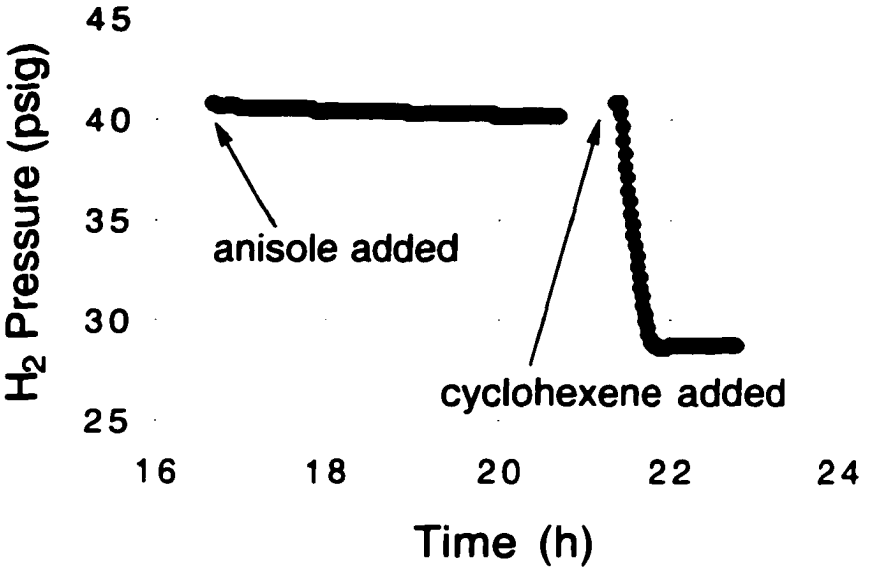

Figure 5.A. Plot of the H_2 pressure vs time for an experiment where both anisole and cyclohexene are hydrogenated with the same batch of polyoxoanion- and tetrabutylammonium-stabilized Rh(0) nanoclusters. The nanoclusters were formed in the absence of substrate from 20 mg of $[Bu_4N]_5Na_3[(1,5\text{-COD})Rh{\bullet}P_2W_{15}Nb_3O_{62}]$ in 3.0 mL of propylene carbonate at 22 °C and 40 psig constant H_2 pressure. After allowing 16 h for nanocluster formation, 0.14 mL of anisole was added and the subsequent H_2 uptake rate was found to be 0.11 psig/h. After 4 h of anisole hydrogenation, at which point the anisole hydrogenation was about 4% complete, 0.5 mL of cyclohexene was added to the reaction solution. The hydrogenation of cyclohexene occurred at diffusion controlled rates (37 psig/h initial rate) and was complete in less than 30 min. This experiment shows that the Rh(0) nanoclusters do have the expected (high) catalytic activity for cyclohexene hydrogenation under conditions where the anisole hydrogenation is found to be comparatively slow.

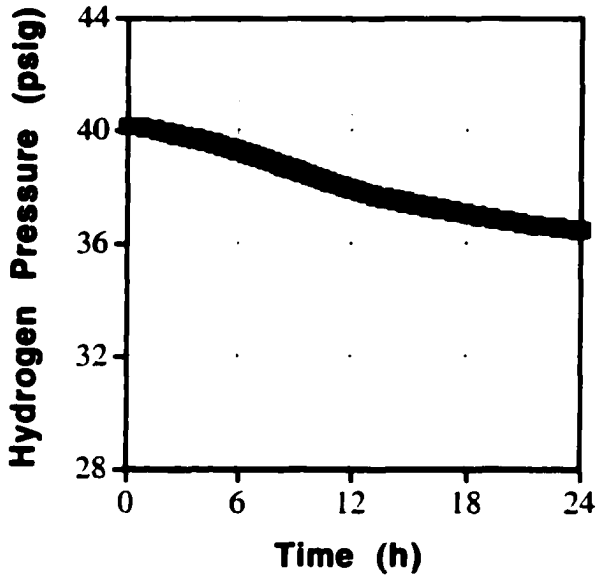

Figure 5.B. Plot of hydrogen pressure vs time for an anisole hydrogenation experiment with $[Bu_4N]_5Na_3[(1,5\text{-COD})Rh{\bullet}P_2W_{15}Nb_3O_{62}]$ as the precatalyst. In this experiment 0.5 μL of water (8 equivs vs Rh) was added. Experimental conditions include 2.9 mL of propylene carbonate, 0.14 mL of anisole, 20 (± 0.5) mg of precatalyst, 22 °C and 40 (± 1) psig initial H_2 pressure. The total pressure loss in 24 h was 3.9 psi, which corresponds to 36% conversion (i.e., 130 catalytic turnovers). The maximum rate of hydrogen uptake was 0.25 psi/h (i.e., 8 turnovers/h). There was no visible precipitate at the end of this reaction. The final reaction solution was a clear, light-brown.

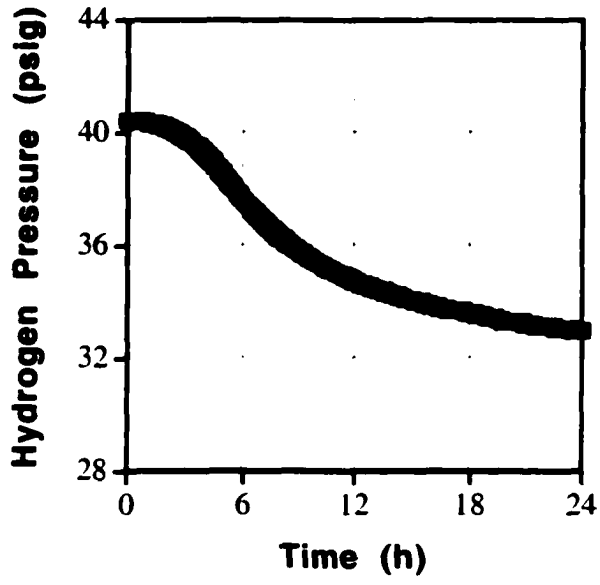

Figure 5.C. Plot of hydrogen pressure vs time for an anisole hydrogenation experiment with $[Bu_4N]_5Na_3[(1,5\text{-COD})Rh{\bullet}P_2W_{15}Nb_3O_{62}]$ as the precatalyst. In this experiment 2.0 μL of water (30 equivs vs Rh) was added. Experimental conditions include 2.9 mL of propylene carbonate, 0.14 mL of anisole, 20 (± 0.5) mg of precatalyst, 22 °C and 40 (± 1) psig initial H_2 pressure. The total pressure loss in 24 h was 7.7 psi, which corresponds to 70% conversion (i.e., 250 catalytic turnovers). The maximum rate of hydrogen uptake was 0.83 psi/h (i.e., 27 turnovers/h). The final reaction solution was clear and black-brown with no visible precipitate. GLC of the final reaction solution showed 1.0 (± 0.1) equivs of cyclooctane had evolved (i.e., reduction of the precatalyst and nanocluster formation were complete).

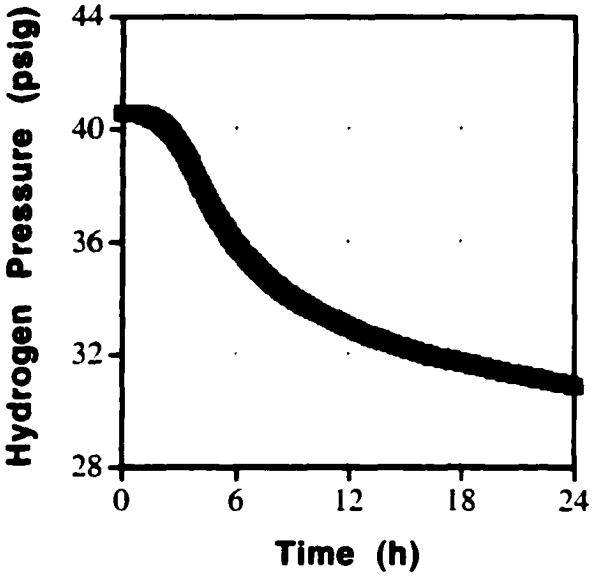

Figure 5.D. Plot of hydrogen pressure vs time for an anisole hydrogenation experiment with $[Bu_4N]_5Na_3[(1,5\text{-COD})Rh{\bullet}P_2W_{15}Nb_3O_{62}]$ as the precatalyst. In this experiment 4.0 μL of water (60 equivs vs Rh) was added. Experimental conditions include 2.9 mL of propylene carbonate, 0.14 mL of anisole, 20 (± 0.5) mg of precatalyst, 22 °C and 40 (± 1) psig initial H_2 pressure. The total pressure loss in 24 h was 9.9 psi, which corresponds to 90% conversion (i.e., 320 catalytic turnovers). The maximum rate of hydrogen uptake was 1.43 psi/h (i.e., 47 turnovers/h). A small amount of dark precipitate was visible at the end of the reaction; the final reaction solution was clear and brown-black. GLC of the final reaction solution showed 1.1 (± 0.1) equivs of cyclooctane had evolved (i.e., reduction of the precatalyst and nanocluster formation were complete).

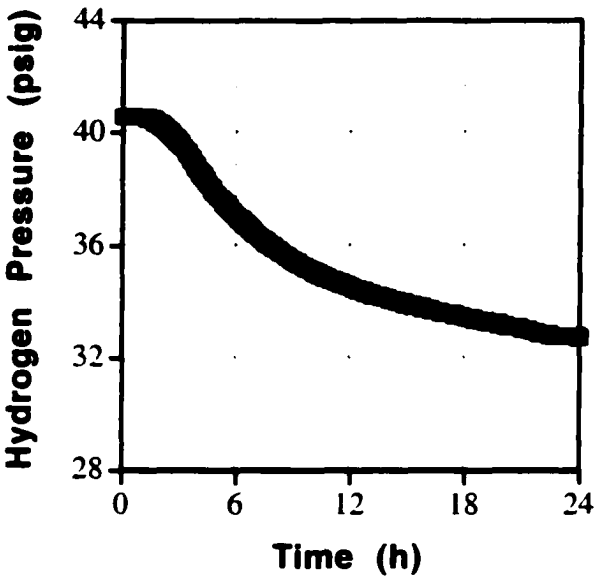

Figure 5.E. Plot of hydrogen pressure vs time for an anisole hydrogenation experiment with $[Bu_4N]_5Na_3[(1,5\text{-COD})Rh{\bullet}P_2W_{15}Nb_3O_{62}]$ as the precatalyst. In this experiment 6.0 μL of water (90 equivs vs Rh) was added. Experimental conditions include 2.9 mL of propylene carbonate, 0.14 mL of anisole, 20 (± 0.5) mg of precatalyst, 22 °C and 40 (± 1) psig initial H_2 pressure. The total pressure loss in 24 h was 8.1 psi, which corresponds to 73% conversion (i.e., 260 catalytic turnovers). The maximum rate of hydrogen uptake was 1.00 psi/h (i.e., 32 turnovers/h). A dark precipitate was visible at the end of the reaction; the final reaction solution was clear and brown-black. GLC of the final reaction solution showed 1.0 (± 0.1) equivs of cyclooctane had evolved (i.e., reduction of the precatalyst and nanocluster formation were complete).

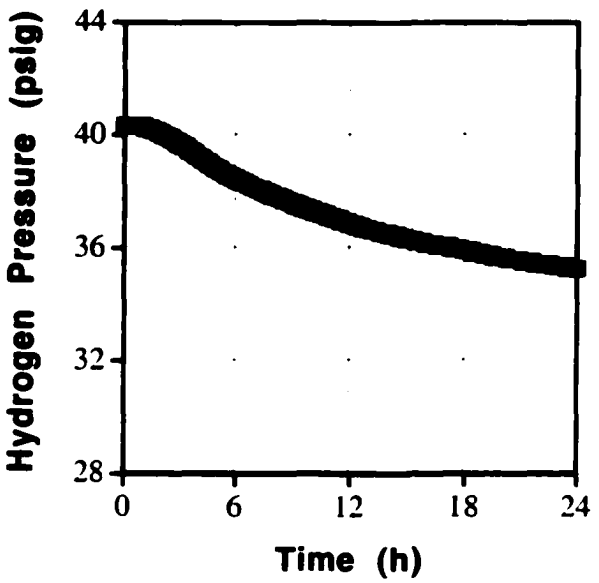

Figure 5.F. Plot of hydrogen pressure vs time for an anisole hydrogenation experiment with $[Bu_4N]_5Na_3[(1,5\text{-COD})Rh{\bullet}P_2W_{15}Nb_3O_{62}]$ as the precatalyst. In this experiment 8.0 μL of water (120 equivs vs Rh) was added. Experimental conditions include 2.9 mL of propylene carbonate, 0.14 mL of anisole, 20 (± 0.5) mg of precatalyst, 22 °C and 40 (± 1) psig initial H_2 pressure. The total pressure loss in 24 h was 5.3 psi, which corresponds to 48% conversion (i.e., 170 catalytic turnovers). The maximum rate of hydrogen uptake was 0.45 psi/h (i.e., 15 turnovers/h). A dark precipitate was visible at the end of the reaction; the final reaction solution was brown-black. GLC of the final reaction solution showed 0.9 (± 0.1) equivs of cyclooctane had evolved (i.e., reduction of the precatalyst and nanocluster formation were complete).

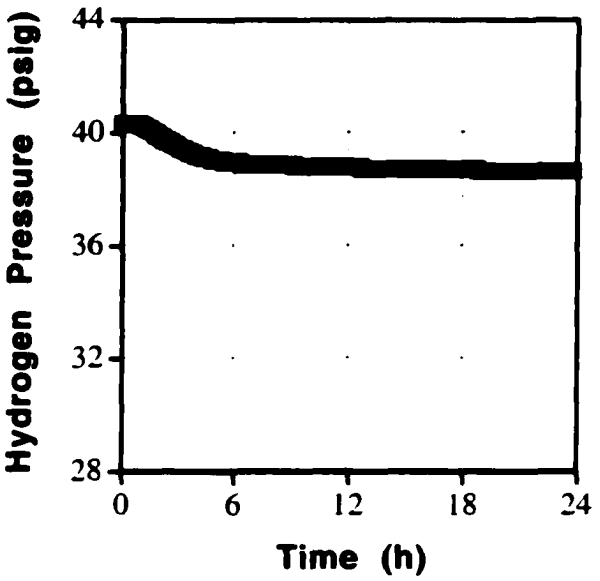

Figure 5.G. Plot of hydrogen pressure vs time for an anisole hydrogenation experiment with $[Bu_4N]_5Na_3[(1,5\text{-COD})Rh{\bullet}P_2W_{15}Nb_3O_{62}]$ as the precatalyst. In this experiment 30 μL of water (465 equivs vs Rh) was added. Experimental conditions include 2.9 mL of propylene carbonate, 0.14 mL of anisole, 20 (± 0.5) mg of precatalyst, 22 °C and 40 (± 1) psig initial H_2 pressure. The total pressure loss in 24 h was 1.9 psi, which corresponds to 17% conversion (i.e., 61 catalytic turnovers). The maximum rate of hydrogen uptake was 0.40 psi/h (i.e., 13 turnovers/h). A dark precipitate was visible at the end of the reaction; the final reaction solution was black. GLC of the final reaction solution showed 1.0 (± 0.1) equivs of cyclooctane had evolved (i.e., reduction of the precatalyst and nanocluster formation were complete).

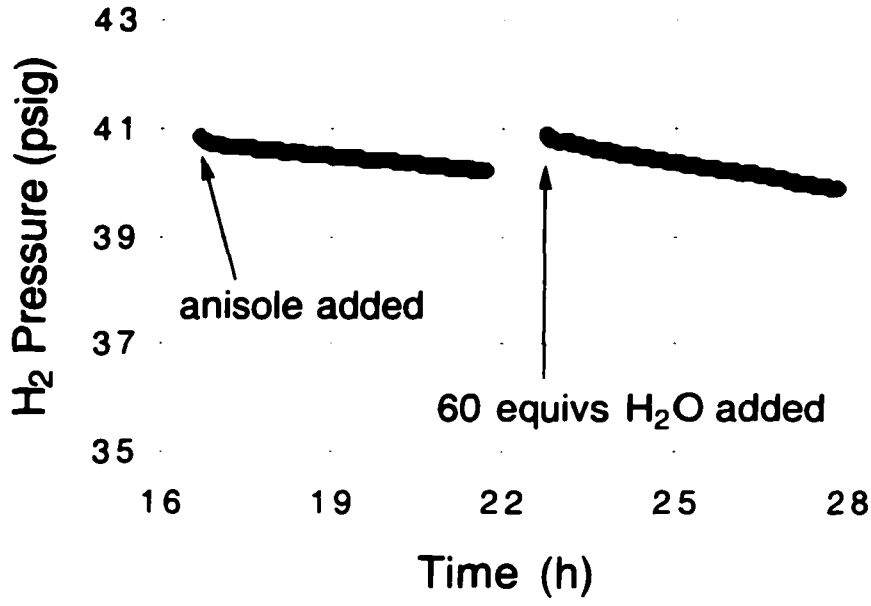

Figure 5.H. Plot of the H_2 pressure vs time for an experiment where anisole is hydrogenated under anhydrous conditions to begin with, and then 60 equivs of H_2O are added, using the same batch of polyoxoanion- and tetrabutylammonium-stabilized Rh(0) nanoclusters. The nanoclusters were formed in the absence of substrate from 20 mg of $[Bu_4N]_5Na_3[(1,5\text{-COD})Rh{\bullet}P_2W_{15}Nb_3O_{62}]$ in 3.0 mL of propylene carbonate at 22 °C and 40 psig constant H_2 pressure. After allowing 16 h for nanocluster formation, 0.14 mL of anisole was added and the subsequent H_2 uptake rate is 0.094 psig/h. After 5 h of anisole hydrogenation, at which point the anisole hydrogenation was about 4% complete, 4.0 μL of H_2O (60 equivs vs Rh) was added to the reaction solution. The subsequent H_2 uptake rate is 0.22 psig/h, about twice as fast as before the H_2O was added. This experiment shows that H_2O increases the rate of hydrogenation, even for preformed Rh(0) nanoclusters.

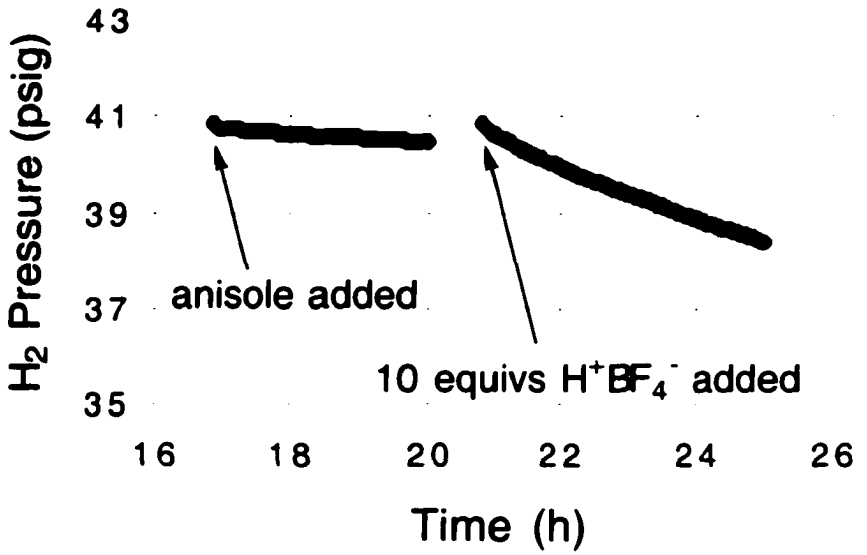

Figure 5.I. Plot of the H_2 pressure vs time for an experiment where anisole is hydrogenated without acid to begin with, and then 10 equivs of $HBF_4 \bullet Et_2O$ are added, using the same batch of polyoxoanion- and tetrabutylammonium-stabilized Rh(0) nanoclusters. The nanoclusters were formed in the absence of substrate from 20 mg of $[Bu_4N]_5Na_3[(1,5\text{-COD})Rh \bullet P_2W_{15}Nb_3O_{62}]$ in 3.0 mL of propylene carbonate at 22 °C and 40 psig constant H_2 pressure. After allowing 16 h for nanocluster formation, 0.14 mL of anisole was added and the subsequent H_2 uptake rate is 0.11 psig/h. After about 3 h of anisole hydrogenation, at which point the anisole hydrogenation was about 3% complete, 5.0 μL of $HBF_4 \bullet Et_2O$ (10 equivs vs Rh) was added to the reaction solution. The subsequent H_2 uptake rate is 0.63 psig/h, about 6 fold faster than before the acid was added. This experiment shows that acid increases the rate of hydrogenation, even for preformed Rh(0) nanoclusters.

Use of Effective Carbon Number (ECN) for GLC Quantitation.

For most hydrocarbons the relative response factors (with FID detection) are directly proportional to the number of carbon atoms in the molecule (e.g., the relative response factor of propane is about three times that of methane).[1] The situation is complicated by the presence of heteroatoms, which generally decrease the response.[1] Nevertheless, large lists of experimental relative response factors allow one to estimate rather closely, based on the groups of atoms in the molecule, the relative response factor of many molecules. This makes the concept of ECN useful for estimating the relative response factor for compounds that cannot be obtained in sufficient purity for an experimental determination. Such was the case—methoxycyclohexane is available commercially (from the Sigma-Aldrich Library of Rare Chemicals), but was found to be only about 80% pure by GLC, and 1-methoxycyclohexene is not available commercially. Only anisole is available commercially in pure form.

Using Table 5.3 elsewhere[1] we were able to calculate the ECN for each compound using the following entries in that table: aliphatic and aromatic carbons give an ECN contribution of 1.0, olefinic carbons give an ECN contribution of 0.95, ethers give an ECN contribution of -1.0. Therefore, the ECN for anisole is 6.0 (i.e., 1 aliphatic carbon, 6 aromatic carbons and 1 ether give: 1 + 6 – 1 = 6). Similarly, the ECN of methoxycyclohexane is also 6.0. The ECN of 1-methoxycyclohexene is 5.9 (i.e., 5 aliphatic carbons, 2 olefinic carbons and 1 ether give: 5 + 1.9 – 1 = 5.9). These simple calculations suggest the relative response factors of all three compounds are within 2% of being the same; therefore, all three compounds were assumed to have the same relative response for the purpose of quantitating our GLC results (no correction was made for the 2% difference expected in the relative response of the enol ether).

As a control we tested the validity of the ECN estimated response factors by ^{1}H NMR for one experiment (see Figure 5.J). In that experiment the reaction solution gave a GLC trace with the following ratio of peaks: anisole, 59.1; 1-methoxycyclohexene, 8.1; methoxycyclohexane, 32.8. A ^{1}H NMR of the same reaction solution gave a spectrum with the following ratio of integrals (for the resonance of the methyl group protons of each compound): 61.2 for anisole (δ 3.8), 8.1 for 1-methoxycyclohexene (δ 3.5), 30.7 for methoxycyclohexane (δ 3.3). The two methods give identical results to within less than ±5% (which is less than the experimental error of integration), so our assumption that all three compounds have identical relative response factors in the FID is correct.

Reference:

(1) Grob, R. L.; Editor *Modern Practice of Gas Chromatography, Third Edition*, 1995.

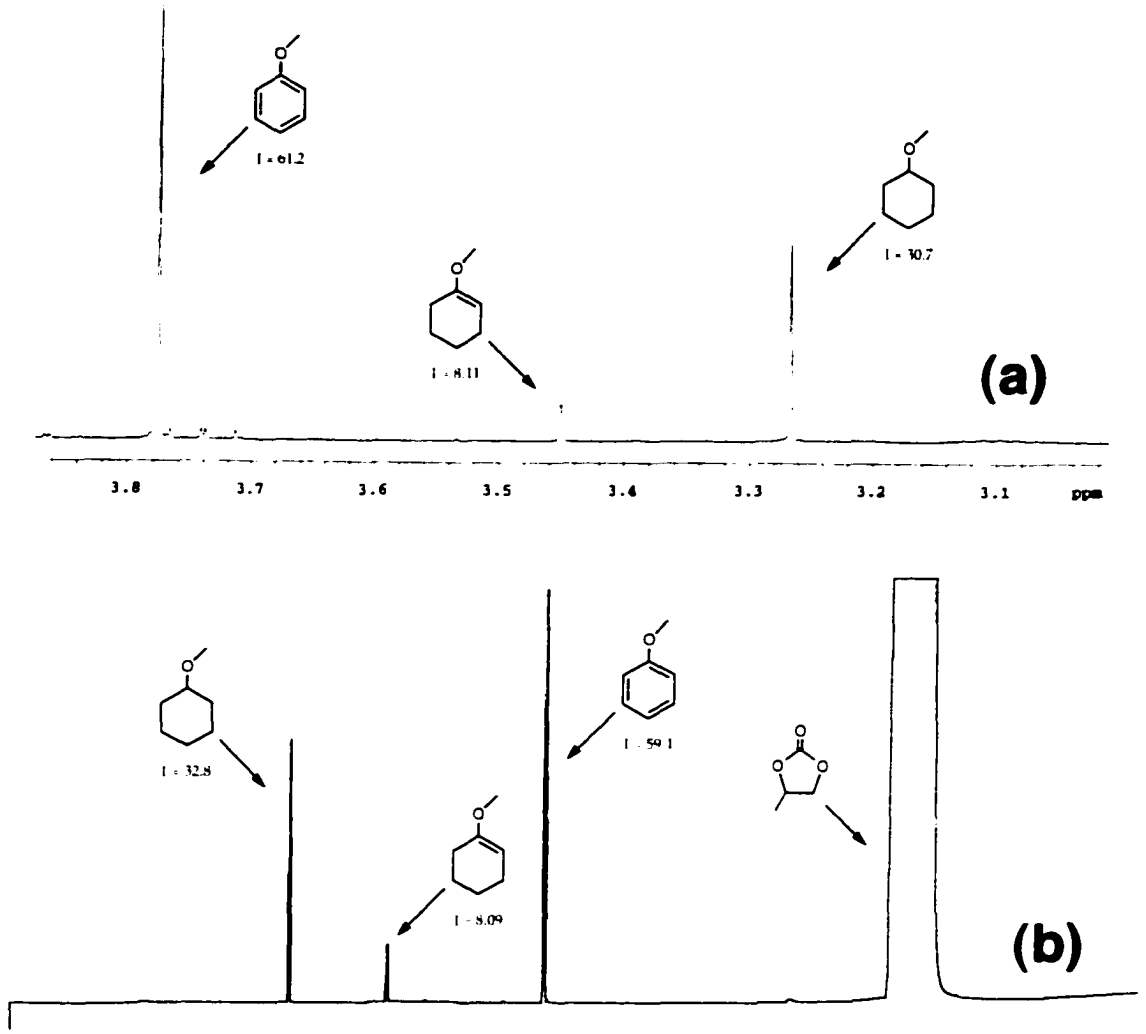

Figure 5.J. (a) The ^{1}H NMR spectrum and (b) the GLC trace of the reaction solution in an anisole hydrogenation with $[Bu_4N]_5Na_3[(1,5\text{-COD})Rh{\bullet}P_2W_{15}Nb_3O_{62}]$ at 78 °C (see the main text for further details about this experiment and for the GLC conditions). This figure demonstrates the validity of the "effective carbon number" (ECN) approximation used to quantitate the GLC data. The ^{1}H NMR shows the resonances and relative integrals for the methyl group protons of anisole, 1-methoxycyclohexene and methoxycyclohexane. The GLC trace shows the peaks and relative integrals for the same compounds (retention times: 5.8 min, 7.9 min and 11.2 min). Since the relative integrals are the same (within experimental error) for the two methods (see the Experimental section on ECN in the main text), the ECN approximation works for this system (and to $<\pm 5\%$). This result also shows that there is no formation of 1-methoxycyclohexene on the GLC injector port. Additionally, the clean GLC trace shows that 1-methoxycyclohexene and methoxycyclohexane are the only significant products in the reaction.

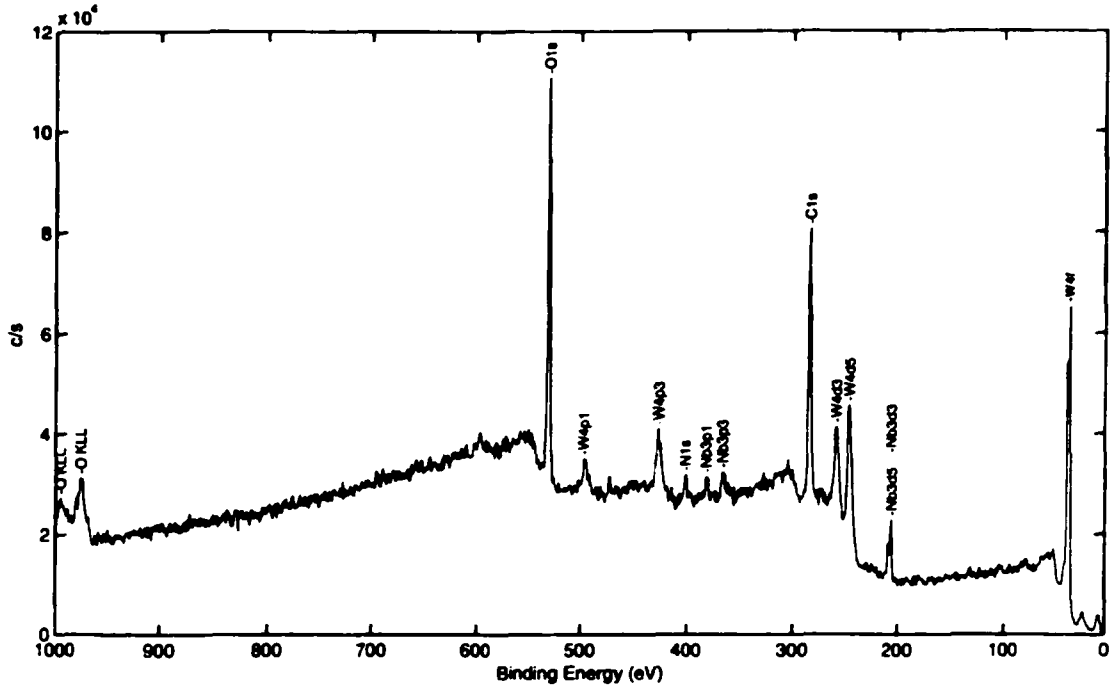

Figure 5.K(a). X-ray photoelectron spectrum of the polyoxoanion- and tetrabutylammonium-stabilized nanoclusters from a Standard Conditions anisole hydrogenation. The conditions of the experiment included 2.9 mL of propylene carbonate, 0.14 mL of anisole, 20 (± 0.5) mg of $[Bu_4N]_5Na_3[(1,5\text{-COD})Rh{\bullet}P_2W_{15}Nb_3O_{62}]$, 22 °C and 40 (± 1) psig initial H_2 pressure (see the main text for further details). The XPS sample was prepared by precipitating the nanoclusters and stabilizer onto a glass substrate with diethyl ether (see the main text for further details). Lines from the polyoxoanion and tetrabutylammonium stabilizer are prominent in this survey scan. Note, however, the absence of Rh lines in the spectrum (e.g., the Rh $3d_{5/2}$ line at ~308 eV and the $3d_{3/2}$ line at ~312.3 eV are missing); high-resolution scans also showed no Rh 3d lines. Hence, and at least for samples prepared by diethyl ether precipitation, the Rh nanoclusters appear to be "buried" in the excess of nanocluster stabilizer material, and are not observed by this surface analysis technique. In this regard, one must consider that a single layer of polyoxoanion stabilizer is 15 Å thick, and already approaches the depths which XPS probes (20–50 Å).

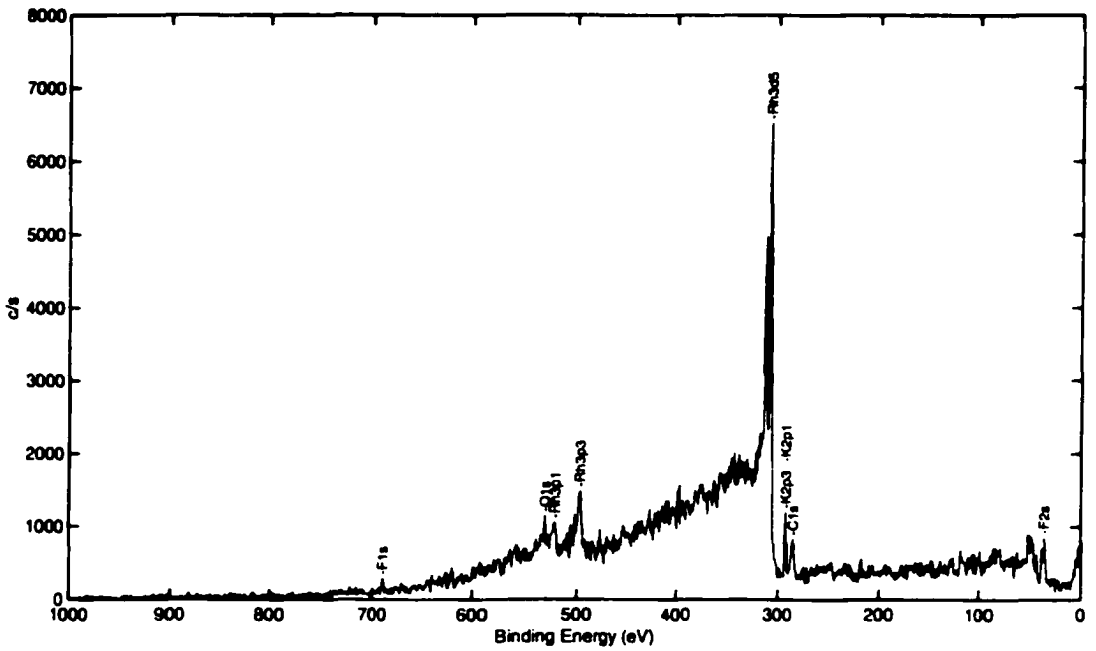

Figure 5.K(b). XPS spectrum of the black precipitate from an anisole hydrogenation with 60 equivalents of H_2O added. The conditions of the experiment included 2.9 mL of propylene carbonate, 0.14 mL of anisole (1.29×10^{-3} mol), 4.0 μL of H_2O, 20 (± 0.5) mg of $[Bu_4N]_5Na_3[(1,5\text{-COD})Rh{\bullet}P_2W_{15}Nb_3O_{62}]$ (3.58×10^{-6} mol), 22 °C and 40 (± 1) psig initial H_2 pressure (ca. 3.6 atm). The presence of bulk Rh(0) is confirmed by the $3d_{5/2}$ line at 307.5 eV and the $3d_{3/2}$ line at 312.3 eV. Note also the lack of the tungsten 4f line, which demonstrates the absence of polyoxoanion stabilizer in the black precipitate.

Is the Selectivity of the Polyoxoanion- and Tetrabutylammonium-Stabilized Nanoclusters Unique?

Anisole and other aryl ethers are common substrates in arene hydrogenation studies. For example, anisole or some other aryl ether was used as a substrate in fourteen of the references in Table 2.1. *However, the partial hydrogenation of an aryl ether has never been observed with a soluble nanocluster catalyst.* There is one paper in which the partial hydrogenation of anisole is reported[1] where it is not clear if the true catalyst is a homogeneous metal complex or a soluble nanocluster. The catalyst in this system was originally claimed to be homogeneous on the basis of light scattering evidence. [1] A later paper by Collman et al. suggests that the true catalyst may be heterogeneous, though the evidence presented is not definitive, as they are careful to point out.[2] Briefly, the evidence presented elsewhere[2] includes (i) the observation of dark colored reaction solutions, (ii) the routine observation of 1 to 2 h induction periods, (iii) the deposition of Rh metal on the reactor walls, and (iv) the observation that the catalyst was much more active for the hydrogenation of benzene and cumene than it was for the hydrogenation of polystyrene. The partial hydrogenation of *any* monocyclic arene using a proven soluble nanocluster catalyst has apparently only been reported once in the literature.[3] (The nano-colloidal nature of the true arene hydrogenation catalyst in that system[3] was discovered several years after the catalyst was developed.[4]) In that work it was noted that cyclohexene derivatives are observed only when very sterically hindered substrates like durene (1,2,4,5-tetramethylbenzene) are hydrogenated. Some researchers even specifically mention that no partial hydrogenation intermediates are observed. [5,6] For example, Roucoux et al. say, "Unfortunately, we did not observe any cyclohexene or cyclohexadiene derivatives as intermediates which ideally would have been desirable".[6] Additionally, many of the reports in this area include careful product studies and most of the reports mention GLC as a means of product quantitation. Of course, it is possible that other researchers using soluble nanocluster catalysts for arene hydrogenation simply missed the alkene intermediate because of low yields or the eventual complete hydrogenation to alkane. Nevertheless, based on the available data one is forced to conclude that, at least among known soluble nanocluster catalysts, our polyoxoanion- and tetrabutylammonium-stabilized Rh(0) nanoclusters display a unique selectivity for the partial hydrogenation of arenes.

References:

(1) Russell, M. J.; White, C.; Maitlis, P. M. *J. Chem. Soc., Chem. Commun.* **1977**, 427.
(2) Collman, J. P.; Kosydar, K. M.; Bressan, M.; Lamanna, W.; Garrett, T. *J. Am. Chem. Soc.* **1984**, *106*, 2569.
(3) Blum, J.; Amer, I.; Vollhardt, K. P. C.; Schwarz, H.; Hoehne, G. *J. Org. Chem.* **1987**, *52*, 2804.
(4) Weddle, K. S.; Aiken, J. D., III; Finke, R. G. *J. Am. Chem. Soc.* **1998**, *120*, 5653.
(5) James, B. R.; Wang, Y.; Hu, T. Q. *Chem. Ind. (Dekker)* **1996**, *68*, 423.
(6) Schulz, J.; Roucoux, A.; Patin, H. *Chem.--Eur. J.* **2000**, *6*, 618.

Discussion of the Horiuti–Polanyi Mechanism for the Hydrogenation of Monocyclic Arenes with Group VIII Heterogeneous Metal Catalysts

The hydrogenation of monocyclic arenes with group VIII heterogeneous metal catalysts is generally discussed in terms of the widely accepted Horiuti–Polanyi mechanism (Figure 5.L).[1,2] For the following discussion we assume that the Horiuti–Polanyi mechanism, or something rather similar to it, is operative for our catalyst. It will be important, however, to obtain concrete evidence to support or refute this mechanism so that the following discussion can be less speculative.

The rate constants that determine the selectivity and yield of the alkene product are shown in Figure 5.L. The rate constant for the desorption of alkene from the surface of the catalyst into the reaction solvent is k_{des}, the rate constant for the adsorption of alkene from the reaction solvent onto the surface of the catalyst is k_{ads}, and the rate constant for the hydrogenation of adsorbed alkene is k_H. The initial selectivity to alkene depends upon the relative values of k_{des} and k_H (i.e., the larger k_{des} is compared to k_H, the higher the initial selectivity to the alkene). We observe an initial selectivity to the alkene of about 30%, with no significant change in initial selectivity over a 56 °C temperature range (22–78 °C), so we are either working near the isokinetic point[3] or the activation energy for alkene desorption is similar to the activation energy for hydrogenation of adsorbed alkene. We do observe a 4-fold increase in the maximum yield of alkene over the same temperature range (22–78 °C). Presumably, the increase in yield at higher temperatures is due to a relative increase in the k_{des}/k_{ads} equilibrium constant (i.e., higher temperatures favor the entropically preferred desorbed alkene) compared k_H.

References:

(1) Hu, S.-C.; Chen, Y.-W. *J. Chin. Inst. Chem. Eng.* **1998**, *29*, 387.
(2) Struijk, J.; D'Angremond, M.; Lucas-De Regt, W. J. M.; Scholten, J. J. F. *Appl. Catal., A* **1992**, *83*, 263.
(3) Giese, B. *Acc. Chem. Res.* **1984**, *17*, 438.

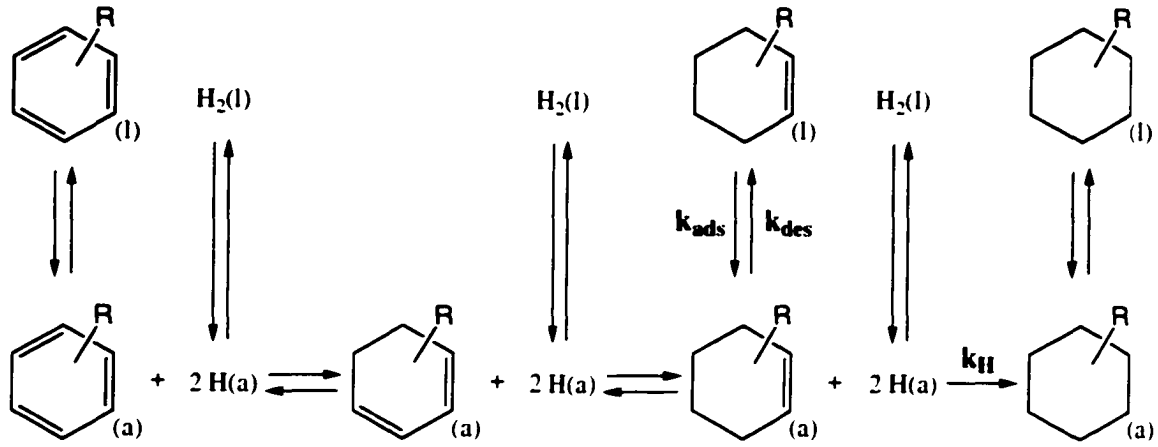

Figure 5.L. Adapted Horiuti-Polanyi mechanism for the catalytic hydrogenation of arenes on group VIII metals. The (l) indicates that the compound is freely dissolved in the liquid state and the (a) indicates that it is adsorbed on the catalyst surface.

Control Experiment Showing the Activity and Lifetime of the 5% Rh/Al_2O_3 for Cyclohexene Hydrogenation.

This control experiment was performed to check the catalytic performance of the heterogeneous catalyst for olefin hydrogenation. This experiment involves repeating a cyclohexene hydrogenation experiment reported elsewhere.[1] In this experiment the catalytic lifetime and activity for cyclohexene hydrogenation were tested using conditions similar to those used for anisole hydrogenation (this experiment was performed *before* the catalyst was re-activated, see the "Materials" section for details). In the drybox 1.5 mg of 5% Rh/Al_2O_3 (7.3×10^{-7} mol Rh) and 20 mL of cyclohexene (1.97×10^{-1} mol) were placed in a new 22 × 175 mm culture tube containing a new 5/8" × 5/16" Teflon-coated magnetic stir bar. This was accomplished by weighing the 5% Rh/Al_2O_3 into a 2-dram vial, adding some cyclohexene to the vial, agitating the suspension of 5% Rh/Al_2O_3 with a polyethylene pipet and then transferring it to the culture tube with the same pipet. Similarly, the vial was rinsed with 4–5 more portions of cyclohexene, and these washings were also added to the culture tube with the same pipet. In all, 20 mL of cyclohexene was added to the culture tube. The culture tube was placed inside the F–P bottle, which was then sealed, brought out of the drybox, placed in the temperature-controlled water bath (22 °C) and attached to the H_2 line via the Quick-Connects. Stirring was started (at >600 rpm) and, using the top (purge) valve, the F–P bottle was purged 15 times with 40 psig H_2 (15 s between each purge). The H_2 pressure was then set at 40 (± 1) psig for the entire course of the reaction. Five minutes after the beginning of the purges was designated as $t = 0$. After 24.0 hours the hydrogenation was nearing completion, so an additional 6.0 mL of cyclohexene was added to the culture tube (in the drybox). The F–P bottle was then reconnected to the hydrogenation apparatus in the same manner as at the beginning of the reaction. After a total of 46.5 hours another 6.0 mL of cyclohexene was added. Complete conversion (433,000 TO) was observed after 73.1 h of reaction. In the previously reported experiment (which was also performed with catalyst that had not been re-activated) 340,000 TO were observed after 68 h.[1] This control experiment shows that the 5% Rh/Al_2O_3 is still highly active for cyclohexene hydrogenation under conditions similar to those used for anisole hydrogenation. The reaction progress was monitored by periodically withdrawing aliquots of the reaction solution for analysis by ^1H NMR spectroscopy. The sampling procedure is described in detail in the section in the Experimental of the main text titled "Anisole Hydrogenation Catalytic Lifetime Experiments".

Reference:

(1) Aiken, J. D., III; Finke, R. G. *J. Am. Chem. Soc.* **1999**, *121*, 8803.

Identification of the White Precipitate in the Total Turnovers Experiment with $HBF_4 \bullet Et_2O$ Added

A white precipitate built up over the course of the total turnovers experiment with 10 equivs of $HBF_4 \bullet Et_2O$ added (see the main text for a detailed description of that experiment). The precipitate was isolated by first collecting it on a medium glass frit. It was then extracted with Et_2O to separate it from the nanoclusters and polyoxoanion stabilizer (neither of which is soluble in Et_2O). Almost all of the material was extracted in this way, leaving behind only a very small amount of black solid. The isolated white precipitate was then obtained by drying overnight under vacuum.

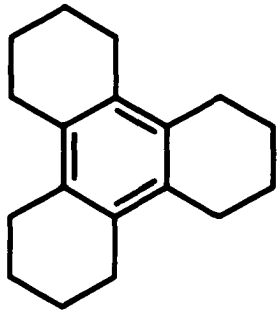

(1)

By comparison to a library of compounds, electron ionization mass spectrometry identified the isolated white precipitate as dodecahydrotriphenylene (1). This assignment was verified by melting point and by ^1H and ^{13}C NMR. The melting point of the precipitate was 226–231 °C (heating rate, 0.9 °C/min), compared to a literature value[1] of 230–231 °C for dodecahydrotriphenylene. A ^1H NMR spectrum of the precipitate in CD_2Cl_2 (referenced to the residual solvent impurity at δ 5.32) showed multiplets of equal intensity at δ 2.53 and δ 1.75, compared to literature values[1] of δ 2.50 and δ 1.73 for dodecahydrotriphenylene. (By ^1H NMR the isolated precipitate is 95% pure.) A proton-decoupled ^{13}C NMR spectrum of the precipitate in CD_2Cl_2 (referenced to the residual solvent impurity at δ 54.0) showed resonances at δ 132.7, 27.3 and 23.8, compared to literature values[1] of δ 132.4, 26.9 and 23.1 for dodecahydrotriphenylene.

Figure 5.M shows a GLC trace for the reaction solution (sampled at 44.3 h) from the total turnovers experiment with 10 equivs of $HBF_4 \bullet Et_2O$ added. (See the Experimental section in the main text for the GLC conditions.) The GLC trace shows that anisole hydrogenation is about 40% complete after 44.3 h, and shows that methanol, methoxycyclohexane, cyclohexanone and anisole are all present in significant quantities in the reaction solution. The partially hydrogenated intermediate 1-methoxycyclohexene is not observed by GLC (is present in <1% yield) in this experiment, Figure 5.M. Instead, cyclohexanone is observed as the partially hydrogenated intermediate. Even though it is known to be present by other techniques (vide supra), dodecahydrotriphenylene is not observed in the GLC trace.

We believe that dodecahydrotriphenylene is formed from the 1-methoxycyclohexene intermediate, via cyclohexanone, with the stoichiometry of formation shown below (2). Apparently, the 1-methoxycyclohexene is converted to cyclohexanone under the acidic reaction conditions, since cyclohexanone is observed by

GLC. The two products shown below (2), methanol and dodecahydrotriphenylene, are both observed (vide supra), but were not quantitated (methanol's volatility makes it difficult to accurately quantitate in our hydrogenation apparatus and dodecahydrotriphenylene is difficult to quantitate because of its (in)solubility in the reaction solution). Our qualitative verification of the stoichiometry shown below (2) strongly suggests that dodecahydrotriphenylene is formed via the well-known[1,2,3] acid-catalyzed condensation of cyclohexanone.

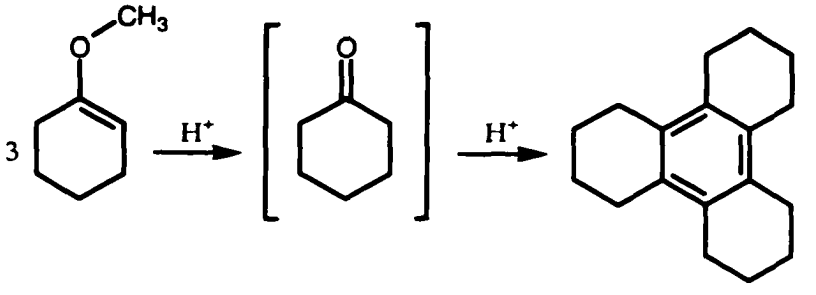

(2)

Although the acid-catalyzed condensation of cyclohexanone has literature precedent, we cannot rule out the possibility that some or all of the dodecahydrotriphenylene is formed directly from the acid-catalyzed condensation of 1-methoxycyclohexene (i.e., in a parallel pathway that bypasses the cyclohexanone intermediate). Scheme 5.A shows a reasonable arrow-pushing mechanism for such a reaction.

The formation of dodecahydrotriphenylene does not require the presence of the precatalyst $[Bu_4N]_5Na_3[(1,5\text{-COD})Rh{\bullet}P_2W_{15}Nb_3O_{62}]$. In a control experiment we found that dodecahydrotriphenylene was formed from a solution containing only 2.0 mL of propylene carbonate, 0.7 mL of anisole, 0.3 mL of 1-methoxycyclohexene and 0.02 mL of $HBF_4{\bullet}Et_2O$ (see the Materials section in the main text for a description of the reagents used). Upon stirring this solution in the drybox, a white precipitate formed within an hour. The precipitate was isolated and characterized as described above, confirming its identity.

References:

(1) Shirai, H.; Amano, N.; Hashimoto, Y.; Fukui, E.; Ishii, Y.; Ogawa, M. *J. Org. Chem.* **1991**, *56*, 2253.

(2) Elmorsy, S. S.; Pelter, A.; Smith, K. *Tetrahedron Lett.* **1991**, *32*, 4175.

(3) Mannich, C. *Chem. Ber.* **1907**, *40*, 153.

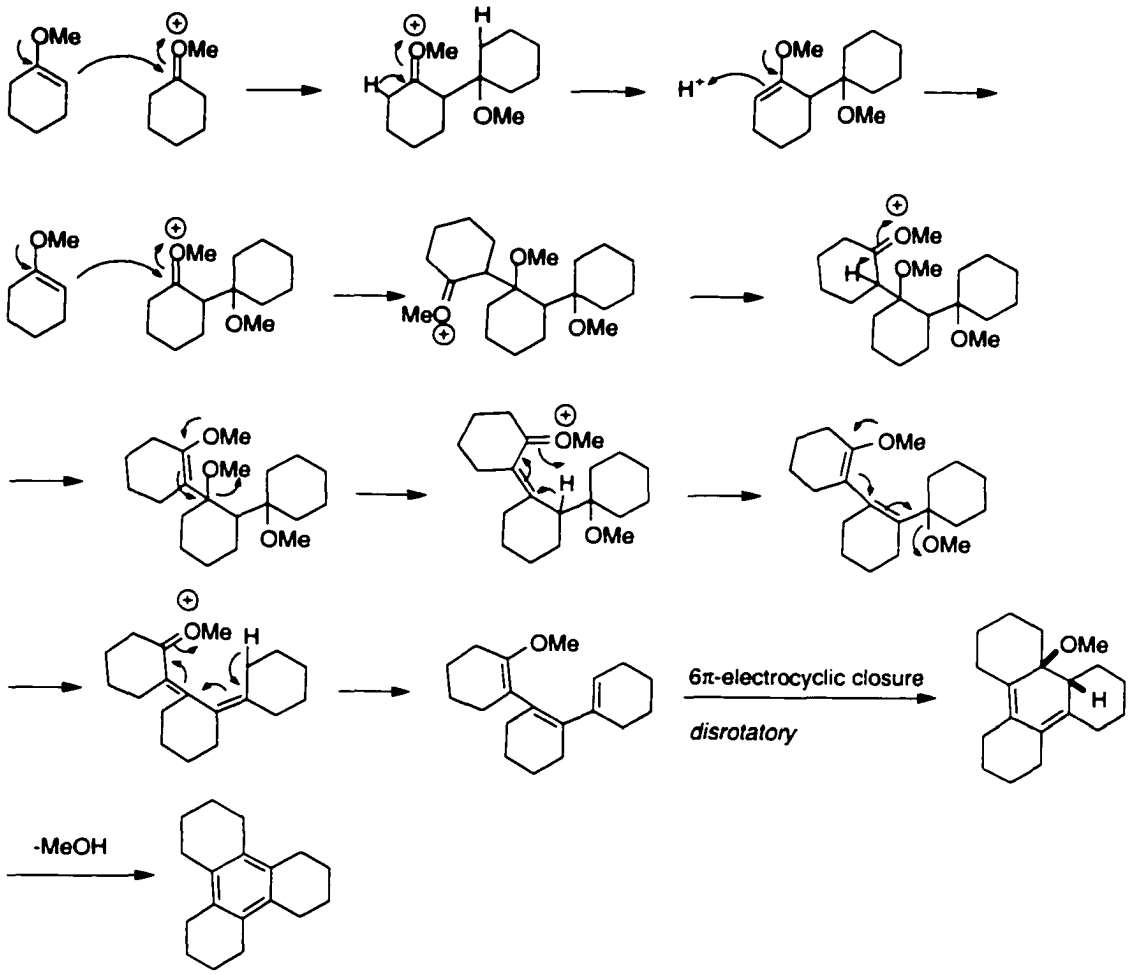

Scheme 5.A. Arrow-pushing mechanism for the formation of dodecahydrotriphenylene from the acid-catalyzed condensation of 1-methoxycyclohexene. We thank Professor Robert M. Williams for his assistance with this mechanism.

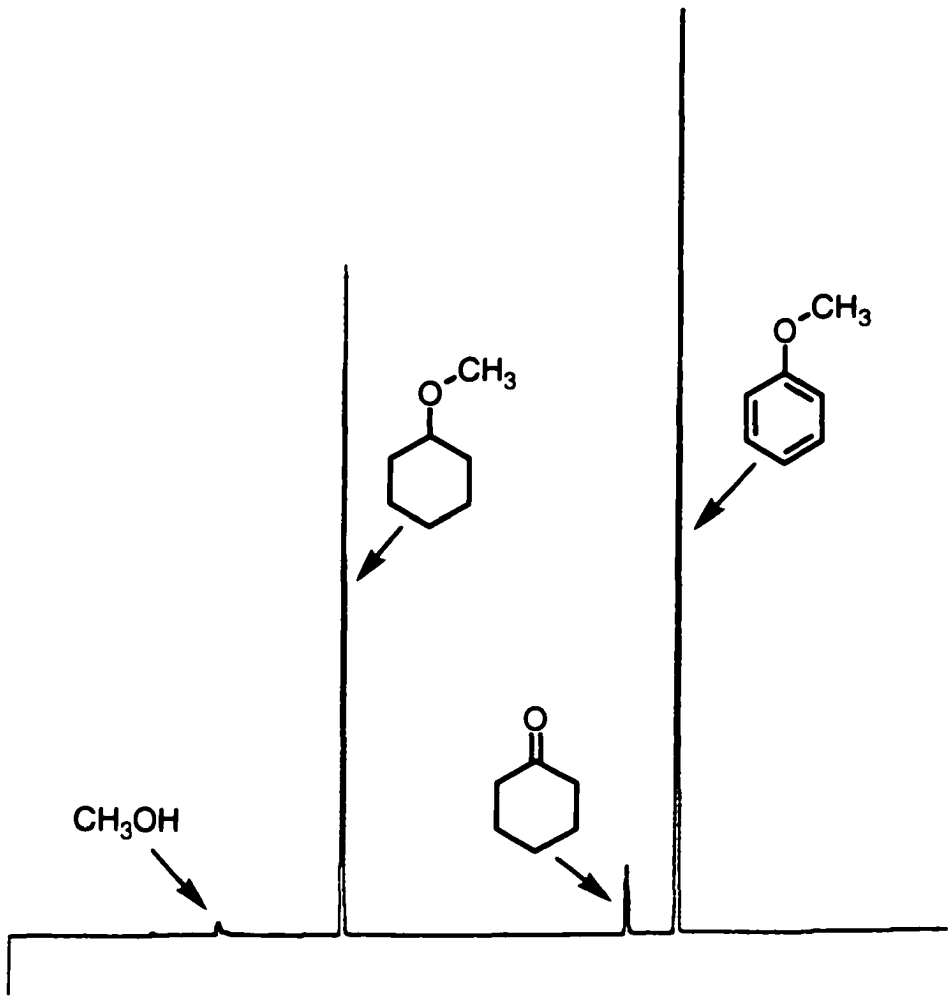

Figure 5.M. The GLC trace of the reaction solution (sampled at 44.3 h) in a total turnovers experiment for anisole hydrogenation with $[Bu_4N]_5Na_3[(1,5\text{-}COD)Rh{\bullet}P_2W_{15}Nb_3O_{62}]$ and with 10 equivs $HBF_4{\bullet}Et_2O$ added (see the main text for further details about this experiment and for the GLC conditions). The GLC trace shows peaks for methanol, methoxycyclohexane, cyclohexanone and anisole (retention times: 3.3, 5.3, 9.8 and 10.6 min). The dodecahydrotriphenylene is not visible using these GLC conditions. Note the absence of a 1-methoxycyclohexene peak.

CHAPTER VI

IS IT HOMOGENEOUS OR HETEROGENEOUS CATALYSIS? IDENTIFICATION OF RUTHENIUM METAL PARTICLES AS THE TRUE CATALYST IN BENZENE HYDROGENATIONS STARTING WITH THE MONOMETALLIC PRECURSOR, $Ru(II)(\eta^6\text{-}C_6Me_6)(OAc)_2$

This dissertation chapter presents a re-investigation of the benzene hydrogenation system based on the monometallic precatalyst, $Ru(II)(\eta^6\text{-}C_6Me_6)(OAc)_2$. The question asked and answered in this chapter is, "is it homogeneous or heterogeneous catalysis?" Compelling kinetic (and other) evidence implicates ruthenium metal particles as the true catalyst in this system. The methods and experiments used for this study are described in Chapter III.

The experiments described in this chapter were performed by J.A.W. The manuscript, which will be submitted to an American Chemical Society journal, was prepared by J.A.W. with assistance and editing (about 10 hours total) by R.G.F. To date, M.A.B.'s (Prof. M. A. Bennett; see page 242) contribution has been to suggest looking at this particular system, and to suggest relatively minor corrections to the manuscript.

Is It Homogeneous or Heterogeneous Catalysis? Identification of Ruthenium Metal Particles as the True Catalyst in Benzene Hydrogenations Starting with the Monometallic Precursor, $Ru(II)(\eta^6\text{-}C_6Me_6)(OAc)_2$

Jason A. Widegren, Martin A. Bennett and Richard G. Finke

Abstract

A reinvestigation of the true catalyst in a benzene hydrogenation system beginning with $Ru(II)(\eta^6\text{-}C_6Me_6)(OAc)_2$ as the precatalyst is reported. Our previously developed, four-step, mechanistic approach is used to answer the question "Is it homogeneous or heterogeneous catalysis?" The key observations leading to the conclusion that the true catalyst is bulk ruthenium metal, and *not* a homogeneous metal complex or a soluble nanocluster, are: (i) the catalytic benzene hydrogenation reaction follows the nucleation ($A \rightarrow B$) and then autocatalytic surface-growth ($A + B \rightarrow 2B$) mechanism recently elucidated for metal(0) nanocluster formation; (ii) bulk ruthenium metal forms from the

nanoclusters during the hydrogenation; (iii) the bulk ruthenium metal is a kinetically competent catalyst; (iv) the soluble nanoclusters aggregate too fast to be kinetically competent catalysts; (v) the addition of Hg(0), a known heterogeneous catalyst poison, completely inhibits further catalysis; and (vi) transmission electron microscopy fails to detect nanoclusters. Overall, the studies presented herein call into question any claim of homogeneous *benzene* hydrogenation with a Ru(arene) precatalyst.

Introduction

The use of transition-metal complexes as precatalysts for reductive processes is widespread. The true catalyst may be a transition-metal complex, *but it can also be a metal film, a metal powder, or a metal nanocluster that forms from the precatalyst under reducing conditions.*[1] In fact, the *in situ* formation of nanoclusters or agglomerated-metal-particle catalysts appears to be common under reducing conditions.[2] However, distinguishing metal-complex homogeneous catalysis from metal-particle heterogeneous catalysis is not trivial; it can be especially difficult to rule out the *in situ* formation of a nanocluster catalyst.[2] Methods for distinguishing homogeneous vs heterogeneous catalysis began to be developed in about 1980 and include contributions from Maitlis,[3] Whitesides,[4] Crabtree,[5,6,7] Collman,[1,8] Lewis,[9,10] and our[11,12] own group. As emphasized elsewhere,[2,5,11] *no single experiment can convincingly determine if the true catalyst in such a system is homogeneous or heterogeneous*; rather, it is necessary to perform a series of experiments, as illustrated in the more general protocol shown in Figure 1.[11] The main features of this protocol are: (1) catalyst isolation and characterization,

especially by initial TEM studies; (2) kinetic studies—a key since catalysis is a wholly kinetic phenomenon[13,14]; (3) quantitative catalyst poisoning experiments; and (4) the perhaps obvious, but still important, concept that the identity of the true catalyst must be consistent with all the data.

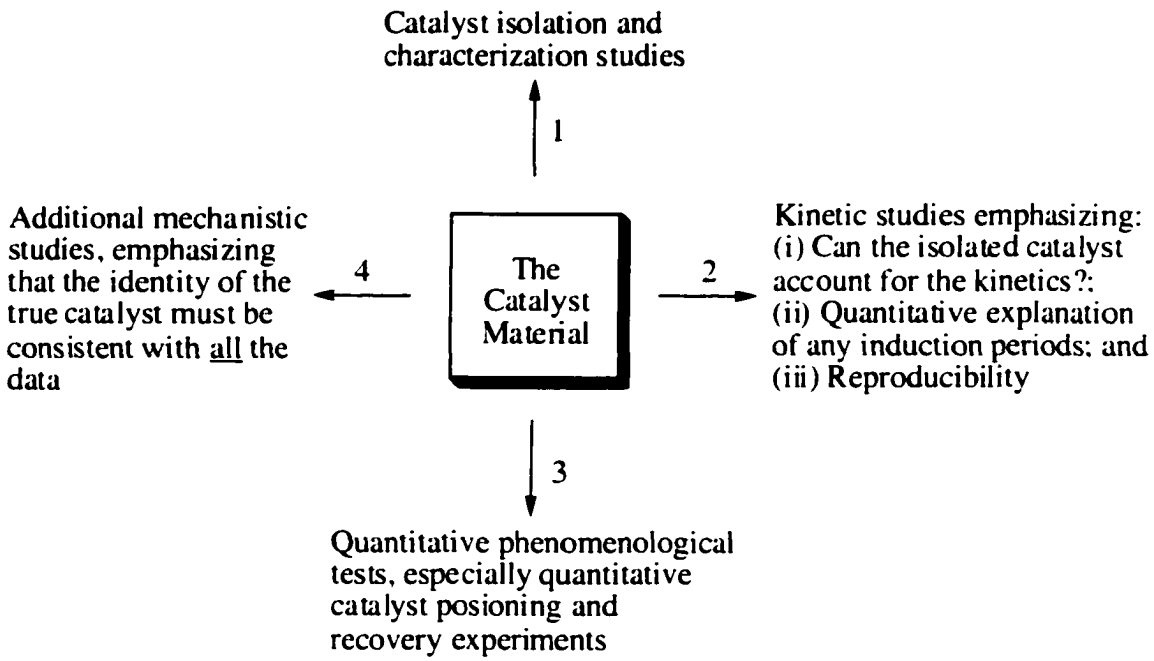

Figure 6.1. The most recent approach to distinguishing between a metal-particle "heterogeneous" catalyst and a metal-complex "homogeneous" catalyst. An expanded version of this approach is available in Figure 5 elsewhere.[11]

The hydrogenation of monocyclic arenes (e.g., benzene) is a difficult reaction to catalyze.[15,16,17] Typically it is accomplished with heterogeneous catalysts of Group VIII metals, such as Rh/Al_2O_3 or Raney nickel.[18] The first *ostensibly* homogeneous benzene hydrogenation catalyst, a Ziegler-type system based on Et_3Al and Ni(II) 2-ethylhexanoate, was reported in 1963;[19] in the intervening ~40 years there have been many more claims of homogeneous, transition-metal complexes capable of monocyclic

arene hydrogenation catalysis.[1,2,20,21] However, (i) there is usually little evidence to support the hypothesis that the true catalyst in these systems is homogeneous; (ii) one claimed "homogeneous" system[22,23] based on $RhCl_3$ and $[(C_8H_{17})_3NCH_3]Cl$ has been shown to be catalyzed by $Rh(0)_n$ nanoclusters that form under the reaction conditions[24]; and (iii) there is some evidence that several other monocyclic arene hydrogenation systems are heterogeneous as well.[2] To our knowledge, the only examples of well-established,[25] monometallic, homogeneous catalysts for benzene hydrogenation are those developed by Rothwell and co-workers based on Nb^V and Ta^V hydrido complexes.[26]

Hence, the question of whether several Ru-complex-based benzene hydrogenation systems[27,28,29,30,31,32,33,34,35,36,37] (see also Table 10.2 and Table S1 elsewhere[1,2]) reported in the literature are truly homogeneous catalysts remains to be answered. We suspect that in many of these systems the true catalyst is either a Ru nanocluster or bulk Ru metal, either of which may be present in only trace amounts, and therefore be hard to detect. Note here the point made elsewhere[11,24] that metal-particle catalysis is the crucial alternative hypothesis,[38] one that must be carefully considered and ruled out, before any claim of a homogeneously catalyzed reaction can be accepted *for which heterogeneous catalysis of the same reaction is well established.*

The goal of present work, which is of significance across the areas of organometallic chemistry,[1,39] nanocluster science,[40,41,42,43,44,45] nanocluster catalysis,[46] and arene hydrogenations,[20] is to answer the following question: what is the true catalyst in benzene hydrogenations beginning with Ru(arene) precatalysts such as $Ru(II)(\eta^6\text{-}C_6Me_6)(OAc)_2$?[21,27,47] One of us (M. A. B.) has been aware of and concerned with the "is it homogeneous or heterogeneous catalysis" issue since the original[27,47] catalytic studies

with Ru(II)(η^6-C_6Me_6)$(OAc)_2$. A telling quote from our earlier work[27] is: "The reduction of benzene to cyclohexane using arene ruthenium(II) catalysts occurs at high hydrogen pressure under a variety of conditions. The homogeneity of these catalytic reactions could not be established unequivocally, and in some cases decomposition to give a heterogeneous component was observed." However, at the time that work was being performed, the methods for answering the "homogeneous or heterogeneous" question were not yet available. Since others of us (R. G. F.) developed a more general approach to the "is it homogeneous or heterogeneous catalysis" question in 1994,[11] we decided to combine forces and see if that methodology would discover the true catalyst in benzene hydrogenations beginning with Ru(II)(η^6-C_6Me_6)$(OAc)_2$.

Herein we present compelling kinetic, transmission electron microscopy (TEM), x-ray photoelectron spectroscopy (XPS), and catalyst poisoning data indicating that the true benzene hydrogenation catalyst when starting with Ru(II)(η^6-C_6Me_6)$(OAc)_2$ is Ru metal. In addition, a heterogeneous catalyst is consistent with data gleaned from the original catalytic studies with Ru(II)(η^6-C_6Me_6)$(OAc)_2$.[27,47] Our demonstration that the true catalyst is not a monometallic Ru complex is relevant to the broader, often vexing question in catalysis of "is the true catalyst homogeneous or heterogeneous?"[2,48] Studies of arene hydrogenation, such as the present work, are of broader current interest due to: (i) the industrial importance of full[49,50] and partial[51,52,53,54] benzene hydrogenation; (ii) the demand for cleaner-burning, low-aromatic-content diesel fuels;[55] and (iii) the chemically demanding problem of hydrogenating aromatic polymers[56,57,58,59,60] such as polystyrene[61] to yield poly(cyclohexylethylene) for DVD disks and other applications.

Results

Benzene Hydrogenation Beginning with the Precatalyst Ru(II)(η^6-C_6Me_6)$(OAc)_2$. The "Standard Conditions" for benzene hydrogenation with the precatalyst Ru(II)(η^6-C_6Me_6)$(OAc)_2$, **1**,[61] in a Parr autoclave are (eq 1): 10.0 mL of benzene, 15.0 mL of 2-propanol, 40 (± 1) mg of **1**, 100 °C, and an initial H_2 pressure of 60 atm. These conditions are taken from the literature,[27,47] except that the temperature is 100 °C vs the literature's 50 °C, for reasons that will become clear in a moment.

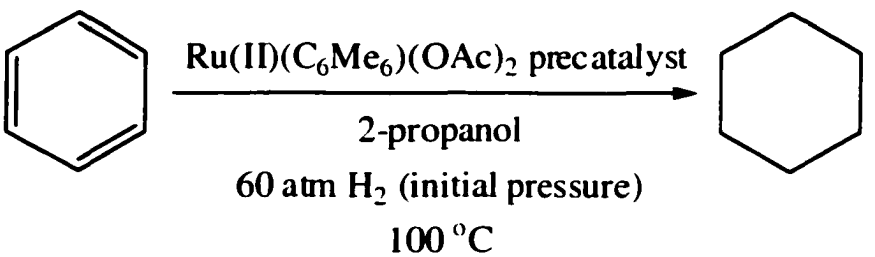

(1)

Catalyst Evolution Kinetic Studies. Figure 2 shows a plot of reaction progress vs time monitored by following the loss of hydrogen pressure vs time. Following a ~3 h induction period, the hydrogenation rate increases rapidly and is complete after a total of ~11 h. The experimental data are well fit to the analytic kinetic equations[65,66] for the pseudoelementary[62,63,64,65,66] steps for *nucleation*, A → B (rate constant k_1), and *autocatalytic surface-growth*, A + B → 2B (rate constant k_2).[65,66] The rate constants determined from the non-linear least squares curve-fit in Figure 2 are $k_1 = 3.1 \times 10^{-3}$ h^{-1} and $k_2 = 2.6 \times 10^{2}$ $M^{-1}h^{-1}$ (the mathematically required correction has been made to k_2 for the stoichiometry factor of 1/100 as described elsewhere,[65,66] but not for the "scaling

factor", that is, for the changing number of Ru atoms on the metal-particle surface[65,66,67]). The experiment shown in Figure 2 was performed a total of six times (by two different researchers), using three different batches of **1** (synthesized by two different researchers). In every case we observed sigmoidal kinetics, as seen in Figure 2. Such a sigmoidal, autocatalytic curve and curve-fit are *prima facie* evidence for the *in situ* formation of a nanocluster catalyst from a soluble transition-metal complex under H_2 given the prior work connecting such kinetics to nanocluster catalyst formation.[2,11,24,65,66,68,69,70,71] Note also that the $A \rightarrow B$ and $A + B \rightarrow 2B$ equations demand, to the precision of the curve-fit, that "A" (i.e., the precatalyst **1**) is *not* the catalyst, as it must first be turned into "B" (i.e., Ru(0) in this case).

An interesting, but not unexpected, observation from the six experiments is that the value of k_1 varies over three orders of magnitude, from 4.8×10^{-1} h^{-1} to 5.4×10^{-4} h^{-1}, yet the value of k_2 varies less than three-fold, from 1.3×10^{2} $M^{-1}h^{-1}$ to 3.7×10^{2} $M^{-1}h^{-1}$. The observation of irreproducible kinetics is consistent with the *in situ* formation of a heterogeneous catalyst.[2] Note that k_1 is the rate constant for nucleation, which is the hardest, most variable part in nanocluster formation reactions due to the potential for homogeneous and heterogeneous nucleation, trace impurities, etc. Even in the best controlled literature case,[11,66,67,68] in which $[Bu_4N]_5Na_3[(1,5\text{-COD})Ir{\bullet}P_2W_{15}Nb_3O_{62}]$ is used as a precursor for $Ir(0)_n$ nanoclusters, the value of k_1 varies by more than an order of magnitude (e.g., the independently determined values of k_1 in references 65 and 66 are 5.6×10^{-4} h^{-1} and 1.0×10^{-2} h^{-1}, respectively). Hence, the kinetic variability observed in benzene hydrogenations with **1** is both expected and precedented for the *in situ* formation

of a heterogeneous catalyst. On the other hand, such kinetic variability is difficult to explain in terms of a homogeneous Ru(arene) complex catalyst.

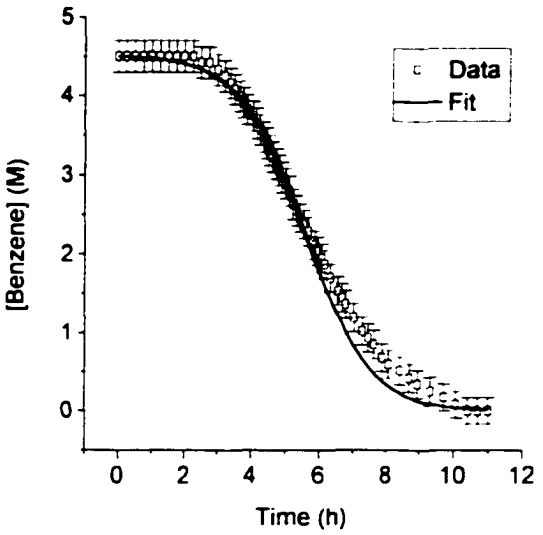

Figure 6.2. Data and curve-fit for a typical benzene hydrogenation experiment at 100 °C with 10 mL of benzene, 15 mL of 2-propanol, 39.8 mg of **1**, and an initial H_2 pressure of 60 atm. Following a ~3 h induction period, the reaction rate increases rapidly and the reaction is complete after a total of ~11 h, that is, a sigmoidal curve typical of slow continuous nucleation, A → B (rate constant k_1), then autocatalytic surface-growth, A + B → 2B (rate constant k_2). The experimental data are well fit to the analytic kinetic equations for these two processes. The rate constants determined from this curve-fit are $k_1 = 3.1 \times 10^{-3}\ h^{-1}$ and $k_2 = 2.6 \times 10^{2}\ M^{-1}h^{-1}$; however, in repeat experiments, k_1 varied over about 3 orders of magnitude and k_2 varied over a factor of ~3 for reasons discussed in the main text. The slight tailing (decreased rate, slower than the prediction of the curve-fit) is probably real due to expected agglomeration to lower surface area, and thus lower reactivity, bulk metal because of the absence of any good nanocluster stabilizer in this system.[70]

Transmission Electron Microscopy (TEM) and X-ray Photoelectron Spectroscopy (XPS) Data. As expected,[27,47] the reaction solution from the Standard Conditions benzene hydrogenation experiment with **1** had changed from yellow-orange to

a dark red-brown, and a dark film coated the glass liner, impeller, and the other parts of the reactor in contact with the reaction solution. Analysis of the red reaction solution by TEM failed to show any soluble nanoclusters; only micrometer-size particles were observed (see Figure S1 of the Supporting Information for an example micrograph).[72] The dark film coating the glass liner, etc., was confirmed to be Ru metal by XPS (see Figure S2 of the Supporting Information).

Testing the Kinetic Competence of the Metallic Film and the Red Reaction Solution. A Standard Conditions benzene hydrogenation experiment was started, and was allowed to proceed to 55% completion (Figure 3, the triangles); the rate of H_2 uptake was 80 psi/h at that point. The reaction was then stopped and the reactor was taken into a nitrogen-atmosphere drybox and opened. The dark-red reaction solution was removed from the reactor and stored in a vial, leaving the dark metallic film in the reactor. Then 10.0 mL of benzene and 15.0 mL of 2-propanol were added to the reactor, and the activity of the metallic film was tested at the normal 100 °C and 60 atm initial H_2 pressure. The benzene hydrogenation proceeded rapidly without a detectable induction period (Figure 3, the squares), showing that the metallic film is indeed an active catalyst for benzene hydrogenation. Additionally, the rate of hydrogen uptake immediately following 55% completion was the same as before, 80 psi/h, *showing that the metallic film is a kinetically competent catalyst*. Similar experiments were performed following two other benzene hydrogenations with **1**, and comparable results were obtained for those experiments as well (i.e., the metallic film hydrogenated benzene rapidly with no detectable induction period).

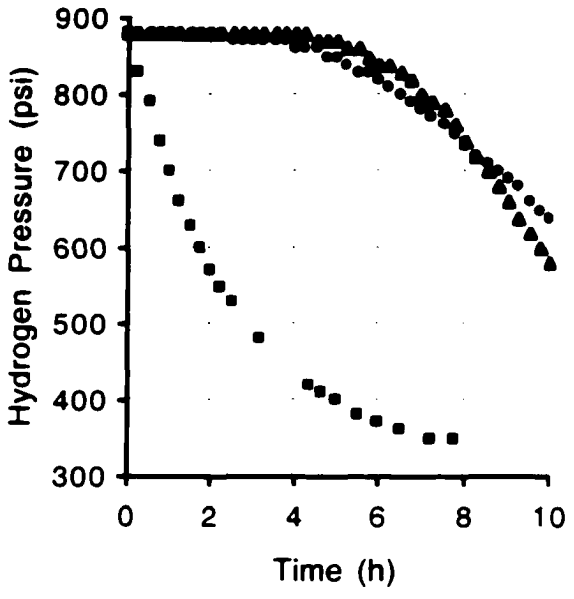

Figure 6.3. Plot of the hydrogen pressure vs time data for three separate benzene hydrogenation reactions. The triangles (Δ) show pressure vs time data for a Standard Conditions hydrogenation starting with **1**; that reaction was stopped after 10 h, at which point it was 55% complete. After the hydrogenation reaction with **1**, the final dark-red reaction solution was separated from the metallic film and, in separate experiments, each was used to catalyze a benzene hydrogenation reaction. The squares (□) show the data for the hydrogenation with the bulk metal, while the circles (O) show the data for the hydrogenation with the dark-red filtrate. With the bulk metal as catalyst, the hydrogenation starts without an induction period and proceeds at a kinetically competent rate. With the dark-red filtrate as catalyst, the hydrogenation begins after an hours-long induction period. These experiments show that within experimental error *all* of the hydrogenation activity observed for this system is due to the bulk metal film.

The catalytic activity of the dark-red reaction solution was also tested. First, 15 mL of the red solution (i.e., two thirds of the final reaction solution from the benzene hydrogenation with **1**) was filtered through a micropore filter to remove any traces of bulk metal. Then 7 mL of benzene and 6 mL of 2-propanol were added[73] and a

hydrogenation reaction was performed at 100 °C and an initial H_2 pressure of 60 atm. Hydrogenation activity was observed only after an induction period of several hours (Figure 3, the circles), similar to the hydrogenation reaction in which **1** was used as the precatalyst. A dark film coated the glass liner and the wetted reactor parts at the end of this reaction. This simplest interpretation of this result is that the soluble Ru complex(es) in the red reaction solution is (are) also just a precursor to a heterogeneous catalyst.

Mercury-poisoning Experiment. The ability of added Hg(0) to poison metal-particle heterogeneous catalysts,[4,74,75] by amalgamating the metal catalyst or adsorbing on its surface, has been known for >80 years[76]; this is the single most widely used test of homogeneous vs heterogeneous catalysis.[2] The suppression of catalysis by Hg(0) is evidence for a heterogeneous catalyst; if Hg(0) does not suppress catalysis, the implication is that the catalysis is homogeneous. The Hg(0)-poisoning experiment is easy to perform, *but is not definitive by itself, and not universally applicable*. Hg(0) is known to react with some single-metal complexes.[4,77,78,79,80] To avoid incomplete poisoning and erroneous conclusions, one must be able to insure intimate contact of the Hg(0) bead with the entire reactor; hence, using a large excess of Hg(0) in a well stirred solution is key.[11,24,81]

A Standard Conditions benzene hydrogenation experiment with **1** was started as described above. After about 30% conversion, the reaction was stopped, ~320 equivs of Hg(0) (vs Ru) were added, and the reaction was then re-started, as shown in Figure 4. The addition of Hg(0) *completely eliminated further catalysis* (i.e., for the next 13 h over which it was monitored). This result is consistent with and strongly supportive of a

heterogeneous catalyst.[2,4,11,24] A control experiment[80] showed that Hg(0) does not react with the precatalyst (see the Supporting Information for details).

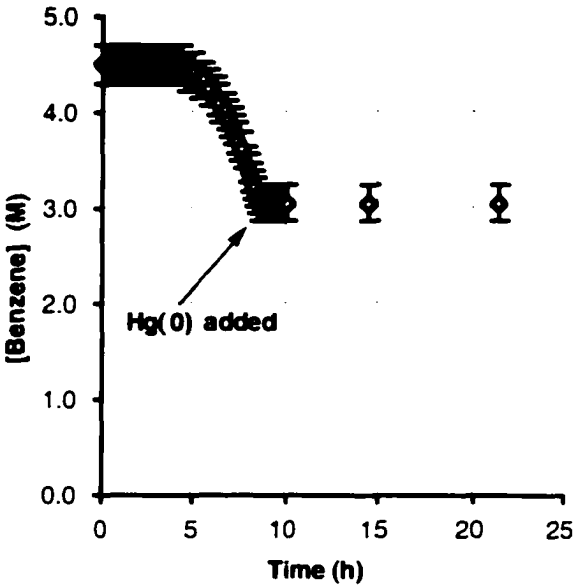

Figure 6.4. Plot of the benzene concentration vs time for a mercury-poisoning experiment. A Standard Conditions benzene hydrogenation with **1** was allowed to proceed for 8.5 h, at which point the benzene hydrogenation was ~30% complete. Then the H_2 pressure was released and 6.61 g of Hg(0) was added (320 equivs vs Ru). The reactor was repressurized with H_2 and the reaction was allowed to continue. However, following addition of the Hg(0), no further benzene hydrogenation catalysis was observed.

Quantitating the Amount of Precatalyst Decomposition by ^{1}H NMR. In order to estimate the amount of Ru metal that forms from **1** during benzene hydrogenation, we used ^{1}H NMR to estimate the amount of free hexamethylbenzene in the reaction solutions. At the end of the experiment shown in Figure 2 about 40% of the precatalyst has been reduced to Ru metal (see the Supporting Information for further details). At the

end of the initial benzene hydrogenation reaction shown in Figure 3 (i.e., a benzene hydrogenation at 55% completion beginning with **1**), <15% of the precatalyst has been reduced to Ru metal. This result illustrates an important logic point: the ability to isolate a large percentage of the precatalyst complex (or some other soluble metal complex) following catalysis is not good evidence for homogeneous catalysis. Such a result *does not rule out the possibility that a small percentage of highly active nanoclusters or bulk metal is responsible for the observed catalysis* (see elsewhere[3,11] for further discussion of this point). In hindsight, the failure to recognize this point in several literature reports[28,29,82,83,84] may have caused misidentification of the true catalyst in those systems.

Benzene Hydrogenation at <<100 °C. For benzene hydrogenations at <<100 °C we observe very long induction periods (i.e., there is no significant nanocluster nucleation at <<100 °C). For example, in a 50 °C experiment (i.e., the exact literature conditions[27,47]), there was no observable activity during 17 h of reaction (as monitored by H_2 pressure and GLC); the reaction solution became dark red, but, significantly, no visible metallic film formed. An experiment at 75 °C also failed to give significant activity during the first 22 h of reaction. However, *after raising the temperature to 100 °C*, both of these benzene hydrogenation reactions went to completion in <12 additional hours and both formed metallic films. The exact difference(s) between our work and the literature work[27,47] is not clear, but there is a high probability that it is in the crucial nucleation step.[65,66] Nucleation did occur at 50 °C in the literature work, but occurs only at higher temperatures in the present work in which we follow strict protocols of reactor cleaning and testing to try to avoid the more facile, lower $\Delta G^{\ddagger}$, heterogeneous nucleation

from trace Ru(0) metal.[85,86] Hence, the most likely explanation for 50 °C vs 100 °C nucleation and growth pathways in the two studies is that a trace amount of metallic Ru was present in the literature reactor, resulting in facile heterogeneous nucleation. It is also possible that our (or the literature's) precatalyst or solvent contains a small amount of some impurity that affects the nucleation step; such effects are well-precedented for H_2O, solvent impurities, etc.[11,65,68] Of note here is that a Standard Conditions benzene hydrogenation with a low-purity batch of precatalyst (74% pure by ^{1}H NMR) yielded a rate constant for nucleation of $k_1 = 4.8 \times 10^{-1}$ h^{-1}, >30 times higher than any of the values of k_1 obtained with 96–97% pure precatalyst. Nevertheless, a benzene hydrogenation experiment at 50 °C (but otherwise Standard Conditions) with the 74% pure precatalyst still had an induction period of >24 hours.

Even though we try to avoid heterogeneous nucleation from trace Ru(0) metal by carefully cleaning the reactor between hydrogenation reactions, we cannot rule out the possibility that nucleation occurs on the glass and monel surfaces of the reactor. In fact, the typically lower $\Delta G^{\ddagger}$ of heterogeneous nucleation,[85] the formation of a metallic film on the wetted parts of the reactor, and the variability in the reaction kinetics all point to heterogeneous nucleation. Interestingly, though, the kinetic curves for benzene hydrogenation with **1** have the same sigmoidal shape that is observed for the *in situ* formation of a transition-metal nanocluster catalyst known to form via *homogeneous* nucleation.[65] This implies (i) that the nucleation in benzene hydrogenations with **1** is actually homogeneous (i.e., occurs in solution), but that the metal eventually plates out on the reactor; (ii) that sigmoidal kinetics are observed for metal-particle formation

regardless of the type of nucleation; or (iii) that the observation of sigmoidal kinetics in the present case is simply coincidental. We favor explanation (ii).

Discussion

We will use the more general approach for distinguishing homogeneous and heterogeneous catalysts, Figure 1, to guide the following discussion. The experiments in the first "prong" of Figure 1, which involve catalyst isolation and characterization and emphasize early use of TEM, are not intended to unequivocally identify the true catalyst: rather, they are intended as scouting experiments to determine if metal particles form under the catalytic conditions. A key point regarding the observation of bulk metal when starting with a single-metal precatalyst: *this demands that nanoclusters were formed en route to the bulk metal*, since there is no other known way to go from a monometallic complex to bulk metal.[11] Hence, in such cases nanoclusters as the true catalyst is the highest priority hypothesis demanding testing.[2] In benzene hydrogenations with **1** as the precatalyst, the *in situ* formation of bulk metal is evidenced by the visible formation of a dark film on the glass liner and the reactor; verification that the film is indeed bulk metal was accomplished using XPS. The formation of nanoclusters is easier to miss because nanocluster solutions may appear homogeneous to the naked eye. Indeed, highly catalytic solutions of well-stabilized nanoclusters will remain completely soluble and apparently "homogeneous".[11,68,69,87] TEM, the single most powerful and broadly applicable method to test for the presence of nanoclusters,[2] failed to detect nanometer-

size particles in the evaporated reaction solution in the present case, however. This is not unexpected: from the literature of colloid/nanocluster stabilization,[70] there is every reason to expect that a Ru nanocluster would not be stable at 100 °C in this system. In addition to the high temperature, good nanocluster stabilizers are not present; carboxylates, such as acetate, have recently been shown to be relatively poor stabilizers.[70] Additionally, in this system the acetate is protonated during the reduction of the precatalyst: H_2 + $Ru(II)(\eta^6\text{-}C_6Me_6)(CH_3COO)_2 \rightarrow Ru(0) + C_6Me_6 + 2CH_3COOH$. Consequently, only acetic acid is present and it is not known nor expected to stabilize nanoclusters.[88]

A relatively small percentage of **1** is reduced to $Ru(0)_n$ in this system (e.g., <15% of the Ru is present as $Ru(0)_n$ at 55% conversion of benzene); however, this is *not* good evidence for homogeneous catalysis, as pointed out earlier. Additionally, the observation of a metallic film demands nanoclusters were formed during the reaction.[11] Hence, soluble Ru complexes, Ru(0) nanoclusters, and bulk Ru(0) metal are all present during the catalytic reaction. To determine which is responsible for the observed catalysis, one must turn to kinetic experiments, which provide the most compelling evidence for the identity of the true catalyst.[89] Three observables containing kinetic information help distinguish homogeneous from heterogeneous catalysis in the present case: (i) the observation of induction periods and sigmoidal kinetics for the catalytic reaction; (ii) the kinetic (ir)reproducibility; and (iii) the testing of any putative catalyst for kinetic competence. If an induction period is observed then the "catalyst" added to the reaction must actually be a *precatalyst* (i.e., the precatalyst, "A", must convert to the catalyst, "B", before catalysis is observed). Any time an induction period is observed in reductive catalysis, one should suspect the *in situ* formation of a heterogeneous catalyst. If the

overall kinetics of a hydrogenation reaction is sigmoidal, and if the kinetics can be fit to the A → B nucleation, and A + B → 2B autocatalytic surface-growth, kinetic scheme that has been previously elucidated for transition-metal nanocluster formation under H_2,[2,11,20,24,65,66,68,69,70,71] that is as compelling a single piece of evidence as exists for the *in situ* formation of a heterogeneous catalyst, at least for hydrogenation catalysis.[2] Note that the curve-fit in Figure 2 is excellent until late in the reaction, where the loss of catalyst surface area due to bulk metal formation, for example, would account for the slower-than-predicted rate.[90,91] Consistent with the *in situ* formation of a heterogeneous catalyst, we observe a great deal of kinetic variability for this catalyst system, especially for the k_1 values, which are a measure of the induction period.[65] As noted earlier, such variability in the induction period is precedented and expected for the *in situ* formation of a heterogeneous catalyst. The experiment shown in Figure 3 demonstrates that the isolated metallic film is a kinetically competent catalyst for the hydrogenation of benzene. On the other hand, the dark-red reaction solution catalyzed benzene hydrogenation only after an induction period; therefore, any soluble species that form during the reaction are simply precursors to the true (heterogeneous) catalyst. Note how, in hindsight, the single kinetic experiment shown in Figure 3 compellingly identifies bulk Ru metal as the true catalyst; hence, we strongly recommend that such an experiment be performed in any catalytic hydrogenation system in which a metallic precipitate forms.

The third prong of the method shown in Figure 1 emphasizes quantitative poisoning studies with CS_2 and other ligand-based poisons.[92] As discussed elsewhere,[2] if one can show that <<1 equivalent of CS_2 completely poisons catalysis, that is compelling evidence for a heterogeneous catalyst because such a result is consistent with the

geometric features of metal-particle heterogeneous catalysis,[93] but difficult to explain for homogeneous catalysis. One limitation of the quantitative CS_2-poisoning experiment is that exothermically binding ligands will dissociate from a metal-particle heterogeneous catalyst at higher temperatures.[94,95,96] Indeed, a control experiment shows that $Rh(0)_n$ nanoclusters, which are completely poisoned by 0.05 equivalents of CS_2 (vs Rh) at 25 °C, are not poisoned *at 100 °C* (see the Supporting Information for the details of that experiment). Hence, we were forced to turn to the more commonly used, but non-quantitative, Hg(0)-poisoning experiment; an excess of Hg(0) must be used, so, in contrast to the CS_2-poisoning experiment, the poison/metal ratio required for complete poisoning does not provide any useful information. However, and consistent with a heterogeneous catalyst, no further catalysis was observed following the addition of ~320 equivalents of Hg(0), Figure 4. A control experiment showed that Hg(0) does not to react with **1** (see the Supporting Information for details), and even though Hg(0) is known to react with some single-metal complexes.[4,77,78,79]

The fourth prong of the method shown in Figure 1 emphasizes the perhaps obvious, but crucial, concept that the identity of the true catalyst must be consistent with all the data.[97] The hypothesis that the true catalyst is bulk Ru metal is consistent with all the data presented herein and with a key observation about the prior literature[27,30,47,83] of arene hydrogenation with Ru(arene) complexes—*visible precatalyst decomposition (to form metallic precipitates, presumably) is commonly observed in the more active systems.*[27,83] In short, only metal-particle heterogeneous catalysis can account for all the observed data.

Summary and Conclusions

We have compelling kinetic (and other) evidence that bulk Ru metal is the true catalyst in the benzene hydrogenation system using Ru(II)(η^6-C_6Me_6)$(OAc)_2$ as the precatalyst. We suspect that the same may be true for other benzene hydrogenation catalysts based on Ru(arene) precatalysts (see the listing of these catalysts in the Introduction),[2] and are testing some of these in separate experiments.[98] The paradigm in Figure 1 does appear to be more generally applicable to the "homogeneous or heterogeneous" problem.

Telltale Indicators of Metal-Particle Heterogeneous Catalysis. The formation of a metal-particle heterogeneous catalyst from a monometallic precatalyst is more likely under certain circumstances. It is important to be familiar with those circumstances so that one can be on the lookout for the telltale signs of heterogeneous catalysis. As discussed in greater detail elsewhere,[2] the conditions under which a heterogeneous catalyst is likely to form include: (i) when easily reduced transition-metal complexes are used as precatalysts; and (ii) when forcing reaction conditions are employed—higher temperatures in particular appear to be thermodynamically conducive to metal-particle formation since the $nM(0)L_x \leftrightarrows M(0)_n + n{\bullet}xL$ equilibrium is probably often endothermic.[2] Heterogeneous catalysis is also favored (iii) when nanocluster stabilizers are present,[70] and is likely (iv) when *monocyclic* arene hydrogenation is observed (with the typically more forcing conditions used for this more difficult reaction). Other telltale signs of heterogeneous catalysis include[2] (v) the formation of dark reaction solutions and metallic

precipitates[99]; and especially (vi) the observation of induction periods and sigmoidal kinetics.[65,66]

The More General Problem of "Is It Homogeneous or Heterogeneous Catalysis?" Although we focus on hydrogenation catalysis in this paper, the problem of distinguishing homogeneous and heterogeneous catalysis is not limited to hydrogenation reactions. *In situ* formation of metal-particle heterogeneous catalysts has also been identified as an issue in hydrosilylation reactions,[9,10,79] ring-opening polymerization catalysis,[100] alkane activation,[101] and C–C coupling reactions.[102] The pervasiveness of the "homogeneous or heterogeneous" problem in catalytic science is further illustrated by the identification of *homogeneous species* as the true catalysts for initially *heterogeneous* oxidation catalysts based on molecular sieves,[103,104] and for carbonylation and Heck coupling catalysts where Pd/C and Pd/Al_2O_3 are the *precatalysts*.[105] Hence, the present work addressing the "is it homogeneous or heterogeneous catalysis" problem is of broader significance.

Lastly, the work herein and a recent review[2] indicate that it is important to use the paradigm in Figure 1 to test a variety of other systems where the *in situ* formation of a heterogeneous catalyst from a homogeneous precatalyst is suspected. A list and brief description of about 30 such systems are available as Table S1 of the Appendix elsewhere.[2]

Experimental

Materials. Benzene (Aldrich, 99.8%, anhydrous, packaged under N_2), 2-propanol (Aldrich, 99.5%, anhydrous, packaged under N_2) and Hg(0) (Aldrich, 99.9995%) were transferred into the glovebox and used as received. Hydrogen gas (General Air, 99.5%) was used as received. Deuterated NMR solvents were purchased from Cambridge Isotope Laboratories, Inc. "Nanopure" water (distilled water filtered through a Barnstead filtration system) was used to wash the reactor between reactions (*vide infra*).

The ruthenium precatalyst complex Ru(II)(η^6-C_6Me_6)$(OAc)_2$, **1**, was prepared (and, unlike the literature, stored) in a nitrogen-atmosphere drybox from [{Ru(η-C_6Me_6)Cl_2}$_2$] and silver acetate (Aldrich, 99%) following literature methods.[31] The [{Ru(η-C_6Me_6)Cl_2}$_2$] was prepared according to the literature procedure[106] from hexamethylbenzene (Aldrich, 99+%, sublimed) and the p-cymene complex [{Ru(η-$C_{10}H_{14}$)Cl_2}$_2$] (Strem, 98%). Three batches of **1** were used for the present study. ^{1}H NMR showed the batches of **1** to be 97% pure, 96% pure, and 74% pure (see Figure S3 of the Supporting Information for the ^{1}H NMR of the 97% pure batch). The 74% pure batch was only used for a repeat benzene hydrogenation experiment; this experiment showed that the presence of impurities from the preparation of **1** have an effect on the kinetics of catalyst formation.[107] The decomposition point of the 97% pure batch of **1** was 163–165 °C, compared to a literature value of 162–165 °C.[31] The literature[31] formulates compound **1** as the monohydrate, [Ru(II)(η^6-C_6Me_6)$(OAc)_2$]•H_2O, based on IR spectra, complete elemental analysis, and ^{1}H NMR. In this paper we have written **1** as the anhydrous compound because we do not observe water by ^{1}H NMR. The absence of a resonance for

water in the ^{1}H NMR does not definitively rule out a hydrate since the water peak is broad and easy to miss,[27] but it is consistent with our strict use of anhydrous conditions for the preparation, handling, and storage of **1**. In any case, the presence or absence of one water of hydration introduces an acceptable weighing error of only ~5%, and the solvent itself contains about one equivalent of water vs Ru in a standard benzene hydrogenation reaction.

Analytical Procedures. Nuclear magnetic resonance (NMR) spectra were obtained at 25 °C on a Varian Inova 300 MHz instrument. Chemical shifts were referenced to the residual proton resonance of the solvent. Spectral parameters for ^{1}H NMR (300 MHz) include: tip angle, 30°; acquisition time, 2.667 s; relaxation delay, 0.0 s; sweep width, 6000 Hz.

X-ray photoelectron spectroscopy (XPS) was performed using a Physical Electronics 5800 spectrometer equipped with a hemispherical analyzer and using monochromatic Al Kα radiation (1486.6 eV, the x-ray tube working at 15 kV and 350 W) and a pass energy of 23.5 eV. An XPS sample was prepared in the following manner. A glass liner that had been used in a benzene hydrogenation reaction was broken with a hammer. A flat piece of the glass liner that was coated with the black film was selected. It was rinsed with acetone and allowed to dry on the bench before being introduced into the instrument.

Two samples for transmission electron microscopy (TEM) were prepared on 300-mesh copper TEM grids with a carbon support film. Following a hydrogenation reaction with precatalyst **1**, the reactor was immediately brought into the glovebox and opened.

The samples were prepared by diluting an aliquot of the dark red-brown reaction solution 30:1 or 180:1 with 2-propanol. A small drop of the diluted solution was placed on a TEM grid and the excess liquid was blotted with a piece of filter paper. The TEM grids were packaged in glass vials and sent to the University of Oregon where TEM analysis was performed as before[65,68] with the expert assistance of Dr. Eric Schabtach. As described previously, micrographs of the nanoclusters were obtained with a Philips CM-12 microscope (with a 2.0 Å point-to-point resolution) operating at 100 KeV.[65,68]

General Procedures for Hydrogenations. All hydrogenation reactions were performed in a Parr pressure reactor (model No. 4561) made of Monel 400 alloy. The reactor is equipped with an automatic temperature controller (±5 °C) and a pressure gauge marked in intervals of 20 psi. Additionally, the bomb head assembly includes a turbine type impeller, a thermocouple, a dip tube for taking liquid samples, and a cooling loop, all four of which contact the reaction solution. A glass liner was used to avoid contacting the reaction solution with the rest of the reactor. The glass liner was dried overnight in a 160 °C drying oven before being transferred into the glovebox while still hot. All catalyst reaction solutions were prepared under oxygen- and moisture-free conditions in a Vacuum Atmospheres glovebox (<2 ppm of O_2 as continuously monitored by a Vacuum Atmospheres O_2-level monitor).

Cleaning the Reactor between Hydrogenation Reactions, and Testing the Residual Hydrogenation Activity of the Reactor Itself. During hydrogenation reactions with precatalyst **1**, deposits of metallic Ru form on the parts of the reactor that

contact the reaction solution (i.e., on the impeller, the thermocouple, the dip tube, and the cooling loop). Because of this, the reactor had to be carefully cleaned between hydrogenation reactions. After each hydrogenation, the metallic film was removed by polishing the reactor with a steel wool pad and soapy water. After polishing, the reactor was rinsed with water, nitric acid, water, and finally acetone (Burdick and Jackson).

Since parts of the reactor become coated with metallic Ru, the reactor itself can have significant hydrogenation activity if not carefully cleaned. Therefore, a control experiment was done each time the reactor was cleaned to insure that any residual activity of the reactor itself was negligible. Specifically, a "blank" hydrogenation, in which no precatalyst was added to the reactor, was performed in the following manner. In the drybox 10.0 mL of benzene and 15.0 mL of 2-propanol were placed in an oven-dried glass liner. The glass liner was sealed in the reactor and the reactor was then removed from the glovebox, equilibrated at 100 °C (while stirring at 600 rpm), and pressurized to 880 psi with H_2 (~60 atm). If the pressure in the reactor decreased by >20 psi within the first 2 h, the reactor was cleaned again and another "blank" hydrogenation performed. In order to keep the residual hydrogenation activity of the reactor at a negligible level, we found it necessary to replace the impeller following each hydrogenation with **1**.

Standard Conditions Benzene Hydrogenation Beginning with the Precatalyst Ru(II)(η^6-C_6Me_6)$(OAc)_2$. In the glovebox 40 (± 1) mg of **1** was transferred into an oven-dried glass liner and dissolved in 10.0 mL of benzene and 15.0 mL of 2-propanol, yielding a clear, yellow-orange solution. The glass liner was sealed in the reactor and the

reactor was then removed from the glovebox, equilibrated at 100 °C (while stirring at 600 rpm), and pressurized to 880 psi with H_2 (~60 atm). Pressurizing the reactor took about 2 minutes, and t = 0 was set once the reactor was fully pressurized. Pressure vs time data were collected by reading the pressure gauge at selected time intervals. Under these conditions complete conversion of benzene to cyclohexane corresponds to a pressure loss of about 550 psi. At the end of each hydrogenation reaction the percent conversion was verified directly by ^{1}H NMR analysis (the NMR sample was prepared by dissolving a drop of the final reaction solution in CD_2Cl_2).

The pressure data were converted to benzene concentration data by a simple proportional relationship: $[\text{benzene}] = [\text{benzene}]_{\text{initial}} \times (\text{pressure} - \text{pressure}_{\text{final}}) / (\text{pressure}_{\text{initial}} - \text{pressure}_{\text{final}})$. This treatment assumes that $\text{pressure}_{\text{final}}$ corresponds to complete conversion of benzene to cyclohexane; this assumption was verified experimentally by ^{1}H NMR (i.e., ≥95% conversion was observed by ^{1}H NMR at the end of the reaction). The error bars shown for the H_2 pressure (or the benzene concentration) assume an error of ±20 psi in the pressure gauge reading and ±5 °C in the temperature control, and probably correspond to the maximum error for this system. Curve-fitting the benzene concentration vs time data was performed as before[66] using the commercial software package Microcal Origin.

Testing the Kinetic Competence of the Metallic Film and of the Red Reaction Solution. A Standard Conditions benzene hydrogenation experiment was started, and was allowed to proceed until the hydrogenation was 55% complete by pressure loss (verified by ^{1}H NMR). At that point the reactor was cooled to room temperature, vented,

brought into the glovebox and opened. The dark-red reaction solution was removed with a pipette, taking care not to remove any of the dark precipitate (this is easy since the "precipitate" is a dark film that adheres to the glass liner and the wetted reactor parts); the dark-red solution was stored in a screw-capped glass vial. Next, 10 mL of benzene and 15 mL of 2-propanol were placed in the precipitate-containing liner. The reactor was resealed, brought out of the glovebox, equilibrated at 100 °C (while stirring at 600 rpm), and pressurized to 880 psi with H_2 (~60 atm). Pressurizing the reactor took about 2 minutes, and t = 0 was set once the reactor was fully pressurized. Pressure vs time data were collected by reading the pressure gauge at selected time intervals.

After cleaning the reactor in the normal way (*vide supra*), the catalytic activity of the dark-red reaction solution was also tested. In the glovebox, 15 mL of the reaction solution was filtered through a disposable nylon syringe filter (0.2 μm pore size) into a clean, oven-dried, glass liner. Then 7 mL of benzene and 6 mL of 2-propanol were added[73] before sealing the glass liner in the reactor. After removing the reactor from the glovebox, it was equilibrated at 100 °C (while stirring at 600 rpm), and pressurized to 880 psi with H_2 (~60 atm). Pressurizing the reactor took about 2 minutes, and t = 0 was set once the reactor was fully pressurized. Pressure vs time data were collected by reading the pressure gauge at selected time intervals.

Mercury-poisoning Experiment. This experiment was started as if it were Standard Conditions benzene hydrogenation experiment (i.e., 40 mg of **1**, 10 mL of benzene, 15 mL of 2-propanol, 100 °C and an initial pressure of 880 psi). Pressure vs time data were collected until the pressure had decreased to 700 psi, at which point the

reaction was about one third complete (complete conversion corresponds to a pressure change of ~550 psi). Then the reactor was cooled to room temperature, vented, taken into the glovebox, and opened. Next, 6.61 g of Hg(0) was added to the dark-red reaction solution (~320 equivs vs Ru). The reactor was then re-sealed, brought out of the glovebox, equilibrated at 100 °C, and stirred for 1.0 h at that temperature to ensure that the Hg(0) had fully contacted the reaction solution and the reactor. Finally, the reactor was pressurized to 700 psi with H_2. At this point, the collection of pressure vs time data was recommenced (ignoring the ~2 h gap required for the poisoning procedure).

Quantitating the Amount of Precatalyst Decomposition by ^{1}H NMR. See the Supporting Information for details.

Control Experiment Showing that Ru(II)(η^6-C_6Me_6)$(OAc)_2$ Does Not React with Hg(0). See the Supporting Information for details.

CS_2-poisoning Experiment. See the Supporting Information for details.

Acknowledgments. The TEM data for this study were expertly obtained by Dr. Eric Schabtach at the University of Oregon's Microscopy Center; it is a pleasure to acknowledge Dr. Schabtach's expertise and continued collaboration. The XPS work was expertly performed by Dr. Sandeep Kohli at the Colorado State University Central Instrument Facility. We thank Dr. Brooks Hornstein and Ms. Lisa Starkey for

experimental assistance. We also thank Mr. Collin Hagen for repeating the Standard Conditions benzene hydrogenation experiment. Financial support was provided by the Department of Energy, Chemical Sciences Division, Office of Basic Energy, grant DOE FG06-089ER13998.

Supporting Information Available: Figure S1, transmission electron micrograph of the evaporated reaction solution following a benzene hydrogenation with the precatalyst Ru(II)(η^6-C_6Me_6)$(OAc)_2$; Figure S2, XPS of the dark film formed during a benzene hydrogenation with the precatalyst Ru(II)(η^6-C_6Me_6)$(OAc)_2$; Figure S3, ^{1}H NMR of the Ru(II)(η^6-C_6Me_6)$(OAc)_2$ precatalyst in $CDCl_3$; details regarding the determination of the extent of precatalyst decomposition during a benzene hydrogenation experiment with Ru(II)(η^6-C_6Me_6)$(OAc)_2$; details regarding the control experiment showing that Ru(II)(η^6-C_6Me_6)$(OAc)_2$ does not react with Hg(0); description of the CS_2-poisoning experiment with $Rh(0)_x$ nanoclusters at 25 and 100 °C.

References:

(1) Collman, J. P.; Hegedus, L. S.; Norton, J. R.; Finke, R. G. *Principles and Applications of Organotransition Metal Chemistry*; University Science Books: Mill Valley, CA, 1987. The uncertainty about the identity of the true catalyst when beginning with several Ru organometallics, Table 10.2, entries F.-I., p. 550, is discussed on p. 555 therein.

(2) Widegren, J. A.; Finke, R. G. A review of the problem of distinguishing true homogeneous catalysis from soluble-metal-particle heterogeneous catalysis under reducing conditions. *J. Mol. Catal. A: Chem.*, submitted. Table S1 of the Appendix lists about 30 catalyst systems for which metal-particle heterogeneous catalysts are suspected, including arene hydrogenation systems with Ru-based precatalysts.

(3) Hamlin, J. E.; Hirai, K.; Millan, A.; Maitlis, P. M. *J. Mol. Catal.* **1980**, *7*, 543.

(4) Whitesides, G. M.; Hackett, M.; Brainard, R. L.; Lavalleye, J. P. P. M.; Sowinski, A. F.; Izumi, A. N.; Moore, S. S.; Brown, D. W.; Staudt, E. M. *Organometallics* **1985**, *4*, 1819.

(5) Anton, D. R.; Crabtree, R. H. *Organometallics* **1983**, *2*, 855.

(6) Crabtree, R. H.; Mellea, M. F.; Mihelcic, J. M.; Quirk, J. M. *J. Am. Chem. Soc.* **1982**, *104*, 107.

(7) Crabtree, R. H.; Mihelcic, J. M.; Quirk, J. M. *J. Am. Chem. Soc.* **1979**, *101*, 7738.

(8) Collman, J. P.; Kosydar, K. M.; Bressan, M.; Lamanna, W.; Garrett, T. *J. Am. Chem. Soc.* **1984**, *106*, 2569.

(9) Lewis, L. N.; Lewis, N. *J. Am. Chem. Soc.* **1986**, *108*, 7228.

(10) Lewis, L. N. *J. Am. Chem. Soc.* **1990**, *112*, 5998.

(11) Lin, Y.; Finke, R. G. *Inorg. Chem.* **1994**, *33*, 4891.

(12) Lin, Y. Ph.D. Dissertation, Department of Chemistry, University of Oregon, March 1994.

(13) Halpern, J. *Inorg. Chim. Acta* **1981**, *50*, 11.

(14) Halpern, J.; Okamoto, T.; Zakhariev, A. *J. Mol. Catal.* **1977**, *2*, 65.

(15) March, J. *Advanced Organic Chemistry: Reactions, Mechanisms, and Structure*, 4th ed.; Wiley-Interscience: New York, 1992; pp. 780.

(16) Stanislaus, A.; Cooper, B. H. *Catal. Rev. – Sci. Eng.* **1994**, *36*, 75.

(17) Fessenden, R. J.; Fessenden, J. S. *Organic Chemistry*, 5th ed.; Brooks/Cole Publishing Company: Pacific Grove, 1993; Chap. 11.

(18) Augustine, R. L. *Heterogeneous Catalysis for the Synthetic Chemist*; Marcel Dekker: New York, 1996; Chap. 17.

(19) Lapporte, S. J.; Schuett, W. R. *J. Org. Chem.* **1963**, *28*, 1947.

(20) Widegren, J. A.; Finke, R. G. A review of soluble transition-metal nanoclusters as arene hydrogenation catalysts. *J. Mol. Catal. A: Chem.*, in press.

(21) Fish, R. H. *Aspects Homogeneous Catal.* **1990**, *7*, 65.

(22) Blum, J.; Amer, I.; Vollhardt, K. P. C.; Schwarz, H.; Hoehne, G. *J. Org. Chem.* **1987**, *52*, 2804.

(23) Blum, J.; Amer, I.; Zoran, A.; Sasson, Y. *Tetrahedron Lett.* **1983**, *24*, 4139.

(24) Weddle, K. S.; Aiken, J. D., III; Finke, R. G. *J. Am. Chem. Soc.* **1998**, *120*, 5653.

(25) The Nb^{V} and Ta^{V} hydrido aryloxide complexes, such as $[Ta\{OC_6H_3(C_6H_{11})_2\text{-}2,6\}_2(H)_3(PMe_2Ph)_2]$, developed by Rothwell and coworkers are well-established examples of monometallic catalysts capable of monocyclic arene hydrogenation based on the following evidence[26]: (i) the reduction of Nb^{V} or Ta^{V} by hydrogen is implausible under the reaction conditions, so that the formation of Nb(0) or Ta(0) metal particles is extremely unlikely; and (ii) the observed selectivity of the catalyst for the intramolecular hydrogenation of the aryloxide ligands is consistent with a homogeneous mononuclear catalyst, but difficult to explain if the true catalyst is heterogeneous (*ortho*-phenyl substituents on the aryloxide ligand are hydrogenated, while hydrogenation of phenyl rings *meta* or *para* to the aryloxide oxygen is not observed nor is hydrogenation of the phenoxide nucleus itself ever observed).

(26) Rothwell, I. P. *Chem. Commun.* **1997**, 1331.

(27) Ennett, J. P. Ph.D. Dissertation, Research School of Chemistry, Australian National University, 1984.

(28) Süss-Fink, G.; Faure, M.; Ward, T. R. *Angew. Chem. Int. Ed.* **2002**, *41*, 99.

(29) Johnson, J. W.; Muetterties, E. L. *J. Am. Chem. Soc.* **1977**, *99*, 7395. These authors specifically state that they were unable to detect free hexamethylbenzene following catalytic reactions. Nevertheless, and even if their (unstated) detection limits for

hexamethylbenzene are low, in the absence of kinetic studies this cannot be used to rule out heterogeneous catalysis.

(30) Bennett, M. A.; Huang, T.-N.; Turney, T. W. *J. Chem. Soc., Chem. Commun.* **1979**, 312.

(31) Tocher, D. A.; Gould, R. O.; Stephenson, T. A.; Bennett, M. A.; Ennett, J. P.; Matheson, T. W.; Sawyer, L.; Shah, V. K. *J. Chem. Soc., Dalton Trans.* **1983**, 1571.

(32) Garcia Fidalgo, E.; Plasseraud, L.; Süss-Fink, G. *J. Mol. Catal. A: Chem.* **1998**, *132*, 5.

(33)Plasseraud, L.; Süss-Fink, G. *J. Organomet. Chem.* **1997**, *539*, 163.

(34) Dyson, P. J.; Ellis, D. J.; Welton, T.; Parker, D. G. *Chem. Commun.* **1999**, 25.

(35) Bennett, M. A.; Ennett, J. P.; Gell, K. I. *J. Organomet. Chem.* **1982**, *233*, C17.

(36)Bennett, M. A.; Ennett, J. P. *Organometallics* **1984**, *3*, 1365.

(37) Cook, J.; Hamlin, J. E.; Nutton, A.; Maitlis, P. M. *J. Chem. Soc., Dalton Trans.* **1981**, 2342.

(38) Platt, J. R. Strong Inference. *Science* **1964**, *146*, 347.

(39) Crabtree, R. H. *The Organometallic Chemistry of Transition Metals*; Wiley & Sons: New York, 2001.

(40) Schmid, G. *Chem. Rev.* **1992**, *92*, 1709.

(41) Lewis, L. N. *Chem. Rev.* **1993**, *93*, 2693.

(42) Bradley, J. S. in *Clusters and Colloids. From Theory to Applications*; Schmid, G., Ed.; VCH: New York, 1994; p. 459-544.

(43) Bönnemann, H.; Braun, G.; Brijoux, W.; Brinkmann, R.; Tilling, A. S.; Seevogel, K.; Siepen, K. *J. Organomet. Chem.* **1996**, *520*, 143-162 and the collection of "key publications" cited as references 2-61 therein.

(44) Schmid, G.; Bäumle, M.; Geerkens, M.; Heim, I.; Osemann, C.; Sawitowski, T. *Chem. Soc. Rev.* **1999**, *28*, 179.

(45) Finke, R. G. in *Metal Nanoparticles: Synthesis, Characterization, and Applications*; Feldheim, D. L. and Foss, C. A., Jr. (Eds.); Marcel Dekker, Inc.: New York, 2001; Chap. 2.

(46) Aiken, J. D., III; Finke, R. G. *J. Mol. Catal. A: Chem.* **1999**, *145*, 1. See references 1-35 therein for additional reviews and introductory references to the interest, uses, and current research problems of nanoclusters and colloids in catalysis and other areas of science.

(47) Bennett, M. A.; Ennett, J. P. *Inorg. Chim. Acta* **1992**, *198-200*, 583.

(48) Sheldon, R. A.; Wallau, M.; Arends, I. W. C. E.; Schuchardt, U. *Acc. Chem. Res.* **1998**, *31*, 485.

(49) Weissermel, K.; Arpe, H.-J. *Industrial Organic Chemistry*; 2nd ed.; VCH: New York, 1993.

(50) Parshall, G. W.; Ittel, S. D. *Homogeneous Catalysis, 2nd Edition. The Applications and Chemistry of Catalysis by Soluble Transition Metal Complexes*; Wiley: New York, 1992.

(51) In *Chem. Engr. (N.Y.)* **1990**, *97* (December 20), 25.

(52) Hu, S.-C.; Chen, Y.-W. *J. Chin. Inst. Chem. Eng.* **1998**, *29*, 387.

(53) Struijk, J.; Moene, R.; Van der Kamp, T.; Scholten, J. J. F. *Appl. Catal., A* **1992**, *89*, 77.

(54) Struijk, J.; D'Angremond, M.; Lucas-De Regt, W. J. M.; Scholten, J. J. F. *Appl. Catal., A* **1992**, *83*, 263.

(55) Stanislaus, A.; Cooper, B. H. *Catal. Rev. - Sci. Eng.* **1994**, *36*, 75.

(56) Hu, T. Q.; James, B. R.; Lee, C. L. *J. Pulp Pap. Sci.* **1997**, *23*, J200.

(57) Hu, T. Q.; James, B. R.; Lee, C. L. *J. Pulp Pap. Sci.* **1997**, *23*, J153.

(58) Hu, T. Q.; James, B. R.; Wang, Y. *J. Pulp Pap. Sci.* **1999**, *25*, 312.

(59) Hu, T. Q.; James, B. R. *J. Pulp Pap. Sci.* **2000**, *26*, 173.

(60) Tullo, A. New DVDs Provide Opportunities for Polymers. In *Chemical and Engineering News*, **1999**, *77*, 14.

(61) Unlike the literature,[31] we formulate **1** as the anhydrous complex. The justification for this is that **1** is synthesized *and stored* in a drybox, and because we have no evidence for waters of hydration. See further comments in the Materials section.

(62) Noyes, R. M.; Field, R. J. *Acc. Chem. Res.* **1977**, *10*, 273.

(63) Field, R. J.; Noyes, R. M. *Acc. Chem. Res.* **1977**, *10*, 214.

(64) Field, R. J.; Noyes, R. M. *Nature* **1972**, *237*, 390.

(65) Watzky, M. A.; Finke, R. G. *J. Am. Chem. Soc.* **1997**, *119*, 10382.

(66) Widegren, J. A.; Aiken, J. D., III; Özkar, S.; Finke, R. G. *Chem. Mater.* **2001**, *13*, 312.

(67) Watzky, M. A.; Finke, R. G. *Chem. Mater.* **1997**, *9*, 3083.

(68) Lin, Y.; Finke, R. G. *J. Am. Chem. Soc.* **1994**, *116*, 8335.

(69) Aiken, J. D., III; Finke, R. G. *Chem. Mater.* **1999**, *11*, 1035.

(70) Özkar, S.; Finke, R. G. *J. Am. Chem. Soc.* **2002**, *124*, 5796.

(71) Özkar, S.; Finke, R. G., Hydrogenphosphate as a Simple, Effective and Readily Available Stabilizer for Transition-Metal Nanoclusters: Hydrogenphosphate- and Tetrabutylammonium-Stabilized, Isolable and Redissolvable Iridium(0) Nanoclusters. Manuscript in preparation.

(72) Rigorously, TEM cannot be used to rule out the presence of a nanocluster catalyst; however, the absence of nanometer-size particles in these micrographs is supporting evidence that nanocluster catalysis is not important in this system.

(73) We chose to add 7 mL of benzene and 6 mL of 2-propanol because this gives a reaction solution that closely approximates the initial reaction solution in a Standard Conditions benzene hydrogenation experiment. Specifically, the reaction solution for this experiment contains ~15 mL of 2-propanol, ~10 mL of benzene, and ~3 mL of cyclohexane (i.e., the same as a Standard Conditions benzene hydrogenation experiment, except for the presence of ~3 mL of cyclohexane). The volumes are approximate because, among other things, they assume exactly 50% conversion in the benzene hydrogenation reaction with **1**, and they assume that there is no volume change associated with the conversion of benzene to cyclohexane. The volume of the initial reaction solution for this experiment is 28 mL, instead of the normal 25 mL. This only changes the headspace in the (300-mL) reactor by ~1%, so no correction was made to H_2 pressure uptake curve shown in Figure 3.

(74) The Hg(0)-poisoning experiment is occasionally performed improperly. In one literature example[28] a solution of precatalyst was stirred with Hg(0) for 1 h, the solution was filtered, and a catalytic hydrogenation reaction was then started. The hydrogenation proceeded with the same catalytic activity as an experiment in which Hg(0) was never

present, and this was used (erroneously) to rule out the presence of a nanocluster catalyst. The problem with this experiment is that the Hg(0) was removed by filtration *before the catalytic reaction was allowed to start* (i.e., before a metal-particle heterogeneous catalyst could have formed). As performed, the experiment only shows that the precatalyst does not react with Hg(0), which is a nice control experiment, but not quite to the point. The Hg(0) should have remained in the reaction solution for the duration of the catalytic reaction or added after the catalytic reaction had already begun, as done elsewhere.[11,24]

(75) For a hydrogenation reaction, the following protocol is recommended. Allow the catalytic hydrogenation reaction to proceed to ~50% completion, release the H_2 pressure, add the (excess of) Hg(0) to the reaction solution, let the reaction solution stir so that the Hg(0) has a chance to contact any and all metal particles that may be present, re-pressurize the reactor with H_2, and then check for catalytic activity.[11,24]

(76) Paal, C.; Hartmann, W. *Chem. Ber.* **1918**, *51*, 711.

(77) van Asselt, R.; Elsevier, C. J. *J. Mol. Catal.* **1991**, *65*, L13.

(78) Jones, R. A.; Real, F. M.; Wilkinson, G.; Galas, A. M. R.; Hursthouse, M. B. *J. Chem. Soc., Dalton Trans.* **1981**, 126.

(79) Stein, J.; Lewis, L. N.; Gao, Y.; Scott, R. A. *J. Am. Chem. Soc.* **1999**, *121*, 3693.

(80) Hg(0) is probably most effective in poisoning metals that form an amalgam, such as Pt, Pd and Ni; metals that do not form amalgams with Hg(0), such as Ir, Rh and Ru are probably more difficult to poison with Hg(0).[4] Hence, if the addition of Hg(0) to the reaction solution suppresses the catalytic activity, one should perform a control experiment showing that the precatalyst complex does not react with Hg(0); if Hg(0) does react with the precatalyst, then this test becomes ambiguous. Similarly, if the addition of Hg(0) to the reaction solution has little effect on the catalytic activity, one should perform a control experiment showing that an authentic heterogeneous catalyst of the same metal *is* poisoned under the same conditions.

(81) As evidence for this statement, experiments show that a large excess of Hg(0) is necessary to poison completely an authentic Rh(0)$_n$ nanocluster.[11,24] Hence, an improperly performed poisoning experiment (i.e., one in which a large excess of Hg(0) is not used) can lead to incorrect conclusions about the nature of the catalyst.

(82) Muetterties, E. L.; Bleeke, J. R. *Acc. Chem. Res.* **1979**, *12*, 324.

(83) Bennett, M. A.; Huang, T.-N.; Smith, A. K.; Turney, T. W. *J. Chem. Soc., Chem. Commun.* **1978**, 582.

(84) Bergbreiter, D. E.; Chandran, R. *J. Am. Chem. Soc.* **1987**, *109*, 174.

(85) Strey, R.; Wagner, P. E.; Viisanen, Y. *J. Phys. Chem.* **1994**, *98*, 7748.

(86) Yu, H.; Gibbons, P. C.; Kelton, K. F.; Buhro, W. E. *J. Am. Chem. Soc.* **2001**, *123*, 9198.

(87) Aiken III, J. D.; Finke, R. G. *J. Am. Chem. Soc.* **1999**, *121*, 8803.

(88) Özkar, S.; Finke, R. G., manuscript in preparation.

(89) TEM and XPS illustrate this point. Neither of these techniques provides any kinetic information and, therefore, neither can compellingly identify the true catalyst.

(90) The curve-fit is easily within experimental error of the data for at least the first half of the benzene hydrogenation reaction. However, at longer times the hydrogenation is slower than predicted by the curve-fit. Deviations between the curve-fit and the data near the end of the reaction can occur for a variety of reasons. For example, the pseudo-elementary step method[65,66] used herein assumes that the catalytic reaction is zero order in substrate. Obviously, at some point later in the reaction, when the substrate concentration approaches zero, this assumption is no longer true. Also, any deactivation process that occurs to a significant extent on the timescale of the experiment will cause deviations like those seen in Figure 2. For example, a loss of catalyst surface area due to (observed) bulk metal formation will cause the reaction to be slower than predicted.[91] For these reasons, only the first half of the data in Figure 2 was used to generate the curve-fit—a precaution we typically employ.[65,66]

(91) Hornstein, B. J.; Finke, R. G., unpublished results.

(92) Hornstein, B. J.; Aiken III, J. D.; Finke, R. G. *Inorg. Chem.* **2002**, *41*, 1625.

(93) For metal-particle heterogeneous catalysts, <<1 equiv of a ligand-based poison like CS_2 is needed to completely inhibit catalysis. For example, 3.5 mol% CS_2 completely poisons a commercial Rh/Al_2O_3 catalyst with an average metal-particle diameter of about 3.6 nm.[92] Geometry is the primary reason that so little poison is needed—only about 1/3 of the metal atoms are on the surface of a metal particle this size, and multiple adjacent surface atoms can be poisoned by a single molecule of poison.[92]

(94) Gonzalez-Tejuca, L.; Aika, K.; Namba, S.; Turkevich, J. *J. Phys. Chem.* **1977**, *81*, 1399.

(95) Frety, R.; Da Silva, P. N.; Guenin, M. *Catal. Lett.* **1989**, *3*, 9.

(96) Butt, J.B. *Catal. Sci. Technol.* **1987**, *6*, 1.

(97) In the past, the absence of H–D scrambling and the formation of all-*cis*-$C_6H_6D_6$ from C_6H_6/D_2 or C_6D_6/H_2 have been taken as strong supporting evidence for a homogeneous process.[82] Nevertheless, with some putatively homogeneous catalysts for monocyclic arene hydrogenation, such as [Ru(η^6-C_6Me_6)(η^4-C_6Me_6)], H–D scrambling does occur.[29] Previously, we obtained good evidence for the formation of all-*cis*-$C_6H_6D_6$ with **1** as the precatalyst.[27] Nevertheless, all the evidence herein points to a heterogeneous catalyst. Clearly, further study of H–D scrambling in monocyclic arene hydrogenation, using systems in which the nature of the true catalyst has been unequivocally determined, is needed.

(98) Hagen, C.; Finke, R. G., experiments in progress.

(99) One should suspect heterogeneous catalysis even if the metallic precipitate is inactive because the following process may be occurring: monometallic precursor (inactive) → high-surface-area nanocluster (active) → low-surface-area bulk metal (low activity to inactive). Note that $M(0)_n$ nanoclusters are the only precedented—*and arguably the only possible*—intermediate between a monometallic precursor and bulk metal, so the observation of bulk metal in a reaction beginning with a single metal catalyst demands that one seriously consider nanoclusters as the true catalyst of that reaction.

(100) Temple, K.; Jäkle, F.; Sheridan, J. B.; Manners, I. *J. Am. Chem. Soc.* **2001**, *123*, 1355.

(101) Crabtree, R. H. *Chem. Rev.* **1985**, *85*, 245.

(102) Reetz, M. T.; Westermann, E. *Angew. Chem., Int. Ed.* **2000**, *39*, 165.

(103) Sheldon, R. A.; Wallau, M.; Arends, I. W. C. E.; Schuchardt, U. *Acc. Chem. Res.* **1998**, *31*, 485.

(104) Arends, I. W. C. E.; Sheldon, R. A. *Appl. Catal., A* **2001**, *212*, 175.

(105) Davies, I. W.; Matty, L.; Hughes, D. L.; Reider, P. J. *J. Am. Chem. Soc.* **2001**, *123*, 10139.

(106) Bennett, M. A.; Huang, T. N.; Matheson, T. W.; Smith, A. K. *Inorg. Synth.* **1982**, *21*, 74.

(107) The rate constants for nucleation, k_1, and autocatalytic surface-growth, k_2, for this less-pure batch of precatalyst were $k_1 = 4.8 \times 10^{-1}$ h^{-1} and $k_2 = 3.7 \times 10^{2}$ M^{-1}h^{-1}. For comparison, in 5 experiments with 96–97% pure precatalyst the values of k_1 ranged from 1.6×10^{-2} h^{-1} to 5.4×10^{-4} h^{-1} and the values of k_2 ranged from 1.3×10^{2} M^{-1}h^{-1} to 2.6×10^{2} M^{-1}h^{-1}.

SUPPORTING INFORMATION

Is It Homogeneous or Heterogeneous Catalysis? Identification of Ruthenium Metal Particles as the True Catalyst in Benzene Hydrogenations Starting with the Monometallic Precursor, $Ru(II)(\eta^6\text{-}C_6Me_6)(OAc)_2$

Jason A. Widegren and Richard G. Finke

Figure 6.A. Transmission electron micrograph of the evaporated reaction solution following a benzene hydrogenation with Ru(II)(η^6-C_6Me_6)$(OAc)_2$. This image, which is representative of several that were taken, shows a particle that is about 1 μm in diameter. Particles in the nanometer size range were not observed in these images.

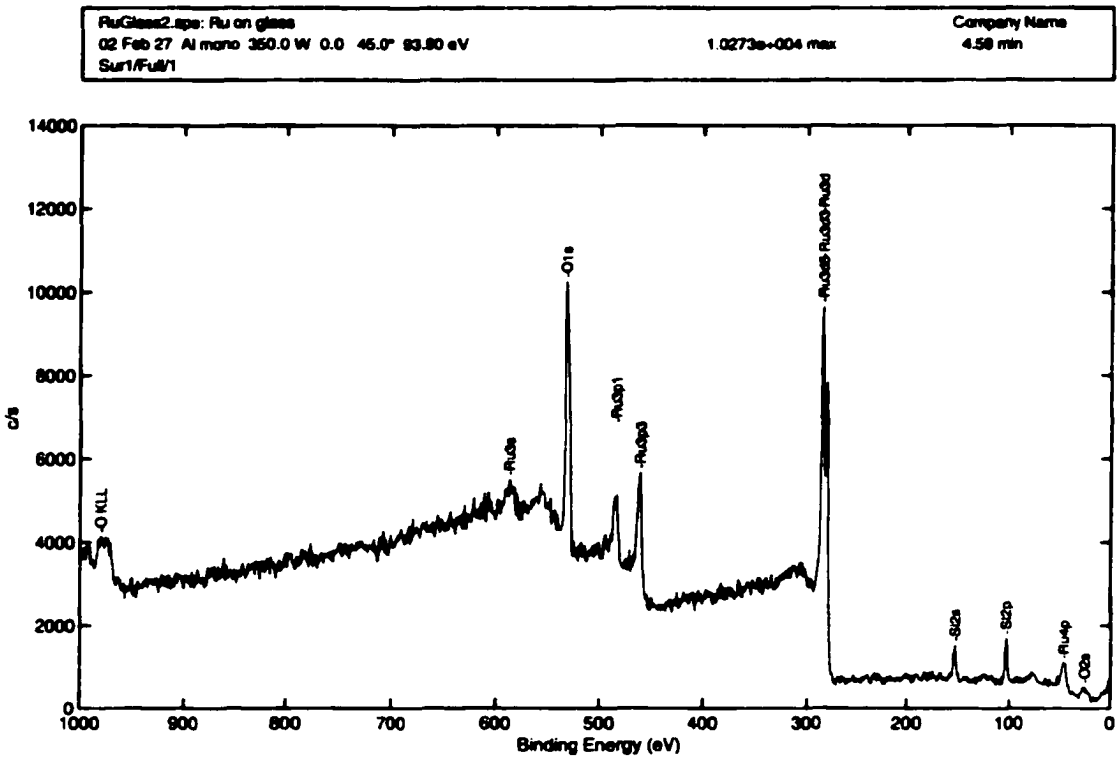

Figure 6.B. XPS of the dark film that forms during benzene hydrogenations with the precatalyst Ru(II)(η^6-C_6Me_6)$(OAc)_2$. During the hydrogenation reaction the glass liner in the reactor becomes coated with dark film; a piece of the precipitate-coated glass liner was rinsed with acetone and used as the XPS sample. Other than silicon and oxygen (from the glass), ruthenium is the only element visible in this survey scan, demonstrating that the precipitate is bulk Ru metal.

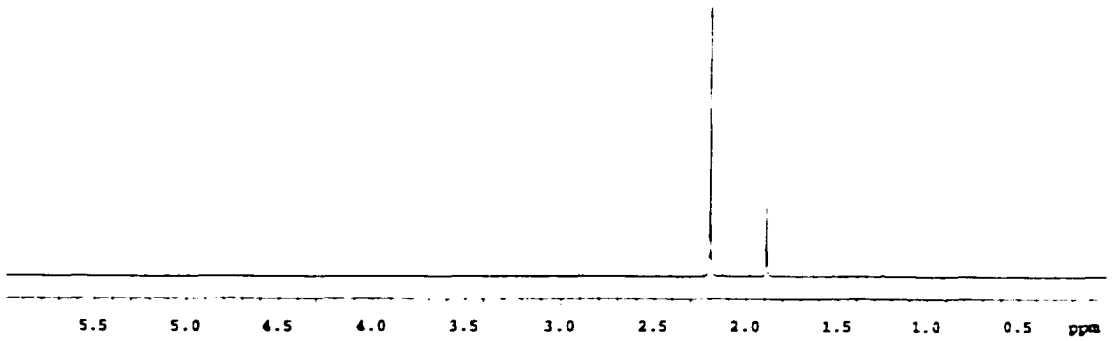

Figure 6.C. ^{1}H NMR of the Ru(II)(η^6-C_6Me_6)$(OAc)_2$ precatalyst in $CDCl_3$. The spectrum is referenced to the residual proton resonance of the solvent at δ 7.27. The peaks at δ 2.2 (singlet, integral = 18.0) and δ 1.9 (singlet, integral = 5.6) correspond to the hexamethylbenzene ligand and the acetate ligands, respectively. This spectrum indicates a purity of 97%.

Determination of the Extent of Precatalyst Decomposition During a Benzene Hydrogenation Experiment with Ru(II)(η^6-C_6Me_6)$(OAc)_2$

A dark-red reaction solution and a metallic film form during the hydrogenation of benzene with the precatalyst Ru(II)(η^6-C_6Me_6)$(OAc)_2$, **1**. To determine the amount of amount of precatalyst decomposition to bulk metal, we quantitated the amount of free (i.e., unbound) hexamethylbenzene in the final reaction solution by ^{1}H NMR. In this experiment, 5 mL of the dark-red reaction solution was evacuated to dryness. The residue was dissolved in 1 g of CD_2Cl_2 and analyzed by ^{1}H NMR. The hexamethylbenzene region of the ^{1}H NMR spectrum is shown below. The peak at δ 2.20 was verified as free hexamethylbenzene by spiking the sample. The peak at δ 2.20 accounts for about 40% of the total integral in this region; hence, we estimate that ~40% of the precatalyst decomposed during the benzene hydrogenation reaction.

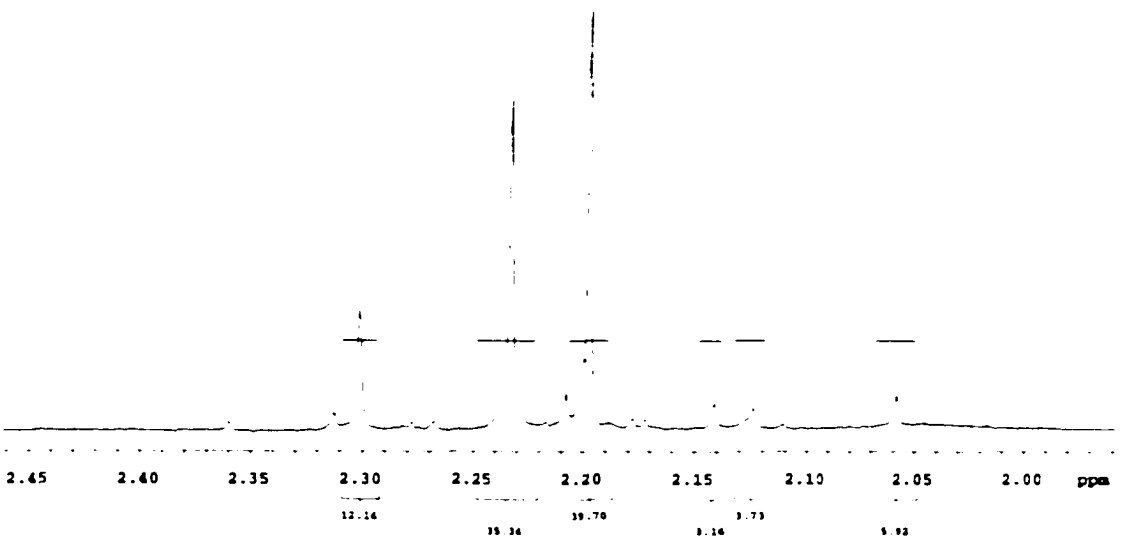

The above experiment assumes that hexamethylbenzene is not hydrogenated during the decomposition of **1**. This assumption was verified experimentally in the following way. We first evaporated to dryness an aliquot of the reaction solution. The residue was dissolved in pentane and analyzed by GC-MS; the GC trace from this experiment is shown below. The peak at about 11.5 min was identified as

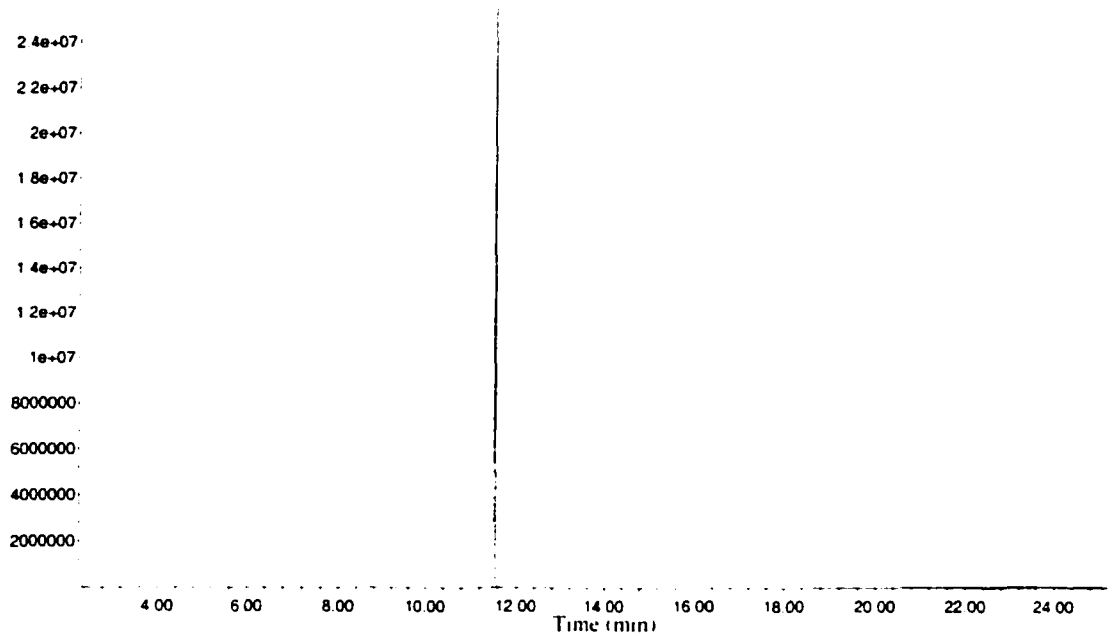

hexamethylbenzene by the MS. No other peaks are visible in the GC trace, which means that the hexamethylbenzene ligand is not hydrogenated to a significant extent during the decomposition of **1** (the solvent peak is not seen because the first 2 min of the GC trace are not shown). Unfortunately, GC could not reliably quantitate the amount of free hexamethylbenzene because the precatalyst complex **1** was found to decompose on the injector port of the GC. That is, a hexamethylbenzene peak is seen by GC even when a solution of pure precatalyst is injected (e.g., about one third of **1** decomposes on the

injector port at a temperature of 275 °C). Nevertheless, the quantitation of free hexamethylbenzene is simplified by the fact that it is not appreciably hydrogenated during the decomposition of **1**.

Control Experiment Showing that Ru(II)(η^6-C_6Me_6)$(OAc)_2$ Does Not React with Hg(0)

In a glovebox a Standard Conditions (see main text) reaction solution was prepared from 39.5 mg of Ru(II)(η^6-C_6Me_6)$(OAc)_2$, 10.0 mL of benzene, and 15.0 mL of 2-propanol. Then 7 mL of the resultant yellow-orange solution was placed in an o-ring-sealed pressure bottle. The rest was placed in a second o-ring-sealed pressure bottle with 4.45 g of Hg(0) (~300 equivalents vs Ru). Both solutions were vortex-stirred in the glovebox at room temperature for 1 hour; neither solution changed in appearance during this time. The stirring was then stopped and a 3-mL aliquot was removed from each solution. Each sample was evacuated to dryness, redissolved in CD_2Cl_2, and analyzed by ^1H NMR; spectrum (a) below shows the sample that was stirred with Hg(0), and spectrum (b) shows the control sample with no Hg(0) present. There is no significant difference between the two spectra, showing that Hg(0) does not react with Ru(II)(η^6-C_6Me_6)$(OAc)_2$ at room temperature.

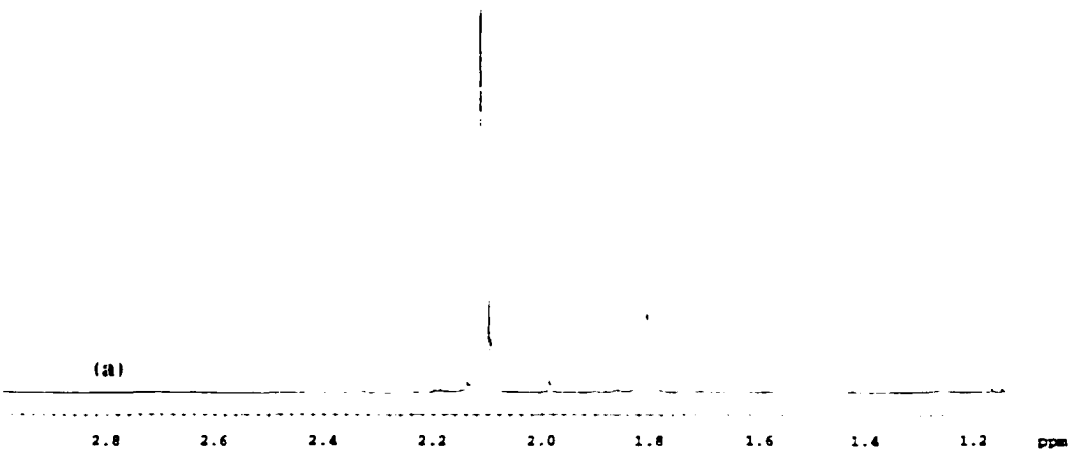

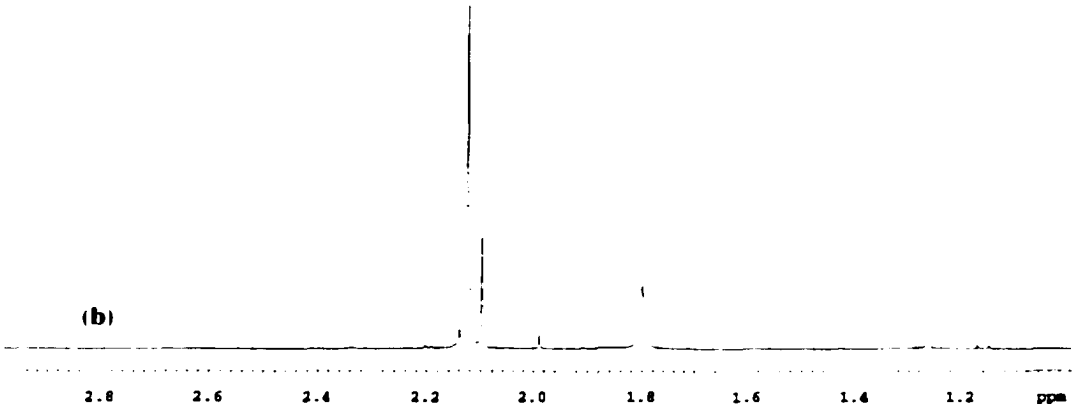

The two sealed pressure bottles were then removed from the glovebox, placed in a 100 °C oil bath, and vortex-stirred for 1 hour. At the end of this period both solutions had changed from yellow-orange to a deep orange (the two samples were visually indistinguishable). The pressure bottles were then taken into the glovebox and opened. Again, 3-mL aliquots were removed from each solution. Each sample was evacuated to dryness, redissolved in CD_2Cl_2, and analyzed by ^1H NMR; spectrum (c) below shows the sample that was stirred with Hg(0), and spectrum (d) shows the control sample with no Hg(0) present. These spectra show that the Ru(II)(η^6-C_6Me_6)$(OAc)_2$ is not stable at 100 °C under these conditions. Nevertheless, there is little difference between the two spectra, showing that Hg(0) does not react with Ru(II)(η^6-C_6Me_6)$(OAc)_2$ at 100 °C.

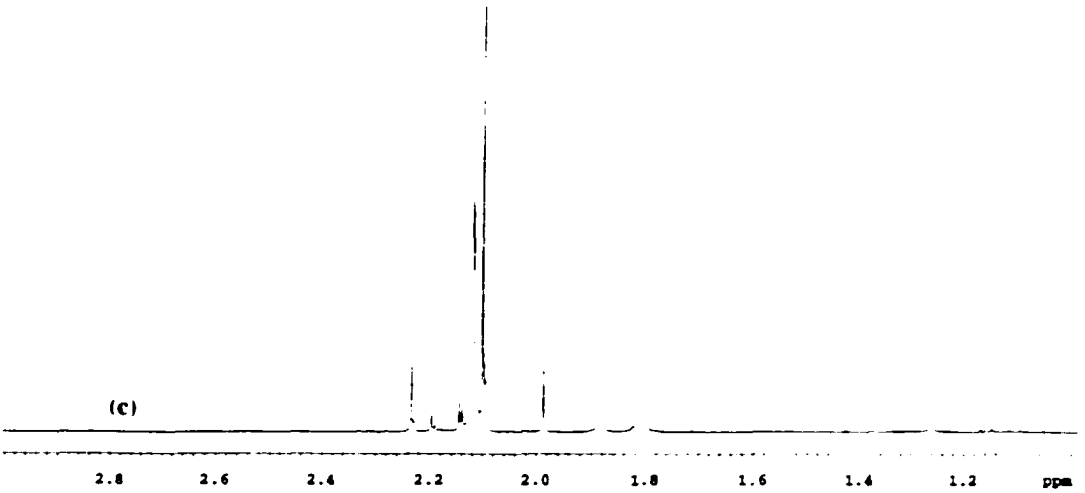

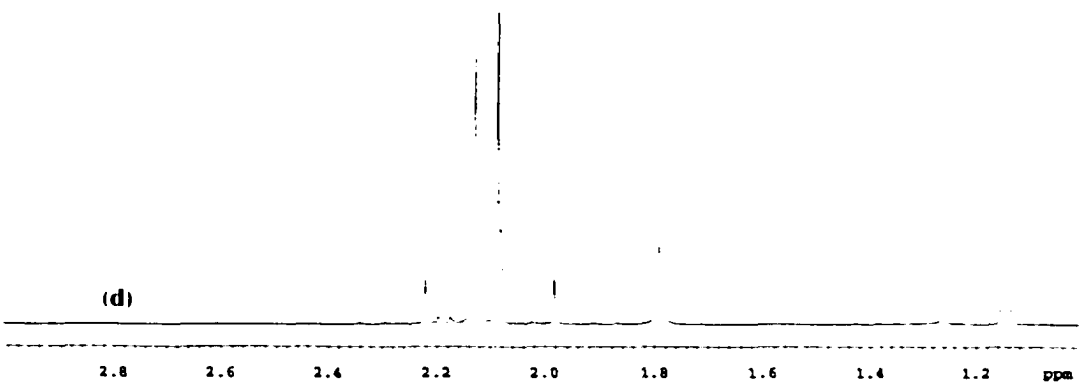

CS_2-Poisoning Experiment with $Rh(0)_x$ Nanoclusters at 25 and 100 °C

Though underutilized, quantitative poisoning experiments using added ligands, such as CS_2, PPh_3, and thiophene, can be very useful for answering the question "Is it homogeneous or heterogeneous catalysis?"[1,2,3,4,5] These poisons bind strongly to metal centers, thereby blocking access of the substrate to the active site. If a catalyst can be poisoned completely with <<1.0 equivalent of the added ligand (per metal atom), that is compelling (kinetic) evidence for a metal-particle heterogeneous catalyst. The logic here is that in a metal-particle catalyst only a fraction of the metal atoms are on the surface; hence, even if every surface atom is active, <<1.0 equivalent of ligand will be sufficient to poison the catalyst.[6] On the other hand, typically ≥1.0 equivalent of ligand is required to completely poison monometallic homogeneous catalysts.[7] See elsewhere[1,2,3] for prototypical examples of this powerful but underutilized "fractional poisoning" experiment. One limitation of this experiment, however, is that it will not work properly at higher temperatures because ligands such as CS_2 will dissociate from a metal-particle catalyst under such conditions.[8,9,10] Because of this limitation we performed a control experiment using a known metal-particle catalyst to see if CS_2 is an effective poison at 100 °C.

We chose polyoxoanion- and tetrabutylammonium-stabilized $Rh(0)_x$ nanoclusters as the metal-particle catalyst to study because of a recent report in the literature where such nanoclusters were poisoned with CS_2 at 25 °C.[3,11] The $Rh(0)_x$ nanoclusters were synthesized under inert atmosphere according to the literature.[3] Briefly, 20.5 mg of $[Bu_4N]_5Na_3[(1,5\text{-COD})Rh{\bullet}P_2W_{15}Nb_3O_{62}$ was dissolved in 2.5 mL of acetone and 0.5 mL

of cyclohexene. This solution was stirred for 19 h at 22 °C under 3.7 atm of H_2. The final dark reaction solution was diluted to 25 mL with acetone.

The cyclohexene hydrogenation activity of the *unpoisoned* $Rh(0)_x$ nanoclusters was then determined. In the glovebox, 9 mL of the nanocluster solution was added to 10 mL of cyclohexene and 6 mL of acetone. This solution was transferred into an oven-dried glass liner and sealed in the pressure reactor. The reactor was then removed from the glovebox, equilibrated at 25 °C (while stirring at 600 rpm), and pressurized to 860 psi with H_2 (~60 atm). After sealing the reactor, pressure vs time data were collected by reading the pressure gauge at selected time intervals. The data for this experiment is shown in the figure below as the circles. The cyclohexene hydrogenation reaction was complete in about 5 h.

In a second experiment, the $Rh(0)_x$ nanoclusters were poisoned with CS_2. A reaction solution containing ~0.05 equivalents of CS_2 (vs Rh) was prepared in the glovebox in the following way: 9 mL of the nanocluster solution was added to 10 mL of cyclohexene and 6 mL of a 1.11×10^{-5} M solution of CS_2 in acetone. This solution was transferred into an oven-dried glass liner and sealed in the pressure reactor. The reactor was then removed from the glovebox, equilibrated at 25 °C (while stirring at 600 rpm), and pressurized to 860 psi with H_2 (~60 atm). After sealing the reactor, pressure vs time data were collected by reading the pressure gauge at selected time intervals. The data for this part of the experiment is shown in the figure below as the darkened triangles. Within experimental error, no hydrogen uptake occurred during the first 3.5 h of reaction. After 3.5 h, the temperature of the *exact same reaction solution* was increased to 100 °C, and data collection continued. The data for this part of the experiment is shown in the figure

below as the hollow triangles. (Note that the increase in temperature caused the pressure to increase by ~200 psi, as seen in the figure below.) Following the increase in temperature the hydrogenation reaction went to completion in about 1.5 h!

This experiment shows that 5 mol% CS_2 completely poisons an authentic $Rh(0)_x$ nanocluster at 25 °C, *but is ineffective as a poison at 100 °C*. Consequently, we did not attempt a quantitative CS_2-poisoning experiment for benzene hydrogenation with $Ru(II)(\eta^6\text{-}C_6Me_6)(OAc)_2$ at 100 °C.

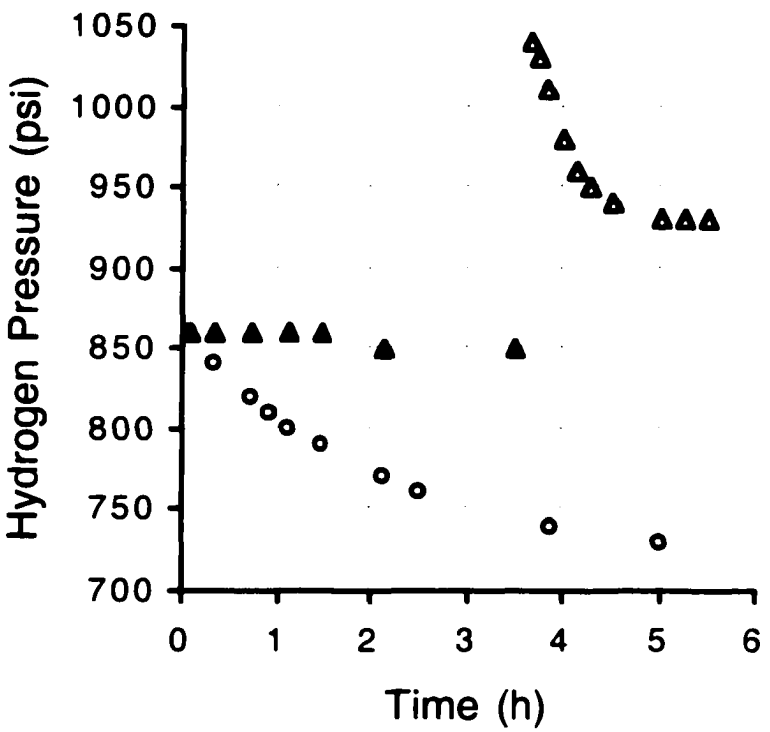

References:

(1) Lin, Y.; Finke, R. G. *Inorg. Chem.* **1994**, *33*, 4891.

(2) Lin, Y. Ph.D. Dissertation, Department of Chemistry, University of Oregon, March 1994.

(3) Hornstein, B. J.; Aiken III, J. D.; Finke, R. G. *Inorg. Chem.* **2002**, *41*, 1625.

(4) Vargaftik, M. N.; Zagorodnikov, V. P.; Stolyarov, I. P.; Moiseev, I. I.; Kochubey, D. I.; Likholobov, V. A.; Chuvilin, A. L.; Zamaraev, K. I. *J. Mol. Catal.* **1989**, *53*, 315.

(5) Johnson, K.A. *Polymer Preprints* **2000**, *41*, 1525.

(6) For metal-particle catalysts, <<1 equiv of a ligand-based poison like CS_2 is needed to completely inhibit catalysis. For example, 3.5 mol% CS_2 completely poisons a commercial Rh/Al_2O_3 catalyst with an average metal particle diameter of about 3.6 nm.[3] Geometry is the primary reason that so little poison is needed—only about 1/3 of the metal atoms are on the surface of a metal particle this size, and several adjacent surface atoms can be poisoned by a single molecule of poison.[3]

(7) This argument assumes a large equilibrium constant for the binding of the poison to the metal particle. Because of this assumption, we recommend using well-established poisons (such as CS_2) and performing appropriate control experiments. One such control experiment is to show that the added ligand is unable to disassemble authentic nanoclusters *of the same metal* into monometallic complexes: $M_n + (n \times x)L \rightarrow nML_x$. Metals with weak M–M bonding (such as first row metals, Pd, and others) are presumably most prone to such a process.

(8) Gonzalez-Tejuca, L.; Aika, K.; Namba, S.; Turkevich, J. *J. Phys. Chem.* **1977**, *81*, 1399.

(9) Frety, R.; Da Silva, P. N.; Guenin, M. *Catal. Lett.* **1989**, *3*, 9.

(10) Butt, J.B. *Catal. Sci. Technol.* **1987**, *6*, 1.

(11) Ideally, we would have used an authentic *ruthenium* metal-particle catalyst for this control experiment. However, the $Rh(0)_n$ nanocluster system (i) is in hand, (ii) is well-studied, and (iii) involves a second-row late transition metal, so the metal-to-ligand bond dissociation energies should be similar.

CHAPTER VII

SUMMARY

Much of the work in this dissertation relies on the ability to follow the kinetics of nanocluster formation. This is accomplished via a "catalytic reporter reaction" and the concept of a pseudoelementary mechanistic step. As the nanoclusters form in solution they promote a fast catalytic reaction, which serves to report (and magnify) their presence. Though indirect, this kinetic method is convenient and quantitative. Herein, this kinetic method for following nanocluster formation is shown to work for several metals and catalytic reactions. A key, take-home message is that nucleation followed by autocatalytic surface-growth, with characteristic sigmoidal kinetic curves, appears to be a general mechanism for transition-metal nanocluster formation under H_2.

The use of *soluble* transition-metal nanoclusters for catalysis is still largely unexplored. Herein, the use of well-characterized polyoxoanion- and tetrabutylammonium-stabilized Rh(0) nanoclusters to catalyze anisole hydrogenation is described. These Rh(0) nanoclusters are capable of ≥2600 catalytic turnovers for anisole hydrogenation, a record catalytic lifetime for a soluble nanocluster catalyst. One point of

special interest is the comparison of soluble nanocluster catalysts with supported-metal-particle catalysts such as Rh/Al_2O_3. Interestingly, polyoxoanion-stabilized Rh(0) nanoclusters are 10-fold more active for anisole hydrogenation than a commercially available 5% Rh/Al_2O_3 catalyst of the same average metal-particle size.

The use of late-transition-metal salts for hydrogenation catalysis is widespread, and the reduction of such salts by H_2 is often thermodynamically favorable under typical hydrogenation conditions. As a result, there are probably many unrecognized cases of nanocluster catalysis (or agglomerated-metal-particle catalysis) under reducing conditions. A re-investigation of the literature benzene hydrogenation system based on the precatalyst $Ru(II)(\eta^6\text{-}C_6Me_6)(OAc)_2$ shows that, within experimental error, agglomerated nanoclusters are responsible for all of the observed benzene hydrogenation catalysis. It would be interesting and useful to re-examine more hydrogenation catalysts in terms of the important question "Is it homogeneous or heterogeneous catalysis?"

There are many avenues for future research related to the material presented in this dissertation. For extensive lists of possible future research please refer to the Summary and Future Outlook sections of Chapters II and III. Three general categories of future research that should be re-emphasized here are: (i) extension of the catalytic reporter reaction methodology for following nanocluster formation by testing other metals and using other catalytic reactions; (ii) further exploration of the use of soluble transition-metal nanoclusters for monocyclic arene hydrogenation catalysis; and (iii) further testing of the hypothesis that metal-particle heterogeneous catalysts commonly form under reducing conditions.

APPENDIX A

GENERAL STATEMENT ON "JOURNALS-FORMAT" THESES

(Written by Professor Richard G. Finke)

The Graduate School at Colorado State University allows, and the Finke Group in particular encourages, so-called journals-format theses. Journals-format theses, such as the present one, consist of a student written and lightly edited literature background section, chapters corresponding (in the limiting, ideal case) to final-form papers either accepted or at least submitted for publication, a summary or conclusions chapter, and short bridge or transition sections between the chapters as needed to make the thesis cohesive and understandable to the reader. The "bridge" sections and summary are crucial so that the thesis fulfills the requirement that the thesis be an entity (an official requirement of most Graduate Schools). All chapters (manuscripts) in a journals-format thesis must of course be written initially by the student, with subsequent (ideally light) editing by the Professor, the student's committee, and even the student's colleagues where appropriate and productive.

The advantages for doing a journals-format thesis are several-fold and compelling. Specifically, some of the major advantages are: the level of science (i.e. of refereed, accepted publications) is at the highest level; the student and Professor must interact closely and vigorously (i.e. to bring both the science and the writing to their highest level), hence the student is getting the best education possible and is being at least exposed to (if not held to) the highest standards; the needed clean-up or control experiments that invariably come up have all been identified and completed before the student leaves; there are no further time demands once the student has left the University (since all the publications are at least submitted; it is terribly inefficient to try to complete either writing or often specialized

experiments once the student has left); and the American tax payers, who ultimately pay the bill for the research, are getting their money's worth since all the research is published and thus widely disseminated in the highest form, as refereed science. Professorial experience teaches that a student who has achieved a journals-format thesis has indeed received a better education and has learned critical thinking and clear writing skills that will serve them well for a lifetime.

Experience also teaches, however, that much more than light editing is often needed in at least some student theses; it follows, then, that considerable professorial writing and editing might be needed for at least the initial chapters of most journals-format thesis. Indeed, a journals-format thesis is not recommended (and may not even be possible) for less strong students. Hence, the issue arises of exactly how much of the science and the writing, in the final (or submittable) chapters, is due to the student vs. the Professor and whether or not this level of contribution constitutes that acceptable of a new Ph.D. and independent investigator. An additional potential problem is that the journals-format thesis does not include unpublished/unpublishable experimental results (i.e., unless they are in footnotes or the Supporting Information), which may have significant value for future members of the research group.

To deal with these issues, several recommendations are made; the recommendations below have been discussed with the committee signing Jason A. Widegren's dissertation. (Mr. Widegren's dissertation is the ninth such thesis from the Finke Group following Dr. C. Garr's, Dr. Y. Lin's, Dr. M. Pohl's, Dr. J. Sirovatka,'s, Dr. J. Aiken's and Dr. R. Suto's dissertations, and Ms. K. Weddle's and Mr. W. White's Masters theses.) The recommendations are:

(i) That the present pages be enclosed in the thesis until such a time as it is no longer needed;

(ii) That for each chapter it is detailed, and to the satisfaction of the committee and the advisor, who made what contributions, both of intellectual substance and writing. [Substantial contributions of other students or Professors should of course also be acknowledged. In the case of disagreements, the various drafts (i.e. as their electronic files) can be examined by the committee (in light of a knowledge of who wrote which draft) to easily determine who contributed what. In possible borderline or controversial cases it may even be advisable to keep all (electronic) drafts of the papers as a record];

(iii) That it be specifically stated whether or not all the experimental work is the Ph.D. candidate's;

(iv) Furthermore, it is recommended that allowances be made for the expectation that a greater degree of involvement of the professorial advisor is likely in a journals-format thesis than in a traditional thesis. [That this is reasonable follows from the fact that some Professors write 100% of all their papers; this, unfortunately, robs the student of the valuable experience of participating in the science and the end product as practiced at the highest levels.];

(v) Notwithstanding (iv), there needs to be ideally no more than ca. 40% Professorial writing contribution in a given *early* chapter in the thesis, and there should be a clear evolution in the thesis of a decreasing professorial involvement to, say, a 10-20% direct contribution in the last chapter or two;

(vi) As a further aid towards separating out the candidate's and the professorial (and other) contributions, it is recommended that the Introductory (usually literature background) chapters(s) and at least the final chapter be lightly edited only, so that authentic examples of the student's contributions are documented in an unambiguous form.

(vii) In order to avoid the loss of useful, but unpublished/unpublishable, experimental work by the student writing a journals format-thesis, the Finke Group requires the following: (1) carefully kept laboratory notebooks; (2) mandatory research reports

detailing the results of any unpublished work; and (3) the extensive use of Supporting Information and textual footnotes, where appropriate, in all published work.

APPENDIX B

Research Proposal

Catalytic hydrogenation in ionic liquids: synthesis of pure 1-butyl-3-methylimidazolium tetrafluoroborate in order to test the effects of impurities on catalytic activity

Abstract / Specific Aims

Air- and moisture-stable ionic liquids (ILs) are receiving much attention as "green" solvents for industrially important catalytic reactions. ILs have no measurable vapor pressure, which is advantageous from an engineering and safety standpoint, but at the same time it makes the purification of these solvents problematic since distillation cannot be used. Recently, it was shown that ILs such as 1-butyl-3-methylimidazolium tetrafluoroborate ([bmim][BF_4]), when prepared via standard syntheses, are contaminated by as much as 1.5% halide. To date, the potential implications of such contamination for catalysis have been largely ignored. The tacitly accepted hypothesis in most of this literature has been that halide (and other) impurities commonly found in ILs have no effect on catalytic reactions in such solvents. The proposed experiments will attempt to quantitatively disprove that hypothesis. The first specific aim of this proposal is to synthesize relatively halide-free [bmim][BF_4] by (i) using anion exchange chromatography to rigorously remove the halide or by (ii) using a completely halide-free synthetic route. The second specific aim is to quantitatively test the effect of halide concentration on catalytic activity for a reaction performed in [bmim][BF_4]; the catalytic reaction chosen for this study is olefin hydrogenation with Wilkinson's catalyst. The effect of halide (and possibly other common) impurities will be tested by systematically adding those impurities into the reaction solution. In general, these experiments will help to establish the acceptable level of halide impurities for catalytic reactions performed in ILs.

Background and Significance

Ionic liquids[1] (ILs) are materials containing only ionic species (i.e., with no neutral molecular species) that are liquid below ~100 °C.[2] ILs have been known for more than 80 years; [$EtNH_3$][NO_3] (melting point 12 °C) was first described in 1914.[3] Nevertheless, widespread use of ILs is a relatively recent phenomenon,[1,4] and is largely a

consequence of the discovery of air- and moisture-stable ILs based on alkylimidazolium cations and fluoroanions.[5] A prototypical example of an air- and moisture-stable IL is 1-butyl-3-methylimidazolium tetrafluoroborate ([bmim][BF_4]).[4]

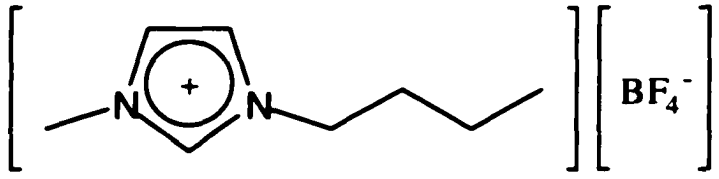

[bmim][BF_4]

ILs have been called "designer solvents" because their chemical and physical properties can be tuned by the proper choice of anion and cation.[6] For example, the coordinating ability of ILs, which is important for this proposal, is governed by the identity of the anion.[2] If weakly coordinating anions[7] such as BF_4^- and PF_6^- are the only anions present in the IL, then the IL will behave as a weakly coordinating solvent. If strongly coordinating anions such as Cl^- are present, then the IL will behave as a strongly coordinating solvent.

Air- and moisture-stable ILs tolerate a variety of functional groups, making possible many applications, including transition-metal catalysis.[2] The potential for using ILs as "green" solvents for industrially relevant catalytic reactions has received much attention recently.[8,9,10,11] Many catalytic reactions have been successfully performed in ILs, including alkene hydrogenation,[12,13,14,15,16] arene hydrogenation,[17] alkene metathesis,[18,19] hydrocarbon oxidation,[20] hydroformylation,[16,21,22] alkene oligomerization,[23] and Heck coupling.[24]

A potential problem with ILs that has not been satisfactorily addressed in the literature is the difficulty of removing non-volatile impurities (volatile impurities are easily removed by evacuation). This is an important consideration since some commonly used synthetic procedures give non-volatile byproducts (see below)! Distillation, the workhorse purification technique for traditional solvents, cannot be used for ILs because they are non-volatile. Therefore, for applications requiring high-purity ILs, special attention must be given to the way in which the ILs are synthesized.

ILs are usually synthesized in one or two steps.[2] The first step involves a quaternization reaction (of a nitrogen atom, for example), eq. 1. This is most often accomplished via an alkylation reaction, commonly with an alkyl halide. The alkylating agent determines the identity of the initially formed anion, eq. 1. If the anion of choice cannot be formed directly in the alkylation reaction, then a second step follows in which the initially formed anion is exchanged for the desired anion, eq. 2. This anion exchange can be accomplished via (i) a metathesis reaction, eq. 2a; (ii) an acid-base reaction, eq. 2b; or (iii) an ion exchange resin, eq. 2c.[2]

$$R_3N + RX \longrightarrow R_4N^+X^- \quad (1)$$

$$R_4N^+X^- \xrightarrow[-X^-]{+Y^-} R_4N^+Y^- \quad (2)$$

$$R_4N^+X^- + M^+Y^- \longrightarrow R_4N^+Y^- + M^+X^- \quad (2a)$$

$$R_4N^+X^- + H^+Y^- \longrightarrow R_4N^+Y^- + H^+X^- \quad (2b)$$

$$R_4N^+X^- + resin^+Y^- \longrightarrow R_4N^+Y^- + resin^+X^- \quad (2c)$$

A problem with anion exhange via either metathesis or acid-base chemistry is that the byproducts must then be removed from the IL. This is typically done (i) by filtration if an insoluble byproduct is formed (e.g., the metathesis byproduct of [bmim][Cl^-] and Ag[BF_4], AgCl, can be removed by filtration), (ii) by evacuation if a volatile product is formed (e.g., in the case of volatile H^+X^-, eq. 2b), or (iii) by extraction if the IL and the impurity have significantly different solubility characteristics (e.g., water can often be used to extract H^+X^- from hydrophobic ILs). Seddon and co-workers recently tested these purification techniques and found that even the best left a considerable amount of the impurity behind.[25] An illustrative example from that work involves the much-used [bmim][BF_4], which is normally synthesized by the metathesis reaction of [bmim][Cl] and Na[BF_4].[25] Using this synthetic route Seddon and co-workers found that, as a consequence of both incomplete metathesis and dissolved NaCl, the resultant [bmim][BF_4] contained 0.43 mol Cl^-/kg (i.e., it contained about 1.5% Cl^-)![25] Even after extracting the [bmim][BF_4] with chilled water ([bmim][BF_4] is miscible with water at room temperature), 0.01 mol Cl^-/kg was present in the IL.[25] In short, because of problems with the metathesis and acid-base reactions, *ion-exchange resins are the method of choice for the high purity synthesis of ILs.*[2]

It must be pointed out, however, that the use of ion exchange resins in the synthesis of ILs has received little attention.[2] In fact, the preparation of [bmim][BF_4] with an ion exchange resin has never been reported. An important conclusion can be drawn from this: much of the extant literature employing ILs such as [bmim][BF_4] is compromised by the possibility that a halide impurity is influencing the experimental results. The possible implications for catalysis in ILs have been largely ignored. To date, only anecdotal evidence exists for a halide effect on catalysis,[15,17] and even in those papers the amount of halide present in the IL was not determined. The presence of halide in an otherwise non-coordinating IL is thought to negatively influence the catalytic rates in reactions such as hydrogenations,[2,15,17,25] although no conclusive experiments have been reported to test this hypothesis. It makes chemical sense that a halide effect exists because a strongly coordinating ligand such as Cl^- can compete with substrate for coordination sites on the transition-metal catalyst.

The hypothesis to be tested in this proposal is that halide impurities have little effect on catalytic reactions performed in [bmim][BF_4] and similar ILs. This hypothesis is tacitly accepted as true in much of this literature, as evidenced by how rarely the halide

concentration is reported in such a catalytic studies.[20] If this hypothesis is disproven (i.e., if halide impurities do have a large effect on catalytic activities), then catalytic activities reported in the literature are suspect unless the halide concentration of the IL is reported! The other implication is that more attention would need to be given to the production and use of "halide-free" ILs.*

Research Design and Methods

This proposal consists of two parts. First, two syntheses of [bmim][BF_4] are proposed, both of which should ensure high-purity IL. Second, this high-purity IL is used to test the effect of halide (and other common impurities) on a prototypical catalytic reaction, alkene hydrogenation with Wilkinson's catalyst.

Synthesis of high-purity [bmim][BF_4] via a two-step approach. In a general sense this synthesis follows the normal two-step approach to preparing [bmim][BF_4], but the details of the synthesis are designed to allow efficient removal of any byproducts or impurities, Scheme 1. The first step in the synthesis, the quaternization reaction to form [bmim][Cl] (or [bmim][Br]), has been described several times in the literature.[25,26,27,28,29] The reagents for this step, 1-methylimidazole, 1-chlorobutane and 1-bromobutane, are commercially available in high purity, though the 1-methylimidazole may need to be freshly distilled.[26,30] The reaction will be performed with an excess of the alkylating agent to force the alkylation to completion (1-bromobutane, the stronger alkylating agent, will be used if complete alkylation of 1-methylimidazole is not possible with 1-chlorobutane). A simple colorimetric method for monitoring this type of alkylation reaction has been described[30] and will be used to ensure complete alkylation. It is important for alkylation reaction to be complete because unreacted 1-methylimidazole is difficult to remove from the IL (due to its high boiling point, 198 °C) and, as a coordinating base, could cause problems with the catalytic studies.[30] The alkylation reaction will be performed at reflux under an inert atmosphere. After complete alkylation of the 1-methylimidazole, the excess alkylating agent will be removed by heating the reaction solution under vacuum.†

The second step in the synthesis, exchanging the halide for BF_4^-, will be accomplished via anion exchange chromatography. Though rarely done, anion exchange chromatography is the best method for producing high-purity ILs in cases where the desired anion cannot be formed in the quaternization reaction.[2] Preparation of an anion exchange resin with BF_4^- as the anion will be accomplished by titrating a Dowex® (or other) type resin in the hydroxide form with commercially available, aqueous $H^+BF_4^-$, eq.

---

* Even if halide is found to have a significant poisoning effect on the catalytic reaction, the IL does not need to be truly halide-free. Rather, the concentration of halide probably just needs to be much lower than the concentration of catalyst. For example, if halide is a quantitative and irreversible poison for a catalytic site, but the halide is present at only 5% the concentration of catalytic sites, then only a 5% decrease in activity should be observed, which is probably not detectable in most systems. The problem is that catalyst concentrations are often quite low, which means that the concentration of any poisons in the solvent must be kept even lower in order to avoid significant effects.

† The IL, [bmim][Cl], is stable to about 250 °C,[27] which is much greater than the boiling points of either 1-chlorobutane (77 °C) or 1-bromobutane (100 °C).

3. Since both [bmim][Cl] and [bmim][BF] are water miscible,[27] water will be used as the solvent for the anion exchange reaction as well, Scheme 1. Lastly, the resultant [bmim][BF_4] will be dried by heating under vacuum.[‡]

$$\text{resin}\text{—}NR_3^+OH^- + H^+BF_4^- \xrightarrow{H_2O} \text{resin}\text{—}NR_3^+BF_4^- + H_2O \qquad (3)$$

The final purity of the [bmim][BF_4] will be checked with a variety of techniques. ^{1}H NMR will be used to check the purity of the cationic component of the IL. GC will be used to check for volatile organic impurities in the IL, the most likely impurities being unreacted starting materials.[§] ^{19}F NMR will be used to check the purity of the BF_4^- anion. Ion-selective electrode will be used to determine the concentration of residual halide; this technique has been validated for the determination of halide impurities in [bmim][BF_4].[25] If halide concentrations are found to be extremely low, atomic absorption spectroscopy will be used instead of ion-selective electrode.

This two-step synthetic approach is based on well-established chemistry, and there is every reason to believe that it will work for the production of pure, essentially halide-free [bmim][BF_4]. Nevertheless, this route is clumsy in that the first step produces halide, which must be carefully removed in the second step. A more elegant approach would be to synthesize [bmim][BF_4] in a single step without introducing any halide in the first place; just such an approach is described next.

Synthesis of high-purity [bmim][BF_4] via a one-step approach. A one-step synthesis of [bmim][BF_4] will be attempted using tributyloxonium tetrafluoroborate,[31] a so-called Meerwein salt, as the alkylating agent. Similar reactions have been reported, including the analogous alkylation of 1-methylimidazole with tri*alkyl*oxonium tetrafluoroborate (*alkyl* = methyl or ethyl).[32] Reaction conditions are reported for those reactions, but, unfortunately, no yield or purity information is available.[32]

Reaction conditions will closely follow the literature[32] as shown in Scheme 2. One equivalent of tributyloxonium tetrafluoroborate[31] will be added to an acetonitrile solution of 1-methylimidazole at 0 °C. The reaction solution will then be warmed to room temperature and stirred until the reaction is complete (as determined by the above-mentioned colorimetric method[30]). The only byproduct in this reaction is dibutyl ether, which can be removed (along with the solvent) by heating the reaction product under vacuum.[‡] The purity of the resultant [bmim][BF_4] will be assessed via the techniques described above.

Some potential problems with this synthesis are worth mentioning. First, Meerwein salts require special handling because they are highly moisture sensitive. Therefore, the 1-methylimidazole and the glassware will have to be carefully dried, and the reaction will have to be performed under inert atmosphere. Second, dibutyl ether has a fairly high boiling point (142 °C) and, therefore, may be difficult to completely remove

---

[‡] The IL, [bmim][BF_4], is stable to about 400 °C,[27] which is much greater than the boiling point of water (100 °C) or dibutyl ether (142 °C).

[§] Of course, the IL is expected to be stable and nonvolatile under normal GC conditions. As such, the IL will tend to build up in the injector port of the GC, necessitating frequent cleanings. Nevertheless, GC is an excellent, inexpensive technique for determining the presence of trace amounts of volatile impurities.

by heating and evacuation. Third, the stoichiometry of the reaction must be carefully controlled. One does not want any unreacted 1-methylimidazole since it is difficult to remove by evacuation.[30] At the same time, an excess of the Meerwein salt would be problematic, since it cannot be removed by evacuation. Fortunately, Meerwein salts are powerful alkylating agents and should react quantitatively with the 1-methylimidazole, so an excess is not required.

Catalytic studies using high-purity [bmim][BF_4] to test the effects of halide and other impurities on a prototype catalytic reaction. Alkene hydrogenation with Wilkinson's catalyst, $RhCl(PPh_3)_3$, was chosen as the catalytic reaction for this proposal because both the catalyst and the reaction have been well studied.[33] This catalytic reaction has been previously performed[14] in [bmim][BF_4], so published reaction conditions are available. Additionally, catalytic activities obtained in the proposed study can be compared with those in the literature, keeping in mind that the [bmim][BF_4] used in the literature study was prepared by the metathesis of [bmim][Cl] with Na[BF_4], which means that it probably contained about 0.4 mol of Cl^- per kg of IL.[25]

Reaction conditions will mirror those found in the literature study.[14] All preparative conditions and reactions will be carried out under dry argon using standard Schlenk techniques, and using cyclohexene that has been distilled from appropriate drying agents under argon. The catalytic reactions will be performed in an autoclave at 25 °C and 10 atm of H_2 with a catalyst concentration of 1.8 mM.[**,††] Wilkinson's catalyst, $RhCl(PPh_3)_3$, is quite soluble in [bmim][BF_4], but cyclohexene and cyclohexane are not, so the reaction is biphasic and the catalyst remains in the IL phase.[14]

Using the above conditions a series of hydrogenations will be performed with cyclohexene as the substrate. The initial reaction will be performed with [bmim][BF_4] prepared by one (or both) of the methods described above. This reaction will provide a baseline activity for Wilkinson's catalyst under "halide-free" conditions.* The effect of halide can then be tested by adding various amounts of [bmim][Cl] (or [bmim][Br]), which is synthesized as an intermediate in the first synthesis described above. The expectation, based on anecdotal evidence from the literature[15,17] is that the presence of halide will cause a decrease in catalytic activity. In a similar manner, the effects of other potential poisons in [bmim][BF_4], such as 1-methylimidazole and water, can also be tested.

A couple of potential outcomes are worth considering. In the worst-case scenario, halide concentration (or one of the other impurities tested) will be found to have a large negative effect on catalytic activity. If this is indeed the case, then all catalytic activities reported in the literature become lower limits if the halide concentration of the IL is not reported! The other implication is that more attention would need to be given to the

---

** As noted earlier, the concentration of Cl in the [bmim][BF_4] used in the literature study[14] is probably about 0.4 mol/kg.[25] This means that there are about 250 equivalents of Cl per Rh! Obviously, the possibility of a significant halide effect exists in that work.

†† As noted above,* the catalyst concentration determines the acceptable level of halide in the [bmim][BF_4] used for the proposed studies. A catalyst concentration 1.8 mM means that the concentration of halide in the "as-synthesized" IL probably needs to be <0.18 mM (i.e., less than 0.1 equiv of halide per Rh), and ideally it should be <0.018 mM (i.e., less than 0.01 equiv of halide per Rh). The best reported synthesis of [bmim][BF_4], in terms of halide concentration, still gives a final Cl concentration of 11 mM,[25] which clearly demonstrates the need for a cleaner synthesis!

production and use of "halide-free" ILs.* A second possible outcome is that halide concentration is found to have little or no effect on catalytic activity. In a sense this would be the most desirable outcome because it allows one to ignore that variable when performing this type of experiment.

Summary

This proposal intends to test the hypothesis that halide (and possibly other common) impurities in air- and moisture-stable ILs have no effect on catalytic reactions performed in such solvents. The first step in testing this hypothesis will be to synthesize previously unavailable, relatively halide-free [bmim][BF_4] by (i) using anion exchange chromatography to rigorously remove the halide or by (ii) using a completely halide-free synthetic route. The second step in testing this hypothesis is to use this relatively halide-free [bmim][BF_4] for a prototype catalytic reaction, olefin hydrogenation with Wilkinson's catalyst. Next, the effect of halide (and possibly other common) impurities on catalytic activity will be tested by systematically adding those impurities into the catalytic reaction. In general, these experiments will help to establish the acceptable level of halide impurities for catalytic reactions performed in ILs.

References:

[1] Welton, T. *Chem. Rev.* **1999**, *99*, 2071.

[2] Wasserscheid, P.; Keim, W. *Angew. Chem., Int. Ed.* **2000**, *39*, 3772.

[3] Sugden, S.; Wilkins, H. *J. Chem. Soc.* **1929**, 1291, and references therein.

[4] Hagiwara, R.; Ito, Y. *J. Fluorine Chem.* **2000**, *105*, 221.

[5] Wilkes, J. S.; Zaworotko, M. J. *J. Chem. Soc., Chem. Commun.* **1992**, 965.

[6] Freemantle, M. *Chem. Eng. News* **1998**, *76*, 32.

[7] Strauss, S. H. *Chem. Rev.* **1993**, *93*, 927.

[8] Seddon, K. R. *Kinet. Catal.* **1996**, *37*, 693.

[9] Olivier, H.; Chauvin, Y. *Chem. Ind.* **1996**, *68*, 249.

[10] Olivier, H.; Chauvin, Y. *Proc. - Electrochem. Soc.* **1996**, *96-7*, 70.

[11] Earle, M. J.; Seddon, K. R. *Pure Appl. Chem.* **2000**, *72*, 1391.

[12] Rony, P. R. *Ann. N. Y. Acad. Sci.* **1970**, *172*, 238.

[13] Parshall, G. W. *J. Amer. Chem. Soc.* **1972**, *94*, 8716.

[14] Suarez, P. A. Z.; Dullius, J. E. L.; Einloft, S.; De Souza, R. F.; Dupont, J. *Polyhedron* **1996**, *15*, 1217.

[15] Suarez, P. A. Z.; Dullius, J. E. L.; Einloft, S.; de Souza, R. F.; Dupont, J. *Inorg. Chim. Acta* **1997**, *255*, 207.

[16] Chauvin, Y.; Mussmann, L.; Olivier, H. *Angew. Chem., Int. Ed. Engl.* **1996**, *34*, 2698.

[17] Dyson, P. J.; Ellis, D. J.; Welton, T.; Parker, D. G. *Chem. Commun.* **1999**, 25.

[18] Buijsman, R. C.; van Vuuren, E.; Sterrenburg, J. G. *Org. Lett.* **2001**, *3*, 3785.

[19] Sémeril, D.; Olivier-Bourbigou, H.; Bruneau, C.; Dixneuf, P. H. *Chem. Commun.* **2002**, 146.

[20] Seddon, K. R.; Stark, A. *Green Chemistry* **2002**, *4*, 119.

[21] Wasserscheid, P.; Waffenschmidt, H. *J. Mol. Catal. A: Chem.* **2000**, *164*, 61.

[22] Brasse, C. C.; Englert, U.; Salzer, A.; Waffenschmidt, H.; Wasserscheid, P. *Organometallics* **2000**, *19*, 3818.

[23] Kohn, R. D.; Haufe, M.; Kociok-Kohn, G.; Grimm, S.; Wasserscheid, P.; Keim, W. *Angew. Chem., Int. Ed.* **2000**, *39*, 4337.

[24] Carmichael, A. J.; Earle, M. J.; Holbrey, J. D.; McCormac, P. B.; Seddon, K. R. *Org. Lett.* **1999**, *1*, 997.

[25] Seddon, K. R.; Stark, A.; Torres, M.-J. *Pure and Appl. Chem.* **2000**, *72*, 2275.

[26] Wilkes, J. S.; Levisky, J. A.; Wilson, R. A.; Hussey, C. L. *Inorg. Chem.* **1982**, *21*, 1263.

[27] Huddleston, J. G.; Visser, A. E.; Reichert, W. M.; Willauer, H. D.; Broker, G. A.; Rogers, R. D. *Green Chemistry* **2001**, *3*, 156.

[28] Bonhôte, P.; Dias, A.-P.; Armand, M.; Papageorgiou, N.; Kalyanasundaram, K.; Grätzel, M. *Inorg. Chem.* **1996**, *35*, 1168.

[29] Huddleston, J. G.; Willauer, H. D.; Swatloski, R. P.; Visser, A. E.; Rogers, R. D. *Chem. Commun.* **1998**, 1765.

[30] Holbrey, J. D.; Seddon, K. R.; Wareing, R. *Green Chemistry* **2001**, *3*, 33.

[31] Schroeder, A.; Sperber, W.; Fuchs, J.; Fehlhammer, W. P. *Chem. Ber.* **1992**, *125*, 1101.

[32] Watkins, B. E.; Rapoport, H. *J. Org. Chem.* **1982**, *47*, 4471.

[33] Collman, J. P.; Hegedus, L. S.; Norton, J. R.; Finke, R. G. *Principles and Applications of Organotransition Metal Chemistry*; University Science Books: Mill Valley, 1987.

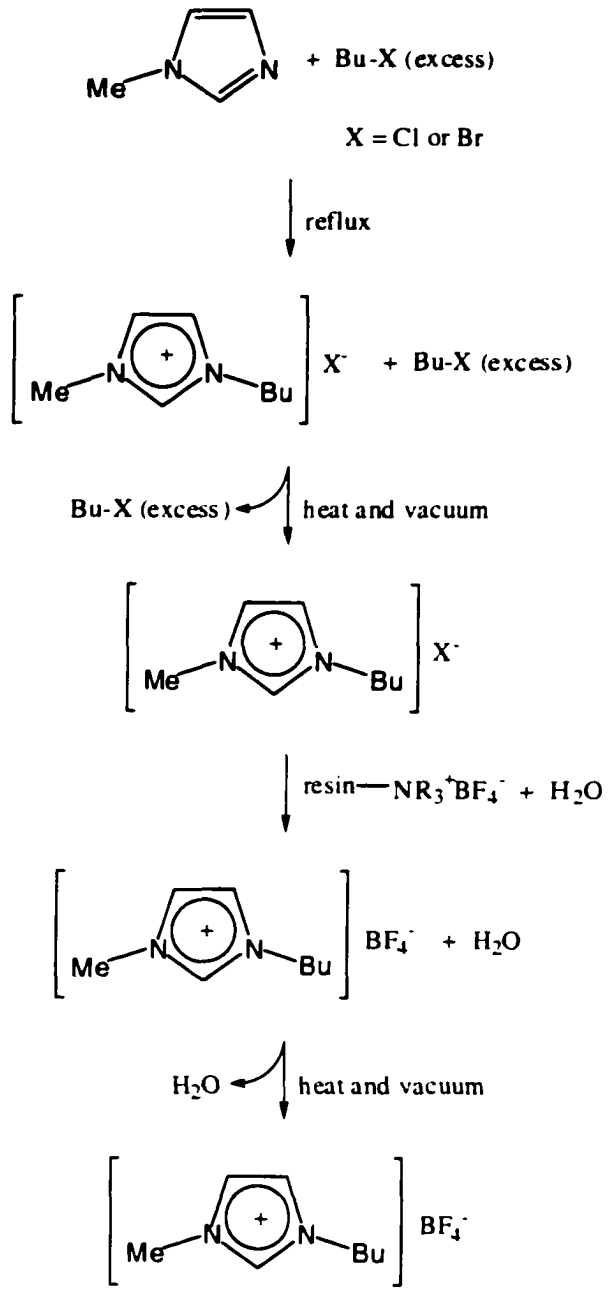

Scheme 1. Two-step synthetic route to high-purity [bmim][BF_4]. The first step involves alkylation of 1-methylimidazole with an excess of alkyl halide (followed by removal of the excess alkylating reagent). The second step involves replacement of the halide with BF_4^- via anion exchange chromatography (followed by drying).

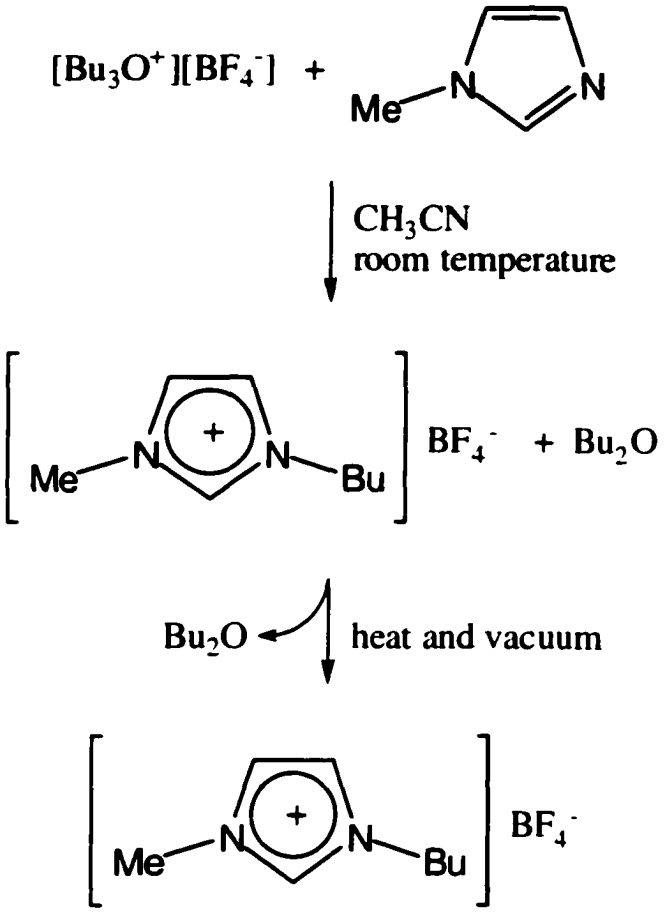

Scheme 2. One-step synthetic route to high-purity [bmim][BF_4]. The alkylation of 1-methylimidazole with a stoichiometric amount of tributyloxonium tetrafluoroborate produces the desired IL in a single step. The only byproduct is dibutyl ether, which is removed by heating the IL under vacuum.